Validation of the IL-36 receptor as a potential therapeutic target in pustular and plaque psoriasis

Mahil, Satveer Kaur

Awarding institution:
King's College London

Validation of the IL-36 receptor as a potential therapeutic target in pustular and plaque psoriasis

Satveer K. Mahil

Genetics and Molecular Medicine PhD

King's College London

Abstract

The term psoriasis describes a phenotypically heterogeneous group of inflammatory skin disorders, associated with major co-morbidity. While progress has been made in illuminating pathways that contribute to specific disease subtypes, shared aetiological mechanisms have not been investigated. In this context, the current project sought to characterise the pathogenic role of IL-36α, -β and -γ, a group of IL-1 family cytokines involved in innate epithelial responses.

The initial focus of the study was on the pathogenesis of pustular psoriasis, a rare autoinflammatory variant of the disease, associated with mutations in *IL36RN* and *AP1S3*. While it has been established that *IL36RN* defects up-regulate IL-36 signalling, the impact of *AP1S3* disease alleles remains poorly understood. Here, the characterisation of *in-vitro* and *ex-vivo* experimental systems demonstrated that *AP1S3* mutations disrupt keratinocyte autophagy. This causes an abnormal accumulation of the p62 NF-κB adaptor, leading to a marked up-regulation of IL-36 production and IL-1 responses.

Having shown that mutations in different pustular psoriasis genes have convergent effects on IL-36 signalling de-regulation, the study sought to determine whether IL-36 cytokines also have a pathogenic role in common plaque psoriasis. The IL-36 transcriptome was first characterised in keratinocyte RNA-seq experiments. This showed a substantial overlap between the genes and pathways that are upregulated by IL-36 cytokines (e.g. IL-17 signalling and leukocyte chemotaxis) and those that are abnormally active in psoriasis. In keeping with these findings, *in-vivo* and *ex-vivo* IL-36 receptor blockade reduced IL-17 over-production and leukocyte infiltration in psoriatic skin.

Finally, the deep phenotyping of human knockouts lacking a functional IL-36 receptor did not identify any anomalies in immune function, as demonstrated by the results of clinical examinations, serology tests and PBMC stimulations. This suggests that pharmacological IL-36 receptor blockade is likely to be well tolerated.

Taken together, these data suggest that IL-36 cytokines play a key role in cutaneous inflammation by amplifying IL-17 and IL-1 signalling in keratinocytes. This highlights IL-36 inhibition as a promising therapeutic approach for the treatment of plaque and pustular forms of psoriasis.

Contents

Tables

Figures

Acknowledgements

I would like to acknowledge the Medical Research Council for giving me the opportunity to pursue this PhD and for their generous funding support.

I am incredibly grateful to Francesca Capon for her wonderful supervision. I feel privileged to have received Francesca's careful, patient guidance at every step of the journey and have aspired to her scientific rigour, resourcefulness and exuberant positivity. I have learnt so much from her; from formulating hypotheses and trouble-shooting experiments to scientific writing and teaching. I am also indebted to Jonathan Barker for his inspirational leadership, invaluable close mentorship and for all of the great opportunities that I have been given throughout my academic clinical fellowship and PhD. I am very thankful to Richard Trembath for his guidance, insight and encouragement. Both Richard and Jonathan were instrumental in forging my path into this PhD and I am grateful and humbled by their ongoing support. I am extremely lucky to have benefited from the mentorship of Catherine Smith and Michael Simpson, who have been invaluable in critiquing this project and ensuring continual progress. It has also been a pleasure to work with Paola Di Meglio and I am grateful for her help with so many experiments over the past 3 years.

I have been most fortunate to have developed collaborations with many other generous and brilliant researchers over the course of this PhD, who readily shared their time, knowledge, ideas and resources to help progress this project. I am grateful to Mark Peakman for welcoming me into his lab to perform the ELISPOTs and to Sefina Arif, Lillian Williams, Laura McLaughlin and Haroon Yusuf for their hands-on guidance. I spent a fantastic week in Boston, USA in the lab of Daniel MacArthur and feel privileged to have experienced first-hand such a productive and inspirational research

environment. I am grateful to Richard, Jonathan and Francesca for facilitating the trip. I am also thankful to the Born in Bradford team (John Wright, Rosie McEachan, Dan Mason, Iram Fayyaz) and Vagheesh Narasimhan for their support with the human knockout work. Finally, it was delightful to work with Helena Ahlfors, who provided invaluable input with the RNA-seq analysis.

I would also like to extend my gratitude to several other friends and colleagues at St John's who have helped me to navigate through the PhD, in particular Niovi Setta-Kaffetzi for her meticulous technical guidance during my first months in the lab, and Nick Dand and Marika Catapano for sharing their bioinformatics expertise. I would like to express further thanks to Rashida Praminik and Meryem Ozgencil for their tuition on keratinocyte culture, Isma Ali for technical help with confocal microscopy, Kasia Grys for immunofluorescence staining advice, Mike Allen for training me to perform skin sectioning, Heather Bax for instruction on ELISAs, Elena Ortiz-Zapater for assistance with protein extraction from skin and Consol Farrera for guidance on co-immunoprecipitation. I am also grateful to friends who have donated hair and blood samples to facilitate my experiments and of course to the amazing patients who have contributed so enthusiastically. It has been a privilege to be part of Francesca's group and a pleasure to work with Niovi, Dorottya Berki, Sophie Twelves, Marta Vergnano, Marika and Lewis Millard. Thank you all for making this PhD such an enjoyable experience.

Finally I would like to thank my wonderful family for their encouragement and abundant positive energy. Two avid followers of this project were my children, who have excitedly shared all of the journey with me. They have inspired and motivated me to keep progressing and I hope that we can continue to flourish together each day.

Contributions

The work presented in this thesis was performed by myself, with the following exceptions. Dr Paola Di Meglio (Non-Clinical Lecturer at King's College London) conducted the experiments on the imiquimod murine model of psoriasis, apart from the mouse skin RNA extraction, cDNA synthesis and real-time PCR downstream analyses, which I performed. Dr Helena Ahlfors (Senior Bio-informatician at University College London Institute for Child Health) kindly provided the basic bash scripts for the RNA-seq analysis, which I modified as needed. Miss Marika Catapano (a PhD student colleague in the group) computed the overlap between the IL-36 and disease transcriptomes, and analysed the enrichment of IL-36 signature genes within GWAS intervals. Miss Sophie Twelves (a PhD student colleague in the group) screened pustular psoriasis patients for *AP1S3* disease alleles. It has been a pleasure to work with all of these colleagues and I am immensely grateful for their contributions to the thesis.

Abbreviations

3MA	3-methyladenine
ACH	acrodermatitis continua of Hallopeau
AP-1	adaptor protein complex 1
AP1S1	adaptor-related protein complex, sigma subunit 1 gene
AP1S2	adaptor-related protein complex, sigma subunit 2 gene
AP1S3	adaptor-related protein complex, sigma subunit 3 gene
bp	base pair
BCG	Bacillus Calmette-Guérin
BSA	bovine serum albumin
CADD	combined annotation dependent depletion
CAPS	cryopyrin-associated autoinflammatory syndrome
CARD14	caspase recruitment domain family, member 14 gene
Cas	CRISPR-associated
CCR5	C-C chemokine receptor type 5
cDNA	complementary DNA
CRISPR	clustered regularly interspaced short palindromic repeats
ctr	control
CXCL	C-X-C motif ligand
DAMP	damage-associated molecular pattern
DC	dendritic cell
DEG	differentially expressed genes
dNTP	deoxynucleotide triphosphate
mDC	myeloid dendritic cell

pDC	plasmacytoid dendritic cell
DIRA	deficiency of the IL-1 receptor antagonist
DLQI	dermatology life quality index
DMEM	Dulbecco's modified Eagle's medium
DNA	deoxyribonucleic acid
dsRNA	double-stranded RNA
EDTA	ethylenediaminetetraacetic acid
ELG&H	East London genes and health
ELISA	enzyme-linked immunosorbent assay
ELISPOT	enzyme-linked immunospot
ERASPEN	European rare and severe psoriasis expert network
ExAC	exome aggregation consortium
FDR	false discovery rate
FBS	fetal bovine serum
FDA	food and drug administration
GFP	green fluorescent protein
GPP	generalised pustular psoriasis
GTEx	genotype tissue expression
GWAS	genome-wide association studies
H_2O_2	hydrogen peroxide
HBSS	Hank's balanced salt solution
HEK293	human embryonic kidney 293 cell line
HIV	human immunodeficiency virus
HLA-C	major histocompatibility complex, class I, C
IB	immune blotting
IFN	interferon

IL	interleukin
Ig	immunoglobulin
IKK	IκB kinase complex
IL-1Ra	IL-1 receptor antagonist
IL1RAcP	interleukin-1 receptor accessory protein
IL1RL2	interleukin-1 receptor-like 2
IL-36R	interleukin 36 receptor
IL-36Ra	IL-36 receptor antagonist
IL36RN	IL-36 receptor antagonist gene
IP	immune precipitation
IMDM	Iscove's modified Dulbecco's medium
IRAK	IL-1 receptor associated kinase
IκB	inhibitor of NF-κB
JAK	janus kinase
KD	knockdown
KO	knockout
LDL	low-density lipoprotein
LoF	loss of function
Lp-PLA2	lipoprotein-associated phospholipase A2
mAb	monoclonal antibody
MAF	minor allele frequency
$MgCl_2$	magnesium chloride
MAPK	mitogen-activated protein kinase
MHC	major histocompatibility complex
ml	millilitre
mm	millimetre
mut	mutated

µl	microlitre
µM	micromolar
NaCl	sodium chloride
ns	not significant
NF-κB	nuclear factor-κB
ng	nanogram
nM	nanomolar
OCT	optimum cutting temperature
PASI	psoriasis area and severity index
PBMC	peripheral blood mononuclear cell
PBS	phosphate buffer saline
PCR	polymerase chain reaction
PCSK9	proprotein convertase subtilisin/kexin type 9
PDE-4	phosphodiesterase type 4
poly(I:C)	polyinosinic:polycytidylic acid
PPIA	cyclophilin A
PPP	palmar-plantar pustulosis
PLA2G7	lipoprotein-associated phospholipase A2 gene
PMA	phorbol 12-myristate 13-acetate
PROMIS	Pakistan risk of myocardial infarction study
PUVA	psoralen/UVA photochemotherapy
PVDF	polyvinylidene fluoride
RNA	ribonucleic acid
rpm	revolutions per minute
RPMI	Roswell Park memorial institute medium
SDS	sodium dodecyl sulphate
SEM	standard error of the mean

shRNA	short-hairpin RNA
siRNA	small-interfering RNA
SNP	single nucleotide polymorphism
STAT	signal transducer and activator of transcription
TBS	Tris-buffered saline
TGF-β	transforming growth factor beta
TIR	toll/IL-1 receptor
TLR	Toll-like receptor
Tm	annealing temperature
TNF	tumour necrosis factor
TRAF	tumour necrosis factor receptor associated factor
VEGF	vascular endothelial growth factor
WCE	whole cell extracts
wt	wild type

1. Introduction

1.1. Psoriasis

1.1.1. Overview

Psoriasis is a common, immune-mediated skin disease that is associated with substantial physical and psychological morbidity [1]. It affects more than 125 million individuals worldwide and has an estimated prevalence of 2% [2]. Males and females are affected equally, with a bimodal distribution of age of onset (peaks are observed at 18-39 and 50-69 years) [3].

Psoriasis can manifest as a broad spectrum of phenotypes, which are not mutually exclusive (Table 1.1, Figure 1.1.1). Diagnosis and assessment of severity are usually based on clinical findings. A crude indicator of severity is the percentage of body surface area that is affected. Using this criterion, approximately one third of patients have 'moderate to severe' psoriasis (>10% body surface area affected). The more refined Psoriasis Area and Severity Index (PASI) ranks the severity and surface area of erythema, as well as the thickness and desquamation of plaques, with scores greater than 12 indicating severe disease [4]. In addition, there are a plethora of patient questionnaires for assessment of quality of life [5]. Although the Dermatology Life Quality Index (DLQI) is routinely used in clinical practice, this is often supplemented by targeted anxiety and depression screens in recognition of the psychological burden of disease [6].

Given that the focus of this thesis is on plaque and pustular psoriasis, these two variants of the disease will be described in more detail.

Table 1.1 Clinical subtypes of psoriasis

Subtype	Clinical features	Sites involved
Plaque psoriasis	Sharply demarcated, erythematous plaques covered with silvery scales.	Scalp, trunk, buttocks, limbs, extensor surfaces.
Pustular psoriasis	Chronic or acute eruption of sterile pustules on erythematous skin.	Generalised or localised to the palms/soles (palmoplantar) or distal digits (acrodermatitis continua of Hallopeau).
Guttate psoriasis	Small, teardrop-shaped salmon pink plaques with a fine, adherent scale. Often self-limited and preceded by group A β-haemolytic streptococcal infection.	Trunk, proximal extremities.
Erythrodermic psoriasis	Generalised erythema and scaling.	Greater than 90% of total body surface involved.
Inverse psoriasis	Erythematous plaques with minimal scale (due to friction and moisture).	Flexural and intertriginous areas.
Nail psoriasis	Pitting, discolouration, subungual hyperkeratosis, onycholysis, dystrophy.	Fingernails or toenails.

Figure 1.1.1 Psoriasis is a clinically heterogeneous disease

The spectrum of psoriasis phenotypes includes (a) guttate psoriasis, (b) plaque psoriasis, (c) pustular psoriasis and (d) nail psoriasis. Adapted from [7].

1.1.2. Plaque psoriasis

1.1.2.1. Clinical and histological features

Plaque psoriasis is the commonest form of the disease and accounts for almost 90% of cases [1]. It classically presents with well demarcated, erythematous plaques with loosely adherent silvery scales. The scalp or extensor surfaces, such as elbows and knees, are commonly affected in a symmetrical distribution.

Co-morbid conditions contribute to the physical burden of the disease and seronegative psoriatic arthritis is one of the most frequent, affecting up to 30% of patients [8]. Although several observational studies have identified increased cardiovascular risk in patients with severe psoriasis, the underlying mechanism and relevance to individuals with milder forms of disease is not clear [9]–[11].

At the histological level [12] (Figure 1.1.2), psoriatic plaques are composed of hyperproliferative keratinocytes that retain their nuclei (parakeratosis) even in the uppermost layers of the epidermis, where they are normally absent. This is due to incomplete terminal differentiation, as demonstrated by reduced expression of keratin 10.

T lymphocytes and dendritic cells (DC) densely infiltrate psoriatic lesions. Neutrophils also collect in 'Kogoj pustules' and 'Munro's microabscesses', which appear in the stratum spinosum and stratum corneum of the epidermis, respectively. Finally, the erythematous appearance of lesions is due to dilated and tortuous blood vessels, which reach into the tips of elongated dermal papillae.

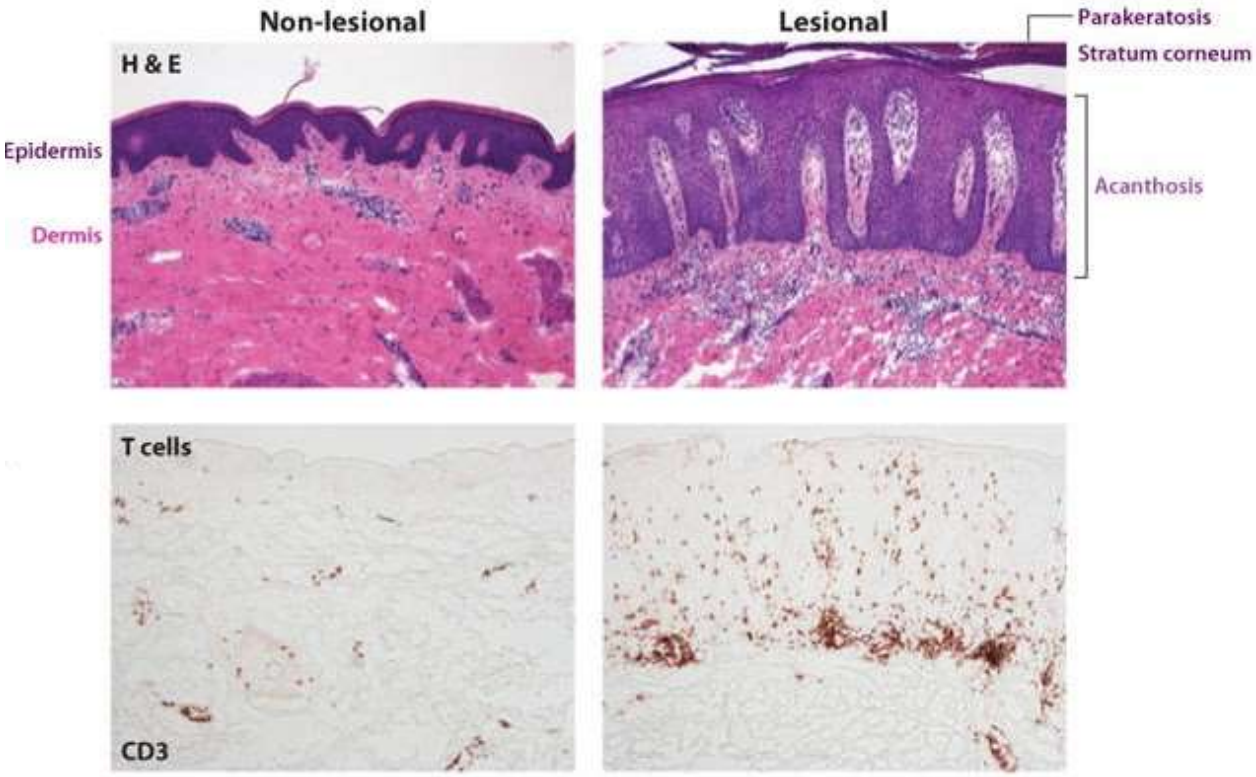

Figure 1.1.2 Psoriatic skin lesions have a characteristic histological appearance

Haematoxylin and eosin stained sections (top panel) of psoriasis skin lesions demonstrate a thickened epidermis (acanthosis) with elongations into the dermis (rete ridges). Retention of nuclei (parakeratosis) is observed in the stratum corneum. The inflammatory infiltrate in the dermis is composed of T cells and dendritic cells. Increased numbers of CD3+ T cells in lesional skin are confirmed using immuno-histochemistry (lower panel). All images x10 magnification [13].

1.1.2.2. Genetic basis of disease

Plaque psoriasis is a complex trait, caused by an interplay between multiple genetic and environmental factors [14]. The existence of a genetic component was initially revealed by epidemiological studies, which showed a greater prevalence of psoriasis amongst near relatives of affected individuals, compared to the general population [15]. Moreover, a higher disease concordance was consistently observed in monozygotic compared to dizygotic twins, with heritability estimates ranging from 60 to 90% [16].

Linkage studies identified at least 9 regions that co-segregated with psoriasis (*PSORS 1-9*) in multiplex pedigrees. However, most of these findings could not be replicated, demonstrating the inadequacy of linkage approaches for the analysis of multi-factorial conditions [17]. A notable exception is the *PSORS1* region, which maps to the class I interval of the major histocompatibility complex (MHC) [18]–[20]. It dominates the genetic landscape of psoriasis as it has the largest effect size and accounts for 35-50% of disease heritability.

Despite the confounding effect of linkage disequilibrium conservation across the MHC [21], *HLA-Cw*0602* is considered the most likely causal susceptibility allele, since single nucleotide polymorphisms (SNPs) that tag this variant generate the most significant association signals in case-control studies [22], [23]. However, fine mapping studies suggest the presence of additional association signals within *PSORS1*, some of which are population-specific [24]–[26].

Outside of the MHC, the only linkage result that was successfully validated was the identification of the *PSORS2* locus on chromosome 17q25. The most likely susceptibility gene in this region is

CARD14, which encodes a nuclear factor-κB (NF-κB) activator and harbours variants associated with rare and common forms of psoriasis [27]–[29].

Following the evolution of techniques for the high-throughput genotyping of SNPs, genome-wide association studies (GWAS) were performed on extended case-control resources. This enabled the identification of numerous psoriasis susceptibility loci, reflecting similar successes in other complex genetic diseases. Although the disease associated regions can span several genes, it is noteworthy that many of the lead SNPs lie in proximity to loci involved in specific adaptive and innate immune pathways. These include genes involved in antigen presentation (*HLA-C, ERAP1*), T17 cell activation (*IL23R, IL23A, IL12B, TRAF3IP2*), innate antiviral immunity (*RNF114, IFIH1*) and skin barrier function (*LCE3B/3D*) [22], [23], [30]–[34]. There is also evidence of gene-gene interactions (epistasis) contributing to disease heritability, since *ERAP1* variants only confer disease susceptibility in individuals also harbouring the *HLA-C* risk allele [23].

Targeted association analyses based on dense SNP arrays such as the Immunochip and exome chip have refined GWAS signals and identified potential susceptibility alleles. These include coding variants in genes such as *IL23R* and *TYK2,* which further underscores the involvement of the IL-23/T17 axis in disease pathogenesis [35]–[37].

There are now over 60 regions that are associated with psoriasis at a genome-wide significant level (Table 1.2). Since only 5% of lead SNPs are likely to be causal, a major future challenge will be the fine mapping and functional annotation of the alleles driving these established association signals [38]. Moreover, as GWAS focused on common SNPs have only accounted for a fraction (~20%) of

psoriasis heritability, further genetic determinants will need to be uncovered [39]–[41]. This could be achieved by assessing rare variants, gene-gene and gene-environment interactions, and using increased sample sizes to identify further common alleles of small effect [14]. With the growing resolution and reducing cost of next-generation sequencing technologies, the potential for future genetic discoveries in psoriasis is promising.

Table 1.2 Genes associated with psoriasis in genome-wide association studies

Gene†	Chromosome	Biological pathway
TNFRSF9 [35]	1	Adaptive immunity, T cell activation
IL28RA [23], [35]	1	Innate immunity, IFN signalling
RUNX3 [35]	1	Adaptive immunity, T cell activation
IL23R [22], [23], [35]	1	Adaptive immunity, IL-23/T17 axis
LRRC7 [36]	1	Neuronal synapse formation
LCE3B/LCE3D [35]	1	Keratinocyte barrier function
DENND1B [42]	1	Adaptive immunity, regulation of T cell receptor signalling
MTHFR [37]*	1	DNA methylation
NPPA [37]*	1	Electrolyte homeostasis
ZNF683 [37]*	1	Adaptive immunity, effector T cell differentiation
C1orf141 [37]*	1	Undetermined
AIM2 [37]*	1	Innate immunity, inflammasome activity
REL [23], [35]	2	Innate immunity, NF-κB signalling
B3GNT2 [35]	2	Adaptive immunity, T cell activation
IFIH1 [23], [25], [35]	2	Innate immunity, antiviral signalling
IL1RL2, IL1RL1 [37]*	2	Innate immunity, IL-1 family signalling
PLCL2 [36]	3	Lipid regulation
NFKBIZ [35]	3	Innate immunity, NF-κB signalling
TP63 [25]	3	Innate immunity, keratinocyte function
CASR [37]*	3	Innate immunity, calcium signalling
GPR160 [37]*	3	Undetermined
NFKB1 [43]*	4	Innate immunity, NF-κB signalling
CARD6 [35]	5	Innate immunity, NF-κB signalling
ERAP1 [23], [35]	5	Adaptive immunity, antigen presentation
IL4, IL13 [22], [35]	5	Adaptive immunity, Th2 signalling

TNIP1 [22], [35]	5	Innate immunity, NF-κB signalling
IL12B [22], [33]–[35], [44]	5	Adaptive immunity, IL-23/T17 axis
ZFYVE16 [37]*	5	TGF-β signalling
LNPEP [45]*	5	Electrolyte homeostasis, NF-κB signalling
PTTG1 [46]*	5	Cell proliferation, DNA repair, angiogenesis
EXOC2 [35]	6	Innate immunity, antiviral signalling
HLA-C [22], [23], [35]	6	Adaptive immunity, antigen presentation
TRAF3IP2 [22], [23], [35]	6	Innate immunity, IL-17 signalling
TNFAIP3 [23], [35]	6	Innate immunity, NF-κB signalling
TAGAP [35]	6	Adaptive immunity, T cell activation
ELMO1 [35]	7	Innate immunity, regulates macrophage engulfment of apoptotic cells, cell migration
CCDC129 [37]*	7	Undetermined
CSMD1 [46]*	8	Keratinocyte differentiation
DDX58 [35]	9	Innate immunity, antiviral signalling
KLF4 [35]	9	Adaptive immunity, differentiation of T17 cells
ZMIZ1 [34], [37]	10	TGF-β signalling
CAMK2G [36]	10	Adaptive immunity, thymic development
PRDX5 [34], [35]	11	Anti-oxidant enzyme
ZC3H12C [35]	11	Innate immunity, macrophage activation
ETS1 [35]	11	Adaptive immunity, T cell differentiation
AP5B1 [37]*	11	Undetermined
IL23A [23], [35]	12	Adaptive immunity, IL-23/T17 axis
COG6 [44]	13	Component of Golgi apparatus
LOC144817 [44]	13	Long intergenic non-protein coding RNA
GJB2 [46], [47]*	13	Keratinocyte barrier function
NFKBIA [23], [48]	14	Innate immunity, NF-κB signalling
SYNE2 [37]*	14	Skin barrier function
AKAP13 [36]	15	Innate immunity, NF-κB signalling

SOCS1 [35]	16	Adaptive immunity, Treg function, negative regulation of JAK signalling
FBXL19 [35], [48]	16	Innate immunity, NF-κB signalling
NOS2 [35], [48]	17	Innate immunity, production of nitric oxide
STAT3, STAT5A/B [35]	17	Adaptive immunity, IL-23/T17 axis
CARD14 [35]	17	Innate immunity, NF-κB signalling
IKZF3 [43]*	17	Adaptive immunity, lymphocyte development
TMC6 [37]*	17	Adaptive immunity, zinc homeostasis
MBD2 [35]	18	Adaptive immunity, T cell activation
SERPINB8 [46]*	18	Innate immunity, cytokine activation
TYK2 [23], [35]	19	Adaptive immunity, IL-23/T17 axis
CARM1 [35]	19	Innate immunity, NF-κB signalling
FUT2 [47]*	19	Innate immunity
ZNF816A [46], [47]*	19	Zinc finger protein, regulatory function, protein recognition
RNF114 [32], [35]	20	Innate immunity, antiviral signalling
RUNX1 [44]	21	Epidermis and T cell development
IFNGR2 [37]*	21	β chain of IFNγ receptor, adaptive immunity, influences T17 cell polarisation
SON [37]*	21	Undetermined
YDJC [49]	22	Undetermined
UBE2L3 [35]	22	Innate immunity, antiviral signalling

IFN, interferon; TGF-β, transforming growth factor beta.

†Most likely candidate gene within the susceptibility locus, based on gene function

*Genome-wide significant association in Han Chinese population only

1.1.2.3. Immunopathogenesis

Genetic studies have provided important mechanistic insights into the aetiology of psoriasis, supporting a pathogenic interplay between immune activation and disruption of skin barrier function.

Psoriasis can be triggered by trauma (Koebner phenomenon), infection (most notably β-haemolytic streptococcus) and medications (such as lithium, β-blockers and IFNα). These events cause keratinocytes to produce the anti-microbial peptide known as LL37, which then complexes with self-RNA or self-DNA and activates plasmacytoid dendritic cells (pDC) via Toll-like receptor (TLR) -7 or -9 [50]. CD11c positive myeloid dendritic cells (mDC) are subsequently activated. This can happen directly, through an engagement of TLR-8 with LL37/RNA complexes or indirectly, via pDC-derived type I interferon [51].

Once activated, mDCs migrate to local skin-draining lymph nodes, where they produce IL-12 and IL-23, which polarise T lymphocytes into Th1 or T17 cells [52]. The latter secrete IL-17 and comprise CD4+ and CD8+ T cells (which express αβ T cell receptors) and the recently characterised γδ T cells. In skin, the main target for IL-17 is the keratinocyte, where downstream signalling mediated by the *TRAF3IP2*/ACT1 adaptor results in the activation of NF-κB and the transcription of pro-inflammatory genes [34], [53]. These include *CCL20* (which attracts DCs and further T17 cells), as well as *IL8*, *CXCL1*, *CXCL2* (which attract neutrophils). Vascular endothelial growth factor (VEGF) is also secreted, which induces vascular dilatation and hyperplasia, thereby facilitating the ongoing influx of inflammatory cells [54]. Thus, IL-17 molecules produced by T17 cells activate keratinocytes to produce chemokines that attract further inflammatory elements into the dermis and the epidermis.

The identity of the antigens that are presented to T lymphocytes by mDCs in psoriasis has historically been elusive. Recent research has indicated that peptides derived from LL37 may act as auto-antigens for T cells in a HLA-C*0602 restricted manner [55], [56]. Further systematic studies have also revealed a potential role for ADAMTS-like protein 5 [57]. Finally, lipid antigens generated by phospholipase A2 group IVD can be presented by skin-resident Langerhan's cells to CD1a-reactive T cells, inducing production of IL-17 [58] [59], [60].

In summary, psoriasis pathogenesis involves local positive feedback loops between keratinocytes, antigen presenting cells and T cells (Figure 1.1.3). The modulation of keratinocyte responses by the IL-23/T17 axis is at the centre of this model and is now a key target for emerging therapies.

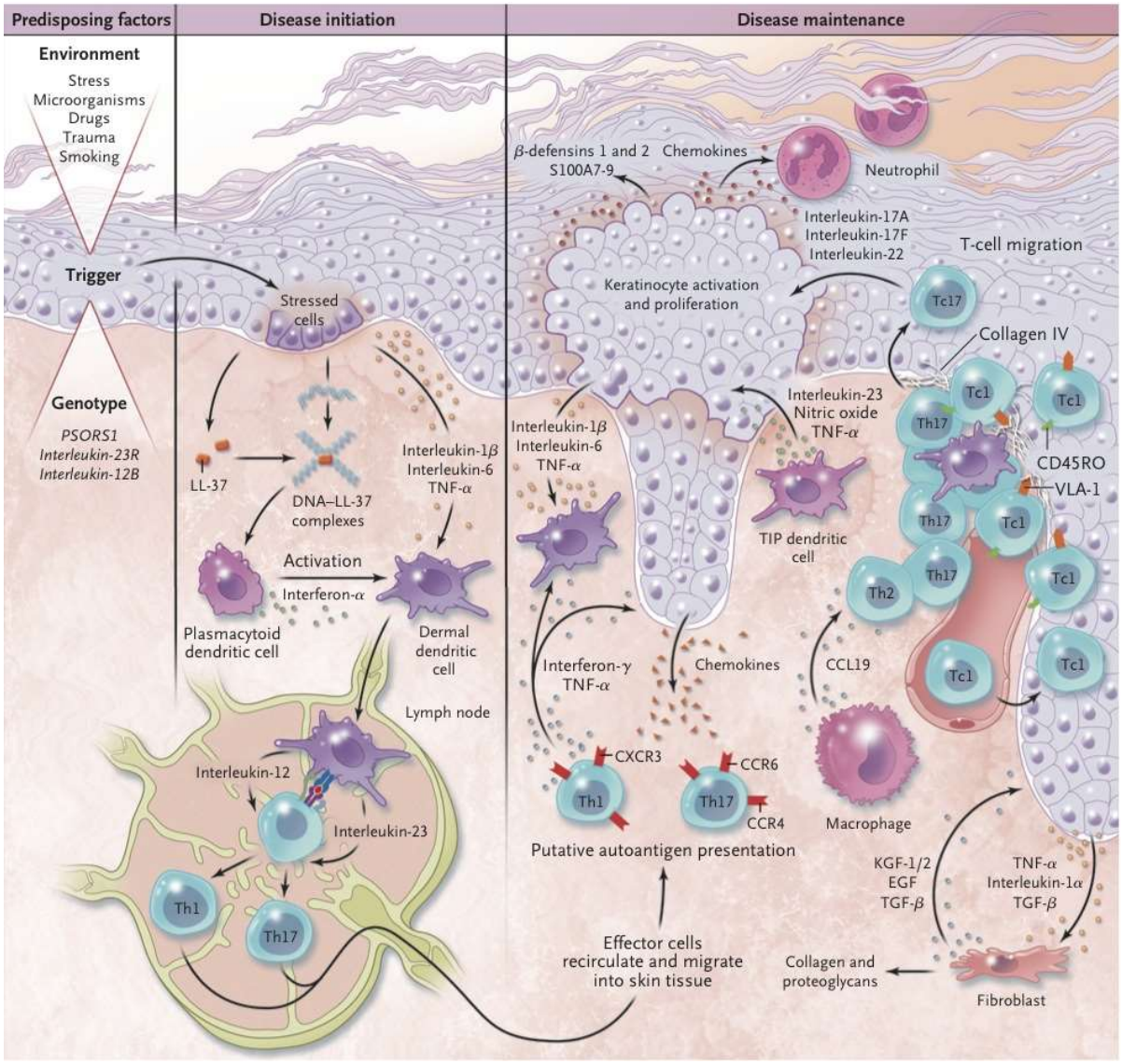

Figure 1.1.3 Pathogenic model for plaque psoriasis

Triggers such as infection and trauma (left panel) lead to the formation of LL-37/DNA complexes and secretion of type I interferons (IFN-α and -β) by plasmacytoid dendritic cells. This promotes antigen presentation by dermal dendritic cells, resulting in the activation of T17 and Th1 lymphocytes (middle panel). These cells release IL-17, IFNγ and TNFα molecules, causing keratinocyte hyper-proliferation (leading to epidermal hyperplasia) and production of further chemokines and cytokines. This in turn drives the recruitment of additional inflammatory cells (T cells, neutrophils and macrophages), in a loop that sustains cutaneous inflammation and contributes to the formation of psoriatic plaques (right panel) [1].

1.1.2.4. Therapies

Although general management guidelines exist in the United States and Europe, treatment choices are individually tailored based on the severity of psoriasis and the presence of co-morbidities [61], [62]. For patients with mild-to-moderate disease (<10% body surface area affected) and no concurrent psoriatic arthritis, topical treatment may suffice. The mainstay of such therapy is corticosteroids, which may be used in a rotational regime with vitamin D analogues, in order to minimise adverse effects such as skin atrophy and dyspigmentation. Phototherapy is effective for short term treatment of moderate-to-severe disease and acts through induction of apoptosis of inflammatory cells, suppression of T17 cells and activation of Th2 and regulatory T cells [63]. However, established phototherapies are time consuming and not suitable for long term use due to their associated carcinogenic potential [64], [65].

Traditional systemic agents such as methotrexate, ciclosporin and acitretin are used for patients with moderate-to-severe disease or milder disease co-existing with psoriatic arthritis. Major limitations of these medications are drug-drug interactions and cumulative organ toxicities, which are less prevalent with the newer targeted immunotherapies.

Several monoclonal antibodies and small molecules antagonising the dysregulated immune response in psoriasis have been developed over the past decade and offer higher efficacy and better safety profiles than conventional therapies (Table 1.3). Based on the mechanistic insights that have emerged from genetic studies, the IL-23/T17 axis has been a particular focus for drug development (Figure 1.1.4).

Table 1.3 Current immunotherapies for psoriasis

Name of agent	Target	Type of agent	Stage of development
Infliximab	TNFα	Chimeric monoclonal antibody	Approved [66]
Etanercept	TNFα	TNFα receptor-Ig fusion protein	Approved [66]
Adalimumab	TNFα	Human monoclonal antibody	Approved [66]
Ustekinumab	IL-12/IL-23p40	Human monoclonal antibody	Approved [66]
Secukinumab	IL-17A	Human monoclonal antibody	Approved [66]
Ixekizumab	IL-17A	Humanised monoclonal antibody	Approved [67]
Brodalumab	IL-17 receptor	Human monoclonal antibody	Phase III complete [67]
Tildrakizumab	IL-23p19	Human monoclonal antibody	Phase III complete [67]
Guselkumab	IL-23p19	Human monoclonal antibody	Phase III in progress [66]
Risankizumab	IL-23p19	Human monoclonal antibody	Phase III in progress [67]
Apremilast	PDE-4	Small molecule inhibitor	Approved [66]
Tofacitinib	JAK1/JAK3	Small molecule inhibitor	Phase III complete [66]
Ruxolitinib	JAK1/JAK2	Small molecule inhibitor	Phase II complete [66]

PDE-4, phosphodiesterase type 4; JAK, Janus kinase; Ig, immunoglobulin.

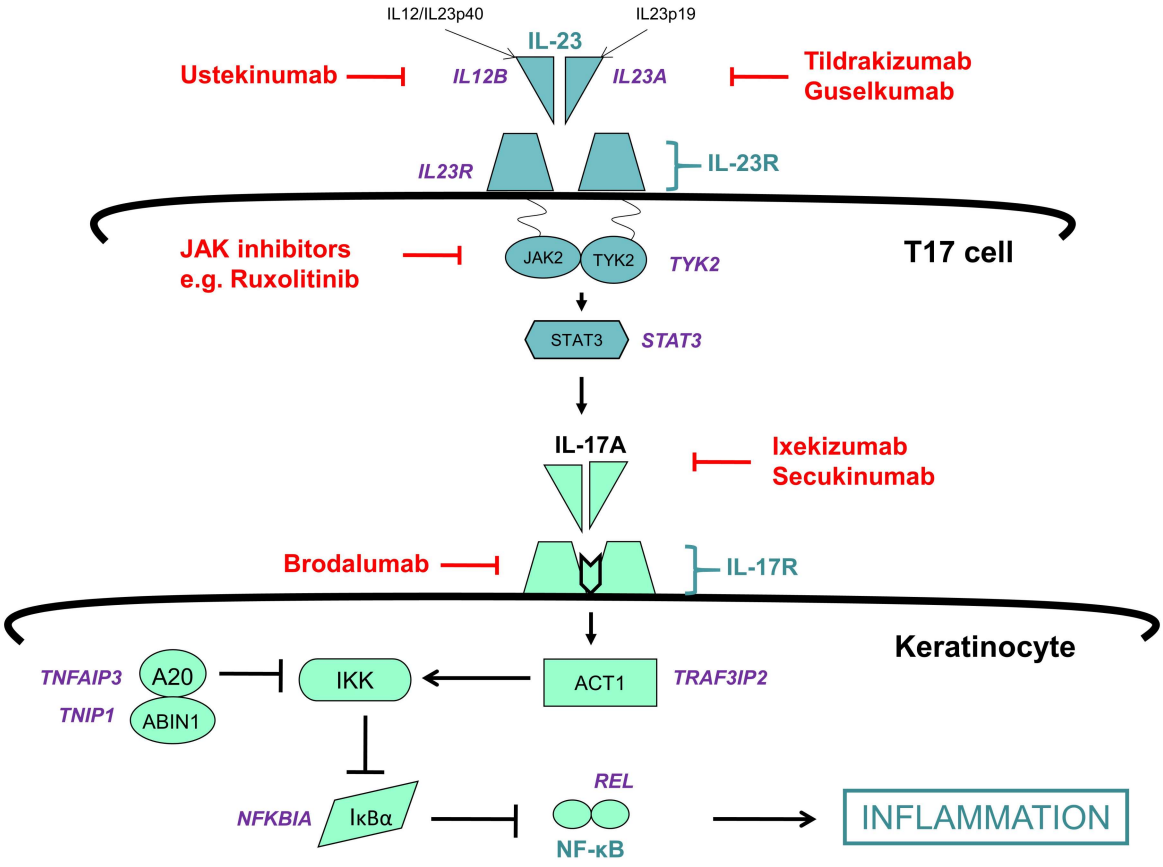

Figure 1.1.4 The IL-23/T17 axis is an important therapeutic target in psoriasis.

Numerous genes (*purple*) encoding proteins in the IL-23/T17 axis have been shown by GWAS to confer psoriasis susceptibility, with several medications for psoriasis (*red*) now targeting components of this pathway. IL-23 binding causes the IL-23 receptor (IL-23R) to associate with Jak2 and Tyk2, which activate STAT3 molecules, resulting in the upregulation of IL-17A by T17 cells. Following activation of IL-17R on keratinocytes, ACT1 (encoded by *TRAF3IP2*) interacts with TRAF proteins and the IκB kinase complex (IKK). IKK subsequently phosphorylates the inhibitory proteins IκB (IκBα is encoded by *NFKBIA*), which are complexed with cytoplasmic NF-κB. Once phosphorylated, IκB is subject to ubiquitin-induced proteasomal degradation, resulting in the nuclear translocation of NF-κB. Further, the protein products of *TNFAIP3* and *TNIP1*, (A20 and ABIN1, respectively) physically interact to enable the ubiquitin-mediated destruction of NEMO (a regulatory protein that activates IKK). JAK; Janus kinase. [66].

TNFα antagonists were the first biologic agents to demonstrate efficacy in psoriasis, and they act by suppressing the differentiation and function of T17 effector cells, in particular by inhibiting IL-23 production by mDCs [68], [69]. Although TNF blockers carry less risk of systemic toxicity compared with conventional systemic agents, they are associated with an increased incidence of infections (e.g. reactivation of latent tuberculosis), demyelination and certain malignancies (e.g. squamous cell carcinoma) [70], [71].

Ustekinumab is an inhibitor of the common p40 subunit of IL-12 and IL-23, which suppresses both Th1 and T17 lymphocyte development and function. It has shown impressive 66-76% PASI-75 (reduction in baseline PASI by $\geq$75%) response rates in phase III clinical trials, and superior efficacy over etanercept [72]–[74]. However, the long-term impact on host immune responses is uncertain and is being monitored in clinical registries [75].

More selective inhibition of T17 responses is achieved through IL-17 antagonists. Secukinumab and ixekizumab are Food and Drug Administration (FDA) approved IL-17A monoclonal antibodies, which have shown superior efficacy to ustekinumab [76]. In fact, phase III clinical trial data demonstrated PASI-75 response rates of 77-82% and 87-90% for secukinumab and ixekizumab, respectively [77], [78]. The rapid and high efficacy of IL-17 antagonists supports the role of IL-17 as a driver of positive feedback loops that modulate keratinocyte function. However, the cytokine also has an important role in host anti-fungal immunity and an increased rate of *Candida* infections have been reported after pharmacological IL-17 blockade [77], [78].

Following the success of ustekinumab, selective IL-23p19 blockers are being developed. Phase I and II clinical trial data demonstrated rapid and sustained clinical improvements with IL-23p19 blockade, alongside reductions in epidermal hyperplasia, CD3+ T cell infiltration, and attenuation of molecular signatures of disease [79], [80]. Phase III clinical trial data are eagerly anticipated.

The oral phosphodiesterase-4 small molecule inhibitor apremilast was recently approved for the treatment of moderate-to-severe psoriasis. It prevents conversion of cAMP to AMP, which downregulates cytokines such as TNFα and IL-23 and upregulates IL-10 [81]. Although reported efficacy is lower than biologic therapies (33% of patients achieve PASI-75), the oral route of administration and favourable safety profile have made this an increasingly popular option for patients [82].

Janus kinase (JAK) inhibitors are a new class of small molecule inhibitors, which act on the tyrosine kinases that activate STAT proteins (Figure 1.1.4). Tofacitinib preferentially inhibits JAK-1 and -3. Phase III trials have demonstrated non-inferiority to etanercept and 69% PASI-75 response rates, with sustained efficacy over 1 year [83], [84]. Promising results have also been reported for the topical JAK 1/2 inhibitor ruxolitinib, with reduced clinical lesion scores over 28 days, alongside improvements in histological and molecular markers of inflammation [85].

In conclusion, scientific advances in characterising the molecular mechanisms of disease have successfully translated into the development of targeted immunotherapies for psoriasis. However, the long term safety profile and efficacy of these agents remain to be determined, including the impact on co-morbid diseases. Moreover, current treatments are not uniformly effective across the

patient population, with low rates of effectiveness demonstrated for both TNF and IL-12/IL-23 antagonists in real world settings [86]. Hence, there is a need for ongoing refinement of the pathogenic model, which will enable the selection of further therapeutic agents.

1.1.3. Pustular psoriasis

1.1.3.1. Clinical and histological features

Pustular psoriasis is an autoinflammatory disease characterised clinically by the presence of sterile pustules on variably erythematous skin, and histologically by diffuse dermal neutrophilic infiltration (Figure 1.1.5) [87], [88]. It can be classified as either acute generalised or chronic localised disease (Figure 1.1.6).

Generalised pustular psoriasis (GPP) is a rare (prevalence 1-9:1,000,000), potentially life-threatening condition. It is characterised by acute episodes of extensive pustulation and widespread erythema, associated with systemic upset (e.g. fever, increased levels of acute phase reactants, leukocytosis) and joint involvement. Triggers for disease flares include pregnancy, infection and drugs [89]. Up to 30% of patients with GPP may present with associated plaque psoriasis [90].

Palmoplantar pustulosis (PPP) and acrodermatitis continua of Hallopeau (ACH) are subtypes of chronic and localised pustular psoriasis. PPP manifests on the palms and soles with painful, sterile pustules appearing on an erythematous base. Triggers include trauma, stress and infections and a higher prevalence of disease is noted in smokers. ACH is characterised by a disabling pustular eruption of the distal fingers and toes that may appear after localised trauma or infection. Pustulation involving the nail folds and nail beds leads to onychodystrophy and anonychia.

Osteolysis of the distal phalanges, distal interphalangeal joint arthritis and skin atrophy may arise in prolonged or refractory cases [89].

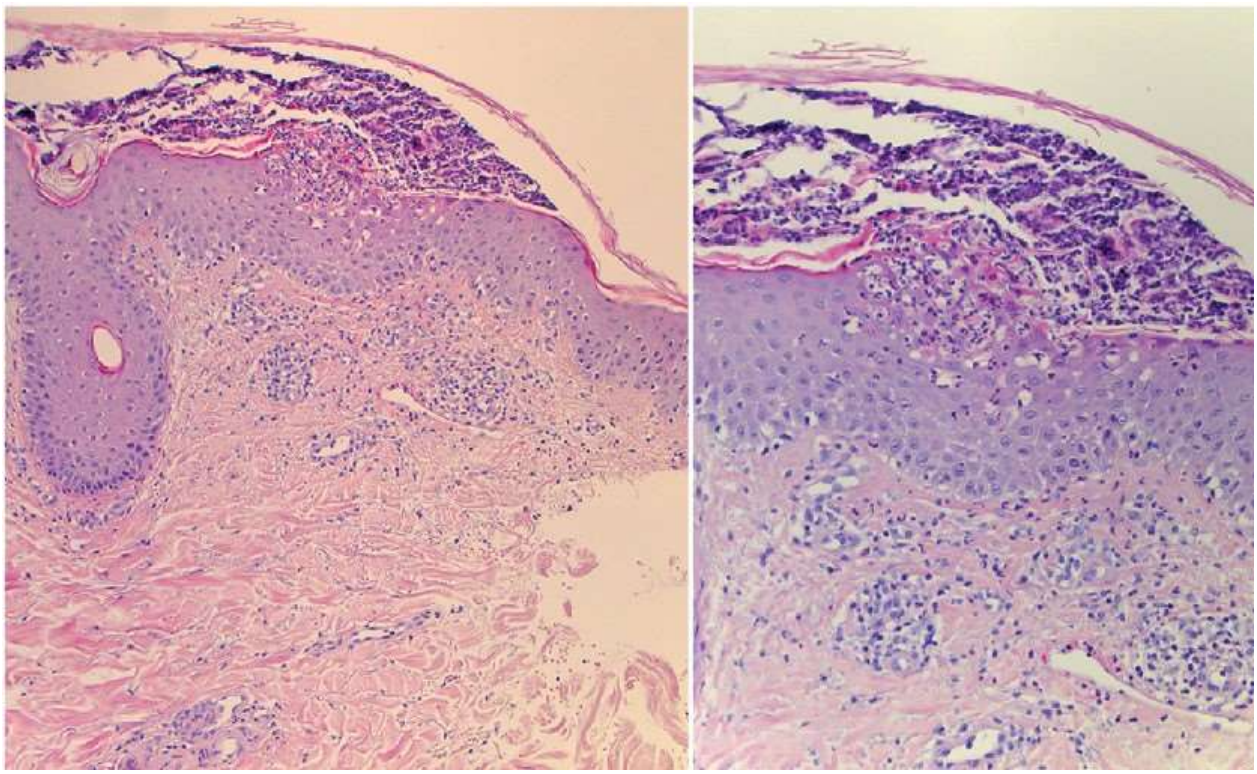

Figure 1.1.5 Pustular psoriasis lesions have characteristic histological features

Haematoxylin and eosin staining of a biopsy from lesional skin shows extensive cutaneous infiltration of neutrophils. The acanthotic epidermis features parakeratosis and there are multifocal, spongiform pustules (of Kogoj) and intracorneal aggregates of neutrophils (Munro microabscesses). (Left x10, right x20) [91].

Figure 1.1.6 Pustular psoriasis can present as generalised or localised disease

(a) Generalised pustular psoriasis, showing widespread lakes of pustules on a background of diffuse erythema. (b) Localised, palmar pustules and scales in palmoplantar pustulosis. (c) Acrodermatitis continua of Hallopeau with pustules and scales limited to the distal fingers and onychodystrophy [92]–[94].

1.1.3.2. Genetic basis of disease

Pustular psoriasis has a distinct genetic architecture to plaque psoriasis, which is underscored by a lack of association with the *PSORS1* locus [95]. Indeed, the severity and rarity of the clinical phenotype indicate that pustular psoriasis could be a monogenic disease. This was confirmed with the advent of next-generation sequencing technologies, which enabled the identification of 3 disease genes: *IL36RN*, *AP1S3* and *CARD14*.

Linkage studies of consanguineous pedigrees and exome sequencing of unrelated GPP patients identified autosomal recessive loss of function mutations in *IL36RN* [96], [97]. As discussed in more detail in section 1.2.3, *IL36RN* encodes the IL-36 receptor antagonist (IL-36Ra), which modulates the activity of the IL-1 family cytokines IL-36α, -β and -γ. Thus, patients harbouring *IL36RN* mutations exhibit uncontrolled IL-36 signalling, leading to excessive IL-1β, IL-8 and IL-6 production by peripheral blood mononuclear cells (PBMCs) [97], [98].

The screening of expanded patient resources has now identified a spectrum of *IL36RN* mutations that are distributed throughout the length of the protein and are associated with pustular psoriasis in a variety of populations (Table 1.4). Although recessive *IL36RN* alleles are typically observed in patients presenting with a severe clinical phenotype (early-onset GPP characterised by a high risk of systemic involvement) [99], deleterious *IL36RN* variants have also been associated with localised pustular disease [100]. Contrary to the expectations for a recessive condition, individuals harbouring a single *IL36RN* mutation are occasionally affected, even though they classically present with disease at a later age [99].

Taken together, the above observations suggest that the genetic architecture of pustular psoriasis is more complex than originally anticipated, with evidence for variable penetrance of disease alleles and a potential role for genetic modifiers and environmental factors.

Table 1.4 *IL36RN* mutations associated with pustular psoriasis

***IL36RN* mutation**	**Country where mutation was first detected**	**Phenotype**	**Reference**
R10X, c.28C>T	Japan	GPP	[101]
L21P, c.62C>T	Pakistan	GPP	[102]
L27P, c.80T>C	Tunisia	GPP	[96]
H32R, c.95A>G	Iraq	GPP	[103]
K35R, c.104A>G	UK	GPP	[100]
c.115+6T>C	Japan	GPP	[104]
I42N, c.125T>A	Japan	GPP	[105]
N47S, c.140A>G	China	GPP	[90]
R48W, c.142C>T	UK	GPP	[97]
P76L, c.227C>T	Germany	GPP	[103]
E94X, c.280G>T	Germany	GPP	[103]
R102W, c.304C>T	UK	GPP, ACH	[100]
R102Q, c.305G>A	China	GPP	[90]
E112K, c.334G>A	Japan	GPP	[106]
S113L, c.338C>T	UK	GPP, ACH, PPP	[97]
T123R, c.368C>G	Japan	GPP	[104]
T123M, c.368C>T	Japan	GPP	[107]

GPP, Generalised pustular psoriasis; ACH, Acrodermatitis continua of Hallopeau; PPP, Palmoplantar pustulosis.

Since *IL36RN* mutations are only found in a minority (~25%) of pustular psoriasis cases [99], exome sequencing was undertaken to gain a better understanding of the genetic basis of the disease. This uncovered two recurring founder mutations in the *AP1S3* gene (p.Phe4Cys and p.Arg33Trp). While these defects accounted for 12% of pustular psoriasis cases of European descent, no *AP1S3* mutations were found in Asian patients [108].

AP1S3 encodes the σ1 subunit of AP-1, an evolutionarily conserved hetero-tetramer that facilitates clathrin-mediated vesicular transport of proteins such as TLR-3 between the trans-Golgi network and endosomes [109]. AP-1 has also been implicated in the formation of autophagosomes. These are the specialised vesicles that mediate autophagy, an intracellular degradation pathway for misfolded proteins and damaged organelles [110]. Interestingly, autophagy has been shown to regulate cutaneous immune responses [111], [112], however the specific mechanisms whereby *AP1S3* mutations contribute to the pathogenesis of pustular psoriasis are yet to be defined.

Caspase recruitment domain family member 14 (*CARD14*) was recently confirmed as a third disease gene for GPP [29]. *CARD14* is highly expressed in keratinocytes and encodes a scaffold protein that, upon oligomerisation, mediates TRAF-2 dependent activation of NF-κB signalling. A deleterious gain of function p.Asp176His substitution in *CARD14* has been associated with GPP in an extended case series and shown to cause spontaneous CARD14 oligomerisation *in-vitro* [29]. The same variant was also found in 2 patients with PPP [113], which provides further evidence for an overlap in the genetic basis of generalised and localised forms of pustular psoriasis. Furthermore, given that gain of function *CARD14* mutations have also been detected in cases of familial plaque psoriasis [27], [28], shared aetiological mechanisms may be present in plaque and pustular subtypes of disease.

1.1.3.3. Immunopathogenesis

The rarity of pustular psoriasis and consequent limited access to patient samples has historically hindered the investigation of pathogenic pathways. The only transcriptional profiling study undertaken to date confirmed a predominance of innate immune transcripts in GPP skin, which is in keeping with the autoinflammatory nature of disease [114]. Specifically, the study documented high expression of IL-1 and IL-36 cytokines, neutrophil chemokines (IL-8, CXCL1 and CXCL2) and neutrophil-derived proteases (e.g. elastase and cathepsin G), which can process IL-36 precursors into mature cytokines [115]. This suggests that keratinocytes activated by IL-36 and IL-1 produce chemokines that drive cutaneous neutrophil influx, which results in the pustular skin phenotype.

The molecular events that cause systemic inflammation in GPP are mostly unexplored. However, insights into potential disease mechanisms may be gained from studies of other autoinflammatory conditions with neutrophilic skin involvement. These disorders are typically mediated by excessive production of IL-1β, a potent pyrogen that also promotes neutrophil recruitment and keratinocyte activation.

An important example is the deficiency of the IL-1 receptor antagonist (DIRA), in which unopposed IL-1 signalling due to recessive *IL1RN* mutations leads to neonatal-onset pustular psoriasis, osteomyelitis, periosteitis and leukocytosis [116]. Likewise, cryopyrin-associated periodic syndromes (CAPS) are caused by autosomal dominant *NLRP3* mutations, which result in constitutive activation of the inflammasome, the multiprotein complex that cleaves pro-IL-1β into a mature cytokine [117]. The ensuing IL-1β over-production results in recurrent episodes of fever and neutrophilic skin inflammation.

Although predominantly expressed by blood monocytes, NLRP1, NLRP3 and AIM2 inflammasomes have been detected in keratinocytes, which are a major source of IL-1β in inflamed skin [118]–[120]. Thus, abnormal inflammasome activation may contribute to the pathology of GPP, given the prominent role of IL-1 cytokines in the modulation of the neutrophil/keratinocyte axis.

1.1.3.4. Therapies

The conventional systemic agents used for the treatment of plaque psoriasis are often ineffective in pustular phenotypes, possibly reflecting a prominent role of innate immune responses in this rarer disease subtype. There is also a paucity of robust clinical trial data, such that current guidelines for pustular psoriasis therapy are mostly based on isolated case reports [121].

First line therapies for GPP are acitretin, methotrexate, cyclosporine and infliximab. The latter agent has particularly rapid effects, with reported attenuation of fever and skin pustules only 2 days after infusion. This may be attributable to the interruption of feedback loops between IL-36 and TNFα. Biologics antagonising IL-17A have also shown promising efficacy in GPP, however the trials undertaken to date were open label and involved only small numbers of patients with no placebo arm, thus limiting interpretation of the results [122], [123].

Given the similar presentation to other autoinflammatory syndromes, IL-1 blockers have been used for the treatment of GPP [124], [125]. The recombinant IL-1 receptor antagonist anakinra initially caused rapid clinical improvements, however full disease remission was seldom achieved. This incomplete response supports the notion that IL-1 itself is not the dominant disease driver, but is part of positive regulatory feedback loops driven by IL-36 [126].

First line therapies for localised pustular psoriasis include topical corticosteroids and psoralen/UVA photochemotherapy (PUVA). Systemic therapies such as cyclosporine and retinoids are used when multiple digits/nails are involved. Although TNFα antagonists can induce worsening or de novo onset of palmoplantar pustular psoriasis, there are several reports of successful treatment in ACH [127], [128]. Finally, data regarding the efficacy of ustekinumab in localised pustular psoriasis is conflicting [92], [129], and attention has now shifted onto IL-1 blockers, with a multi-centre double-blind randomised controlled trial currently underway [130]. Nevertheless, overall, therapeutic options in pustular psoriasis are disappointingly limited and there is a substantial unmet need for effective treatments [121].

Taken together, there are striking differences between plaque and pustular subtypes of psoriasis, namely the cardinal clinical features and genetic architectures [131]. Interestingly, however, the two diseases often co-exist in patients, with the same cytokines (e.g. IL-36 and IL-17) showing an up-regulation in plaque and pustular lesions. Thus there may be common molecular mechanisms at play that, once elucidated, will open avenues for novel, unifying and potentially more efficacious therapies for these two debilitating conditions.

1.2. The interleukin-36 family

1.2.1. Overview of the IL-36 family

The IL-36 cytokines were originally identified through database searches for IL-1 homologues [132]. As the functional properties of these molecules began to emerge, it became apparent that this IL-1 subfamily consists of three agonistic ligands, known as IL-36α (initially labelled as IL-1F6), IL-36β (IL-1F8) and IL-36γ (IL-1F9). The fourth member, called IL-36Ra (IL-1F5), is a receptor antagonist (Table 1.5). All four proteins bind a common heterodimeric receptor, consisting of a signalling subunit (IL-36R, also called IL-1Rrp2 and encoded by the *IL1RL2* gene) and an accessory protein (IL-1RAcP, encoded by *IL1RAP*). The latter is shared with the receptors for IL-33 and IL-1α/β.

Table 1.5 The IL-36 family cytokines

Protein (*gene*)	Previous nomenclature	Homology to IL-1Ra	Homology to IL-1β
IL-36Ra (*IL36RN*)	IL-1F5	47-52%	26%
IL-36α (*IL36A*)	IL-1F6	24%	30%
IL-36β (*IL36B*)	IL-1F8	27%	31%
IL-36γ (*IL36G*)	IL-1F9	20%	31%

IL-1Ra, IL-1 receptor antagonist. Adapted from [133].

1.2.2. Expression and processing of IL-36 cytokines

IL-36 cytokines are encoded by a cluster of genes on chromosome 2q14 and are produced by several epithelial tissues, such as the skin, gut and lung [134]. Immune cells, including dendritic cells, Langerhans cells, monocytes/macrophages and T cell subsets, can also secrete these molecules.

In the skin, keratinocytes are the main IL-36 producers. Even though *IL36A, IL36B* and *IL36G* transcripts are readily detectable under basal conditions, cytokine expression can be up-regulated by IL-17A, TNFα, IL-1α and IL-36 itself [135], [136]. Release of IL-36γ by keratinocytes has also been demonstrated following necrotic cell death, in response to the viral double stranded RNA (dsRNA) analogue polyinosinic:polycytidylic acid (poly(I:C)) and upon exposure to LL37 [137], [138]. IL-36 may thus act as an important damage-associated molecular pattern (DAMP) in mediating the immune response to cutaneous infection and wounding.

Similar to other IL-1 family proteins, IL-36 cytokines are expressed as inactive precursors and require post-translational N-terminal cleavage by proteases to become bioactive [139]. The cysteine protease cathepsin S was recently found to activate IL-36γ [140]. Since this enzyme is expressed by keratinocytes and fibroblasts, and is up-regulated in psoriasis skin, it may represent an important regulator of IL-36 driven cutaneous inflammation. Further studies have shown that the neutrophil-derived proteases cathepsin G, elastase and proteinase-3 can differentially cleave IL-36α, -β, -γ and IL-36Ra in order to increase their biological activity [141]–[143]. The activation of IL-36 cytokines is thus likely to be regulated by complex cross-talk between immune cells and the epithelial barrier.

1.2.3. IL-36 receptor signal transduction

The IL-36 receptor actively traffics between the plasma membrane and endosomes of IL-36 target cells [144]. Following engagement with IL-36α, -β or -γ, IL-36R dimerises with IL-1RAcP, an event which stabilises agonist binding. Intracellular Toll/IL-1 receptor (TIR) domains then recruit the MyD88 adaptor protein, followed by interleukin-1 receptor-associated kinase (IRAK) -1 and -2. This leads to the activation of mitogen-activated protein kinase (MAPK) and NF-κB [145] (Figure 1.2.1). Downstream signalling induces the production of innate immune cytokines (e.g. IL-6 and IL-8) [145], chemokines (CCL3, CCL4, CCL20) [146], anti-microbial peptides (e.g. hBD2, CAMP/LL37) and matrix metalloproteinases [147].

Real-time PCR analyses of *in-vitro* stimulated keratinocytes further demonstrated that IL-36 cytokines synergise with IL-17A and TNFα to induce their own expression and that of other pro-inflammatory cytokines implicated in psoriasis pathogenesis (e.g. TNFα) [135]. However, most of the above studies were based on the use of unprocessed molecules with minimal biological activity, which substantially limited the power to detect the effects of IL-36 stimulation. Moreover, the differences and overlap between the genes induced by IL-36α, -β and -γ (which share between 45% and 57% homology at the amino acid level [148]) have not been investigated.

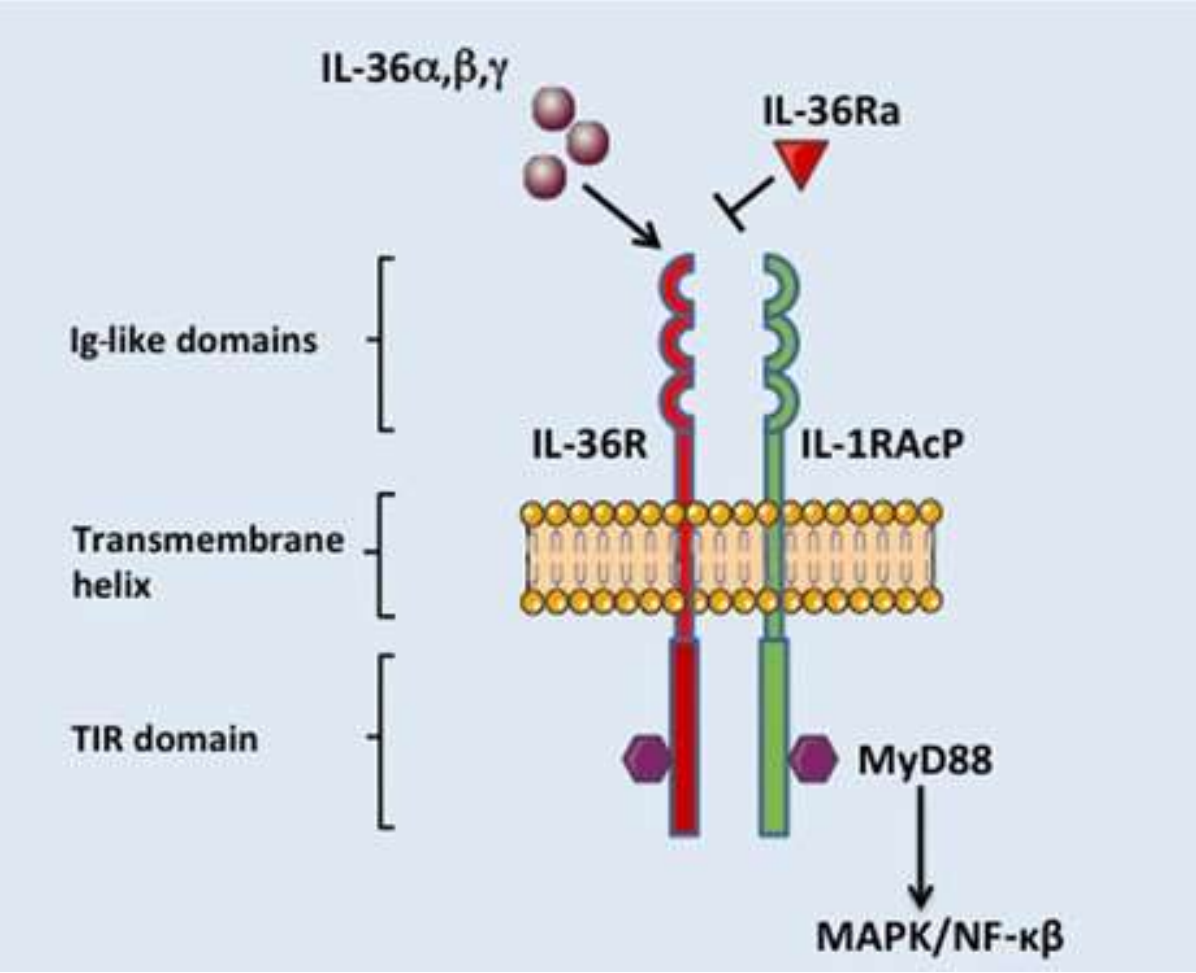

Figure 1.2.1 The interleukin-36 receptor

Binding of IL-36 agonists to IL-36R induces recruitment of the co-receptor IL-1RAcP. The TIR domains found in both receptor subunits bind to the MyD88 adaptor protein, which initiates MAPK and NF-κB intracellular signalling cascades, resulting in pro-inflammatory gene expression. IL-36Ra also binds to IL-36R, however this fails to trigger the recruitment of IL-1RAcP, thus leading to inhibition of signalling [149].

In contrast to IL-36 agonists, IL-36Ra binds to IL-36R but blocks the recruitment of IL-1RAcP [139], thus exerting an antagonistic activity which modulates IL-36 signalling. In this context, the *IL36RN* mutations observed in GPP patients disrupt IL-36Ra activity, causing uncontrolled IL-36 signalling. Conversely, loss of function IL-36R variants, such as the A471T allele found in 2% of the world population, disrupt the interaction with IL-1RAcP and cause a substantial reduction in IL-36 driven NF-κB activation [150]. While these observations were made *in-vitro*, the low frequency of the A471T variant has prevented a phenotypic dissection of its effects in homozygous individuals.

1.2.4. Role of IL-36 in normal immune function

As innate immune mediators, IL-1 family cytokines help the host to eliminate pathogenic microbes that invade epithelial barriers such as the skin and lung. In particular, IL-36 cytokines have been implicated in the defence against the ubiquitous fungal pathogens *Aspergillus fumigatus* and *Candida albicans* [151], [152]. In fact, human PBMCs exposed to *Aspergillus* up-regulate IL-36γ production via TLR-4 and dectin-1 dependent pathways [151].

Importantly, Th1 and T17 anti-fungal responses were shown to be dependent on IL-36R signalling, such that IL-36Ra treatment reduced *Aspergillus*-induced IL-17 and IFNγ production. IL-36Ra also inhibited *Candida*-induced T17 activation, causing decreased IL-17 and IL-22 production [152]. Since the role of IL-17 signalling in anti-fungal defences is well established [153], these studies support the notion that IL-36 cytokines prime T cells and modulate the IL-23/T17 axis.

The role of IL-36 in Th1-mediated responses against intracellular bacteria has also been investigated. *Ex-vivo* stimulated splenocytes from IL-36R deficient mice infected with *Mycobacterium bovis*

Bacillus Calmette-Guérin (BCG) demonstrated reduced production of IFNγ, TNFα and IL-6, compared to wild type littermates [154]. The pulmonary lesions of IL-36R deficient mice were also more extensive than those of wild type animals, indicating that IL-36-mediated immune responses protect from damage induced by BCG infection. While these observations suggest that a lack of IL-36 signalling causes a deficiency of antigen-specific Th1 cell activation, a subsequent study showed that the increased lung pathology in the knockout mice was only transient and there was no overall reduction in bacterial clearance or survival compared with wild type littermates [155].

Although studies of human cells are scarce, recent *in-vitro* findings support a role of IL-36 in immunity to tuberculosis. In fact, *Mycobacterium tuberculosis* can induce IL-36γ production in human macrophages, by activating TLR2/4-MyD88 signalling. IL-36γ was in turn shown to up-regulate antimicrobial peptides such as CAMP/LL37 and hBD2 [156]. Further, *M. tuberculosis* growth inhibition was observed in control but not in *IL36R* deficient macrophages. IL-36 may thus have direct innate effects on intracellular pathogens such as *M. tuberculosis*, in addition to its indirect action mediated by the adaptive modulation of DC-driven T cell responses.

The accumulating evidence for a role of IL-36 in the defence against fungi and mycobacteria has provided valuable insights into the physiological function of this cytokine family. While these molecules have likely evolved to maintain health through such activity, dysregulated IL-36 signalling has increasingly been implicated in the development of inflammatory diseases including psoriasis.

1.2.5. Role of IL-36 in disease

1.2.5.1. Skin disease: psoriasis

Several lines of evidence support a role for IL-36 in the pathogenesis of psoriasis. Overexpression of the IL-36 agonists (in particular IL-36α and IL-36γ) has consistently been demonstrated in the lesions of patients with plaque psoriasis [60], [135], [147], [157]–[159] (Table 1.6). Indeed, IL-36γ was tentatively proposed as a biomarker of psoriasis severity, since serum levels correlated with disease activity (PASI) in a pilot study [159].

Table 1.6 IL-36 cytokines upregulated in human psoriasis skin

Study	*IL36A*	*IL36B*	*IL36G*
Johnston *et al* [147]	√	√	√√
Carrier *et al* [135]	√	√	√√
Keermann *et al* [158]	√	√	√√
D'Erme *et al* [159]	n/a	n/a	√√
Boutet *et al* [157]	√		√√
Quaranta *et al* [60]	√		√√

'√' indicates overexpression was detected in psoriasis skin lesions

'√√' indicates the most over-expressed IL-36 cytokine in each study

n/a indicates that the cytokine was not analysed in the study

Microarray analysis of lesional skin also revealed a significant up-regulation of *IL1RL2* (the gene encoding the signalling subunit of the IL-36 receptor) in severe versus mild psoriasis, further supporting a pathogenic role for abnormal IL-36R signalling [160]. This finding was underscored by the recent discovery of a novel psoriasis susceptibility locus that spans the *IL1RL2* gene [37].

Insights obtained in mouse models have substantiated the above findings. For instance, transgenic mice overexpressing *Il36a* in basal keratinocytes developed transient psoriasiform skin changes [161]. These clinical features were exacerbated when the animals were crossed with *Il36rn* deficient mice and abrogated on a background of *Il1rl2* or *Il1rap* deficiency. Thus, the inflammatory phenotype was dependent on IL-36R signalling.

A pathogenic role for IL-36 has also been demonstrated in imiquimod-induced psoriasiform dermatitis, a widely-used mouse model of psoriasis. In this experimental system, *Il36r* knockout mice were protected from the onset of skin inflammation, since they failed to expand T17 cells upon treatment with imiquimod [162]. Interestingly, these mice showed greater protection from disease compared with IL-23 and IL-17 deficient animals. In contrast, IL-36Ra deficient mice had exacerbated imiquimod-mediated psoriasiform dermatitis.

In keeping with the above observations, it has been shown that murine myeloid dendritic cells express IL-36R and respond to IL-36 stimulation by upregulating pro-inflammatory cytokines (e.g. IL-23, IL-12, IL-1β), co-stimulatory molecules (e.g. CD80, CD86) and MHC class II antigens [163], which collectively drive T17 and Th1 responses. In an independent study, IL-36 was also shown to directly activate murine CD4+ T lymphocytes and promote their differentiation into Th1 cells, in synergy with IL-12 [154].

The stimulatory effect of IL-36 cytokines was confirmed in human monocyte-derived DCs, with evidence of increased expression of HLA-DR, co-stimulatory molecules (CD40, CD83, CD80) and Th1-polarising cytokines (IL-12, IL-18) [164]. Further, human dendritic cells express *IL1RL2* (albeit at lower levels than keratinocytes), such that IL-36 treated DCs cause increased proliferation of allogeneic T cells in co-cultures [146], [165].

In contrast to the results obtained in murine studies, *IL1RL2* expression was not detected in circulating human T cells, which proved unresponsive to direct IL-36 stimulation [146], [165]. Skin-resident T cells, however, have not been analysed, so it is unclear whether they express *IL1RL2* and respond to IL-36.

Based on the above observations, it is becoming increasingly clear that IL-36 mediated cross-talk between DCs and epithelial cells may drive T cell-dependent inflammatory responses in psoriasis (Figure 1.2.2). The current understanding is that IL-36 molecules released from keratinocytes after trauma or infection may promote DC-driven T17 and Th1 activation. The T cell cytokines thus secreted (e.g. IL-17, TNFα) can feedback to up-regulate IL-36 production by keratinocytes. IL-36 then acts in an autocrine and paracrine manner to induce chemokines that attract further immune cells to sites of inflammation. Of note, IL-36γ can also increase the expression of adhesion molecules (ICAM-1, VCAM-1) and chemokines (e.g. CCL20) in dermal microvascular endothelial cells, where it contributes to T cell recruitment [166]. This IL-36 mediated interplay between endothelial and immune cells further emphasises potential mechanisms whereby IL-36 may be important in directing skin immune responses.

While the discovery of *IL36RN* mutations in GPP implicated abnormal IL-36 signalling in the pathogenesis of pustular psoriasis [96], [97], the data summarised above suggest that IL-36 could also contribute to the development of common plaque psoriasis. The potential role of IL-36 as a shared disease driver in rare and common subtypes of psoriasis thus requires further investigation.

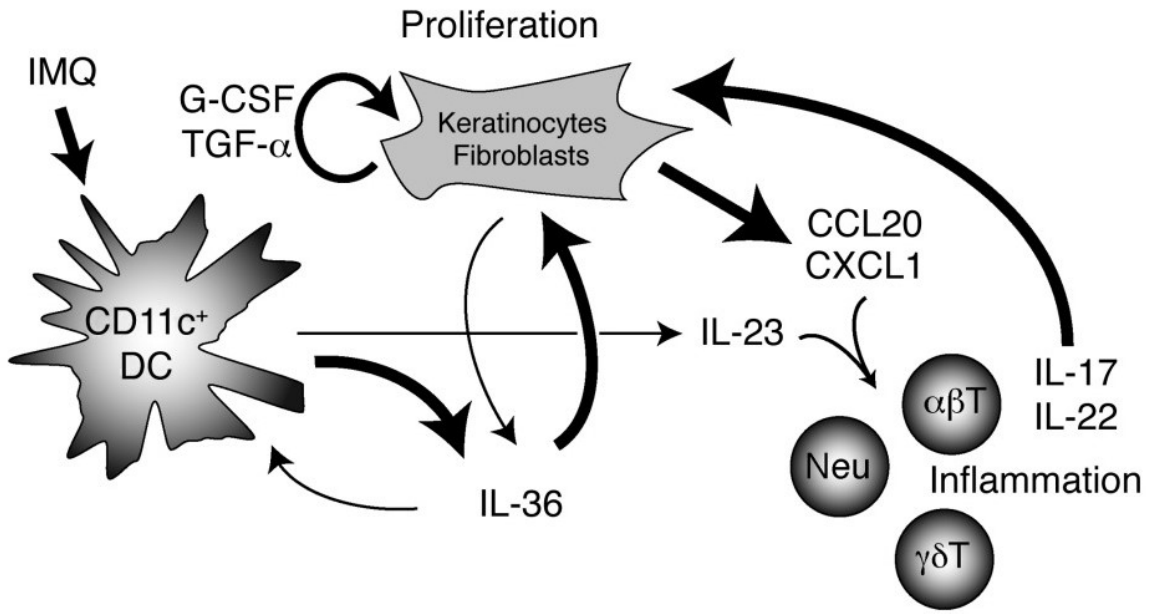

Figure 1.2.2 IL-36 mediated dendritic cell-keratinocyte crosstalk contributes to cutaneous inflammatory responses

Environmental triggers (e.g. the TLR-7 agonist imiquimod (IMQ)) cause the activation of dendritic cells (DC) and keratinocytes, leading to the release of IL-36. This enhances DC and keratinocyte inflammatory responses in an autocrine and paracrine fashion, resulting in the recruitment (via CCL20) and differentiation (via IL-23) of resident T lymphocyte populations into T17 cells. Cytokines produced by T17 effectors potently stimulate keratinocyte activation and proliferation, resulting in further IL-36 production and propagation of skin inflammation [162].

1.2.5.2. Beyond skin

Since IL-36 cytokines are predominantly expressed by epithelial cells [167], research efforts are underway to determine whether these molecules are implicated in the inflammation of other barrier surfaces such as the gut and lung.

Given the similar elevation of IL-36 in lesional psoriasis and ulcerative colitis (UC) [168]–[170], the correlation of cytokine levels with UC severity [170], and the presence of the disease in many psoriatic patients [171], a pro-inflammatory role of IL-36 was expected in UC, and has indeed been described [168], [169].

IL-36 stimulation of human intestinal epithelial cells was shown to upregulate chemokine expression, via MyD88-dependent MAPK and NF-κB signalling [168]. This finding was supported by the analysis of a murine model of acute colitis, in which *Il36r*$^{-/-}$ mice showed decreased disease severity and reduced infiltration of inflammatory cells in the colonic mucosa, compared with wild type controls [169].

An interesting function of IL-36 in the resolution of gut epithelial damage is also emerging [170], [172], as mucosal wound healing was found to be impaired in the absence of a functional IL-36R [172]. In fact, MyD88 dependent IL-36R signalling can promote the resolution of intestinal damage by inducing the production of chemokines (e.g. CXCL1, CCL20) by colonic fibroblasts and the proliferation of intestinal epithelial cells [170]. These observations suggest that IL-36R signalling may be involved in the restoration of epithelial integrity in other tissues. This would have important

implications for the safety of any therapeutics designed to block IL-36 activity in inflammatory diseases.

IL-36 has also been implicated in airway inflammation since elevated IL-36γ levels were detected in primary bronchial epithelial cells from asthma patients versus controls. This IL-36 over-production was further increased after rhinovirus infection, which is a common cause of asthma exacerbations [173]. IL-36γ was subsequently shown to induce MAPK and NF-κB mediated up-regulation of chemokines (e.g. IL-8 and CCL20) in lung fibroblasts [174].

Similar to keratinocytes, bronchial epithelial cells can up-regulate IL-36 cytokines in response to stimulation by dsRNA, IL-17, TNFα and IL-1β. Thus IL-36 may amplify T17 and Th1 responses to viral triggers in lung epithelium, leading to the development of airway inflammation. This hypothesis is supported by data from mouse models, in which intra-tracheal IL-36α administration was shown to promote neutrophil recruitment via the upregulation of CXCL1 and CXCL2 [175]. Increased levels of IL-36γ were also found in the lungs of asthma susceptible A/J mice [176].

The role of IL-36 has additionally been investigated in diseases that are co-morbid with psoriasis. Although levels of IL-36α were found to be upregulated in synovial tissue from patients with psoriatic or rheumatoid arthritis [177], the evidence implicating IL-36 cytokines in the pathogenesis of inflammatory joint disease is not compelling. When all IL-36R ligands were analysed, only a subset of patients with rheumatoid arthritis had elevated agonist/antagonist ratios in synovial tissue [157], and joint disease severity in mouse models was shown to be independent of IL-36 receptor signalling [178], [179].

IL-36 may, however, play a role in obesity, which is potentially relevant to the observed association of increased adiposity and psoriasis [180]. Adipocytes upregulated IL-6 and IL-8 in response to IL-36 stimulation and downregulated PPARγ expression, indicating a reduction in cell differentiation [181].

Overall, IL-36 signalling may contribute to the pathogenesis of several inflammatory diseases, at least in part by promoting the activation of T17 cell responses. While mechanistic studies highlight IL-36 cytokines as key mediators of cross-talk between epithelial and immune cells in disease states, a role for these molecules in host immune responses to fungi and mycobacteria has also emerged. These dichotomous functions of IL-36 in maintaining health and propagating disease require further characterisation before research can create new opportunities for therapeutic intervention and thus realise its full translational potential.

1.3. The role of human gene knockouts in the discovery and validation of novel drug targets

1.3.1. Current challenges in drug discovery and development

Despite the success of biologic agents for the treatment of psoriasis, there is still an unmet need for new therapies, which reflects the challenges faced by the broader medical community. In fact, there is a well-documented gap between the efficacy of biologics in clinical trials and their effectiveness in real-world settings (i.e. the 'efficacy-effectiveness gap') [86], [182]. At the same time, the success of the pharmaceutical industry in producing new treatments has been steadily declining over recent years, despite rising investments [183].

The current drug discovery pipeline spans on average 15 years and costs over US$1 billion per new therapeutic agent (Figure 1.3.1) [184], [185]. The process starts with *in-vitro* target identification and pre-clinical studies in animal models, which determine whether the drug should be tested in humans. Subsequent clinical trials are implemented in 3 phases (Figure 1.3.1). Phase I evaluates safety and dose ranges, by assessing toxicity, pharmacodynamics and pharmacokinetics in small groups of healthy volunteers [186]. Phase II studies seek to demonstrate effectiveness in a relatively small number of affected individuals, while phase III trials assess drug safety and efficacy in larger patient cohorts.

Expenditure is dominated by the drug development programmes that are terminated during the clinical trial phase. In fact, more than 90% of the drugs entering clinical studies fail to demonstrate sufficient safety and efficacy to ultimately gain regulatory approval, which highlights the limitations of current pre-clinical disease models [187]. These are based on *in-vitro* (e.g. cell cultures) and *in-*

vivo (e.g. mouse models) experimental systems, which are limited by their biological simplicity and direct relevance to humans, respectively. In this context, the advent of next generation sequencing has opened a new avenue for pre-clinical drug development, which involves the study of human mutations affecting the function of drug targets.

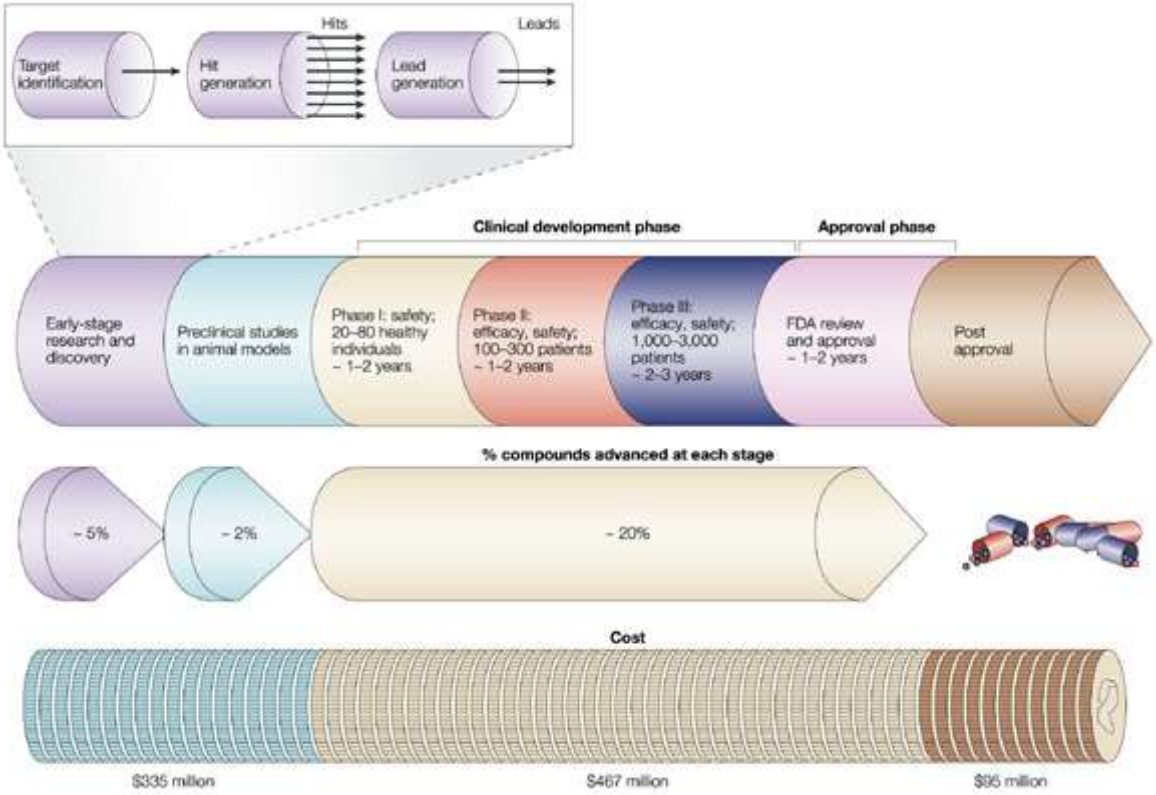

Figure 1.3.1 Pipeline for drug discovery and development

A new drug must pass through discovery, pre-clinical and clinical study phases, which is a costly process that may take several years. Early in the pipeline, compounds that are active against validated targets ('hits') and with desirable drug-like biological properties ('leads'), are tested in pre-clinical studies. Since thousands of compounds are studied before one successfully gains regulatory approval for therapeutic use in patients, the early identification of potential failures is highly desirable [188].

1.3.2. Advantages of studying human knockouts

A 'human knockout' is an individual who harbours bi-allelic mutations that disrupt the function of a particular gene. Such loss of function (LoF) mutations include nonsense variants, frameshift insertions/deletions, splice-site changes and deleterious missense substitutions [189].

Despite limited power to detect rare alleles, whole genome sequencing of 185 individuals from the 1000 Genome Project (encompassing African, Caucasian and East Asian subjects) showed that the average person carries approximately 100 LoF variants, with 20 present in a homozygous state [190]. Although not causing disease, these changes may still impact on phenotypic variation, hence the characterisation of their effects could deliver valuable *'in-vivo*' insights on gene function. Further, if the mutated gene encodes a drug target, then the phenotype of the human knockout will likely re-capitulate the effects of pharmaceutical blockade, which may inform the pre-clinical assessment of novel medications.

1.3.2.1. Insights from phenotyping human knockouts

There are numerous examples illustrating how the study of naturally occurring LoF variants can benefit drug discovery and development. In particular, the landmark study of human *PCSK9* knockouts underscores the translational potential of this research (Figure 1.3.2) [191].

PCSK9 encodes proprotein convertase subtilisin/kexin type 9, an enzyme which modulates lipid homeostasis by mediating the degradation of cell surface low-density lipoprotein (LDL) receptors [192]. In 2003, Abifadel et al demonstrated that gain of function *PCSK9* mutations increased plasma LDL cholesterol levels and caused familial hypercholesterolaemia [193]. Loss of function mutations

with the opposite effect on LDL were subsequently discovered in the Dallas Heart Study, a multi-ethnic population-based longitudinal study. Healthy individuals with rare LoF *PCSK9* mutations had markedly reduced LDL levels and an associated lower risk of cardiovascular disease [191]. These observations prompted the development of PCSK9 blockers, which inhibit the degradation of LDL receptors on the surface of hepatocytes, thus improving the clearance of circulating LDL. After impressive clinical trial results, showing up to 60% reduction in serum LDL levels, PCSK9 inhibitors have recently been FDA-approved for the treatment of hypercholesterolaemia and are amongst the most promising cholesterol-lowering agents since the discovery of statins [194].

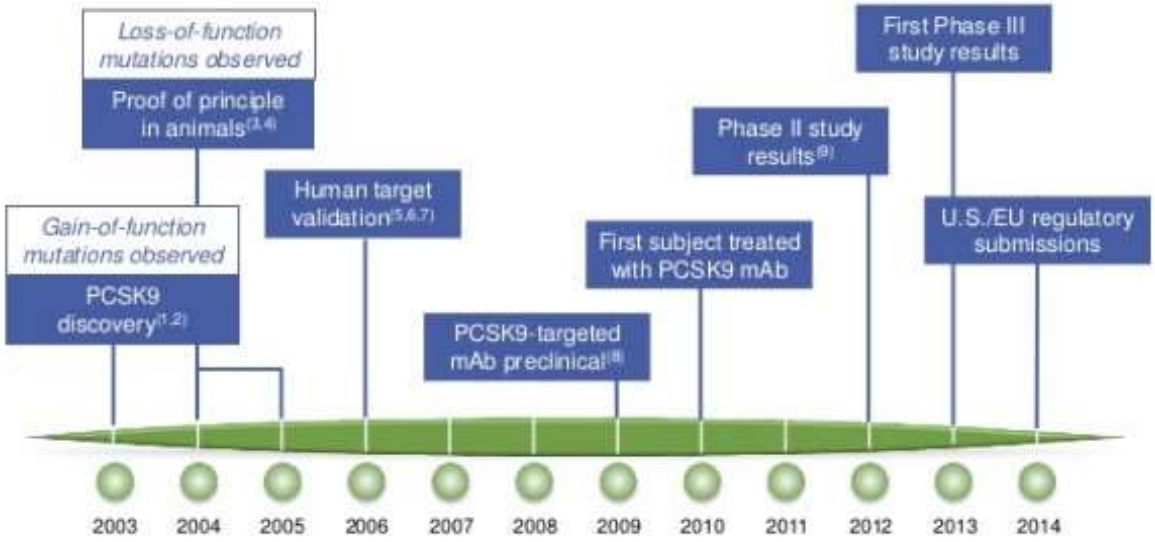

Figure 1.3.2 Timeline for PCSK9 inhibitor development

The phenotype of human *PCSK9* knockouts, which recapitulated the effect of PCSK9 blockade, was critical in the validation of PCSK9 as a novel drug target for hypercholesterolaemia, and expedited the path to clinical trials of anti-PCSK9 monoclonal antibodies (mAb) [195].

Similar therapeutic opportunities were identified from healthy individuals harbouring homozygous LoF alleles in *CCR5* (encoding C-C chemokine receptor 5) who failed to contract HIV despite multiple exposures to the virus [196]. The importance of CCR5 in mediating viral entry in immune cells was subsequently highlighted by a case report of a HIV-infected patient who was cured after receiving a bone marrow transplant from a *CCR5* knockout donor [197]. These findings paved the way for the development of therapeutic CCR5 antagonists, which have now received regulatory approval and form part of a new category of 'entry inhibitor' drugs for HIV [198].

The development of PCSK9 and CCR5 inhibitors are unlikely to be isolated success stories, given the recent identification of other naturally-occurring knockouts with broad-reaching therapeutic relevance (Table 1.7).

This potential was highlighted in a recent large-scale study, which uncovered a dose-dependent relationship between the mutation status of *PLA2G7* and the enzymatic activity of its gene product, lipoprotein-associated phospholipase A2 (Lp-PLA2). Despite prior evidence for a positive correlation between Lp-PLA2 levels and coronary artery disease [199], carriers of LoF *PLA2G7* alleles did not show a reduction in cardiovascular risk [200]. The authors of the study argued that this could have predicted the recent failure of Lp-PLA2 inhibitors in clinical trials, [201], [202], thus highlighting the utility of genetic studies in validating therapeutic targets, prior to major investment in drug development.

Table 1.7 Human knockouts associated with beneficial phenotypic consequences

Gene	Function of protein	Phenotype of human knockout
PCSK9	Enzyme mediating LDL cholesterol receptor degradation	Reduction in plasma LDL levels and risk of cardiovascular disease [191]
CCR5	Cell surface co-receptor, which acts synergistically with CD4 to enable HIV entry into T cells	Protection against HIV infection [196]
LPA	Lipoprotein A; transport of cholesterol and oxidised phospholipids [203]	Reduction in plasma lipoprotein A levels and risk of cardiovascular disease [204]
CASP12	Immune response to bacterial sepsis	Resistance to severe sepsis [205]
ACTN3	Regulator of calcineurin activity in skeletal muscle [206]	Reduced sprinting power and enhanced endurance capacity [207]
APOC3	Regulates clearance of lipoprotein metabolites and inhibits lipoprotein lipase	Reduction of plasma triglycerides and risk of cardiovascular disease. Lower rise in plasma triglycerides after an oral fat challenge. [200], [208], [209]

1.3.2.2. Strategies for the discovery of human knockouts

Although the study of human knockouts holds great promise for drug development, the identification of individuals harbouring relevant homozygous LoF alleles is challenging and requires large sample sizes. The Exome Aggregation Consortium (ExAC) recently collated more than 60,000 exomes from a wide range of population-based studies, and detected an average of 35 (mostly common) homozygous protein truncating variants per individual [210]. Some datasets were found to be more advantageous for the discovery of knockouts, since rare, homozygous LoF mutations were enriched in founder populations and in South Asian cohorts with high rates of parental relatedness (Figure 1.3.3).

Individuals from founder populations share extensive genomic portions that are identical by descent, due to inheritance from a common ancestor. The recent exome sequencing of 100,000 Icelander and 30,000 Finnish individuals have demonstrated how informative such populations can be [204], [211]. Almost 8% of participants from the Icelandic cohort had 1 gene completely knocked out by a rare (minor allele frequency <2%), homozygous LoF variant. Likewise, the average Finn harboured twice as many complete gene knockouts than a non-Finnish European [204], [211]. The sequencing of large bottlenecked populations cohorts thus enabled the discovery of rare LoF variants, in contrast to previous studies, where a smaller sample size [190] or sampling of mixed populations (ExAC, [210]) mostly restricted the analysis to common LoF variation.

Of note, the above studies may have already identified most of the gene knockouts occurring within the relevant populations, as these are limited by the number of LoF alleles originally present in the founders. Thus, attention has recently shifted to South Asian cohorts with high degrees of parental relatedness [200], [212]. In support of this approach, the observed rate of knockout genes was

almost 50 fold higher in the offspring of first cousins than that found in founder populations [212]. In fact, the recent exome sequencing of more than 3,000 British Pakistani individuals (recruited in Bradford and Birmingham) demonstrated that 50% of subjects with first-cousin parents carried a rare deleterious variant [212]. Subsequent research involving 10,000 Pakistani individuals (recruited to the Pakistan Risk of Myocardial Infarction Study, PROMIS) identified >700 genes with homozygous LoF mutations that had not been previously observed [200].

Importantly, the above studies involved the recall and deep phenotyping of individuals with specific LoF alleles [200], [212]. This provided a deeper understanding of the consequences of gene inhibition [213]. Despite the practical and ethical challenges of these 'recall by genotype' approaches (e.g. ensuring an appropriate level of genetic information disclosure during re-contact), such studies are gaining popularity with researchers and have also been welcomed by participants [214], [215]. This represents a paradigm shift in genetics research, away from phenotype-driven genotyping and towards genotype-directed phenotyping.

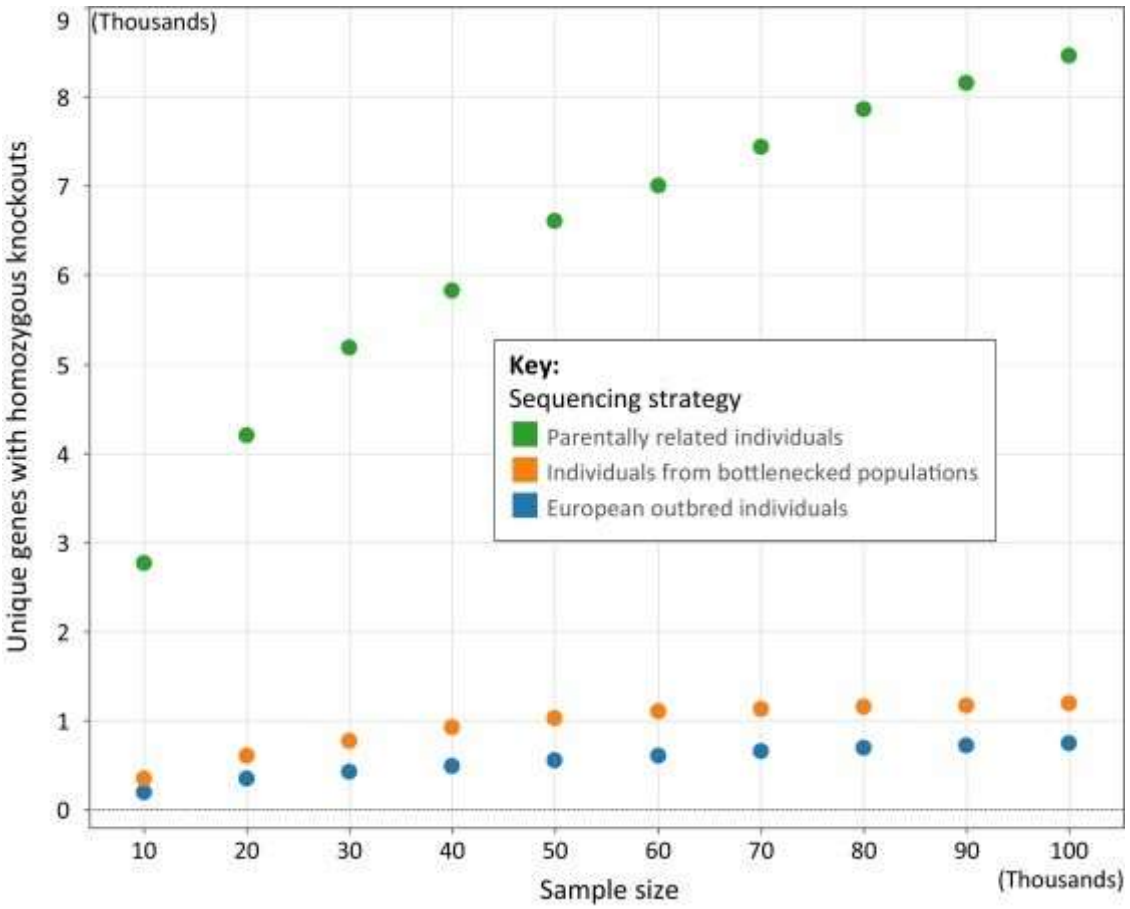

Figure 1.3.3 Human gene knockouts can be discovered in populations with different structures

Sequencing of the offspring of consanguineous unions (green dots) yields higher discovery rates for genes with homozygous loss of function (knockout) variants, compared to the analysis of European outbred (blue) or bottlenecked (orange) populations [216].

A potential limitation of the application of human knockout research to pre-clinical drug discovery is the compensatory mechanisms that could have arisen as a consequence of germline LoF alleles, which may not be present in an individual receiving a drug later in life. Nevertheless, the efficacy and safety data from PCSK9 and CCR5 inhibitors suggest that at least a proportion of human knockouts do accurately recapitulate the effects of pharmacological blockade.

The human knockout research that has so far translated into successful drug development has largely been the result of serendipitous discoveries. In the future, a close collaboration between geneticists, informaticians, clinicians and research participants will be essential to systematically exploit the therapeutic potential of human knockout studies.

1.4 Aims

The aim of this study was to investigate shared aetiological mechanisms in different subtypes of psoriasis, with a particular focus on the role of IL-36 signalling in plaque and pustular forms of the disease.

Thus, the intermediate objectives of the project were:

- To demonstrate that the effects of pustular psoriasis mutations converge on the up-regulation of IL-36 signalling. To prove that *IL36RN* mutations are not the only genetic defects resulting in excessive IL-36 production, the consequences of *AP1S3* disease alleles were investigated. Given that *AP1S3* encodes a subunit of AP-1 [108], an adaptor complex implicated in autophagosome formation [110], it was hypothesised that *AP1S3* mutations could dysregulate IL-36 signalling through the disruption of autophagy. This model was explored in several *in-vitro* experimental systems and in patient keratinocytes.

- To investigate the role of IL-36 signalling in the pathogenesis of common plaque psoriasis. Since the prevalence of plaque psoriasis is increased in pustular psoriasis patients compared to the general population [99], it was next hypothesised that increased IL-36 signalling may also contribute to the development of the common form of the disease. The study thus sought to investigate the presence of an IL-36 signature in lesional skin and to assess the therapeutic potential of IL-36 signalling inhibition, through the analysis of *in-vivo* and *ex-vivo* experimental models.

- To investigate whether therapeutic IL-36 blockade would be safely tolerated. The long-term consequences of IL-36 signalling inhibition were assessed by phenotyping a group of human knockouts bearing homozygous LoF mutations in the IL-36 receptor gene.

This thesis thus integrates model system analyses, transcriptomics and human knockout research to investigate the role of IL-36 as a common disease driver and therapeutic target in pustular and plaque psoriasis.

2. Materials and Methods

2.1. Human subjects

This study was performed in accordance with the declaration of Helsinki after approval by the National Research Ethics Service Committee London - Chelsea (reference 14/LO/2169) and the ethics committees of collaborating institutions. Written informed consent was obtained from all participants. Adult patients with psoriasis were ascertained by trained dermatologists and healthy controls were recruited within King's College London. Additional pustular psoriasis patients screened for *AP1S3* disease alleles (n=85) were recruited from multiple centres across Europe (St John's Institute of Dermatology, London; Birmingham Children's Hospital; University of Manchester; Glasgow Western Infirmary; Our Lady's Children's Hospital, Dublin; University Hospital, Galway; Helsinki University Central Hospital; Radboud University Nijmegen Medical Centre; Hospital Universitari Valld'Hebron, Barcelona; University of Szeged; European Registry of Severe Cutaneous Adverse Reactions), Asia (Hospital Sultanah Aminah, Johor Bahru, Malaysia; National Skin Centre, Singapore) and Australia (Royal Prince Alfred Hospital, Camperdown).

The recall of *IL1RL2* knockouts and access to their medical records was facilitated by the Born in Bradford research team after approval by their executive committee (chaired by Professor John Wright). The human knockouts and ethnically-matched controls were recruited from Bradford Teaching Hospitals NHS Foundation Trust. Full blood counts and serology tests were provided by Viapath, Guy's and St Thomas' Hospitals NHS Foundation Trust.

2.2. Cell culture

All cells were cultured under aseptic conditions, in a laminar flow hood. Cells were grown at 37°C in humidified CO_2/95% air in a NuAire Air-Jacketed Automatic CO_2 Incubator (NU-5500).

2.2.1. CRISPR/Cas-9 genome editing

The protocol described by Ran et al [217] was used by Dr Niovi Setta-Kaffetzi and Mr Lewis Millard (former group members) to generate *AP1S3* knockout cell lines from *in-vitro* spontaneously transformed keratinocytes (HaCaT) and human embryonic kidney (HEK293) cells, maintained in Dulbecco's Modified Eagle Medium (DMEM; Gibco) supplemented with 10% fetal bovine serum (FBS; Biosera) and 1% penicillin-streptomycin (Gibco).

Briefly, CRISPR/Cas-9 guide RNAs were designed with the CRISPR design tool [218] and cloned into a pSpCas9BB-2A-GFP vector (Addgene, #48138), as described elsewhere [217]. The construct was transfected into HEK293 and HaCaT cells using Lipofectamine 2000 (Life Technologies), according to the manufacturer's instructions. After 48 hours, cultures were harvested and GFP-positive cells were isolated by flow cytometry (FACSCanto II, BD Biosciences) and seeded for clonal expansion. The resulting cell lines were validated by the Sanger sequencing (see 2.11) of *AP1S3* exon 2, the paralogous genomic segments in *AP1S1* and *AP1S2* and the off-target sites predicted by the CRISPR design tool. The expression of *AP1S1*, *AP1S2* and *AP1S3* was also measured by real-time PCR. Control cells were transfected with an empty pSpCas9BB-2A-GFP vector and processed in the same way as their knockout counterparts.

2.2.2. Culture and stimulation of immortalised cell lines

All cells were grown in DMEM supplemented with 10% FBS and 1% penicillin-streptomycin. Cultures were passaged upon reaching confluence and stocks were stored in liquid nitrogen, in filter-sterilised freezing medium (90% FBS and 10% dimethyl sulfoxide (Sigma)).

For autophagy induction experiments, stable *AP1S3* knockdown and control HaCaT keratinocytes (previously described elsewhere [108]), and *AP1S3* knockout and control HEK293 cells generated by CRISPR/Cas-9 genome editing (see 2.2.1), were plated in 6-well plates (Corning) at a density of $5x10^5$ cells per well. After 18 hours of starvation in Hank's balanced salt solution (HBSS; Gibco), cells were harvested for western blotting.

For autophagy inhibition experiments, wild type HaCaT keratinocytes were seeded in 24-well plates at a density of $4x10^5$ cells per well and stimulated with 20ng/ml IL-1β (Sigma) for 2 hours in the presence or absence of 10mM 3-methyladenine (3MA; Sigma). Cells were then harvested for RNA isolation.

For the stimulation of TLR-2/6 and IL-1 mediated signalling, control and *AP1S3* knockout HaCaT keratinocytes were seeded in 24-well plates at a density of $4x10^5$ cells per well. Cells were stimulated with 10ng/ml IL-1β for 2 hours, 100ng/ml MALP2 (Bio-techne) for 48 hours, 100ng/ml IL-36Ra (Bio-techne) for 5 hours or starved in HBSS for 18 hours. Cells were then harvested for RNA isolation.

2.2.3. Culture and stimulation of primary cells

2.2.3.1. Establishment of primary cultures

Skin-derived primary keratinocytes and dermal fibroblasts were isolated from healthy skin that was discarded after plastic surgery procedures undertaken at Guy's and St Thomas' NHS Foundation Trust. The skin sample was incubated overnight in 5U/ml dispase (Stem Cell Technologies) at 4°C. Epidermal sheets were separated from the dermis and immersed in 0.05% Trypsin-EDTA (Gibco) for 15 minutes at 37°C. The resulting cell suspension was seeded in 12-well plates pre-treated with coating matrix (Gibco). Cells were maintained in Epilife keratinocyte medium (Gibco) containing supplement 7 (Gibco) and 1% penicillin-streptomycin. All stimulation experiments were carried out at the second passage.

The dermis obtained from the same skin sample was cut into 1.5cm^2 pieces and placed into a 6cm culture dish. DMEM supplemented with 10% FBS and 1% penicillin-streptomycin was added to the tissue and replaced every 2-3 days. Once sufficient cell outgrowth was observed, the fibroblasts were transferred into a T25 culture flask (Corning).

Keratinocytes derived from hair plucks were cultured according to a protocol described by Aasen and Izpisúa Belmonte [219]. Twelve temporal hair plucks were sampled from each subject and transported in DMEM supplemented with 1% penicillin-streptomycin and 250ng/ml amphotericin B (Sigma). Hair plucks were placed in 6-well plates and initially maintained in mTeSR1 medium (Stem Cell Technologies) containing 1% penicillin-streptomycin and 250ng/ml amphotericin B. Once keratinocyte outgrowth was visible, mTeSR1 was replaced with Epilife keratinocyte medium

containing Supplement 7 and 1% penicillin-streptomycin. After approximately 14 days, cells were stimulated, while still in passage zero.

Peripheral blood mononuclear cells (PBMCs) were purified by centrifugation of whole blood on a density gradient (Ficoll-paque plus; VWR International), and cultured in RPMI (Gibco) supplemented with 10% FBS and 1% penicillin-streptomycin.

2.2.3.2. Primary cell stimulation

For autophagy inhibition experiments, primary keratinocytes were seeded in 24-well plates and pre-treated with 10mM 3MA for 5 hours when 80% confluent. Cells were stimulated with 20ng/ml IL-1β for 2 hours in the presence or absence of 10mM 3MA. Keratinocytes were then harvested for RNA isolation.

For the analysis of TLR-2/6 signalling or IL-1 responses, primary keratinocytes were seeded in 24-well plates and transfected with 33nM ON-TARGET plus SMARTpool siRNA for human *AP1S3* or with ON-TARGET plus non-targeting siRNA (both GE Dharmacon) using Lipofectamine 2000 in Epilife medium. Forty-eight hours later, cells were stimulated with 20ng/ml IL-1β for 2 hours or 100ng/ml MALP2 for 42 hours, prior to RNA isolation. Culture supernatants were also collected from non-stimulated *AP1S3* siRNA-knockdown and control primary keratinocytes after 48 hours and frozen at -80°C until use for enzyme-linked immunosorbent assay (ELISA).

For the analysis of cytokine responses in patients bearing *AP1S3* mutations, keratinocytes grown from hair plucks were treated with 20ng/ml IL-1β for 2 hours, 100ng/ml IL-36Ra for 5 hours or starved in HBSS for 18 hours, prior to RNA isolation.

For the definition of IL-36 signature genes, primary keratinocytes were seeded in 24-well plates and stimulated with 20ng/ml IL-36α, -β or –γ (Bio-Techne). After 24 hours, cells were harvested for RNA isolation and RNA sequencing, and culture supernatants were collected for ELISA.

For the assessment of keratinocyte responses to mechanical trauma, primary keratinocytes were grown to complete confluence and uniformly spaced, linear scratch wounds covering 40-50% of the well surface were created with a sterile pipette tip. After 4 hours, cells and culture supernatants were harvested for RNA isolation and ELISA, respectively.

For the phenotyping of human *IL1RL2* knockouts, PBMCs were seeded in 24-well plates at a density of $2.5x10^6$ cells per well and treated with 50ng/ml IL-36α for 7 hours, 50ng/ml phorbol 12-myristate 13-acetate (PMA; Sigma) and 250ng/ml Ionomycin (VWR International) for 5 hours or 5µg/ml poly(I:C) (InvivoGen) for 24 hours. The response to stimulation was investigated by real-time PCR and ELISA.

For the assessment of IL-17 secreting T cells in *IL1RL2* knockouts, T-cell Xtend (Oxford Immunotec) was added to whole blood one day after collection, and PBMC isolation was performed. PBMCs were maintained in RPMI/GlutaMAX (Gibco) supplemented with 10% AB Serum (Sigma), 1% penicillin-

streptomycin and 1% amphotericin B. Cells were pre-incubated with 20µg/ml *Candida albicans* extracts (Greer), 1µl/ml 5-in-1 Infanrix vaccine (GlaxoSmithKline) or phosphate-buffered saline (PBS; Gibco) control for 48 hours prior to analysis by enzyme-linked immunospot (ELISPOT) assay.

2.3. IL-36 signalling blockade

2.3.1. *Ex-vivo* experiments

Patients with a diagnosis of moderate-to-severe plaque psoriasis (PASI >10) who were not receiving immune-modulators (washout at least 2 days for topical agents and 6 weeks for systemic treatment) were selected for inclusion in this part of the study. Paired lesional and non-lesional punch biopsies (6mm) were quartered immediately after sampling from patients and cultured for 24 hours in Iscove's Modified Dulbecco's Medium (IMDM; Sigma) containing 2% penicillin-streptomycin-glutamine solution (Gibco), 10% knockout serum replacement factor (Gibco) and either 5ng/ml IL-36Ra or PBS. The effects of IL-36Ra treatment were determined by real-time PCR, ELISA, immunofluorescence microscopy and western blotting.

2.3.2. *In-vivo* experiments

All mouse work was conducted by Dr Paola Di Meglio at the Francis Crick Institute animal facility under specified pathogen-free conditions, in accordance with institutional guidelines and UK Home Office regulations.

Eight-week old, female BALB/cJ mice were treated for five consecutive days with 5% Imiquimod (Meda AB), while also receiving daily intra-peritoneal injections (150µg) of anti-IL36R antibody

(M616, Amgen) or rat IgG2a isotype control (Bio X Cell), starting on day -2 of Imiquimod administration. Full thickness skin biopsies (8mm) were collected after 7 days for histological analysis, flow cytometry and real-time PCR.

For histological analysis, tissue sections were paraffin-embedded and stained with haematoxylin and eosin. Images were acquired at 10x magnification with an Olympus VS120 slide scanner. Five measurements of epidermal and scale thickness were taken in three sections per mouse by a researcher blinded to the experimental groups.

For flow cytometry analysis of skin-infiltrating immune cells, 1 cm^2 skin was digested in 400 mg/ml Liberase TL (Roche) and 1 mg/ml collagenase D (Roche) in IMDM for 2 hours at 37°C, as described elsewhere [220]. For intracellular cytokine staining, cells were stimulated for 4 hours with phorbol 12, 13-dibutyrate (500 ng/ml) and ionomycin (500 ng/ml) in the presence of brefeldin A (1 mg/ml) and Fc block (BD Bioscience), while being simultaneously stained for surface markers, then fixed with 3.8% paraformaldehyde, permeabilised with 0.1% NP-40, and stained for IL-17A and IL-22 (Biolegend). Cells were acquired on a FACS Fortessa (BD Biosciences).

2.4. RNA isolation and real-time PCR

RNA samples isolated from human monocytes/macrophages/dendritic cells, neutrophils, skin-resident T lymphocytes and B cells were kindly provided by Prof Leonie Taams (King's College London), Dr Benjamin Fairfax (University of Oxford), Dr Richard Woolf (King's College London) and Dr David Fear (King's College London), respectively. The remaining RNAs were isolated using the mirVana kit (Life Technologies) (human skin biopsies); a Polytron PT 3000 tissue homogenizer

(Kinematika) with TRIzol (Life Technologies) (mouse skin); and the RNeasy Mini Plus kit (Qiagen) or GeneJET RNA purification kit (Thermo Fisher Scientific) (all cultured cells), according to the manufacturer's instructions.

Following reverse transcription with the nanoScript2 kit (Primer Design), gene expression was assessed by real-time PCR using TaqMan assays (Life Technologies) or the primers listed in Appendix I. For TaqMan assays, reactions were set up in a final volume of 20µl containing 1X TaqMan Universal Master Mix II (Life Technologies), 1µl probe (Life Technologies) and 2µl of diluted cDNA. All other reactions required a volume of 20µl containing 70nM of primers, 1X KAPA SYBR FAST Universal qPCR Master Mix (KAPA Biosystems) and 2µl of diluted cDNA.

Samples were loaded on a 7900HT Fast Real Time PCR System (Applied Biosystems) and the cycling steps were as follows: 95°C for 10 minutes, (95°C for 15 seconds, 60°C for 60 seconds) x 40. Transcript levels were normalised to *PPIA*, *HuPO*, *B2M* or *B2m* expression. The relative quantification of gene expression was calculated using the ΔΔCt method [221].

2.5. ELISA and ELISPOT

The production of IL-36α, IL-36γ, IL-8, TNFα and IL-17 was measured with the Human IL36A ELISA Kit (Sigma), Human IL36G ELISA Kit (Sigma), Human IL-8 ELISA Kit (Sigma), Human TNFα ELISA Kit (Sigma) and Human IL-17 Quantikine ELISA Kit (Bio-techne), respectively. The absorbance at 450nm was determined using an ELISA reader (BMG Labtech).

IL-17 producing T cells were quantified with an IL-17A T cell ELISPOT assay (U-Cytech Biosciences), which was carried out according to the manufacturer's protocol using Professor Mark Peakman's laboratory facilities at King's College London. The mean number of spots in stimulated samples was normalized to the mean number of spots in untreated samples to derive a stimulation index.

2.6. Plasmids and constructs

The FLAG-*AP1M1* construct was generated by inserting HindIII/BamHI-digested *AP1M1* in frame into a c-Flag pcDNA3 vector (Addgene #20011) using PCR-based amplification. The wild type and mutant (p.Phe4Cys and p.Arg33Trp) myc-tagged *AP1S3* constructs are described elsewhere [108]. The integrity of all constructs was verified by Sanger sequencing (see 2.11) using the primers specified in Appendix I.

2.7. Immunofluorescence confocal microscopy

2.7.1. Analysis of mutagenised constructs

For the AP-1 subunit co-localisation experiments, HEK293 cells were seeded on poly-L-lysine coated coverslips (Becton Dickinson) in a 24-well plate at a density of $1.5x10^5$ cells per well. Cells were transfected with Lipofectamine 2000, so as to over-express Flag-tagged *AP1M1* and either wild type or mutant (p.Arg33Trp) Myc-tagged *AP1S3* constructs.

After 24 hours, cells were fixed with 4% paraformaldehyde (Alfa Aesar), immersed in blocking buffer (1xPBS, 0.3% Triton X-100 (Sigma), 5% goat serum (Sigma)) for 1 hour and incubated overnight at 4°C with 1:500 mouse monoclonal anti-myc (Cell Signalling Technology) and 1:600 rabbit monoclonal

anti-FLAG (Cell Signalling Technology) in PBS containing 1% bovine serum albumin (BSA; Sigma) and 0.3% Triton X-100 (Sigma). Cells were subsequently incubated with secondary antibodies conjugated with a fluorescein dye (1:800 Alexa Fluor 594 goat anti-mouse IgG and 1:800 Alexa Fluor 488 goat anti-rabbit IgG (Thermo Fisher Scientific)) for 70 minutes at room temperature and mounted onto slides using ProLong Diamond Antifade reagent (Life Technologies). Slides were imaged using a C2 confocal microscope (Nikon) in the Nikon Imaging Centre at King's College London and z-stack images of at least 15 cells per slide were taken.

In autophagy induction experiments, *AP1S3* knockout and control HEK293 cells were seeded on coverslips in a 24-well plate at a density of $1x10^5$ cells per well. Cells were transfected with a pEGFP-LC3 plasmid (Addgene; #24920) and either an empty vector or a rescue construct (wild type myc-*AP1S3* or p.Arg33Trp myc-*AP1S3*) using Lipofectamine 2000. After 24 hours, cells were starved for 18 hours in HBSS supplemented with 0.1µM Bafilomycin A1 (Santa Cruz Biotechnology). Cells were imaged as described above and autophagosomes were counted using NIS-Elements Advanced Research software (Nikon).

2.7.2. Analysis of skin sections

For the *ex-vivo* investigation of IL-36 blockade, tissue sections (8µm) cut from optimum cutting temperature (OCT) compound (VWR International)-embedded frozen skin biopsies were fixed with cold acetone (VWR International), permeabilised using 0.6% H_2O_2 (Sigma), 0.1% Triton X-100 in deionised water for 10 minutes, and incubated in blocking buffer (0.1% BSA, 10% goat serum, 0.1% Tween 20 (Sigma) in PBS) for 20 minutes. Sections were sequentially stained with primary antibody (1:50 rabbit anti-human CD3 (Dako) or 1:50 mouse anti-human CD11c (Bio-Rad)) for 1.5 hours and secondary antibody (1:800 goat anti-rabbit IgG Alexa Fluor 594 or 1:800 goat anti-mouse IgG Alexa

Fluor 594 (Thermo Fisher Scientific)) for 30 minutes. Slides were imaged using an A1R confocal microscope (Nikon) and z-stack images of at least 5 images per sample were taken. The number of positive cells per field were counted using NIS-Elements Advanced Research software.

2.8. Thermal stability assay

HEK293 cells were seeded in 24-well plates at a density of $1x10^5$ cells per well and transfected with Lipofectamine 2000, so as to over-express wild type and mutant (p.Phe4Cys) Myc-tagged *AP1S3* constructs. After 24 hours, cells were harvested and protein extracts were prepared using a non-denaturing lysis buffer (50mM TrisHCl pH 7.4; 150mM NaCl; 5mM EDTA; 10% glycerol; 1% NP-40 and 1X protease inhibitor (EDTA-free, Roche)). Six aliquots of each cell lysate were incubated for 5 minutes across a 37°C- 57°C temperature gradient (37.0°C, 38.7°C, 42.9°C, 48.2°C, 55.2°C, 57.2°C) in a Mastercycler Pro (Eppendorf). Samples were centrifuged for 30 minutes at 13,000 rpm at 4°C and the soluble fraction was analysed by western blotting using an anti-myc antibody (see 2.10).

2.9. Co-immunoprecipitation

HEK293 cells were seeded in 6-well plates at a density of $5x10^5$ cells per well and co-transfected with the indicated constructs using Lipofectamine 2000 for 24 hours. Protein extracts were prepared using ice cold lysis buffer (20mM TrisHCl pH 8, 137mM NaCl, 1% NP-40, 2mM EDTA and 1X protease inhibitor). Lysates were subjected to overnight immune precipitation using 1:50 rabbit monoclonal anti-FLAG. Immunocomplexes were precipitated by incubating with 50% protein A-agarose bead slurry (Cell Signalling Technology) for 3 hours at 4°C. After washing, the proteins bound to the beads were eluted and analysed by western blotting.

2.10. Western blotting

All of the equipment used for western blotting was purchased from Bio-Rad and all reagents from Sigma, unless indicated otherwise.

For the analysis of thermal stability assays and autophagy induction experiments, protein extracts were prepared with the non-denaturing lysis buffer described in 2.8, while a slightly modified buffer was used for co-immunoprecipitation experiments (2.9).

For the analysis of *ex-vivo* IL-36 blockade, proteins were isolated from skin biopsies using a Bullet Blender Tissue Homogeniser (Next Advance) with a non-denaturing cell lysis buffer (50 mM TrisHCl pH 7.4, 150 mM NaCl, 2% Triton X-100, 1% SDS, 10mM EDTA, 1:100 protease inhibitor cocktail, 200mM calyculin).

Following denaturation in 1X Laemmli buffer (0.375M Tris-HCl pH 6.8, 9% SDS, 50% glycerol, 5% β-mercaptoethanol, 0.03% bromophenol blue) at 100°C for 5 minutes, protein lysates were loaded onto 10-15% gels alongside a protein marker (Bio-Rad Precision Plus Protein Standards) and electrophoresed at 100V in 1X running buffer (25mM Tris-Base, 1.92M Glycine, 0.1% SDS).

Proteins were transferred onto a polyvinylidene fluoride (PVDF; Roche Diagnostics) membrane that had been equilibrated in cold absolute methanol for 2 minutes and in 1X transfer buffer (25mM Tris-Base, 192mM glycine, 20% methanol) for 5 minutes. Proteins were transferred using a Mini Trans-Blot Electrophoresis transfer cell apparatus at 200mA, for 1 hour at 4°C. To evaluate transfer efficiency, the membrane was stained with Ponceau S (Sigma) red dye.

To inhibit non-specific antibody binding, membranes were blocked by incubation in 5% skimmed milk (Marvel)-1X TBS-T (140mM NaCl, 20mM TrisBase, 0.1% Tween 20) for 1.5 hours at room temperature. Blots were then probed overnight at 4°C with rabbit polyclonal anti-LC3 (1:1000, Cell Signalling Technology), rabbit polyclonal anti-β actin (1:1000, Cell Signalling Technology), rabbit polyclonal anti-p62 (1:1000, Sigma), mouse monoclonal anti-myc (1:1000, Thermo Scientific), rabbit monoclonal anti-FLAG (1:1000), mouse monoclonal anti-p-p38 (1:500, Santa Cruz Biotechnology) or mouse monoclonal anti-hsc70 (1:2000, Santa Cruz Biotechnology). Anti-LC3 was diluted in 5% BSA and all other antibodies were diluted in 5% skimmed milk.

For detection of p38α/β, membranes that had been previously probed with anti p-p38 were incubated in stripping buffer (2% SDS, 0.0625M Tris HCl pH 6.8, 0.8% β-mercaptoethanol) at 50°C for 45 minutes. After rinsing the membrane for 1.5 hours under running water and washing with 1X TBS-T for 5 minutes, membranes were re-probed with mouse monoclonal anti-p38α/β (1:500, Santa Cruz Biotechnology).

Following primary antibody staining, the membranes were washed in 1X TBS-T and incubated with the appropriate peroxidase-linked species specific secondary antibody (GE healthcare) at 1:10000 dilution in 5% skimmed milk-1X TBS-T for 1 hour at room temperature.

Once the membranes had been treated with ECL (Amersham), autoradiography film (FUJI) were developed using an automated film developer (Konica Minolta SRX-101A). All densitometry analysis was undertaken with Image J [222].

2.11. PCR and Sanger sequencing

Genomic DNA was extracted from the saliva of human knockouts and controls (collected using Oragene·DNA kits (DNA Genotek)) by technical staff at St John's Institute of Dermatology. DNA was isolated from *AP1S3* knockout and control cells using the DNeasy kit (Qiagen), according to manufacturers' instructions.

For verification of the DNA sequence of human *IL1RL2* knockouts and controls, primers (Appendix I) were designed to amplify all coding exons and exon–intron junctions of *IL1RL2*.

To validate *AP1S3* knockout cells generated by CRISPR/Cas9 genome editing, primers were designed to amplify the CRISPR/Cas9 *AP1S3* target region (*AP1S3* exon 2), paralogous loci (*AP1S1* exon 2, *AP1S2* exon 2) and off-target sites predicted by the CRISPR design tool. All oligonucleotide sequences are reported in Appendix I.

PCR reactions were set up in a final volume of 15µl containing 1X reaction buffer supplemented with 0.15mM $MgCl_2$ (Thermo Scientific), 0.2mM dNTPs (Thermo Scientific), 0.3µM forward and reverse oligonucleotide primers, 25ng of DNA template and 0.625U Taq DNA Polymerase (Thermo Scientific). Amplification was performed in a Mastercycler Pro under the following conditions: 95°C for 5 minutes, (95°C for 30 seconds, Tm for 30 seconds, 72°C for 30 seconds) x 30, 72°C for 5 minutes. The annealing temperature for each primer pair (Tm, reported in Appendix I), was established by a gradient PCR. Amplification of target DNA was confirmed by agarose gel electrophoresis.

Following enzymatic purification of the PCR products using the ExoSTAR kit (GE Healthcare), sequencing reactions were performed by adding 1X Sequencing Buffer (Applied Biosystems), 2µl primer and 0.25µl of BigDye Terminator v3.1 Ready Reaction Mix (Applied Biosystems) to 1.5µl of purified PCR product. Cycling conditions were: (96°C for 30 seconds, 55°C for 15 seconds, 60°C for 60 seconds) x 35. Following purification of the sequencing reaction products by ethanol precipitation, each sample was dissolved in 10µl of HiDi Formamide (Applied Biosystems) and denatured for 2 minutes at 90°C.

Sequenced PCR products were loaded onto a 3730xl DNA Analyzer (Applied Biosystems) and nucleotide changes detected using Sequencher 4.10.1 (Gene Codes Corporation).

2.12. Computational analyses

2.12.1. Pathogenicity predictions

Individuals with homozygous *IL1RL2* variants were identified by mining the exome sequence data relating to the Born in Bradford cohort [212] (provided by Dr Vagheesh Narasimhan, Sanger Institute). The pathogenic potential of the variants was assessed with the following programs: CADD [223], Condel [224], SIFT [225], PROVEAN [226] and PolyPhen-2 [227]. Nucleotide changes that were predicted to be deleterious by at least four algorithms were considered as pathogenic.

2.12.2. Transcriptome data analysis

RNA-seq libraries were prepared with the Illumina TruSeq Stranded Total RNA preparation kit and sequenced on an Illumina HiSeq 3000 system at the Next Generation Sequencing Facility, Leeds

Institute of Molecular Medicine, University of Leeds. The quality of the sequence data was assessed using FastQC [228] and adapter sequences and low quality 5'ends of reads were removed using Trim Galore [229]. Sequences were next aligned to the Ensembl Human GRCh37 transcriptome using Bowtie 2-2.2.2 [230]. To determine RNA expression, the number of reads that mapped to each gene was quantified by htseq-count [231]. Original bash scripts for the above processing steps were obtained from Dr Helena Ahlfors (Senior Bioinformatician at University College London Institute for Child Health) and modified as needed.

Raw data for the expression profiling of plaque (GSE67785) and pustular psoriasis (GSE79704) skin lesions and IL-4 stimulated keratinocytes (GSE59275) were downloaded from the Gene Expression Omnibus database. Gene names were converted into Entrez IDs using NCG 5.0 [232] by Miss Marika Catapano (a PhD student colleague in the group), who also computed differential expression using DESeq2 [233]. Differentially expressed genes with a fold change $\geq$ 2 and false discovery rate (FDR) <0.05 were selected for pathway enrichment analysis, which was performed using Ingenuity Pathway Analysis (QIAGEN Bioinformatics).

2.12.3. Statistics

Unless otherwise indicated, all experimental data are presented as means +/- standard error of the mean (SEM). Differences between groups were assessed using the unpaired Student's t test or one-way ANOVA with Dunnett's post-test, as appropriate. *P* values ≤ 0.05 were considered as statistically significant.

The significance of the overlap between the up-regulated genes (or enriched pathways) represented in Venn diagrams was calculated by Miss Marika Catapano using the hyper-geometric distribution (phyper function in R (version 3.4.0)). The enrichment of IL-36 signature genes within disease associated intervals was also assessed by Miss Marika Catapano. The lead SNP for each locus was extracted from the National Human Genome Research Institute GWAS catalogue [234] and the susceptibility region was defined as a genomic segment extending 50kb in either direction. The unique genes mapping within each interval were identified using BioMart [235]. Fisher's test and hyper-geometric distribution *P* values were adjusted for multiple testing using the Bonferroni correction.

3. Results

3.1. *AP1S3* mutations cause skin autoinflammation by disrupting keratinocyte autophagy and up-regulating IL-36 production

ORIGINAL ARTICLE

AP1S3 Mutations Cause Skin Autoinflammation by Disrupting Keratinocyte Autophagy and Up-Regulating IL-36 Production

Satveer K. Mahil[1], Sophie Twelves[1], Katalin Farkas[2], Niovi Setta-Kaffetzi[1], A. David Burden[3], Joanna E. Gach[4], Alan D. Irvine[5], László Képíró[6], Maja Mockenhaupt[7], Hazel H. Oon[8], Jason Pinner[9], Annamari Ranki[10], Marieke M.B. Seyger[11], Pere Soler-Palacin[12], Eoin R. Storan[13], Eugene S. Tan[8], Laurence Valeyrie-Allanore[14], Helen S. Young[15], Richard C. Trembath[1], Siew-Eng Choon[16], Marta Szell[2,17], Zsuzsanna Bata-Csorgo[2,6], Catherine H. Smith[1], Paola Di Meglio[18], Jonathan N. Barker[1,19] and Francesca Capon[1,19]

Prominent skin involvement is a defining characteristic of autoinflammatory disorders caused by abnormal IL-1 signaling. However, the pathways and cell types that drive cutaneous autoinflammatory features remain poorly understood. We sought to address this issue by investigating the pathogenesis of pustular psoriasis, a model of autoinflammatory disorders with predominant cutaneous manifestations. We specifically characterized the impact of mutations affecting *AP1S3*, a disease gene previously identified by our group and validated here in a newly ascertained patient resource. We first showed that *AP1S3* expression is distinctively elevated in keratinocytes. Because *AP1S3* encodes a protein implicated in autophagosome formation, we next investigated the effects of gene silencing on this pathway. We found that *AP1S3* knockout disrupts keratinocyte autophagy, causing abnormal accumulation of p62, an adaptor protein mediating NF-κB activation. We showed that as a consequence, *AP1S3*-deficient cells up-regulate IL-1 signaling and overexpress IL-36α, a cytokine that is emerging as an important mediator of skin inflammation. These abnormal immune profiles were recapitulated by pharmacological inhibition of autophagy and verified in patient keratinocytes, where they were reversed by IL-36 blockade. These findings show that keratinocytes play a key role in skin autoinflammation and identify autophagy modulation of IL-36 signaling as a therapeutic target.

Journal of Investigative Dermatology (2016) **136,** 2251–2259; doi:10.1016/j.jid.2016.06.618

INTRODUCTION

Autoinflammatory disorders (AIDs) are a group of inherited conditions caused by abnormal activation of the innate immune system. AIDs typically present with recurrent and seemingly unprovoked episodes of systemic upset, which are almost invariably accompanied by joint and skin inflammation (Aksentijevich and Kastner, 2011). The latter can manifest with urticarial, pustular, or ulcerative eruptions, which are considered important markers of disease activity (Beer et al., 2014).

In the last 15 years, genetic studies have identified more than 30 AID genes, illuminating fundamental innate immune pathways and highlighting pathogenic mechanisms (most notably, abnormal IL-1 production) that have been successfully targeted by therapeutic interventions (de Jesus et al., 2015).

[1]*Division of Genetics and Molecular Medicine, King's College London, London, UK;* [2]*MTA-SZTE Dermatological Research Group, Szeged, Hungary;* [3]*Department of Dermatology, University of Glasgow, Glasgow, UK;* [4]*Department of Dermatology, Birmingham Children's Hospital, Birmingham, UK;* [5]*Paediatric Dermatology, Our Lady's Children's Hospital, Dublin, Ireland;* [6]*Department of Dermatology and Allergology, University of Szeged, Hungary;* [7]*Dokumentationszentrum schwerer Hautreaktionen (dZh) and RegiSCAR-study, Department of Dermatology, Medical Center–University of Freiburg, Freiburg, Germany;* [8]*National Skin Centre, Singapore;* [9]*Department of Medical Genomics, Royal Prince Alfred Hospital, Camperdown, Australia;* [10]*Department of Skin and Allergic Diseases, Helsinki University Central Hospital, Helsinki, Finland;* [11]*Department of Dermatology, Radboud University Nijmegen Medical Centre, Nijmegen, The Netherlands;* [12]*Pediatric Infectious Diseases and Immunodeficiencies Unit, Hospital Universitari Vall d'Hebron, Barcelona, Spain;* [13]*Department of Dermatology, University Hospital, Galway, Ireland;* [14]*Department of Dermatology, Henri Mondor Hospital, Paris, France;* [15]*Department of Dermatology, University of Manchester;* [16]*Department of Dermatology, Hospital Sultanah Aminah, Johor Bahru, Malaysia;* [17]*Institute of Medical Genetics, University of Szeged, Hungary; and* [18]*Mill Hill Laboratory, The Francis Crick Institute, London, UK*

[19]*These authors contributed equally to this work.*

Correspondence: Francesca Capon, Division of Genetics and Molecular Medicine, 9th floor Tower Wing, Guy's Hospital, Great Maze Pond, London SE1 9RT, UK. E-mail: francesca.capon@kcl.ac.uk

Abbreviations: 3-MA, 3-methyladenine; AID, autoinflammatory disorder; CRISPR, clustered regularly-interspaced short palindromic repeats; Cas9, CRISPR-associated endonuclease 9; GFP, green fluorescent protein; MALP-2, macrophage-activating lipopeptide 2; siRNA, small interfering RNA; TLR-2/6, Toll-like receptor 2/6

Received 23 March 2016; revised 15 June 2016; accepted 25 June 2016; accepted manuscript published online 5 July 2016; corrected proof published online 12 August 2016

Despite these successes, the basis of organ-specific disease manifestations is still unclear. This is particularly true of skin pathology, because the nature of the cells and molecular mechanisms that mediate cutaneous inflammation in AID remain poorly defined (Beer et al., 2014).

We sought to address this issue by investigating the pathogenesis of pustular psoriasis, a severe AID manifesting with repeated eruptions of painful skin pustules. These can be localized to the palms and soles (palmar plantar pustulosis), toes and fingertips (acrodermatitis continua of Hallopeau) or affect most of the body surface (generalized pustular psoriasis). Although the lesions can be accompanied by arthritis and systemic upset, cutaneous involvement is the most prominent clinical feature of the disease (Griffiths and Barker, 2010). This makes pustular psoriasis an ideal model for investigating the molecular mechanisms that drive skin inflammation in AID.

We specifically investigated the pathogenic role of *AP1S3*, a gene that we found to be mutated in all forms of pustular psoriasis (Setta-Kaffetzi et al., 2014). *AP1S3* encodes a subunit of AP-1, a heterotetramer that mediates membrane trafficking between the post-Golgi network and the endosome (Robinson, 2004). The complex is composed of two large (AP-1γ1 and AP-1β1), one medium (AP-1μ1) and one small subunit (AP-1σ1). The latter exists in three alternative forms (AP-1σ1A, AP-1σ1B and AP-1σ1C), encoded by paralogous genes (*AP1S1*, *AP1S2*, *AP1S3*), so that the *AP1S3* product is AP-1σ1C (Figure 1a). The σ1 subunit confers stability to AP-1 tetramers, so that mutations in *AP1S* genes are expected to disrupt the entire complex (Robinson, 2004).

The AP-1 complex has also been implicated in the formation of autophagosomes (Guo et al., 2012). These are specialized vesicles that mediate the degradation of cellular components by autophagy, a catabolic process that can be activated by nutrient stress (e.g., starvation). Given that autophagy modulates cytokine production downstream of various pattern recognition receptors (Netea-Maier et al., 2016), we hypothesized that *AP1S3* mutations would disturb autophagic activity, causing innate immune dysregulation. We then validated our pathogenic model in a variety of in vitro experimental systems and in patient cells.

RESULTS

Validation of *AP1S3* as a pustular psoriasis gene

Although we previously reported that two *AP1S3* mutations (p.Phe4Cys and p.Arg33Trp) account for approximately 10% of European pustular psoriasis patients (Setta-Kaffetzi et al., 2014), the rarity of the disease has hindered the replication of this finding. To address this issue, we screened the *AP1S3* coding region in 85 newly ascertained patients (53 European and 32 non-European subjects) (see Supplementary Table S1 online), recruited across Europe and East Asia. This uncovered p.Phe4Cys and p.Arg33Trp alleles in five unrelated individuals (n = 3 generalized pustular psoriasis and n = 2 palmar plantar pustulosis patients) (Table 1). All were of European descent, confirming the limited geographic distribution of the two mutations. Two of the three generalized pustular psoriasis patients carried the *AP1S3* mutation in conjunction with a deleterious change in *IL36RN*, a pustular psoriasis gene encoding the IL-36 receptor antagonist

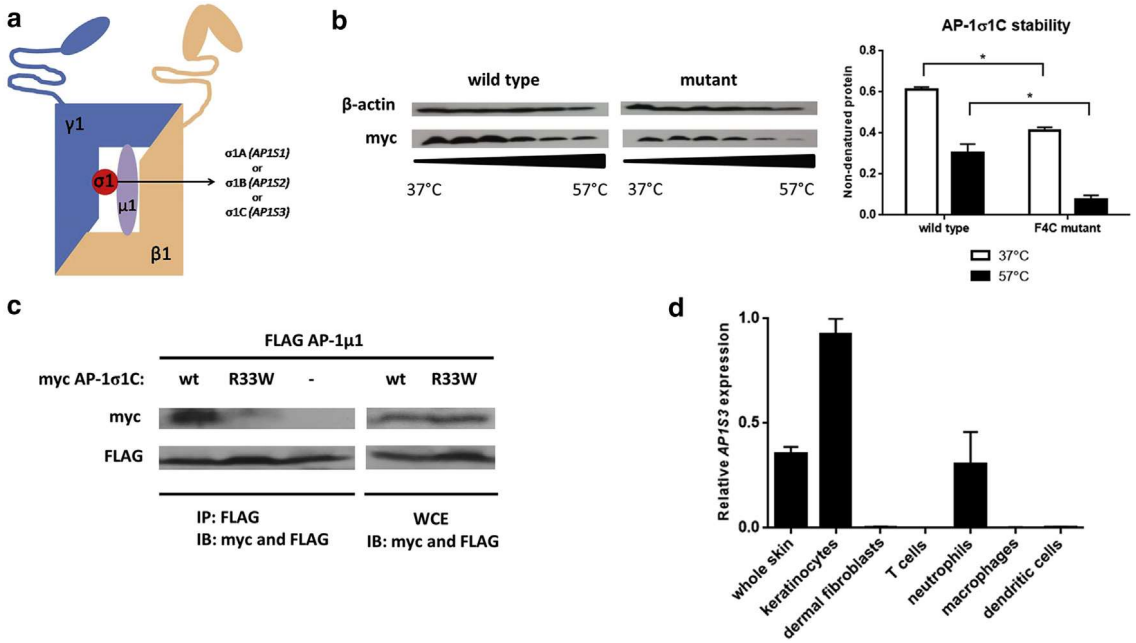

Figure 1. *AP1S3* loss-of-function mutations are most likely to affect skin keratinocytes. (**a**) Schematic representation of AP-1 structure. (**b**) HEK293 cells were transfected with wild-type and mutant *AP1S3* constructs. Lysates were subjected to the indicated temperature gradient, and soluble (nondenatured) proteins were analyzed by Western blotting. The densitometry shows the fraction of nondenatured protein (mean ± standard error of the mean of the results obtained in two experiments). (**c**) HEK293 cells were transfected with myc-tagged *AP1S3* and FLAG-tagged *AP1M1* constructs. Lysates were subjected to immune precipitation (IP) and immune blotting (IB) as indicated. The image is representative of results obtained in two experiments. (**d**) Real-time PCR analysis showing abundant *AP1S3* expression in keratinocytes. The data show the mean ± standard error of the mean of measurements obtained in two donors. $^*P \leq 0.05$. IB, immune blotting; IP, immune precipitation; WCE, whole cell extracts; wt, wild type.

Table 1. Clinical phenotype of affected individuals bearing *AP1S3* disease alleles

Patient ID	Sex	Ethnicity	Diagnosis	Concurrent PV	Age of Onset, years	*IL36RN* Genotype	*AP1S3* Genotype
T010091	F	European	GPP	U	68	p.Ser113Leu/—	p.Phe4Cys/—
T030865	F	European	GPP	N	<1	p.Ser113Leu/—	p.Phe4Cys/—
T016713	F	European	PPP	N	55	—/—	p.Arg33Trp/—
T026517	F	European	PPP	N	50	—/—	p.Arg33Trp/—
T028754	F	European	PPP	N	49	—/—	p.Arg33Trp/—

Abbreviations: F, female; GPP, generalized pustular psoriasis; ID, identifier; N, no; PPP, palmar plantar pustulosis; PV, psoriasis vulgaris; U, unknown.

(Marrakchi et al., 2011; Onoufriadis et al., 2011). One of these individuals exhibited a particularly severe, recalcitrant phenotype and had a sister with a milder form of the disease, who only carried the *IL36RN* mutation (see Supplementary Table S2 online).

Taken together, these observations validate the involvement of *AP1S3* in pustular psoriasis and suggest the possibility of epistasis between *IL36RN* and *AP1S3* alleles.

AP1S3 mutations disrupt protein function in keratinocytes

Structural homology modeling indicates that the p.Phe4Cys change maps to a β-sheet required for protein folding, whereas the p.Arg33Trp substitution is expected to disrupt the interaction between AP-1σ1C and AP-1μ1A (Setta-Kaffetzi et al., 2014). This strongly suggests that both mutations are loss-of-function alleles.

To validate these predictions, we first examined the effect of p.Phe4Cys on the thermal stability of AP-1σ1C. After transfection of wild-type and mutant *AP1S3* constructs into HEK293 cultures, we subjected cell lysates to a temperature gradient and monitored AP-1σ1C levels by western blotting. We found that p.Phe4Cys proteins were denatured significantly more quickly than their wild-type counterparts (Figure 1b), confirming that the mutation disrupts AP-1σ1C stability.

To investigate the impact of the p.Arg33Trp allele, we carried out co-immunoprecipitation experiments, using FLAG-*AP1M1* and myc-*AP1S3* constructs transfected into HEK293 cells. As expected, we found that wild-type myc-AP1σ1C co-precipitated with FLAG-AP1μ1A. This interaction, however, was disrupted when FLAG-*AP1M1* was co-transfected with a p.Arg33Trp myc-*AP1S3* cDNA (Figure 1c). Similar results were obtained in immunofluorescence experiments, showing that wild-type myc-AP1σ1C co-localized with FLAG-AP1μ1A, whereas the mutant p.Arg33Trp protein did not (see Supplementary Figure S1 online). Thus, we concluded that the p.Arg33Trp mutation disturbs the interaction between AP-1σ1C and AP-1μ1A, as predicted in-silico.

Having validated the loss-of-function nature of disease alleles, we sought to establish which cell types are most likely to be affected by *AP1S3* deficiency. We therefore measured gene expression in biologically relevant cell populations. Although transcript levels were low in neutrophils and virtually undetectable in $CD4^+$ T lymphocytes, we observed abundant gene expression in keratinocytes (Figure 1d). The impact of disease alleles was therefore modeled in this cell type.

AP1S3 deficiency causes impaired keratinocyte autophagy

Because autophagosome formation requires a functional AP-1 complex (Guo et al., 2012), we hypothesized that *AP1S3* loss-of-function mutations may disrupt keratinocyte autophagy.

We first examined this possibility in a HaCaT keratinocyte cell line stably transduced with a silencing *AP1S3* small hairpin RNA (Setta-Kaffetzi et al., 2014) (Figure 2a). After inducing autophagy by starvation, we monitored the conversion of the LC3-I protein into its modified form (LC3-II), which is a well-recognized autophagosome marker (Klionsky et al., 2012). We found that LC3-II levels were significantly reduced in *AP1S3* knockdown versus control cell lines (Figure 2b).

We then repeated the experiment in a HEK293 *AP1S3* knockout cell line, generated by clustered regularly interspaced short palindromic repeats (CRISPR)—CRISPR-associated endonuclease-9 (Cas9) genome editing (Figure 2c). This confirmed that *AP1S3* silencing causes a very significant decrease in starvation-induced LC3-II accumulation (Figure 2d).

To further validate our findings, we used fluorescence microscopy to visualize the expression of LC3-green fluorescent protein (GFP) constructs transfected into the HEK293 *AP1S3* knockout cell line. We found that the number of autophagosomes that had incorporated LC3-GFP was significantly reduced in knockout versus control cells. This phenotype was rescued by the overexpression of wild-type but not mutant (p.Arg33Trp) *AP1S3* constructs (Figure 2e).

Thus, *AP1S3* deficiency disrupts autophagy induction in multiple experimental systems.

AP1S3 deficiency results in abnormal p62 accumulation and enhanced Toll-like receptor (TLR) 2/6 signaling

It has been shown that keratinocyte autophagy modulates NF-κB activation downstream of TLR-2/6 by regulating the degradation of the p62 adaptor protein (Lee et al., 2011). This led us to hypothesize that *AP1S3* deficiency would cause an abnormal accumulation of p62, resulting in enhanced NF-κB signaling. We therefore measured p62 protein levels in keratinocytes cultured from the hair plucks of one affected individual (carrying the *AP1S3* p.Arg33Trp mutation) and two healthy control subjects. We found that p62 expression was markedly increased in the patient's cells (Figure 3a). A similar up-regulation was observed in normal primary keratinocytes transfected with *AP1S3* small interfering RNAs (siRNAs) (Figure 3b and 3c) and in a HaCaT *AP1S3* knockout cell line (see Supplementary Figure S2a and b online). We therefore

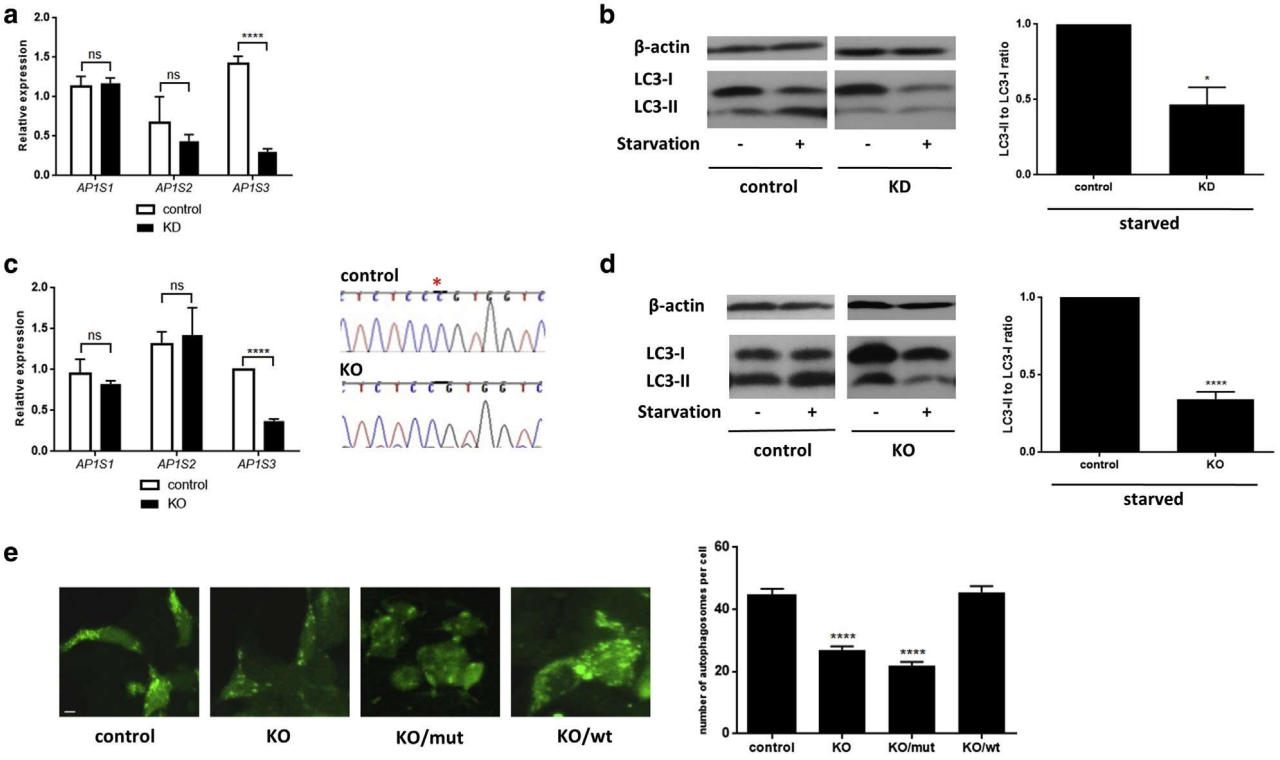

Figure 2. *AP1S3* deficiency results in impaired autophagy. (**a**) After the generation of a HaCaT *AP1S3* knockdown cell line, gene silencing was measured by real-time PCR, because of cross-reactivity of the anti-AP1σ1c antibody with the proteins encoded by *AP1S1* and *AP1S2*. (**b**) Starvation-induced LC3-II accumulation was measured by Western blotting and densitometry. The data are presented as mean ± standard error of the mean of measurements obtained in four independent experiments. (**c**) HEK293 *AP1S3* knockout cell lines harboring a c.124delC change (highlighted by a red asterisk in the chromatogram) were generated by CRISPR/Cas-9 editing. (**d**) Cells were starved to induce autophagy, and LC3-II accumulation was measured by Western blotting. The data are presented as described. (**e**) Control and *AP1S3* KO HEK293 cells were transfected with GFP-LC3 and either an empty vector (control and KO panels) or a rescue construct (wild-type *AP1S3* in KO/wt panel and p.Arg33Trp *AP1S3* in KO/mut). Starvation-induced LC3 punctae were visualized by confocal fluorescence microscopy. The data are presented as mean ± standard error of the mean of measurements obtained in at least 15 cells per experiment. Scale bar = 5 μm. $*P \leq 0.05$, $****P \leq 0.0001$. Cas9, CRISPR-associated protein-9; CRISPR, clustered regularly interspaced short palindromic repeats; GFP, green fluorescent protein; KD, knockdown; KO, knockout; mut, mutated; ns, not significant; wt, wild-type.

concluded that the abnormal p62 accumulation observed in the patient was a result of *AP1S3* deficiency.

To further explore these findings, we measured macrophage-activating lipopeptide 2 (MALP-2)—induced cytokine expression in primary keratinocytes transiently transfected with *AP1S3* siRNAs (Figure 3d). Although there was no *IL1B*, *IL6,* or *IL8* induction at the examined time point, we detected a marked increase in *TNFA* levels. We also observed a significant induction of *IL36A* (but not *IL36B* or *IL36G*), a cytokine that drives abnormal immune signaling in patients with *IL36RN* mutations (Onoufriadis et al., 2011). Importantly, the induction of *TNFA* and *IL36A* was significantly enhanced in *AP1S3*-deficient cells compared with control (Figure 3d).

We then repeated the MALP-2 stimulations in the HaCaT *AP1S3* knockout cell line. This confirmed the abnormal induction of *TNFA* and *IL36A* in knockout cells (see Supplementary Figure S2c).

AP1S3 deficiency causes abnormal IL-1 signaling and up-regulates baseline IL-36 expression

Autophagy-mediated degradation of p62 also regulates IL-1 signaling (Lee et al., 2012), a response that plays a major role in autoinflammation. To determine whether *AP1S3* deficiency would also affect this pathway, we transfected primary keratinocytes with *AP1S3* siRNA pools and measured cytokine levels after IL-1 stimulation. Although *TNFA* expression was unchanged at the examined time point, we observed a clear up-regulation of *IL1B*, *IL8,* and *IL36A* transcripts. The induction of all cytokines was markedly up-regulated in *AP1S3*-deficient cells compared with control (Figure 4a). These observations were replicated in HaCaT *AP1S3*-knockout cells (see Supplementary Figure S3a online), thus validating the effects of gene silencing on IL-1 signaling.

Surprisingly, our experiments showed that baseline *IL36A* expression was markedly increased in *AP1S3*-deficient cells, both at the RNA and protein levels (Figures 4a and b, and see Supplementary Figure S2c). A similar, although less pronounced, effect was also observed for *IL36B* and *IL36G* mRNA expression (see Supplementary Figures S4a and S4b online) and IL-8 protein secretion (Figure 4b).

To determine whether this up-regulation was also a consequence of impaired autophagy, we cultured normal primary keratinocytes in medium supplemented with 3-methyladenine (3-MA), an agent that blocks the formation of autophagosomes (Klionsky et al., 2012). As expected, we found that 3-MA treatment caused an increase in IL-1—dependent cytokine expression. *IL36A* baseline expression

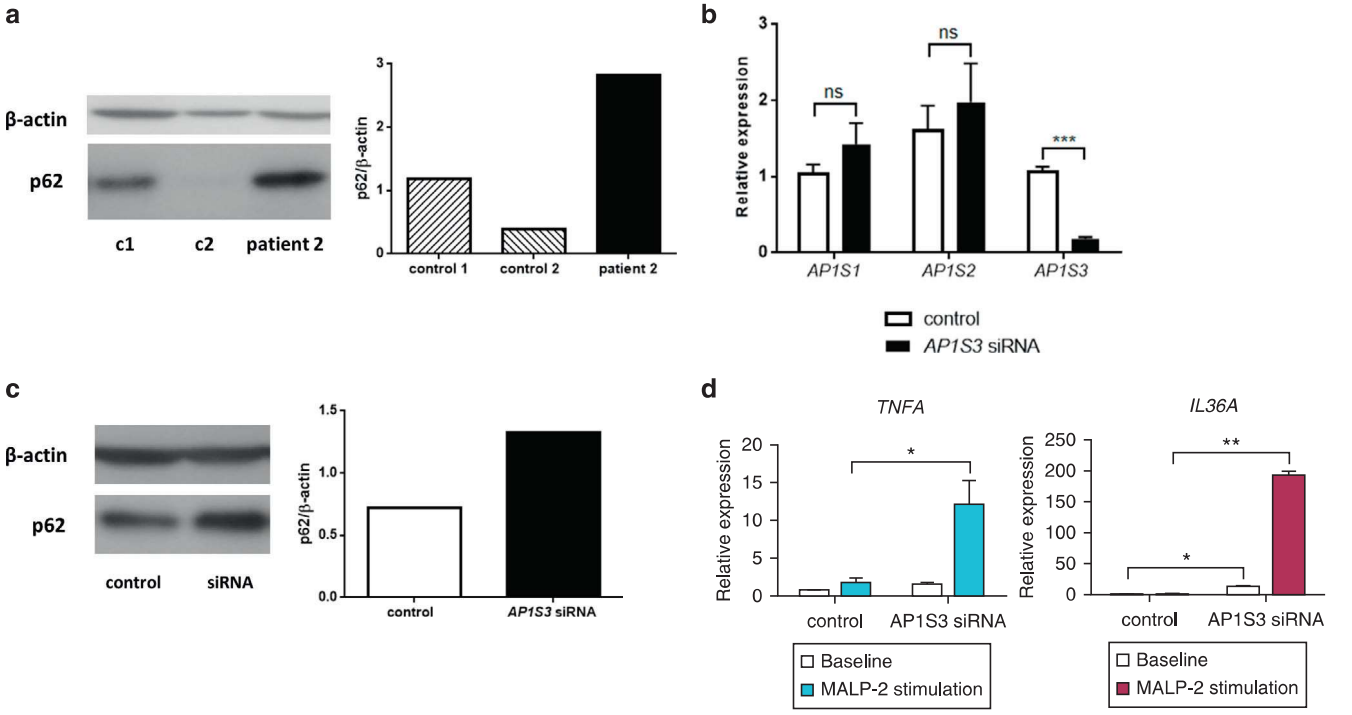

Figure 3. Abnormal p62 accumulation and enhanced TLR-2/6 signaling in *AP1S3*-deficient keratinocytes. (**a**) p62 levels were measured in patient and control subject keratinocytes by Western blotting and densitometry. (**b**) After the transfection of silencing (*AP1S3* siRNA) and nonsilencing (control) siRNA pools into primary keratinocytes, (**c**) baseline p62 levels were measured by Western blotting and densitometry. (**d**) Alternatively, cells were stimulated with MALP-2 in triplicate, and the induction of TLR2/6-dependent genes was measured by real-time PCR. The data are representative of results obtained in at least two independent experiments and are presented as mean ± standard error of the mean of duplicate stimulations. $^{*}P \leq 0.05$, $^{**}P \leq 0.01$, $^{***}P \leq 0.001$. c, control; ns, not significant; siRNA, small interfering RNA; TLR, Toll-like receptor.

was also up-regulated by 3-MA (Figure 4c). These observations, which were replicated in HaCaT keratinocytes (see Supplementary Figure S3b), show that the proinflammatory effects of *AP1S3* deficiency are mediated by a disruption of keratinocyte autophagy.

Patients harboring *AP1S3* mutations up-regulate IL-36 expression and IL-1 signaling

To validate the pathophysiological relevance of our findings, we cultured keratinocytes from the hair plucks of two affected individuals (each carrying an *AP1S3* mutation and a wild-type *IL36RN* sequence) and two healthy control subjects. Although we observed only a weak response to MALP-2 stimulation, we found that cytokine levels were robustly up-regulated after IL-1 treatment. Importantly, the induction of *IL1B, IL8,* and *IL36A* transcripts was increased in the keratinocytes of patients compared with control (Figure 5a), replicating the results generated in *AP1S3*-knockdown cells.

The basal expression of IL-36 cytokines was also up-regulated in patient keratinocytes (Figure 5a and b and see Supplementary Figure S4c), further validating the data obtained in *AP1S3*-deficient cells. *IL1B* and *IL8* baseline transcripts were also significantly overexpressed in the examined individuals (Figure 5a).

To further investigate the mechanisms underlying these observations, we measured transcript levels after autophagy induction by starvation, or blockade, of the IL-36 receptor with a recombinant antagonist (IL-36Ra). We found that both treatments could lower patient cytokine expression to the levels observed in healthy control subjects (Figure 5c, and see Supplementary Figure S4d). Although the experiment was carried out in a single patient, the results were also replicated in *AP1S3*-knockout cells (see Supplementary Figure S5 online), suggesting that impaired autophagy and enhanced IL-36 signaling both contribute to the abnormal immune profile associated with *AP1S3* mutations.

DISCUSSION

The aim of our study was to characterize the molecular mechanisms underlying the cutaneous features of AIDs. We therefore investigated the pathogenesis of pustular psoriasis, focusing our attention on *AP1S3,* a gene that is specifically mutated in this disease. We first validated the pathogenic involvement of this locus by demonstrating the presence of disease alleles in five of the 53 European patients (9.4%) who were included in our screening. We observed that *AP1S3* mutations can be inherited in conjunction with *IL36RN* changes, modifying the phenotypic effect of the latter. This suggests that *AP1S3* alleles may exacerbate the effects of *IL36RN* deficiency by disturbing IL-36 homeostasis, a notion that is borne out by the results of our functional studies.

First, our experiments showed that *AP1S3* expression was low or undetectable in cells that do not respond to IL-36 stimulation (neutrophils and $CD4^{+}$ T cells), whereas transcript levels were abundant in keratinocytes, where IL-36 signaling can be activated by TLR agonists (Gabay and Towne, 2015). The only other known gene for pustular psoriasis (*CARD14*) is also abundantly expressed in keratinocytes (Berki et al., 2015), suggesting that these cells play an

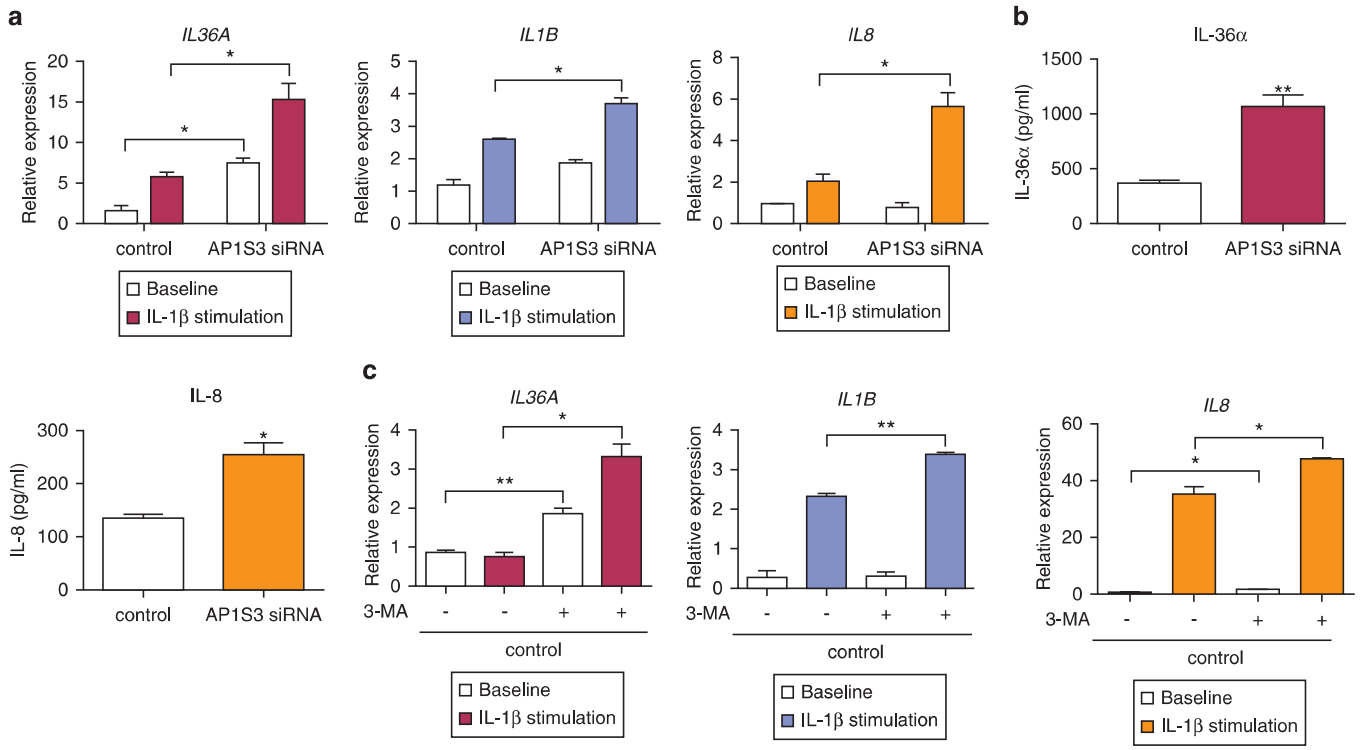

Figure 4. *AP1S3*-deficient primary keratinocytes exhibit an abnormal immune profile, which can be recapitulated by autophagy inhibition. (**a**) After siRNA-mediated *AP1S3* silencing, primary keratinocytes were stimulated with IL-1β, and gene expression was determined by real-time PCR. (**b**) Alternatively, cells were cultured for a further 48 hours in the absence of stimuli, and cytokine production was measured by ELISA. (**c**) Normal primary keratinocytes were cultured in the presence or absence of 3-MA and subsequently stimulated with IL-1β. Gene expression was determined by real-time PCR. All data are representative of results obtained in two independent experiments and are presented as mean ± standard error of the mean of (**a**) duplicate or (**b, c**) triplicate measurements. $^{*}P \leq 0.05$, $^{**}P \leq 0.01$. 3-MA, 3-methyladenine; siRNA, small interfering RNA.

important role in cutaneous autoinflammation. This is in keeping with the emerging view of keratinocytes as immune sentinels contributing to host defense through the engagement of innate receptors and the production of proinflammatory mediators (Di Meglio et al., 2011; Lowes et al., 2013).

The involvement of *AP1S3* in IL-36 regulation is also supported by repeated observations of increased *IL36A* expression in *AP1S3*-deficient cells and in nonlesional keratinocytes, derived from patient hair plucks. Of note, stable *AP1S3* knockout also led to constitutive up-regulation of *IL1B* and *IL8* (see Supplementary Figure S3). Although this phenotype mirrored the expression profile observed in patients, it was not replicated in the transient gene-silencing experiments, where mRNA levels were measured shortly after knockdown initiation. Although *IL36A* was up-regulated at this early time point, the other two cytokines were not, suggesting that the overexpression of *IL1B* and *IL8* may be secondary to IL-36 accumulation. Indeed, our experiments showed that IL-36 receptor blockade is sufficient to normalize *IL1B* and *IL8* levels in patient keratinocytes.

Thus, our observations place IL-36 at the center of a proinflammatory loop that drives enhanced cytokine production in skin autoinflammation (see Supplementary Figure S6 online). This is in keeping with the results of recent studies, indicating that *IL36A* is markedly up-regulated in psoriatic skin and that this is unlikely to be a secondary consequence of inflammation (Swindell et al., 2016). Given that therapeutics blocking IL-36 are now under development (Wolf and Ferris, 2014), these discoveries have important translational implications.

Our experiments show that the effects of *AP1S3* mutations on cytokine production are mediated by disruption of keratinocyte autophagy, causing abnormal p62 accumulation and enhanced NF-κB activation downstream of TLR-2/6 and IL-1R. Of note, p62 transcripts are up-regulated in psoriatic lesions, whereas the expression of molecules that contribute to skin inflammation is reduced in p62-deficient keratinocytes (Lee et al., 2011).

Here, IL-1 treatment of patient cells (which overexpress p62) caused a moderate (~2-fold) induction of *IL1B* transcripts (Figure 5) but a substantial up-regulation of *IL8* (>20-fold). Given that the latter cytokine plays a fundamental role in driving neutrophilic skin infiltration, this finding has a clear pathological relevance.

Autophagy can also modulate cytokine production at the posttranslational level, by degrading components of the inflammasome, the molecular complex that cleaves pro-IL1β into a bioactive molecule (Shi et al., 2012). Although this process has been chiefly investigated in mouse macrophages, it might also be active in human keratinocytes, where it could amplify the effects of *AP1S3* mutations.

It is now widely accepted that perturbations of protein degradation play a pathogenic role in various AIDs with prominent dermatological features (Martinon and Aksentijevich, 2015). Evidence recently generated in

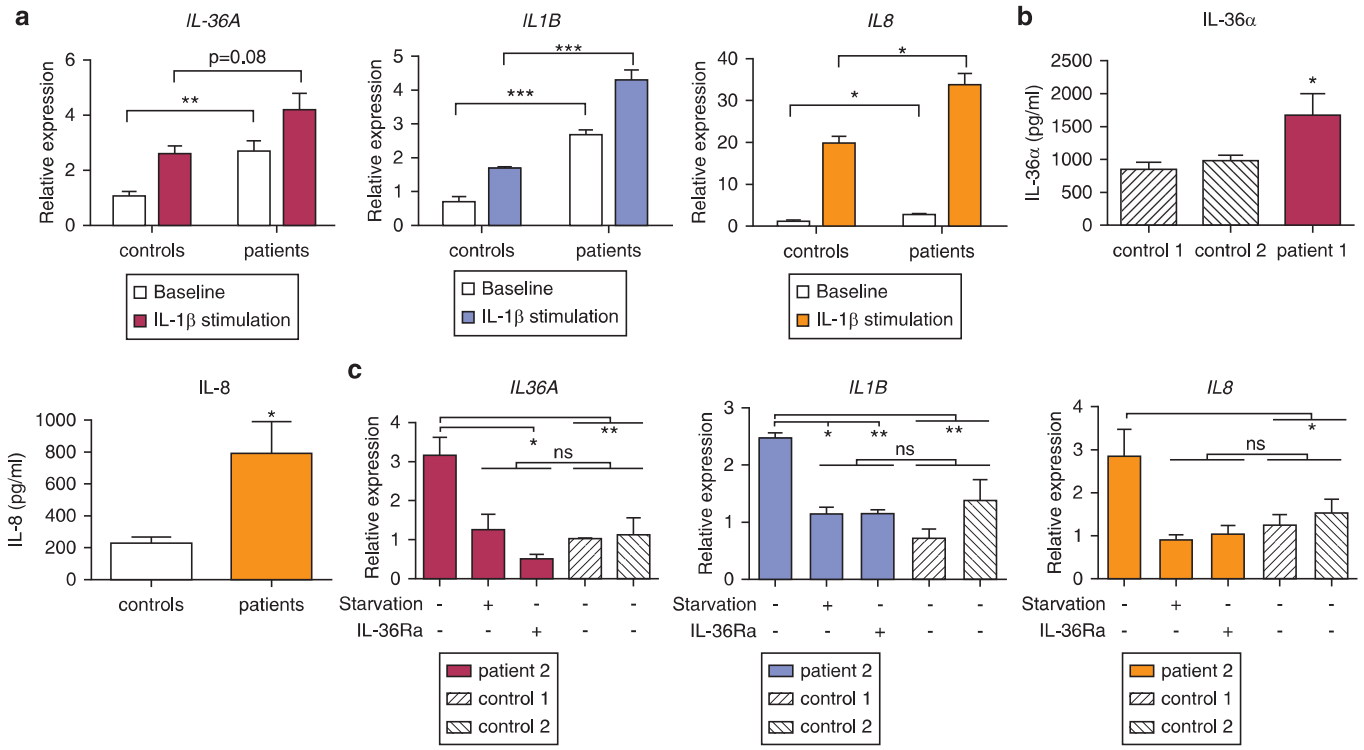

Figure 5. Abnormal cytokine expression in the keratinocytes of patients harboring *AP1S3* mutations. (**a**) Primary keratinocytes were stimulated with IL-1β, and cytokine induction was measured by real-time PCR. The data are presented as mean ± standard error of the mean of duplicate stimulations carried out in the cells of two unrelated patients and two healthy control subjects. (**b**) IL-36α and IL-8 production was measured in culture supernatants by ELISA. Data are presented as mean ± standard error of the mean of triplicate measurements. (**c**) Primary keratinocytes were starved to induce autophagy or cultured in the presence of IL-36Ra. Gene expression was measured by real-time PCR. The data are presented as mean ± standard error of the mean of triplicate measurements, obtained in one patient and two healthy control subjects. $*P < 0.05$, $**P < 0.01$, $***P < 0.001$. ns, not significant.

animal models also indicates that therapeutic effects of anakinra (an IL-1 blocker widely used for the treatment of AIDs) are partly mediated by the rescue of defective autophagy (Iannitti et al., 2016). In the light of this evidence, our work warrants further studies of impaired keratinocyte autophagy as a pathogenic mechanism and therapeutic target in skin autoinflammation.

METHODS

Participants

This study was performed in accordance with the declaration of Helsinki and was approved by the ethics committees of participating institutions. Written informed consent was obtained from all participants. Patients were ascertained by trained dermatologists (see Supplementary Table S3 online) on the basis of established diagnostic criteria (Griffiths and Barker, 2010). Patients 1 and 2 were described elsewhere as T002206 and T001882, respectively (Setta-Kaffetzi et al., 2014). Healthy volunteers were recruited within King's College London. All affected individuals were screened for *IL36RN* and *AP1S3* mutations as described (Onoufriadis et al., 2011; Setta-Kaffetzi et al., 2014).

Plasmids and constructs

The wild-type and mutant myc-tagged *AP1S3* constructs are described elsewhere (Setta-Kaffetzi et al., 2014). The FLAG-*AP1M1* construct was generated by cloning the gene coding sequence into a c-Flag pcDNA3 vector (Addgene #20011). CRISPR/Cas9 guide RNAs (see Supplementary Table S4 online) were designed with the CRISPR design tool (http://crispr.mit.edu/) and cloned into a pSpCas9BB-2A-GFP vector (Addgene #48138), as described elsewhere (Ran et al., 2013). All constructs were validated by Sanger sequencing.

Primary cell culture

Primary keratinocytes and dermal fibroblasts were isolated from healthy skin discarded after plastic surgery. The keratinocytes were maintained in Epilife keratinocyte medium supplemented with Supplement 7 and 1% penicillin-streptomycin, and the fibroblasts were grown in DMEM supplemented with 10% fetal bovine serum and 1% penicillin-streptomycin (all reagents from Gibco, Waltham, MA).

Keratinocytes were derived from hair plucks as described elsewhere (Aasen and Izpisua Belmonte, 2010). Briefly, 12 hairs were plucked from the temporal scalp and placed in mTeSR1 medium (Stem Cell Technologies, Vancouver, Canada) containing 1% penicillin-streptomycin and 250 ng/ml amphotericin B (Sigma, St. Louis, MO). Once outgrowths were visible, mTeSR1 was replaced with Epilife keratinocyte medium containing Supplement 7 and 1% penicillin-streptomycin. After 14 days, cells were stimulated.

Thermal stability assay

HEK293 cells were transfected with the indicated constructs, using Lipofectamine 2000 (Life Technologies, Waltham, MA). Cell lysates were then incubated for 5 minutes across a 37–57 °C temperature gradient. Samples were centrifuged for 30 minutes at 13,000 rpm at 4 °C, and the soluble fraction (supernatant) was analyzed by Western blotting.

CRISPR/Cas9 genome editing

The protocol described by Ran et al. (2013) was used to edit HaCaT and HEK293 cells maintained in complete DMEM. Briefly, the guide

RNA construct was transfected into the cells, using Lipofectamine 2000. After 48 hours, GFP-positive cells were isolated by flow cytometry and seeded for clonal expansion. The resulting cell lines were validated by Sanger sequencing of the target region, paralogous loci, and off-target sites predicted by the CRISPR design tool. The expression of *AP1S1*, *AP1S2,* and *AP1S3* was also measured by real-time PCR. Control cells were transfected with an empty pSpCas9BB-2A-GFP vector.

Cell stimulation

For autophagy induction, cells were starved for 18 hours in Hank's Balanced Salt solution (Gibco), and protein extracts were analyzed by Western blotting. For autophagy inhibition, cells were pretreated with 10mmol/L of 3-MA (Sigma) for 5 hours and then stimulated with 20ng/ml of IL-1β (Sigma) for 2 hours, in the presence 3-MA.

Alternatively, primary or immortalized keratinocytes were treated with 100ng/ml of MALP2 (Bio-techne, Minneapolis, MN) for 42 hours, 20ng/ml of IL-1β for 2 hours, 100ng/ml of IL-36Ra (Bio-techne) for 5 hours or were starved as described.

For transient gene-silencing experiments, cells were transfected for 48 hours with 33 nmol/L of *AP1S3* ON-TARGET plus SMARTpool siRNA or ON-TARGETplus nontargeting siRNA (GE Dharmacon, Lafayette, CO) using Lipofectamine 2000 and stimulated as described above.

Real-time PCR and ELISA

RNAs isolated from skin, lymphocytes, in vitro derived macrophages/dendritic cells, and neutrophils were provided by Frank Nestle, Susan John, Leonie Taams (King's College London), and Benjamin Fairfax (Wellcome Trust Centre for Human Genetics, Oxford), respectively. All remaining RNAs were isolated using the RNeasy Mini Plus kit (Qiagen, Hilden, Germany). Gene expression was assessed by real-time PCR by using the primers listed in Supplementary Table S4 online. Transcript levels were normalized to *PPIA* or *B2M* expression, measured with Applied Biosystems (Foster City, CA) TaqMan probes. IL-36α and IL-8 production was measured with the Human IL36A ELISA Kit (Sigma) and Human IL-8 ELISA Kit (Sigma).

Co-immunoprecipitation and Western blotting

A rabbit monoclonal anti-FLAG (1:50, Cell Signaling Technology, Danvers, MA) was used in co-immunoprecipitation experiments, whereas Western blots were probed with rabbit polyclonal anti-LC3 (Cell Signaling Technology), rabbit polyclonal anti-β actin (Cell Signaling Technology), rabbit polyclonal anti-p62 (Sigma), or mouse monoclonal anti-myc (Thermo Scientific, Waltham, MA) (all 1:1,000). Densitometry was undertaken with Image J software (Schneider et al., 2012).

Immunofluorescence microscopy

In the co-localization experiments, HEK293 cells were co-transfected with the indicated constructs, using Lipofectamine 2000. After 24 hours, cells were fixed and incubated with 1:500 mouse monoclonal anti-myc (Cell Signaling Technology) and 1:600 rabbit monoclonal anti-FLAG. Slides were imaged by using a C2 confocal microscope (Nikon, Tokyo, Japan), and z-stack images of at least 15 cells per slide were taken.

In autophagy induction experiments, HEK293 cells were transfected with a pEGFP-LC3 plasmid (Addgene #24920) and the indicated construct, using Lipofectamine 2000. After 24 hours, cells were starved for 18 hours in Hank's Balanced Salt solution supplemented with 0.1 μmol/L of Bafilomycin A1 (Sigma). Cells were imaged as described above and autophagosomes were counted by using NIS-Elements Advanced Research software (Nikon).

Statistics

Means were compared with unpaired Student *t* tests. Error bars represent standard error of the mean.

ORCID

Francesca Capon: http://orcid.org/0000-0003-2432-5793
Alan Irvine: http://orcid.org/0000-0002-9048-2044

CONFLICT OF INTEREST

Maja Mockenhaupt is the coordinator of the international RegiSCAR-project, which was/is funded (among others) by a consortium of pharmaceutical companies (Bayer Vital, Boehringer-Ingelheim, Cephalon, GlaxoSmithKline, MSD Sharp and Dohme, Merck, Novartis, Pfizer, Roche, Sanofi-Aventis, Servier, Tibotec, Grünenthal, Falk Pharma, UCB Biopharma, AB-Science). Maja Mockenhaupt is also a member of expert panels/advisory boards in the field of severe cutaneous adverse reaction coordinated by pharmaceutical companies (Boehringer Ingelheim, Merck, Sanofi). She has also been an expert in litigations concerning Stevens Johnson syndrome/toxic epidermal necrolysis. Helen Young is/has been a consultant or speaker to Abbott/Abbvie, Amgen, Janssen-Cilag, Leo-Pharma, Novartis, Lily, Stiefel, Teva Pharmaceuticals, and Wyeth/Pfizer.

ACKNOWLEDGMENTS

This work was supported by the Department of Health via the National Institute for Health Research comprehensive Biomedical Research Centre award to Guy's & St. Thomas' National Health Service Foundation Trust in partnership with King's College London, King's College Hospital National Health Service Foundation Trust. FC, RCT, and JNB are supported by the Medical Research Council (award MR/L011808/1). ZB and MS were supported by Orszagos Tudomanyos Kutatasi Alap (National Scientific Research Fund) grants OTKA K105985 and OTKA K111885. MM and LV are part of The International Registry of Severe Cutaneous Adverse Reaction (RegiSCAR) Consortium, funded by the European Commission (QLRT-2002-01738), GIS-Institut des Maladies Rares, and Institut National de la Santé et de la Reserche Médicale (INSERM) (4CH09G) in France and by a consortium of pharmaceutical companies. SKM is funded by a Medical Research Council Clinical Training Fellowship (MR/L001543/1). ST is supported by the King's Bioscience Institute and the Guy's and St Thomas' Charity Prize PhD Programme in Biomedical and Translational Science. NSK received a British Skin Foundation PhD studentship (grant 3007s).

SUPPLEMENTARY MATERIAL

Supplementary material is linked to the online version of the paper at www.jidonline.org, and at http://dx.doi.org/10.1016/j.jid.2016.06.618.

REFERENCES

Aasen T, Izpisua Belmonte JC. Isolation and cultivation of human keratinocytes from skin or plucked hair for the generation of induced pluripotent stem cells. Nat Protoc 2010;5:371–82.

Aksentijevich I, Kastner DL. Genetics of monogenic autoinflammatory diseases: past successes, future challenges. Nat Rev Rheumatol 2011;7:469–78.

Beer HD, Contassot E, French LE. The inflammasomes in autoinflammatory diseases with skin involvement. J Invest Dermatol 2014;134:1805–10.

Berki DM, Liu L, Choon SE, David Burden A, Griffiths CE, Navarini AA, et al. Activating CARD14 mutations are associated with generalized pustular psoriasis but rarely account for familial recurrence in psoriasis vulgaris. J Invest Dermatol 2015;135:2964–70.

de Jesus AA, Canna SW, Liu Y, Goldbach-Mansky R. Molecular mechanisms in genetically defined autoinflammatory diseases: disorders of amplified danger signaling. Annu Rev Immunol 2015;33:823–74.

Di Meglio P, Perera GK, Nestle FO. The multitasking organ: recent insights into skin immune function. Immunity 2011;35:857–69.

Gabay C, Towne JE. Regulation and function of interleukin-36 cytokines in homeostasis and pathological conditions. J Leukocyte Biol 2015;97:645–52.

Griffiths CEM, Barker JN. Psoriasis. In: Burns T, Breathnach S, Cox N, Griffiths CEM, editors. Rook's textbook of dermatology. Chichester, UK: Wiley-Blackwell; 2010. p.20.1—.60.

Guo Y, Chang C, Huang R, Liu B, Bao L, Liu W. AP1 is essential for generation of autophagosomes from the trans-Golgi network. J Cell Sci 2012;125: 1706—15.

Iannitti RG, Napolioni V, Oikonomou V, De Luca A, Galosi C, Pariano M, et al. IL-1 receptor antagonist ameliorates inflammasome-dependent inflammation in murine and human cystic fibrosis. Nat Com 2016;7:10791.

Klionsky DJ, Abdalla FC, Abeliovich H, Abraham RT, Acevedo-Arozena A, Adeli K, et al. Guidelines for the use and interpretation of assays for monitoring autophagy. Autophagy 2012;8:445—544.

Lee HM, Shin DM, Yuk JM, Shi G, Choi DK, Lee SH, et al. Autophagy negatively regulates keratinocyte inflammatory responses via scaffolding protein p62/SQSTM1. J Immunol 2011;186:1248—58.

Lee J, Kim HR, Quinley C, Kim J, Gonzalez-Navajas J, Xavier R, et al. Autophagy suppresses interleukin-1beta (IL-1beta) signaling by activation of p62 degradation via lysosomal and proteasomal pathways. J Biol Chem 2012;287:4033—40.

Lowes MA, Russell CB, Martin DA, Towne JE, Krueger JG. The IL-23/T17 pathogenic axis in psoriasis is amplified by keratinocyte responses. Trends Immunol 2013;34:174—81.

Marrakchi S, Guigue P, Renshaw BR, Puel A, Pei XY, Fraitag S, et al. Interleukin-36-receptor antagonist deficiency and generalized pustular psoriasis. N Engl J Med 2011;365:620—8.

Martinon F, Aksentijevich I. New players driving inflammation in monogenic autoinflammatory diseases. Nat Rev Rheumatol 2015;11:11—20.

Netea-Maier RT, Plantinga TS, Van De Veerdonk FL, Smit JW, Netea MG. Modulation of inflammation by autophagy: consequences for human disease. Autophagy 2016;12:245—60.

Onoufriadis A, Simpson MA, Pink AE, Di Meglio P, Smith CH, Pullabhatla V, et al. Mutations in IL36RN/IL1F5 are associated with the severe episodic inflammatory skin disease known as generalized pustular psoriasis. Am J Hum Genet 2011;89:432—7.

Ran FA, Hsu PD, Wright J, Agarwala V, Scott DA, Zhang F. Genome engineering using the CRISPR-Cas9 system. Nat Protoc 2013;8:2281—308.

Robinson MS. Adaptable adaptors for coated vesicles. Trend Cell Biol 2004;14:167—74.

Schneider CA, Rasband WS, Eliceiri KW. NIH Image to ImageJ: 25 years of image analysis. Nat Methods 2012;9:671—5.

Setta-Kaffetzi N, Simpson MA, Navarini AA, Patel VM, Lu HC, Allen MH, et al. AP1S3 mutations are associated with pustular psoriasis and impaired Toll-like receptor 3 trafficking. Am J Hum Genet 2014;94: 790—7.

Shi CS, Shenderov K, Huang NN, Kabat J, Abu-Asab M, Fitzgerald KA, et al. Activation of autophagy by inflammatory signals limits IL-1beta production by targeting ubiquitinated inflammasomes for destruction. Nat Immunol 2012;13:255—63.

Swindell WR, Sarkar MK, Liang Y, Xing X, Gudjonsson JE. Cross-disease transcriptomics: Unique IL-17A signaling in psoriasis lesions and an autoimmune PBMC signature. J Invest Dermatol 2016;136:1820—30.

Wolf J, Ferris LK. Anti-IL-36R antibodies, potentially useful for the treatment of psoriasis: a patent evaluation of WO2013074569. Expert Opin Ther Pat 2014;24:477—9.

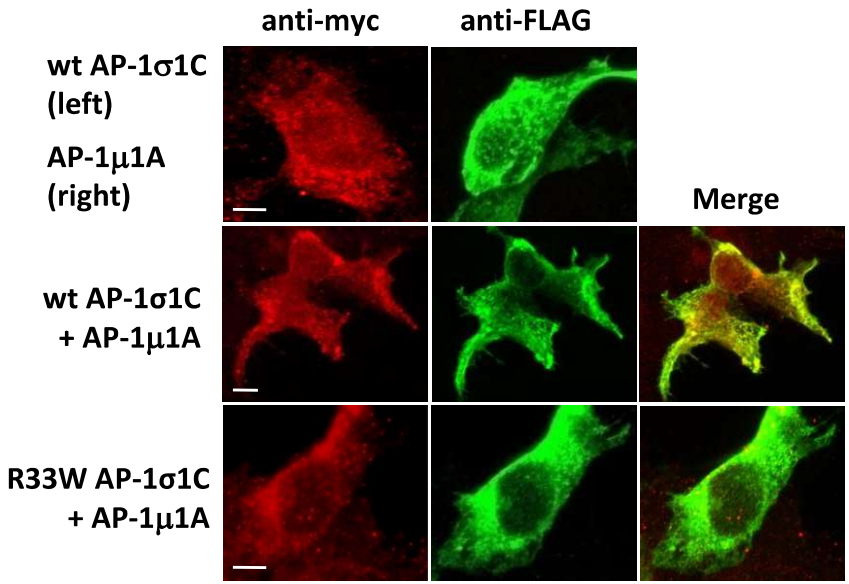

Figure S1. *AP1S3* mutation disrupts the interaction between σ1C and μ1A subunits of AP-1.
HEK293 cells were transfected with myc-tagged *AP1S3* and FLAG-tagged *AP1M1* constructs. The localisation of AP-1σ1C and AP-1μ1A proteins was visualised by confocal fluorescence microscopy. The images are representative of data obtained in ≥15 cells per experiment. Scale bar 5μm.

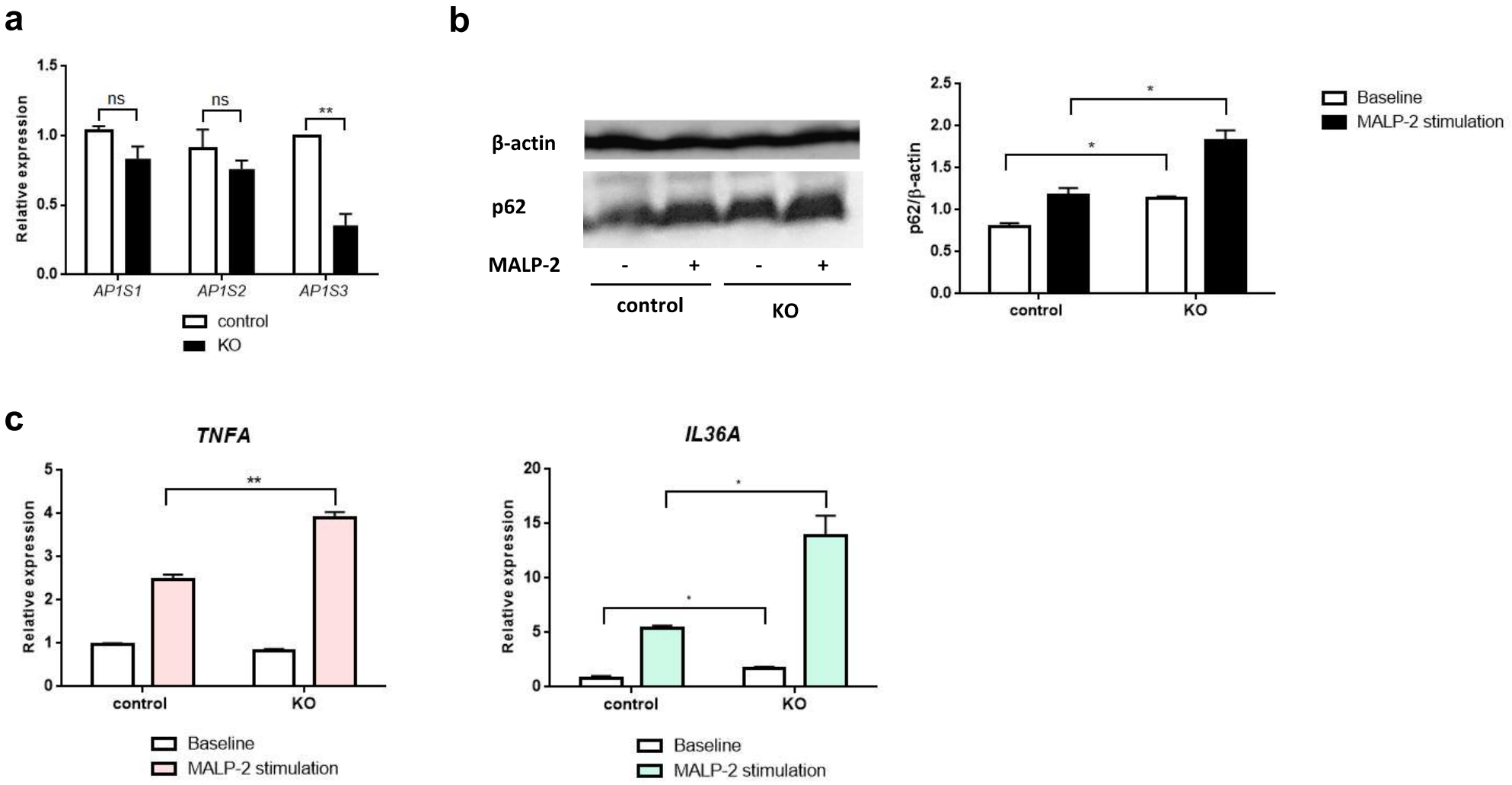

Figure S2. *AP1S3* deficient HaCaT keratinocytes exhibit abnormal p62 accumulation and enhanced TLR-2/6 signalling.
Following AP1S3 silencing by CRISPR/Cas9 genome editing (a), HaCaT keratinocytes were stimulated with MALP-2. p62 accumulation in control and knockout (KO) cells was monitored by western blotting and densitometry (b), and gene expression was determined by real-time PCR (c). The data are representative of results obtained in at least two independent experiments, and are presented as mean ± SEM of duplicate stimulations. *P≤0.05, **P≤0.01.

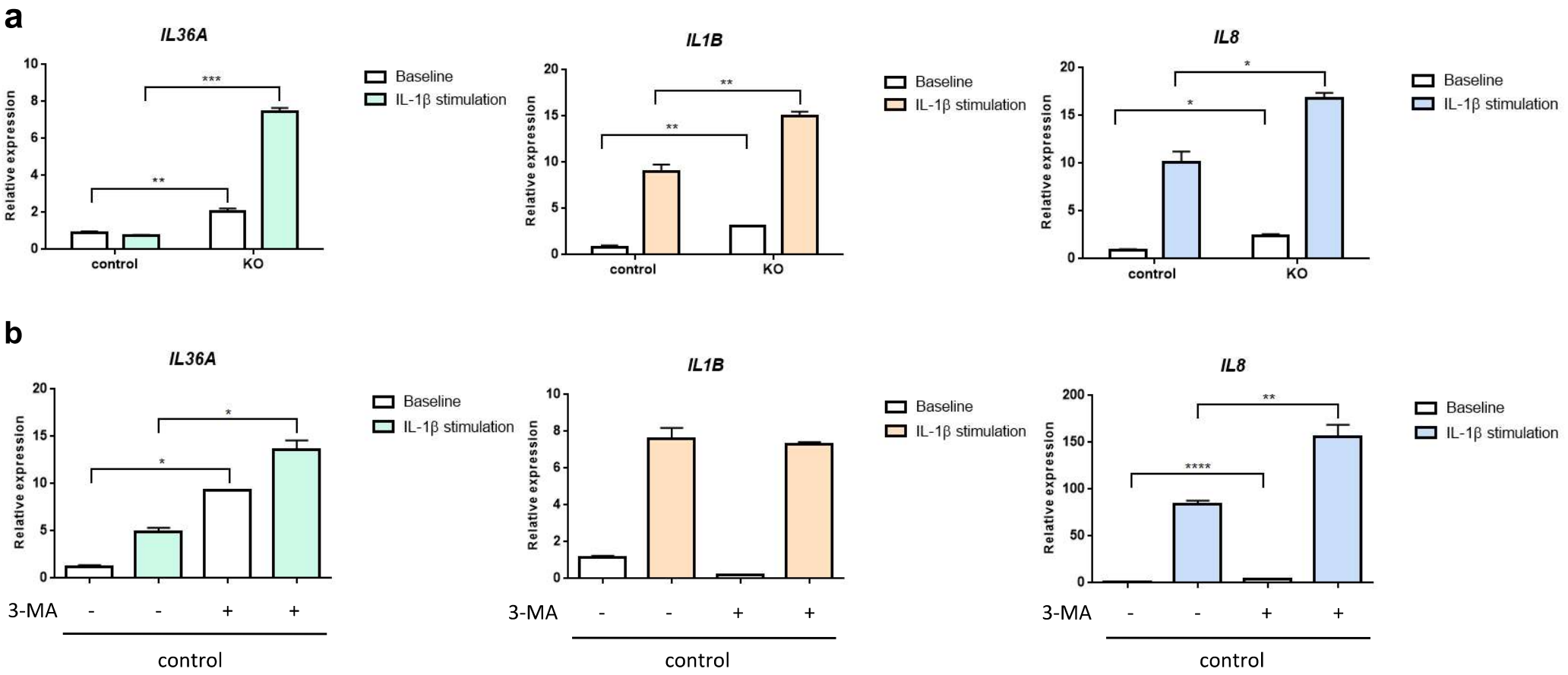

Figure S3. *AP1S3* deficient HaCaT keratinocytes exhibit an abnormal immune profile, which can be recapitulated by autophagy inhibition.

(a) Following *AP1S3* silencing by CRISPR/Cas-9 genome editing, control and *AP1S3* knockout (KO) cells were stimulated with IL-1β and gene expression was determined by real-time PCR. (b) Cells were cultured in the presence or absence of 3-MA and subsequently stimulated with IL-1β. Gene expression was determined by real-time PCR. All data are representative of results obtained in 2 independent experiments and are presented as mean ± SEM of triplicate measurements. **P≤0.01, ***P≤0.001, ****P≤0.0001.

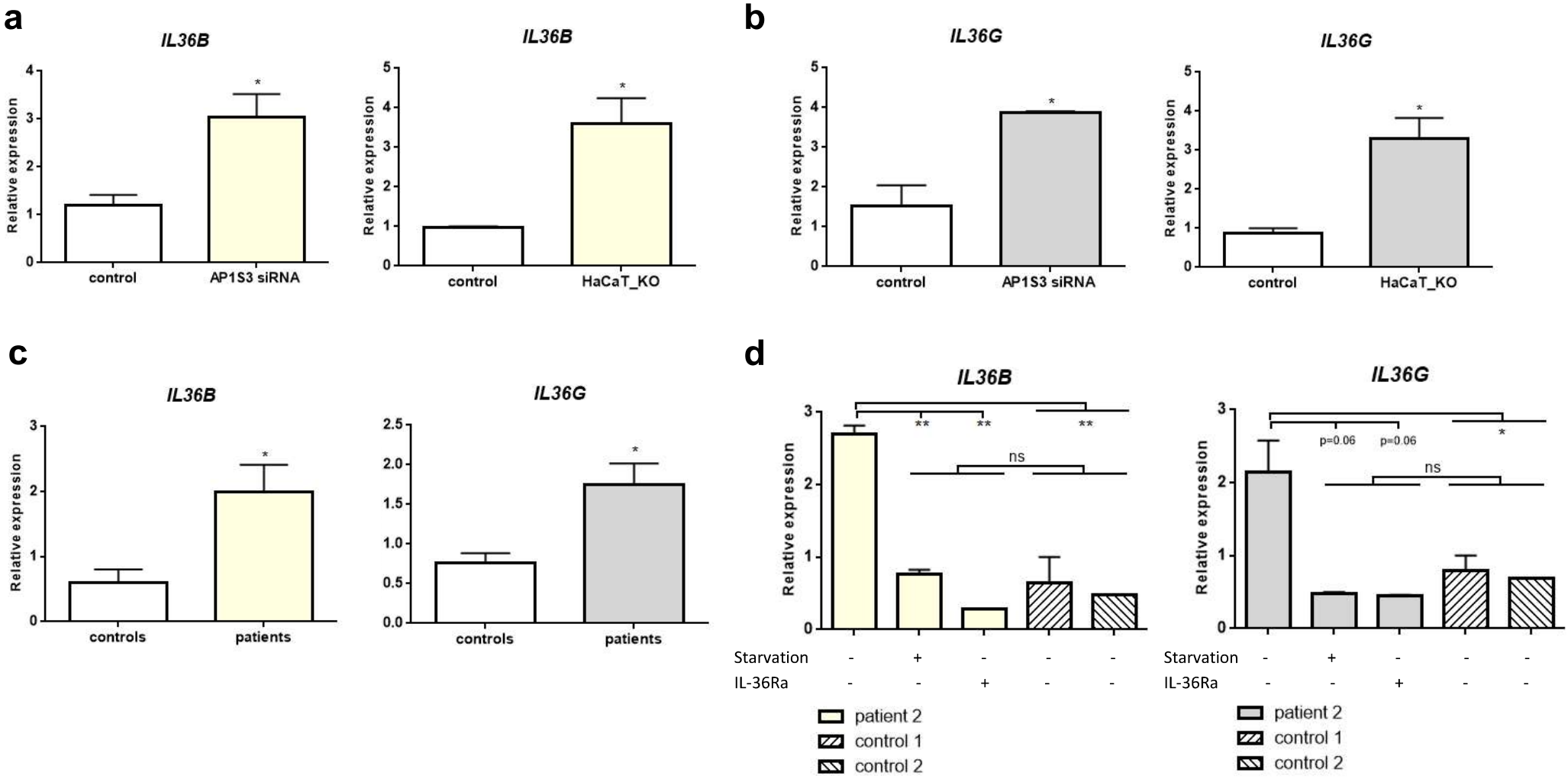

Figure S4. *IL36B* and *IL36G* expression is increased in *AP1S3* deficient cells. (a-b) Baseline gene expression was determined by real-time PCR, following *AP1S3* silencing by transient transfection of siRNA pools into primary keratinocytes (*AP1S3* siRNA) or CRISPR/Cas-9 genome editing of HaCaT keratinocytes (HaCaT_KO). Data are presented as mean ± SEM of triplicate measurements. (c) Baseline *IL36B* and *IL36G* expression was measured in primary keratinocytes from 2 unrelated patients harbouring *AP1S3* mutations and 2 healthy controls. The data are presented as mean ± SEM of duplicate measurements. (d) Primary keratinocytes were starved to induce autophagy or cultured in the presence of IL-36Ra. The data are presented as mean ± SEM of triplicate measurements, obtained in 1 patient and 2 healthy controls. KO, knockout. *P≤0.05, **P≤0.01.

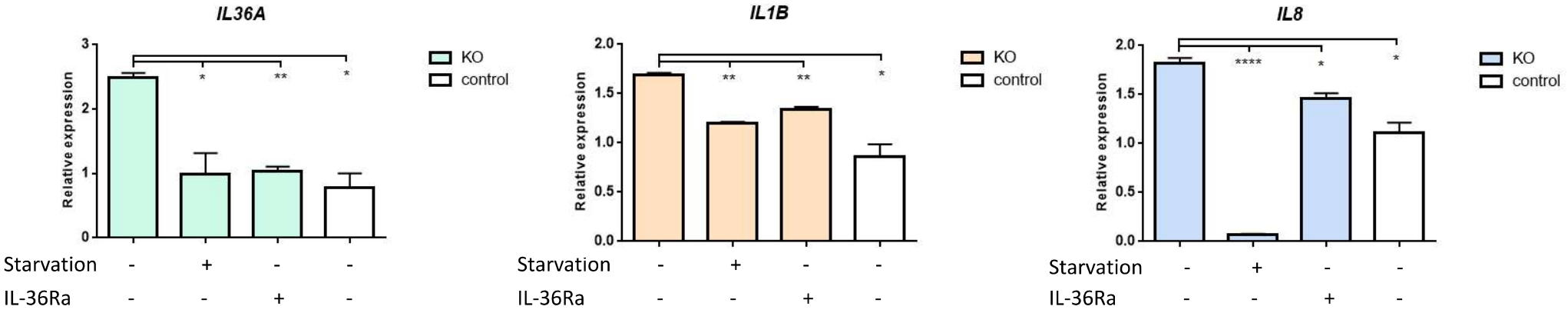

Figure S5. Autophagy induction and IL-36 blockade have anti-inflammatory effects on *AP1S3* deficient HaCaT keratinocytes.
Control and *AP1S3* knockout (KO) HaCaT keratinocytes were starved to induce autophagy or cultured in the presence of IL-36Ra. Gene expression was determined by real-time PCR. The data are representative of results obtained in two independent experiments and are presented as mean ± SEM of triplicate measurements. *P≤0.05, **P≤0.01, ****P≤0.0001.

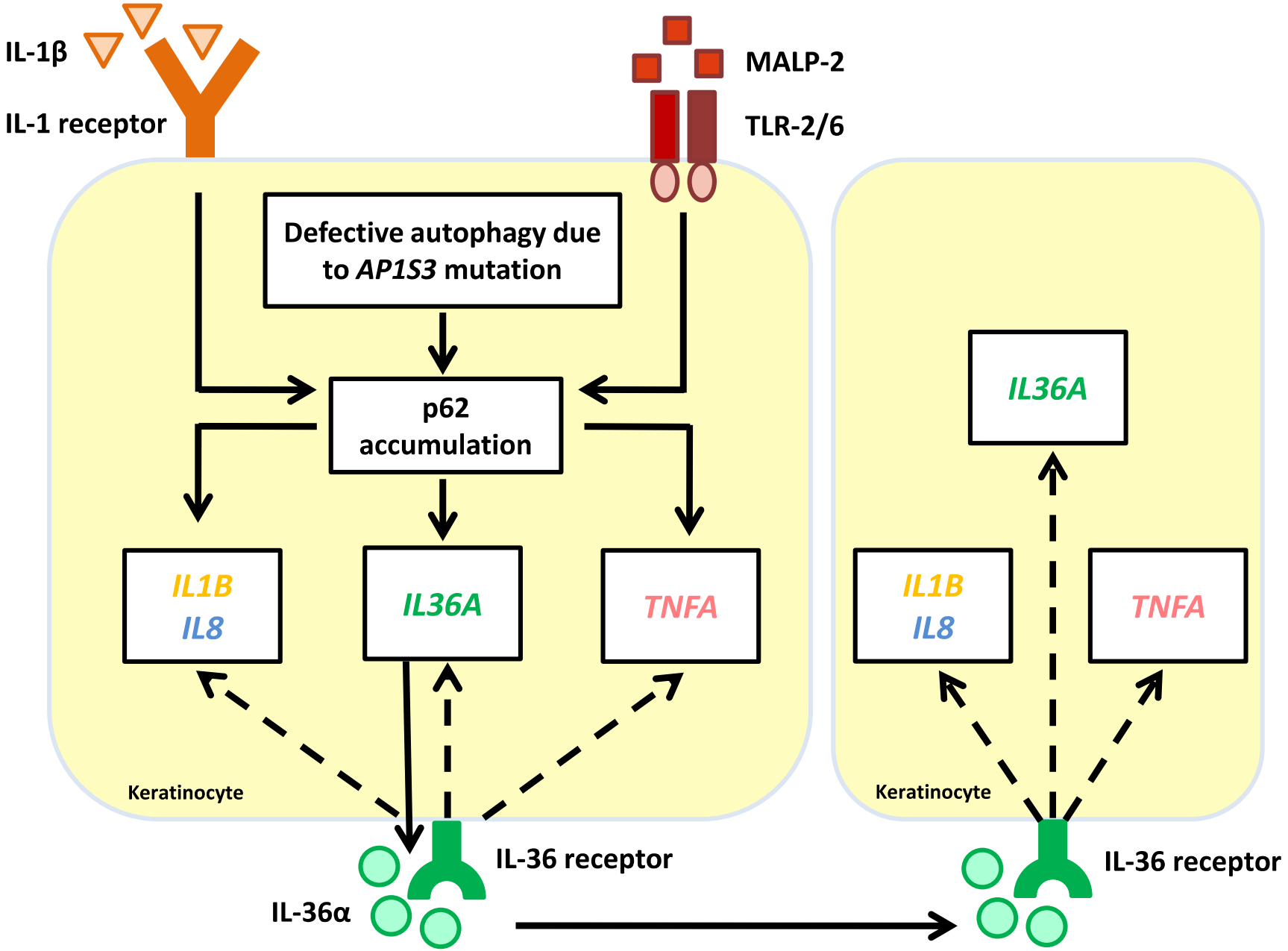

Figure S6. Proposed pathogenic model illustrating the pro-inflammatory effects of *AP1S3* deficiency.
AP1S3 mutations disrupt autophagy, causing abnormal accumulation of p62 and increased cytokine expression downstream of the IL-1 receptor and TLR-2/6. Among the cytokines that are up-regulated, IL-36 drives a positive feedback loop by inducing *IL36A*, *IL1B, IL8* and *TNF* expression.

Supplementary Table S1: Study cohort summary statistics

	Clinical Diagnosis			Sex		Ethnicity		
	GPP	**ACH**	**PPP**	**M**	**F**	**European**	**Asian**	**Other**
Patient n.(%)	43 (50.6%)	1 (1.2%)	41 (48.2%)	26 (30.6%)	59 (69.4%)	53 (62.3%)	27 (31.8%)	5 (5.9%)

GPP: Generalised pustular psoriasis; ACH: Acrodermatitis continua of Hallopeau; PPP: Palmar plantar pustulosis. NB: all cases were pre-screened to exclude the presence of bi-allelic *IL36RN* mutations

Supplementary Table S2: Mutation status and disease features observed in two sisters with generalised pustular psoriasis

Patient id	**Sex**	***AP1S3* genotype**	***IL36RN* genotype**	**Age of onset**	**Disease course**	**PV concurrence**	**Systemic involvement**	**Drug response**
T030865	F	p.Phe4Cys/-	p.Ser113Leu/-	<1	Multiple flares	No	Yes	Partial response to infliximab
T030866	F	-/-	p.Ser113Leu/-	34	Single flare	No	Yes	Remission with methotrexate

Systemic involvement during flares was defined as the concurrence of fever>38°C and a neutrophil count >15*10^9/ml; PV: Psoriasis vulgaris

Supplementary Table S3: Details of patient recruitment centres

Patient ethnicity	Recruiting centre
European	European Registry of Severe Cutaneous Adverse Reactions
	Glasgow Western Infirmary, Glasgow, UK
	Helsinki University Central Hospital, Helsinki, Finland
	Our Lady's Children's Hospital, Dublin, Ireland
	Radboud University Nijmegen Medical Centre, Nijmegen, The Netherlands
	Royal Prince Alfred Hospital, Camperdown, Australia
	St John's Institute of Dermatology, London, UK
	University Hospital, Galway, Ireland
	University of Manchester, Manchester, UK
	University of Szeged, Szeged, Hungary
Asian	Birmingham Children's Hospital, Birmingham, UK
	Helsinki University Central Hospital, Helsinki, Finland
	Hospital SultanahAminah, Johor Bahru, Malaysia
	Hospital UniversitariValld'Hebron, Barcelona, Spain
	National Skin Centre, Singapore
Other	St John's Institute of Dermatology, London, UK

Supplementary Table S4: Oligonucleotide sequences used in the study

Target region	Primer ID	Sequence (5' to 3')	Annealing Temp (°C)	Application
AP1S3 Exon 1	AP1S3_ex1_Fwd	CTCCAGCGCTCCTTGCTC	56	Genome editing validation
	AP1S3_ex1_Rev	GGATCGAATGAATGAATGGA		
AP1S3 Exon 2	AP1S3_ex2_Fwd	TTTCAGTGTCTTTGCAGAACG	59	Genome editing validation
	AP1S3_ex2_Rev	CCCCAGCCTTCAAAGATTTC		
AP1S3 Exon 3	AP1S3_ex3_Fwd	GACTGCATATTCGTGGGAAAA	59	Genome editing validation
	AP1S3_ex3_Rev	GCTGAGATGGGGACTGTAGC		
AP1S3 Exon 4	AP1S3_ex4_Fwd	GGCAGATGTTTCCCCTGATA	59	Genome editing validation
	AP1S3_ex4_Rev	TCATCATCATCATCATCATCTTTC		
AP1S3 Exon 5	AP1S3_ex5_Fwd	ATTTCACAGTCTGCGGAAGG	59	Genome editing validation
	AP1S3_ex5_Rev	TGGGAGGCGTTGCTTATTTA		
AP1S2 Exon 2	AP1S2_ex2_Fwd	CATGTAAATGCCCCATCCCC	59	Sequencing of potential CRISPR off-target site
	AP1S2_ex2_Rev	TCACTGAAGTCTGCAATTTCCT		
AP1S1 Exon 2	AP1S1_ex2_Fwd	GGGCTGGATGTTGGAAGAAA	59	Sequencing of potential CRISPR off-target site
	AP1S1_ex2_Rev	GTCCTCCAGATGTCCTCAGC		
TREM1	TREM1_Fwd	CTGAAAAGCACAGGGTCAGG	56	Sequencing of potential CRISPR off-target site
	TREM1_Rev	ATGGATGTGGCTGGAAGTCA		
PALD1	PALD1_Fwd	TTTTGGTGAGGGTGCAAGC	59	Sequencing of potential CRISPR off-target site
	PALD1_Rev	CAGAAGGTGGAAAAGTGACCA		

FBXL5	FBXL5_Fwd	AGGACATTGTTGGACTAAGGACT	56	Sequencing of potential CRISPR off-target site
	FBXL5_Rev	TGAAGTAGGGCAGATCTTGGT		
TG	TG_Fwd	GCCTTCAACTCTGCCTTTATTCA	56	Sequencing of potential CRISPR off-target site
	TG_Rev	AAACCACAGAGCCAGCAGAA		
AP1S3	AP1S3_Fwd	GCTCTTCAGTCGACAAGGGA	60	Real-time PCR
	AP1S3_Rev	GCGTCAAGAGCTCATTGTCC		
AP1S2	AP1S2_Fwd	ACTGCAGGAGGAAGCTGAAAC	60	Real-time PCR
	AP1S2_Rev	GAAGCGGCTTAGCAAAACAGT		
AP1S1	AP1S1_Fwd	ATACTTTGGCAGTGTGTGCG	60	Real-time PCR
	AP1S1_Rev	CCTCTTGCAGTAGGTCAGCC		
TNF	TNF_Fwd	CCCAGGGACCTCTCTCTAATCA	60	Real-time PCR
	TNF_Rev	GCTACAGGCTTGTCACTCGG		
IL8	IL8_Fwd	TTGGCAGCCTTCCTGATTTC	60	Real-time PCR
	IL8_Rev	AACTTCTCCACAACCCTCT		
IL1B	IL1B_Fwd	GCCCTAAACAGATGAAGTGCTC	60	Real-time PCR
	IL1B_Rev	GAACCAGCATCTTCCTCAG		
IL36A	IL36A_Fwd	GGCCTGAATGGACTCAATCT	60	Real-time PCR
	IL36A_Rev	ACTTCACAGGCTCGGGTTG		
IL36B	IL36B_Fwd	CAGCATTAAGCCTGTCACTC	60	Real-time PCR
	IL36B_Rev	GCACAGAAGAGACAGAGATC		
IL36G	IL36G_Fwd	GGGCCGTCTATCAATCAATG	60	Real-time PCR
	IL36G_Rev	TGATAACAGCAACAGTGACTG		

AP1S3 exon 2	sgRNA-top	CACCGTTCAGATTATTCTCTCCCG	n/a	CRISPR guide RNA
AP1S3 exon 2	sgRNA-bottom	AAACCGGGAGAGAATAATCTGAAC	n/a	CRISPR guide RNA
Non-targeting	ON-TARGET plus Non-targeting pool siRNA	UGGUUUACAUGUCGACUAA UGGUUUACAUGUUGUGUGA UGGUUUACAUGUUUUCUGA UGGUUUACAUGUUUUCCUA	n/a	Control oligonucleotides for siRNA mediated gene silencing
AP1S3 coding region	ON-TARGET plus SMARTpool Human *AP1S3*siRNA	CUACACAUGUUCUGGAUAA AAGAAGAUCACCCGGGAAA GGAAAUUACGGCUACAGAA CAUUCAUAUUAGAGUGGUU	n/a	siRNA mediated gene silencing
AP1M1 coding region	AP1M1_HindIII_Fwd AP1M1_BamHI_Rev	GTAAAGCTTATGTCCGCCAGCGCCGTCTAC GATGGATCCCTGGGTCCGGAGCTGGTAATC	60	Cloning of *AP1M1* into c-Flag pcDNA3 plasmid

3.2. An analysis of IL-36 signature genes and individuals with *IL1RL2* knockout mutations validates IL-36 as a psoriasis therapeutic target

PSORIASIS

An analysis of IL-36 signature genes and individuals with *IL1RL2* knockout mutations validates IL-36 as a psoriasis therapeutic target

Satveer K. Mahil,[1] Marika Catapano,[1,2] Paola Di Meglio,[1,3] Nick Dand,[1] Helena Ahlfors,[4] Ian M. Carr,[5] Catherine H. Smith,[1] Richard C. Trembath,[1] Mark Peakman,[6] John Wright,[7] Francesca D. Ciccarelli,[2,8]* Jonathan N. Barker,[1]* Francesca Capon[1]†

Interleukin (IL)–36α, IL-36β, and IL-36γ are innate mediators of acute epithelial inflammation. We sought to demonstrate that these cytokines are also required for the pathogenesis of plaque psoriasis, a common and chronic skin disorder, caused by abnormal T helper 17 (T_H17) cell activation. To investigate this possibility, we first defined the genes that are induced by IL-36 cytokines in primary human keratinocytes. This enabled us to demonstrate a significant IL-36 signature among the transcripts that are up-regulated in plaque psoriasis and the susceptibility loci associated with the disease in genome-wide studies. Next, we investigated the impact of in vivo and ex vivo IL-36 receptor blockade using a neutralizing antibody or a recombinant antagonist. Both inhibitors had marked anti-inflammatory effects on psoriatic skin, demonstrated by statistically significant reductions in IL-17 expression, keratinocyte activation, and leukocyte infiltration. Finally, we explored the potential safety profile associated with IL-36 blockade by phenotyping 12 individuals carrying knockout mutations of the IL-36 receptor gene. We found that normal immune function was broadly preserved in these individuals, suggesting that IL-36 signaling inhibition would not substantially compromise host defenses. These observations, which integrate the results of transcriptomics and model system analysis, pave the way for early-stage clinical trials of IL-36 antagonists.

INTRODUCTION

Interleukin (IL)–36α, IL-36β, and IL-36γ are a group of IL-1 family cytokines that signal through a common dimeric receptor, composed of the IL-36 receptor (IL-36R) and IL-1R accessory protein (IL-1RAcP) subunits. The activation of this complex triggers nuclear factor κB and mitogen-activated protein kinase (MAPK) signaling, leading to the production of proinflammatory molecules such as IL-1α/β, IL-6, and IL-8 (*1*). Conversely, binding of IL-36R by the IL-36R antagonist (IL-36Ra) (encoded by the *IL36RN* gene) blocks downstream signal transduction (*1*). The importance of this immunomodulatory mechanism was underscored by the discovery of loss-of-function *IL36RN* mutations in patients with generalized pustular psoriasis (GPP) (*2*). This is a severe autoinflammatory disorder, which is characterized by recurrent episodes of neutrophilic skin pustulation and systemic inflammation (manifesting as an acute phase response with neutrophilia) (*3*). Notably, most GPP patients also present with plaque psoriasis (hence, psoriasis), a chronic and disfiguring skin disease that affects 1 to 3% of the population (*3*).

Research carried out in the last decade has demonstrated that the abnormal activation of T helper 17 (T_H17) lymphocytes is a major disease driver in psoriasis (*4*). At the same time, several lines of evidence suggest that IL-36 cytokines are also likely to have a pathogenic role. First, individuals with GPP show elevated IL-36 expression in the skin (*5*) and present a risk of psoriasis that is 10 times higher than that observed in the general population (*6*). Second, the gene encoding the IL-36R (*IL1RL2*) maps to a locus showing genome-wide significant association with psoriasis (*7*). Finally, work carried out in animal models has demonstrated that IL-36 cytokines can activate dendritic cells and thus promote T_H17 lymphocyte polarization (*8*). Because the IL-17 molecules released by T_H17 cells can, in turn, up-regulate IL-36 production, it has been proposed that the two cytokines drive a powerful feedback loop, which effectively propagates skin inflammation (*9*).

Together, the above observations suggest that germline *IL36RN* mutations cause widespread up-regulation of IL-36 signaling and severe autoinflammation (GPP), whereas localized, T_H17-dependent overexpression of IL-36 cytokines amplifies cutaneous immune responses in psoriasis. Thus, we propose that IL-36 is a shared disease driver, which contributes to the onset of plaque and pustular psoriasis through different molecular mechanisms.

Here, given that the role of IL-36 in GPP is well established, we have investigated IL-36 signaling as a pathogenic mediator and therapeutic target in psoriasis. By following up the results of IL-36 transcription profiling with targeted inhibition experiments, we demonstrated that in vivo and ex vivo IL-36 blockade can reverse the inflammatory phenotype of psoriasis skin lesions. We also showed that mutations that abolish IL-36 signaling do not substantially compromise human immune function, suggesting that pharmacological IL-36 blockade is likely to have an acceptable safety profile.

[1]Division of Genetics and Molecular Medicine, King's College London, London SE1 9RT, UK. [2]Cancer Systems Biology Laboratory, Francis Crick Institute, London NW1 1AT, UK. [3]AhRimmunity Laboratory, Francis Crick Institute, London NW1 1AT, UK. [4]UCL Institute of Child Health, Great Ormond Street Hospital for Children NHS Foundation Trust, London WC1N 3JH, UK. [5]School of Medicine, University of Leeds, Leeds, LS9 7TF, UK. [6]Department of Immunobiology, King's College London, London SE1 9RT, UK. [7]Bradford Royal Infirmary, Bradford Institute for Health Research, Bradford BD9 6RJ, UK. [8]Division of Cancer Studies, King's College London, London SE1 1UL, UK.
*These authors contributed equally to this work.
†Corresponding author. Email: francesca.capon@kcl.ac.uk

RESULTS

IL-36 signature genes are up-regulated in psoriatic skin lesions and enriched within psoriasis susceptibility loci

To explore the role of IL-36 in psoriasis, we first assessed the presence of an IL-36 signature in the disease transcriptome. To date, IL-36 target genes have only been profiled in a single microarray study based on the stimulation of keratinocyte cultures with unprocessed IL-36 cytokines

(*10*). Because these precursor molecules were later found to have minimal biological activity (*11*), the power to detect differential expression was limited. Here, we sought to generate a reference IL-36 transcriptome through the RNA sequencing (RNA-seq) of healthy primary keratinocytes treated with bioactive IL-36α, IL-36β, or IL-36γ (table S1). The principal components analysis of our data set demonstrated a complete separation between treated ($n = 3$ for each cytokine) and untreated samples ($n = 3$) as well as an overlap between the profiles of keratinocytes stimulated with individual cytokines (Fig. 1A). This pattern was confirmed by unsupervised hierarchical clustering (Fig. 1B), suggesting important similarities between the three IL-36 transcriptomes.

We found that 4096, 4459, and 3468 genes were differentially expressed [false discovery rate (FDR), <0.05] upon treatment with IL-36α, IL-36β, and IL-36γ, respectively (Fig. 1C). Of these, 207, 352, and 229 were up-regulated by at least twofold (Fig. 1C and table S2). In keeping with the results of the principal components analysis and hierarchical clustering, we observed a substantial overlap between these data sets, with 182 genes (hereafter referred to as the *IL36_182* set) induced by all three cytokines (Fig. 1C). These included previously described IL-36–dependent loci (*CCL20*, *CXCL1*, *IL8*, *DEFB4A*, and *STEAP4*) (*5*, *10*), as well as novel targets such as the chemotactic proteins *S100A7*, *S100A8*, and *S100A9* and the phospholipase *PLA2G4D*, which generates the lipid antigens presented by Langerhans cells (Fig. 1C and table S2) (*12*).

In keeping with the notion that IL-36 is a dominant cytokine in the GPP skin transcriptome, we found 58 *IL36_182* genes among the 500 that were most significantly up-regulated in a recently described (*5*) GPP cohort (Fig. 1D). We then reanalyzed a publicly available psoriasis data set (*13*) and found 68 *IL36_182* loci among the 500 most overexpressed genes (Fig. 1D). The overlap between the *IL36_182* set and the genes up-regulated in psoriasis or GPP was highly significant ($P < 10^{-30}$ for both diseases), but the same did not apply to the gene set induced by IL-4 ($P > 0.03$ for both GPP and psoriasis), a T_H2 cytokine that was analyzed as a negative control (fig. S1).

To complement the above observations, we also examined the overlap between IL-36 target genes and psoriasis susceptibility intervals previously detected in genome-wide association studies (GWAS). We found that the *IL36_182* set was significantly enriched among the genes that lie within psoriasis-associated regions ($P = 9.1 \times 10^{-4}$), but not among those that map to unrelated susceptibility loci, linked to autism or schizophrenia ($P > 0.05$ for both diseases) (Fig. 1E). Thus, our analyses identified a clear IL-36 gene signature in GPP and psoriasis.

IL-36 signature genes cluster to pathways implicated in the pathogenesis of psoriasis

To further explore the biological significance of our differential expression findings, we undertook a gene set enrichment analysis of the IL-36α, IL-36β, and IL-36γ transcriptomes. This demonstrated a marked overrepresentation of inflammatory processes implicated in the pathogenesis of psoriasis. The pathway showing the most significant enrichment in our data set was "Role of IL-17A in psoriasis," with an FDR of $<10^{-10}$ observed for all three cytokines. In keeping with this result, a reanalysis of a published IL-17 transcriptome (*14*) revealed that 26 of 46 (56%) of the genes that are up-regulated by IL-17 in keratinocytes are part of the *IL36_182* set (table S3).

Very significant FDRs were also detected for pathways related to the infiltration of inflammatory elements into lesional skin ("Granulocyte adhesion and diapedesis" and "Agranulocyte adhesion and diapedesis;" FDR < 10^{-6} for both) and the activation of p38 MAPK signaling (FDR ≤ 10^{-5}) (Fig. 2A and table S4). There was a marked overlap between the processes driven by IL-36α, IL-36β, and IL-36γ, with 45 pathways enriched in all three transcriptomes ($P < 10^{-30}$ for all pairwise comparisons) (Fig. 2B).

We next extended our gene set enrichment analysis to the disease data sets. As expected, we found a substantial overlap between the pathways that were driven by IL-36 and those that were enriched in the GPP transcriptome ($P = 9.4 \times 10^{-31}$) (fig. S2). We then examined the psoriasis data set, where we identified 71 enriched pathways (FDR < 0.05), 37 (52%) of which were shared with the IL-36 transcriptome ($P = 5.8 \times 10^{-35}$) (Fig. 2C and table S4). In keeping with the results of the differential expression analysis, we found that the genes underlying these enrichment signals were all part of the *IL36_182* set (table S4).

To validate the effects of IL-36 cytokines on genes that are relevant to the pathogenesis of psoriasis, we stimulated keratinocyte cultures obtained from additional healthy donors ($n = 3$). We focused our attention on a representative set of loci (highlighted in red font in Fig. 1C) that were markedly up-regulated in psoriatic skin and mapped to pathways that were enriched in the disease transcriptome. These included *IL36G*, *S100A7*, and *LCN2* ("Role of IL-17A signaling in psoriasis") and *CCL20*, *IL8*, and *MMP9* ("Granulocyte/agranulocyte adhesion and diapedesis"), as well as *IRAK2* and *PLA2G4D* ("p38 MAPK signaling"). Real-time PCR analyses confirmed that these genes were all strongly up-regulated by IL-36α, IL-36β, and IL-36γ (Fig. 3A). The induction was especially robust for *S100A7* (all fold changes > 50) and *IL36G* (fold changes > 8.5). The latter result was also validated at the protein level (Fig. 3B), suggesting the presence of a feedforward loop that sustains IL-36 expression in inflamed skin. These results indicate that IL-36 cytokines [produced upon infection or trauma (fig. S3)] amplify keratinocyte inflammatory responses by up-regulating their own expression and that of molecules which attract T_H17 cells (CCL20) and directly or indirectly potentiate IL-17 signaling (S100A7, LCN2, and PLA2G4D) (fig. S4).

In vivo IL-36R blockade improves the phenotypic appearance of murine psoriasiform dermatitis

Having demonstrated that IL-36 cytokines drive immune pathways that are critical to the pathogenesis of psoriasis, we proceeded to assess the anti-inflammatory effects of IL-36 signaling inhibition. We first investigated the potential of IL-36 blockade in imiquimod-induced psoriasiform dermatitis, an IL-17–mediated mouse model of the disease, which is widely used in preclinical studies (*15*, *16*). As expected, we found that imiquimod administration resulted in an inflammatory skin phenotype characterized by increased acanthosis (epidermal thickness) (Fig. 4, A and B), abundant leukocyte infiltration (Fig. 4, C and D), up-regulation of IL-17–producing T cells (Fig. 4E and fig. S5), and IL-17 mRNA (Fig. 4F). These pathological manifestations, however, were substantially mitigated by 48-hour pretreatment with an anti–IL-36R neutralizing antibody.

First, the mice that had received the IL-36R blocking antibody presented with less severe skin lesions compared to littermates treated with an immunoglobulin G2a (IgG2a) isotype control (Fig. 4A). IL-36 inhibition was also associated with a ~30% reduction in acanthosis, which was accompanied by a comparable decrease in scale thickness (Fig. 4A). This was consistent with the observed up-regulation of *Krt10* (a marker of keratinocyte terminal differentiation) and the reduced expression of *Krt16* (a marker of keratinocyte hyperproliferation) (Fig. 4B).

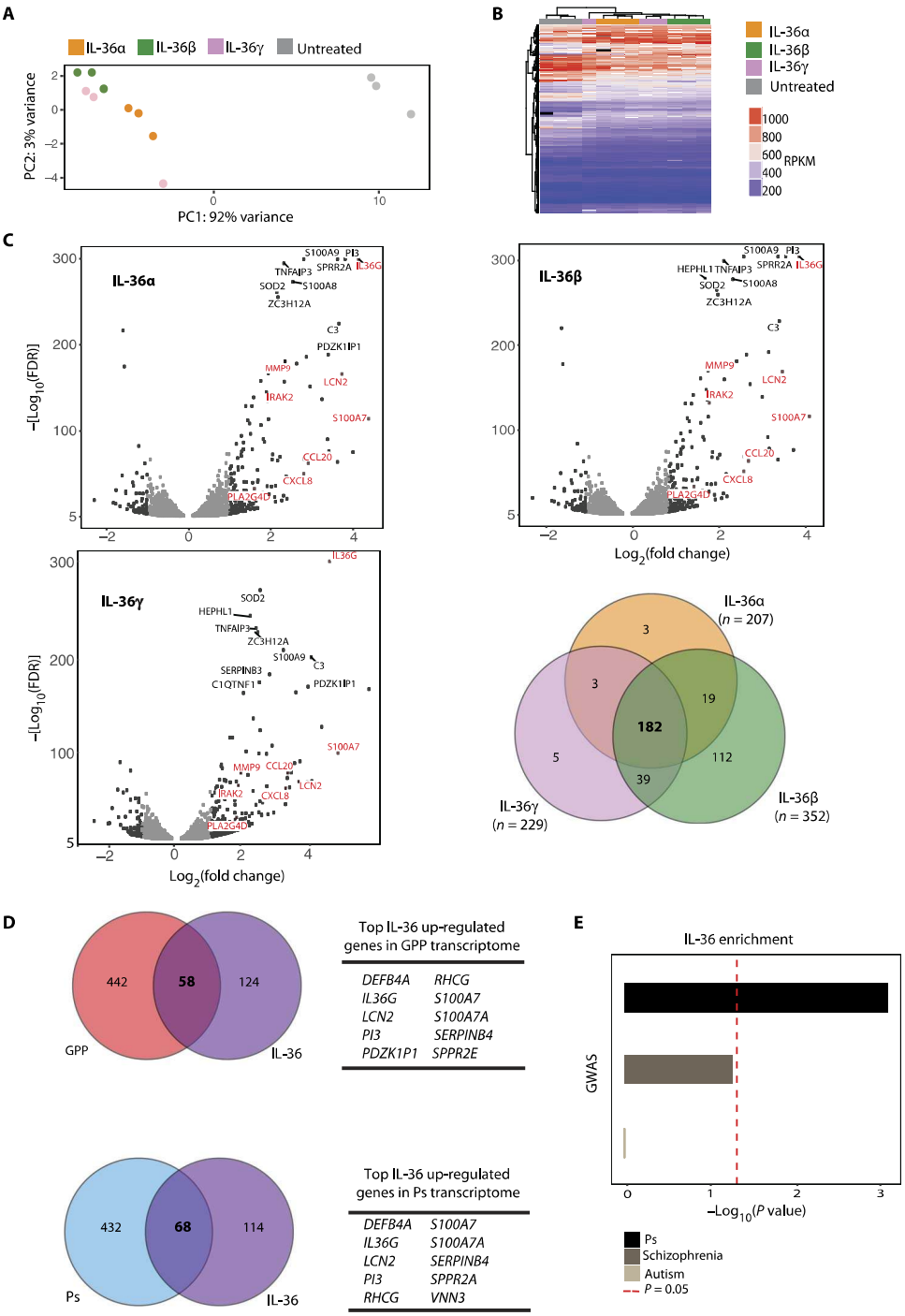

Fig. 1. Identification of IL-36 signature genes in human keratinocytes. (**A**) Principal components analysis of RNA-seq data from IL-36–treated and IL-36–untreated keratinocytes. Each dot represents an experimental replicate. (**B**) Heat map generated from unsupervised clustering of differentially expressed genes (FDR < 0.05) transcript levels. RPKM, reads per kilobase per million mapped reads. (**C**) Volcano plots show the genes that are most strongly induced by IL-36 treatment. Black dots refer to genes showing a $\log_2|$fold change$|$ > 1. Labels indicate the 10 most significantly up-regulated genes in each data set (black font) and the loci selected for real-time polymerase chain reaction (PCR) validation (red font). The Venn diagram displays the intersection of up-regulated genes (FDR < 0.05; fold change ≥ 2) across the IL-36α, IL-36β, and IL-36γ transcriptomes. The number of up-regulated genes for each data set is reported in parentheses. (**D**) The Venn diagrams show the intersection of the core IL-36 transcriptome (*IL36_182* set) with the genes overexpressed in GPP or psoriasis (Ps) skin lesions. The 10 IL-36 signature genes that are most significantly up-regulated in the psoriasis and GPP data sets are listed beside each diagram. (**E**) Bar chart showing the overrepresentation of the *IL36_182* set among genes lying within psoriasis susceptibility regions detected in GWAS. Schizophrenia and autism susceptibility intervals were analyzed as negative controls.

Second, flow cytometry analyses of skin cell suspensions demonstrated a substantial decrease in neutrophil infiltration in mice treated with the anti–IL-36R antibody (Fig. 4C). These animals also showed a substantial decline in the number of γδ T cells (Fig. 4D), which was especially pronounced for the IL-17–producing subpopulation (Fig. 4E). This decrease, which was mirrored by a reduced accumulation of IL-17$^+$ αβ T lymphocytes (fig. S5), was especially noteworthy, given the key pathogenic role of IL-17$^+$ γδ T cells in imiquimod-induced dermatitis (*17*).

Finally, and in keeping with the diminished infiltration of inflammatory elements, real-time PCR analysis of lesional skin showed reduced cytokine (*Il36g*, *Il17a*, *Il22*, *Tnf*, *Csf2*, and *Csf3*) and chemokine (*Cxcl1*, *Cxcl2*, and *Cxcl5*) expression in mice treated with the anti–IL-36R antibody (Fig. 4F). Together, these results show that in vivo IL-36 signaling inhibition has powerful anti-inflammatory effects on psoriasiform dermatitis.

Ex vivo IL-36R blockade improves the inflammatory phenotype of human psoriasis skin

To further investigate the therapeutic potential of IL-36 blockade, we investigated a validated ex vivo model of human psoriasis, which is based on the short-term culture (24 hours) of paired skin biopsies, obtained from lesional and nonlesional skin of patients (*18*). This system reflects the complexity of the disease and effectively recapitulates the pathogenic cross-talk between keratinocytes and immune cells. Here, real-time PCR analysis of cultures obtained from five independent patients confirmed the up-regulation of *IL36G* and *IL17A* in lesional skin (Fig. 5A). Supplementation of the culture medium with recombinant IL-36Ra markedly reduced the overexpression of these cytokines, alongside that of chemokines such as *IL8* and *CCL20* (Fig. 5A). The treatment also reduced the levels of *KRT16* while increasing *KRT10* expression (Fig. 5A). Parallel ELISA measurements confirmed that IL-36Ra

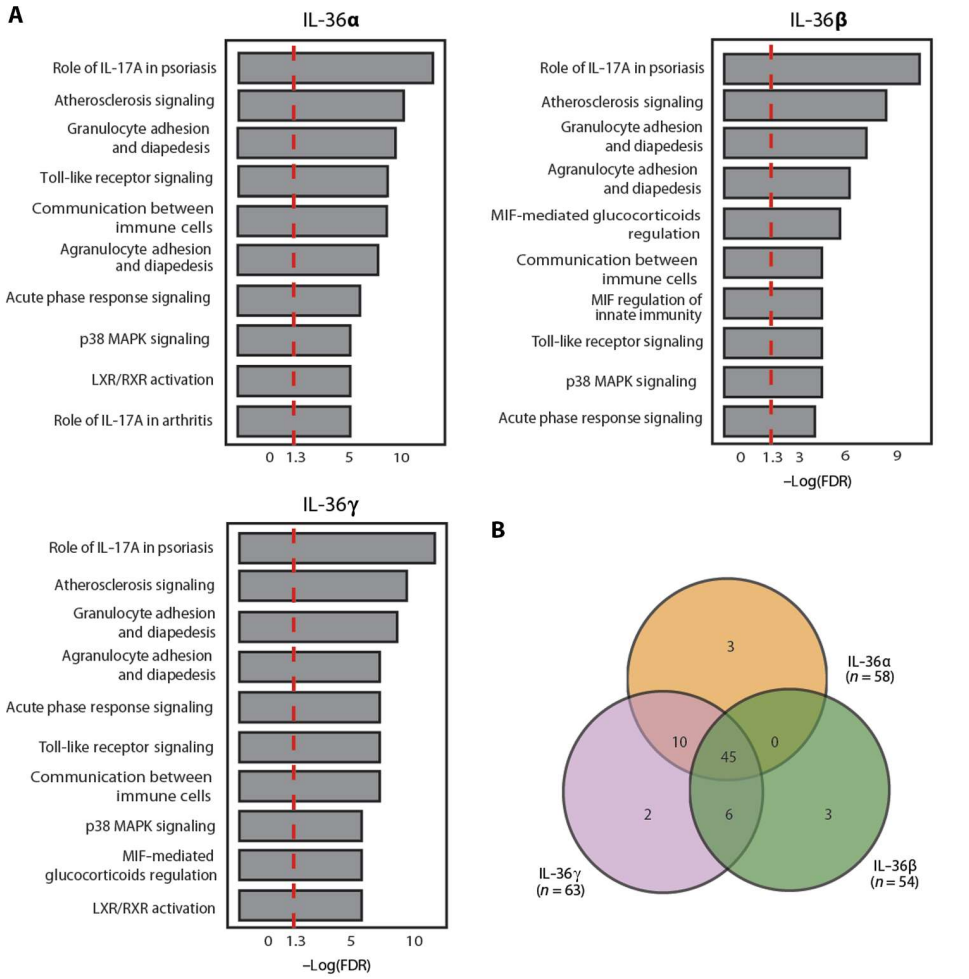

Most significantly enriched pathways shared between IL-36 and Ps

Canonical pathway	–Log(FDR)			
	IL-36α	IL-36β	IL-36γ	Ps
Role of IL-17A in psoriasis	13.1	11.0	12.6	11.0
Atherosclerosis signaling	9.8	9.6	10.2	11.0
Granulocyte adhesion and diapedesis	7.8	7.3	9.2	19.9
Agranulocyte adhesion and diapedesis	6.8	6.2	6.9	13.2
Communication between immune cells	7.0	5.1	6.7	9.1
LXR/RXR activation	5.2	4.0	5.8	5.4
Toll-like receptor signaling	7.0	5.1	6.7	3.4
Differential regulation of cytokines production in intestinal cells by IL-17A and IL-17F	4.5	3.4	4.3	8.4
TREM1 signaling	4.1	3.4	3.8	3.9
Role of IL-17 in arthritis	5.2	3.7	5.0	3.3

Fig. 2. The pathways that underlie the pathogenesis of psoriasis are enriched within the IL-36 transcriptome. (**A**) Pathways displaying the most significant enrichment in the IL-36α, IL-36β, and IL-36γ transcriptomes. The red dashed line shows the –log(FDR) level corresponding to an FDR of <0.05. (**B**) The Venn diagram shows the intersection of the pathways that are enriched (FDR < 0.05) in the three IL-36 transcriptomes. The number of enriched pathways for each data set is reported in parentheses. (**C**) The Venn diagram shows the intersection of the pathways that are enriched in psoriasis and in the three IL-36 transcriptomes. The 10 most significantly enriched pathways are reported on the right.

supplementation inhibited the release of IL-17 and IL-36γ into the culture medium (Fig. 5B), thus validating the gene expression results at the protein level.

Finally, immunofluorescence microscopy demonstrated a highly significant (albeit not absolute) reduction in the number of T lymphocytes and dendritic cells in IL-36Ra–treated lesional skin (Fig. 5C). Given the decreased expression of chemokines such as CCL20, this is likely to reflect a reduced retention of immune cells within the tissue.

To complement these findings, we sought to investigate the mechanisms underlying the effects of IL-36Ra on psoriatic lesions. We first examined the expression of the IL-36R gene (*IL1RL2*) in disease-relevant cell types. Although transcript levels were low in normal skin-resident T lymphocytes, in vitro–differentiated macrophages, and in vitro–differentiated dendritic cells, *IL1RL2* was very strongly expressed in keratinocytes (Fig. 5D). This suggests that IL-36Ra treatment mostly affects the latter cell type, where it inhibits IL-36R–dependent chemokine and cytokine production. To further explore this model, we examined the impact of IL-36Ra on MAPK signaling, one of the main mediators of IL-36–driven cytokine induction. We found that p38 phosphorylation, which was examined as a representative readout of MAPK activation on the basis of the results of pathway enrichment analysis, was markedly reduced in IL-36Ra–treated skin (Fig. 5E and fig. S8). These experiments demonstrate that ex vivo IL-36 inhibition reduces cytokine expression and leukocyte infiltration in psoriatic skin lesions, most likely through an effect on keratinocyte MAPK signaling.

Phenotyping of individuals carrying *IL1RL2* knockout mutations supports the safety of IL-36 signaling blockade

Having demonstrated the anti-inflammatory effects of IL-36 signaling inhibition in different experimental systems, we sought to establish whether pharmacological IL-36 blockade would compromise human immune function. We hypothesized that naturally occurring mutations in *IL1RL2* (the gene encoding the IL-36 signaling receptor) would mimic the effects of IL-36 signaling blockade. We therefore proceeded to ascertain a sample of individuals with homozygous *IL1RL2* loss-of-function alleles.

To maximize the likelihood of identifying subjects carrying *IL1RL2* knockout mutations, we focused our attention on a population displaying high rates of parental relatedness. We therefore queried the exome profiles of 2162 unrelated British-Pakistani individuals recruited by Born in Bradford, a community-based project that aims to investigate health outcomes in Bradford, UK (*19*). We found that 28 unrelated study participants (1.3%) harbored low-frequency homozygous changes in *IL1RL2*. Twelve of these individuals carried likely knockout mutations, that is,

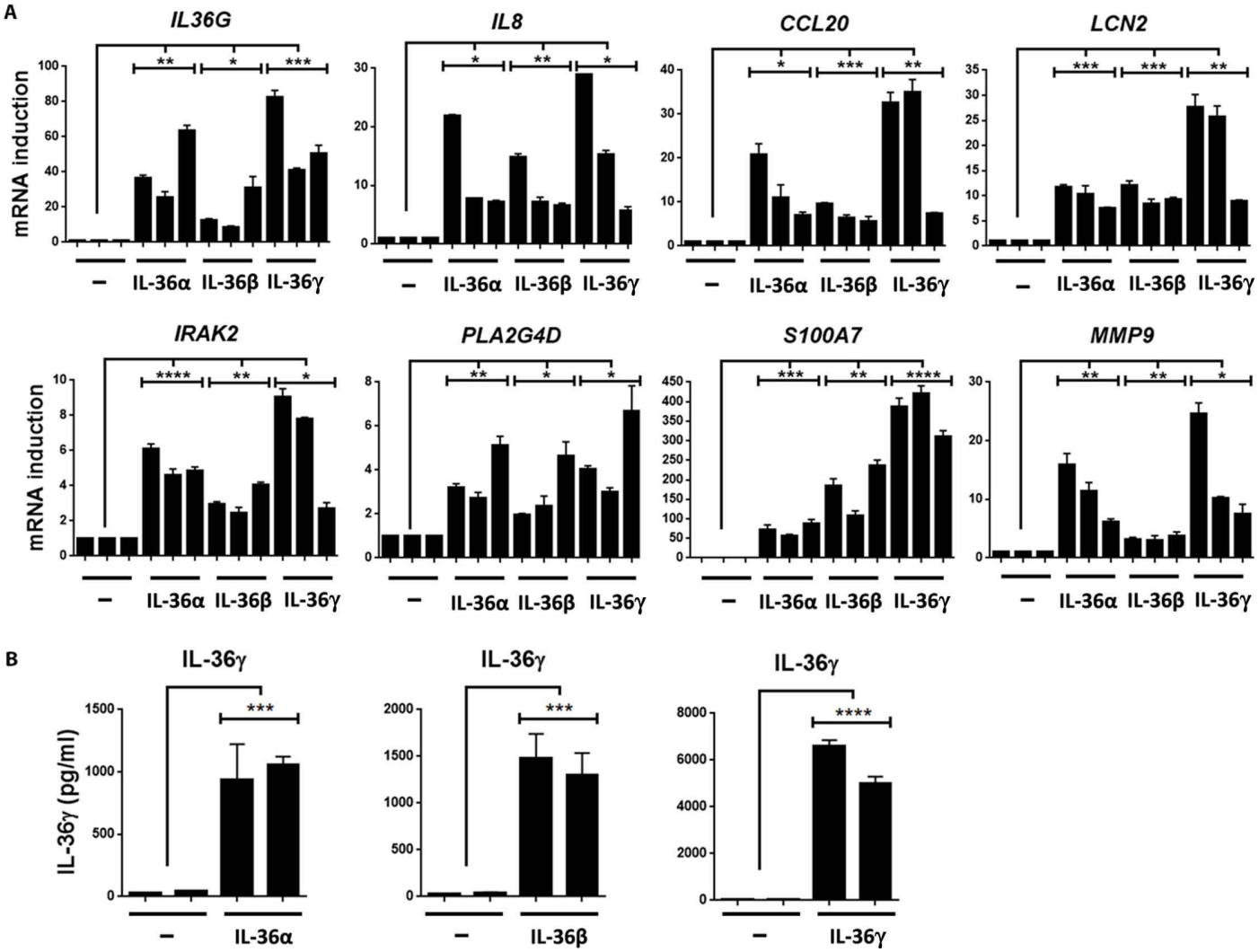

Fig. 3. IL-36 cytokines amplify immune responses implicated in psoriasis pathogenesis. (**A**) Validation of IL-36 responsiveness in genes that contribute to the pathogenesis of psoriasis. Primary keratinocytes from three independent healthy donors were treated with IL-36α, IL-36β, IL-36γ, or vehicle (–). Gene expression was compared in treated versus untreated keratinocytes, using real-time PCR. Data for each individual donor were normalized to transcript levels in untreated cells and are presented as the mean ± SEM of measurements obtained in triplicate stimulations. (**B**) Effect of IL-36 cytokines on the secretion of IL-36γ by keratinocytes. IL-36γ release was quantified by enzyme-linked immunosorbent assay (ELISA) after the stimulation of primary keratinocytes with IL-36α, IL-36β, and IL-36γ. Data for each individual donor are presented as the mean ± SEM. *P* values were calculated by Student's *t* test. $^{*}P < 0.05$, $^{**}P < 0.01$, $^{***}P \leq 0.001$, $^{****}P \leq 0.0001$.

homozygous missense alleles classified as damaging by multiple algorithms (table S5). Notably, the most prevalent change was a p.Ala471Thr substitution, found in 9 of 12 subjects and previously characterized in vitro as a deleterious allele (*20*).

To investigate the impact of these damaging *IL1RL2* changes on immune function, we first reviewed the medical records of the 12 individuals harboring deleterious homozygous mutations. One had always lived in the United Kingdom, whereas the other 11 had grown up in rural Pakistan and only left the country as young adults. We found that all were in good health, and none had suffered from cardiovascular disease, cancer, or immune-mediated conditions. None of the 12 subjects had a history of recurrent infections. Although IL-36 signaling has been implicated in host defense against *Mycobacterium tuberculosis* (*21*), none of the 12 individuals had contracted tuberculosis, a condition that is endemic in Pakistan (*22*). All showed normal leukocyte counts (table S6).

To further explore these findings, we recalled six subjects with deleterious *IL1RL2* mutations, five of whom were p.Ala471Thr homozygotes (the sixth was homozygous for a p.Ile229Met deleterious change). In parallel, we also recruited four age-, sex-, and ethnicity-matched controls, who carried wild-type *IL1RL2* sequences (Fig. 6, A and B). Clinical examination confirmed that none of the individuals with *IL1RL2* mutations presented with anomalies of the skin, oral mucosa, or lymph nodes. Serology tests showed that total IgA, IgG, and IgM levels were normal. The same applied to *Aspergillus* IgG levels, which were investigated because IL-36 signaling has been implicated in the response to this particular pathogen (*23*). Finally, we found that all individuals with *IL1RL2* mutations had circulating antibodies against varicella zoster virus and tetanus toxoid, showing that they had mounted an adequate immune response after antigen exposure (table S7).

To investigate in more detail the immune phenotype associated with deleterious *IL1RL2* alleles, we obtained peripheral blood mononuclear

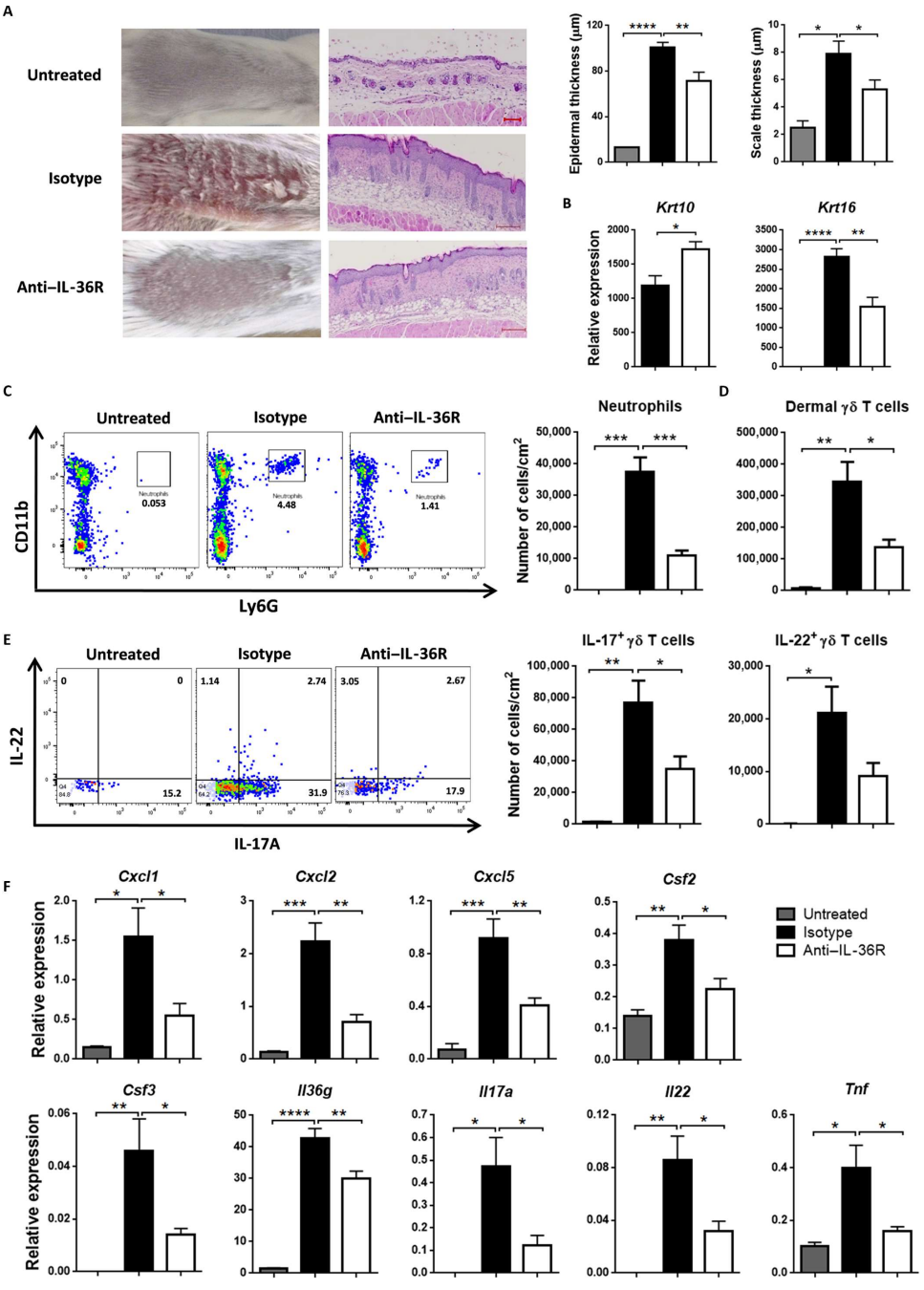

Fig. 4. In vivo IL-36 signaling blockade ameliorates imiquimod-induced psoriasiform dermatitis. Mice received an anti–IL-36R or isotype-matched control antibody (n = 5 per group) for 7 days, starting 2 days before imiquimod treatment. The experiment was carried out twice with comparable results. (**A**) Representative photographs (left) and hematoxylin and eosin staining (center) of imiquimod-treated mice receiving either anti–IL-36R or an isotype antibody. Untreated skin is shown as a reference. Measurements of the epidermis and scale thickness are plotted on the right. Scale bars, 100 μm. (**B**) Real-time PCR analysis of skin differentiation (*Krt10*) and hyperproliferation (*Krt16*) markers in imiquimod-treated mice receiving either an isotype antibody or anti–IL-36R. (**C**) Quantification of neutrophils infiltrating the skin of untreated versus imiquimod-treated mice receiving either an isotype antibody or anti–IL-36R. Representative fluorescence-activated cell sorting (FACS) plots of $CD11b^+Ly6G^+$ neutrophils gated within live $CD45^+$ cells are also shown. (**D**) Quantification of dermal γδ T cells infiltrating the skin of untreated versus imiquimod-treated mice receiving either an isotype antibody or anti–IL-36R. (**E**) Representative FACS plot (left) and quantification (right) of IL-17– and IL-22–producing dermal γδ T cells gated within live $CD45^+$ cells in the skin of untreated versus imiquimod-treated mice receiving either an isotype antibody or anti–IL-36R. (**F**) Real-time PCR of genes encoding chemokines and cytokines relevant to psoriasis in untreated versus imiquimod-treated mice receiving either an isotype antibody or anti–IL-36R. All data were normalized to the transcript levels observed in untreated mice and are presented as means ± SEM. *P* values were calculated with one-way analysis of variance (ANOVA) and Dunnett's posttest. $^*P < 0.05$, $^{**}P < 0.01$, $^{***}P \leq 0.001$, $^{****}P \leq 0.0001$.

cells (PBMCs) from the six individuals with homozygous knockout mutations and the four control subjects. We first demonstrated that *IL1RL2* and *IL1RAP* (the gene encoding the IL-36R co-receptor) are both expressed in these cells (fig. S6). Next, we stimulated PBMCs with a representative IL-36 cytokine (IL-36α). We found that this treatment failed to up-regulate downstream gene expression in individuals with *IL1RL2* knockout mutations (Fig. 6, C and D), despite a normal response to a control stimulation with phorbol 12-myristate 13-acetate (PMA)/ionomycin (Fig. 6E). This confirmed that the p.Ala471Thr and p.Ile229Met alleles abolish IL-36R activity and formally demonstrated that the individuals who harbor these mutations lack a functional IL-36R.

Next, we treated PBMCs with Infanrix, a vaccine mix conferring protection against diphtheria, tetanus, pertussis, polio, and *Haemophilus influenzae* type B. We then measured the number of $IL\text{-}17^+$ T lymphocytes so as to investigate the effect of *IL1RL2* mutations on adaptive responses to bacterial and viral antigens. We found that the induction of T cell–mediated IL-17 production was comparable in individuals with knockout changes and control subjects (Fig. 6F). We obtained similar results when we stimulated PBMCs with *Candida albicans* extracts, showing that the response to this fungal pathogen was also unaffected (Fig. 6F). Finally, we treated PBMCs with polyinosinic: polycytidylic acid [poly(I:C)], a synthetic double-stranded RNA that has been reported to up-regulate IL-36γ, suggesting an involvement of IL-36 cytokines in antiviral defenses (*24*). Again, we found that the induction of antiviral (*IFIT1* and *RSAD2*) and anti-inflammatory gene products (IL-8) was comparable in control and knockout cells (Fig. 6, G and H). These observations demonstrate that normal immune function is largely preserved in the presence of *IL1RL2* knockout mutations, suggesting that IL-36 blockade is likely to be well tolerated.

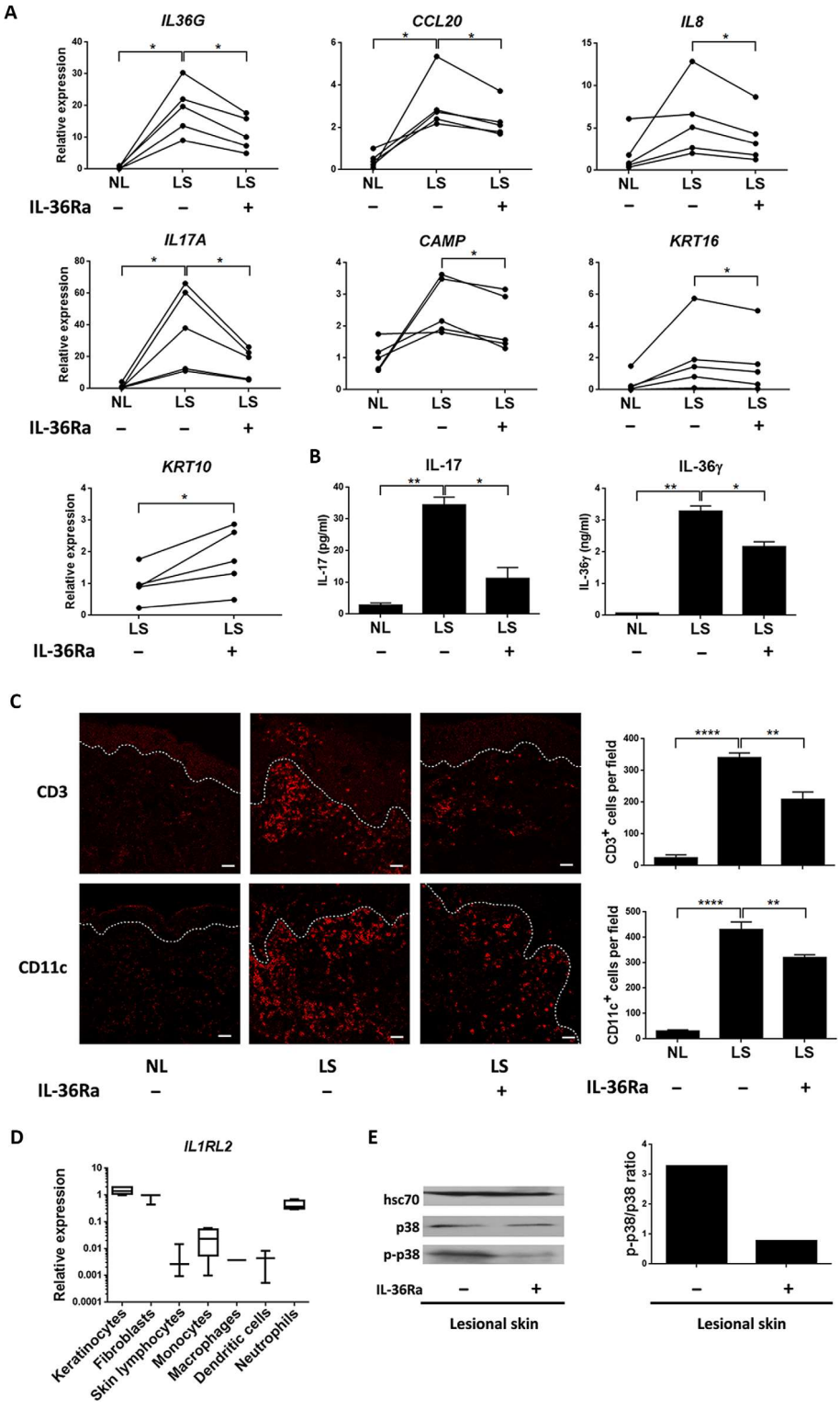

Fig. 5. Ex vivo IL-36R blockade reduces inflammation in psoriasis skin lesions. (**A** and **B**) Lesional (LS) skin biopsies were cultured for 24 hours in the presence or absence of IL-36Ra. For each patient, a paired nonlesional (NL) sample was analyzed as a reference. Cytokine expression was assessed by real-time PCR (A; $n = 5$ patients, each represented by one line per graph), whereas IL-17 and IL-36 release were quantified by ELISA (B; $n = 3$ patients; data are presented as means ± SEM). All P values were calculated by one-way repeated-measures ANOVA with Greenhouse-Geisser correction. (**C**) Representative confocal microscopy images of $CD3^+$ T cells and $CD11c^+$ dendritic cells in lesional skin samples treated with IL-36Ra ($n = 3$) (left). The number of positive cells per field, quantified in ≥5 images per sample, is presented as means ± SEM (right). P values were calculated by one-way ANOVA followed by Dunnett's posttest. $^*P < 0.05$, $^{**}P < 0.01$, $^{****}P \leq 0.0001$. Scale bars, 50 μm. The dermal-epidermal junction is highlighted by a dotted line. (**D**) Real-time PCR of *IL1RL2* expression in disease-relevant cell types. Each bar shows the median and range of expression values in two to five healthy donors. (**E**) Western blotting (loading control, hsc70) (left) and densitometric analysis of p-p38/p38 ratios (right) after IL-36Ra treatment of lesional skin. The data are representative of results from two independent skin samples.

DISCUSSION

Here, we have investigated the IL-36 signaling pathway as a shared pathogenic driver for plaque and pustular psoriasis. We initially examined the genes that are up-regulated by IL-36 treatment in skin keratinocytes. This is the cell type where the expression of IL-36R is highest and the effects of its stimulation are likely to be most pronounced. Keratinocyte RNA-seq allowed us to define a robust IL-36 signature, which is readily detectable among the genes that are overexpressed in psoriasis and those that map to disease susceptibility intervals. Our pathway enrichment analyses support a pathogenic model whereby IL-36–dependent genes drive several interconnected feedback loops that potentiate IL-17 signaling and leukocyte chemotaxis

IL-36 is initially produced upon exposure to viral infection (*24*) and skin trauma, two well-known triggers of psoriasis exacerbation (*3*). IL-36 cytokines can then induce the expression of *IL36G* in an autocrine and paracrine fashion. Our real-time PCR and ELISA data indicate that this is a very robust up-regulation, which is likely to play an important role in the propagation of cutaneous inflammatory responses. The induction of *IL36A* and *IL36B* is much weaker (table S2). This suggests a prominence of IL-36γ in early disease pathogenesis that could potentially be exploited for targeted therapeutic intervention.

IL-36 cytokines also drive the production of molecules that attract neutrophils (for example, IL-8 and CXCL1), dendritic cells (for example, CCL20), and T lymphocytes (CXCL10 and CCL20) to sites of inflammation. The strongest effect was demonstrated for S100A7, a potent inducer of T cell chemotaxis (*25*), which is up-regulated more than 100-fold by IL-36β and IL-36γ. The expression of LCN2,

Fig. 6. Individuals with homozygous *IL1RL2* mutations show no signs of abnormal immune function. (**A**) Demographics and mutation status of the Born in Bradford participants analyzed in the study. Bold font denotes individuals recalled for further phenotyping. (**B**) Representative chromatograms confirming the genotypes of recalled subjects. The nucleotide changes are highlighted by red asterisks. (**C** and **D**) PBMCs obtained from individuals with *IL1RL2* knockout mutations ($n = 6$) and control ($n = 4$) subjects were treated for 7 hours with IL-36α. Cytokine production was determined by real-time PCR (C; data are presented as the mean of triplicate stimulations) and ELISA (D; data are presented as the mean of duplicate stimulations). KMutH, knockout mutation homozygotes; Ctr, controls. (**E** to **H**) PBMCs obtained from individuals with *IL1RL2* knockout mutations and control subjects were treated with PMA/ionomycin (E), Infanrix 5-in-1 vaccine (F), and *C. albicans* extracts (F), or poly(I:C) (G and H). Gene expression was measured by real-time PCR (E and G; data are presented as the mean of triplicate stimulations), numbers of IL-17–secreting T cells were quantified by enzyme-linked immunospot (ELISPOT) (F; data are presented as the mean stimulation index observed in triplicate stimulations) (example photomicrographs are shown), and cytokine release was determined by ELISA (H; data are presented as the mean of duplicate stimulations). All *P* values were calculated by Student's *t* test. $^{**}P < 0.01$. ns, not significant.

A

Participant ID	Sex	Age (years)	Ethnicity	IL1RL2 genotype
P1	F	48	Pakistani	p.Ala471Thr/p.Ala471Thr
P2	F	41	Pakistani	p.Ala471Thr/p.Ala471Thr
P3	F	38	Pakistani	p.Ala471Thr/p.Ala471Thr
P4	F	41	Pakistani	p.Ala471Thr/p.Ala471Thr
P5	F	39	Pakistani	p.Ile229Met/p.Ile229Met
P6	F	30	Pakistani	p.Ala471Thr/p.Ala471Thr
P7	F	33	Pakistani	p.Ala471Thr/p.Ala471Thr
P8	F	31	Pakistani	p.Ala471Thr/p.Ala471Thr
P9	F	30	Pakistani	p.Ala471Thr/p.Ala471Thr
P10	F	29	Pakistani	p.Ala471Thr/p.Ala471Thr
P11	F	31	Pakistani	p.Pro543Leu/p.Pro543Leu
P12	F	30	Pakistani	p.Ala197Asp/p.Ala197Asp
C1	F	49	Pakistani	Wild type
C2	F	31	Pakistani	Wild type
C3	F	21	Pakistani	Wild type
C4	F	48	Pakistani	Wild type

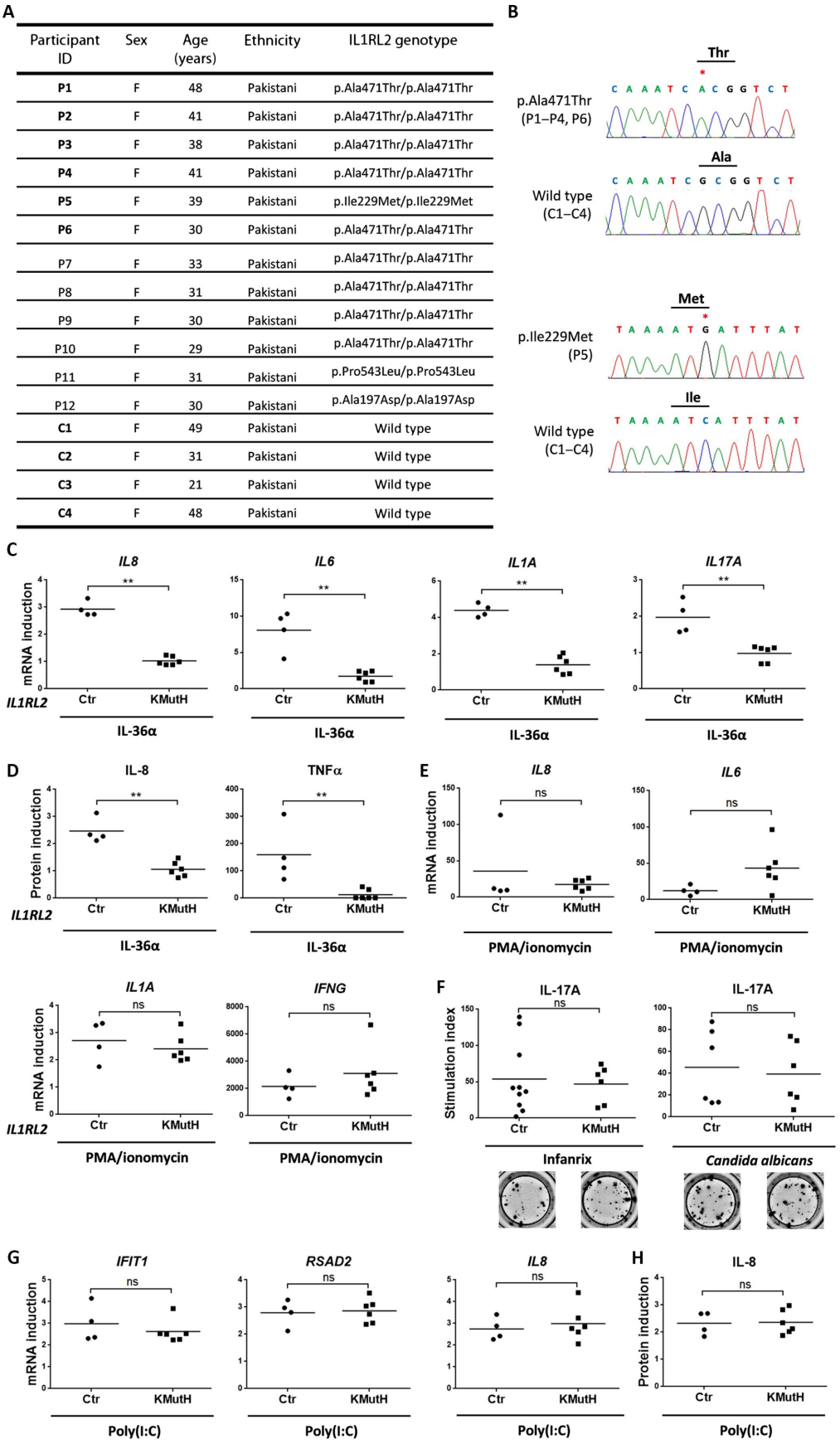

a molecule promoting neutrophil activation and infiltration (*26*), was also markedly increased by IL-36 treatment.

In parallel, we showed that IL-36 can up-regulate the PLA2G4D phospholipase. This enzyme, repeatedly found to be overexpressed in psoriasis (*27*), generates lipid antigens for presentation to CD1a-reactive T lymphocytes (*12*). Given that the activation of the latter cells results in the production of IL-17 and IL-22 (*12*), *PLA2G4D* induction is another mechanism whereby IL-36 potentiates T_H17 activity. It is also possible that PLA2G4D might, like other molecules that are chronically overexpressed in psoriatic skin (*28*), be recognized as an autoantigen by human leukocyte antigen–restricted T cells.

This in silico–derived pathogenic model is in keeping with the experimental characterization of IL-36γ and PLA2G4D as psoriasis biomarkers (*27*, *29*). It is also borne out by the

results of our ex vivo and in vivo studies, where IL-36 blockers reduced IL-17 and IL-36 expression in lesional skin while also decreasing chemokine induction and T cell infiltration.

The in vivo work was carried out in a single animal model (albeit a widely used one), where IL-36 signaling inhibition could not completely reverse the consequences of imiquimod administration. Although this is an important limitation, the anti-inflammatory effects of the treatment were supported by multiple experimental readouts and further validated by ex vivo studies of patients' skin, as recommended by the latest guidelines on the analysis of imiquimod-induced dermatitis (*15*). In this context, the incomplete resolution of inflammation may simply reflect the short-term nature of the treatment (7 days for in vivo and 24 hours for ex vivo assays). Thus, the analysis of experimental systems enabling prolonged IL-36 blockade (for example, three-dimensional organotypic skin models) may be needed to fully validate the therapeutic potential of IL-36 antagonists.

Real-time PCR analysis of cells obtained from healthy donors showed that *IL1RL2* levels were low in macrophages, dendritic cells, and skin-resident T lymphocytes. Although *IL1RL2* transcripts were present in neutrophils, the significance of this observation is unclear, given that IL-36R surface expression is not detectable in these cells (*30*). Thus, the anti-inflammatory effects of IL-36 blockade are likely mediated by a disruption of keratinocyte activation, resulting from the binding of IL-36Ra to an abundantly expressed receptor.

Having demonstrated the in vivo and ex vivo efficacy of IL-36 signaling inhibition, we sought to investigate its long-term effects on human immune function. We undertook the phenotyping of individuals carrying *IL1RL2* knockout mutations, because the analysis of loss-of-function alleles can generate invaluable insights into the effects of targeted pharmaceutical inhibition. For instance, the safety of cholesterol-lowering PCSK9 inhibitors was supported by the observation that *PCSK9* mutations do not affect human health (*31*).

Here, we identified 12 individuals harboring *IL1RL2* knockout changes through an analysis of the Born in Bradford cohort (*19*). Although all the mutations present in this relatively small data set were missense variants, pathogenicity predictions and IL-36 stimulations showed that these were deleterious alleles, which had a profound impact on receptor function. Conversely, clinical examinations did not uncover any evidence for impaired immune function.

Serology tests also failed to detect any anomalies. Of particular interest, *Aspergillus* IgG levels were unremarkable, responses to *C. albicans* stimulation were normal, and none of the individuals with *IL1RL2* knockout mutations presented with candidiasis, even if IL-36 signaling has been implicated in antifungal defenses (*23*). Although the size of our data set does not allow us to exclude the possibility that IL-36 inhibition may confer vulnerability to rare infections, the data presented here indicate that IL-36 blockade is broadly compatible with normal immune function.

Our observations have important translational implications. Although biologics targeting the IL-23/T_H17 axis (especially IL-17 blockers) have transformed the treatment of psoriasis (*32*), disease management can still be problematic in real-world settings, where the response to existing cytokine blockers does not match the efficacy levels observed in clinical trials (*33*). The efficiency of biologic therapies is even lower in pustular forms of psoriasis, where the need for an effective treatment is especially pressing (*3*).

In this context, the findings obtained in our model systems support the development of IL-36 blockade as a therapeutic strategy for plaque and pustular psoriasis. Although the phenotyping of individuals harboring *IL1RL2* knockout mutations suggests a favorable safety profile for IL-36 antagonists, we cannot exclude the possibility that these subjects may have developed compensatory immune mechanisms in early life. It is also possible that the effects of *IL1RL2* mutations may have been mitigated by genetic modifiers occurring at high frequency within the British Pakistani population. In spite of these limitations, the immunocompromised phenotype of individuals suffering from other receptor deficiencies suggests that IL-36 signaling may indeed be dispensable to host defenses and warrants further characterization of IL-36 antagonists in phase 1 clinical trials.

MATERIALS AND METHODS

Study design

The aim of this study was to demonstrate that IL-36 cytokines play a pathogenic role in psoriasis and to validate the IL-36R as a therapeutic target. The first objective was pursued by demonstrating that IL-36–dependent genes identified in keratinocyte RNA-seq experiments were enriched in the psoriasis skin transcriptome and in disease-associated loci. The second objective was investigated in in vivo and ex vivo studies of IL-36R blockade. Deep phenotyping of individuals who lack a functional IL-36R owing to *IL1RL2* knockout mutations was also undertaken to assess the long-term effects of IL-36 signaling inhibition.

The RNA-seq experiment was carried out in triplicate to maximize the power of detecting differentially expressed genes at a coverage exceeding 2×10^7 reads per sample (*34*). In vivo studies were carried out in two groups of five mice on the basis of previous experience with comparable work (*18*).

For the remaining experiments, sample sizes were dictated by the availability of psoriasis patients and *IL1RL2* knockouts matching our strict inclusion criteria (see the Supplementary Materials). mRNA levels (see table S9 for details of real-time PCR primers), cytokine concentrations, and leukocyte numbers were investigated as predefined end points. Immunofluorescence and ELISPOT images were quantified in a blinded fashion. No randomization of animal groups was necessary. Although drug administration to imiquimod-treated mice was not blinded, epidermal and scale thickness measurements were assessed in a blinded fashion. Primary data are located in table S10. Details of sampling and experimental replicates are provided in each figure legend.

Human subjects

This study was performed in accordance with the Declaration of Helsinki and was approved by the National Research Ethics Service Committee London–Chelsea. Written informed consent was obtained from all participants. Adult patients with psoriasis (n = 10; table S8) were ascertained by dermatologists at Guy's and St. Thomas' NHS Foundation Trust (see the Supplementary Materials for further details). Discarded skin was obtained from four healthy donors undergoing plastic surgery at Guy's and St. Thomas' NHS Foundation Trust. Primary keratinocyte cultures were then established as described elsewhere (*35*).

RNA sequencing

Sequences were aligned to the Ensembl Human GRCh37 transcriptome using Bowtie 2-2.2.2 (*36*), and the number of reads that mapped to each gene was quantified with htseq-count (*37*).

Raw expression data for psoriatic skin and the IL-4 and IL-17 keratinocyte transcriptomes were downloaded from the Gene Expression Omnibus database (GSE67785, GSE59275, and GSE12109, respectively), and differential expression was computed using DESeq2

(*38*). Genes that were up-regulated by individual IL-36 cytokines (fold change ≥ 2, FDR < 0.05) were selected for pathway enrichment analysis, which was implemented with Ingenuity Pathway Analysis (Qiagen Bioinformatics).

In vivo IL-36 signaling blockade

Mice were bred in the Francis Crick Institute animal facility under specific pathogen–free conditions, where experiments were performed in accordance with institutional guidelines and U.K. Home Office regulations. Female BALB/cJ mice (8 weeks old) treated for five consecutive days with 5% imiquimod (Meda AB) received daily intraperitoneal injections (150 μg) of anti–IL-36R antibody (M616, Amgen) or rat IgG2a isotype control (Bio X Cell), starting on day −2 of imiquimod administration. Full-thickness skin biopsies were collected on day 7 for histological staining, RNA extraction, and flow cytometry (see the Supplementary Materials for further details).

Statistical analyses

The significance of the overlap between the up-regulated genes (or enriched pathways) represented in Venn diagrams was calculated using the hypergeometric distribution (phyper function in R). Fisher's exact test was used to assess the enrichment of IL-36 signature genes within non–major histocompatibility complex intervals associated with psoriasis, schizophrenia, and autism. The NHGRI-EBI (National Human Genome Research Institute–European Bioinformatics Institute) Catalog of published GWAS (www.ebi.ac.uk/gwas; March 2017 update) was queried using the search terms "psoriasis," "schizophrenia," and "autism" to generate three lists of disease-associated single-nucleotide polymorphisms (SNPs). A window of ±50 kb was added to the lead SNP at each locus, and the genes mapping to the resulting regions were extracted using BioMart (www.ensembl.org/biomart).

Fisher's test and hypergeometric distribution *P* values were adjusted for multiple testing using the Bonferroni correction. Unless otherwise indicated, experimental data are presented as means ± SEM. Differences between groups were assessed using unpaired Student's *t* test or one-way ANOVA with Dunnett's posttest, as appropriate.

SUPPLEMENTARY MATERIALS

www.sciencetranslationalmedicine.org/cgi/content/full/9/411/eaan2514/DC1

Materials and Methods

Fig. S1. IL-4 target genes are an appropriate negative control for IL-36 enrichment analyses, because there is no overlap between IL-4 and IL-36 signature genes.

Fig. S2. The pathways that underlie the pathogenesis of GPP are enriched within the IL-36 transcriptome.

Fig. S3. Mechanical trauma up-regulates IL-36 production by cultured keratinocytes.

Fig. S4. Proposed pathogenic model illustrating the role of IL-36 as an amplifier of T_H17 signaling in psoriasis.

Fig. S5. In vivo IL-36 signaling blockade reduces the infiltration of IL-17–producing αβ T cells in imiquimod-induced psoriasiform dermatitis.

Fig. S6. The genes encoding the IL-36R subunits are expressed in PBMCs.

Fig. S7. Dose- and time-dependent effects of IL-36 cytokines in primary keratinocytes.

Fig. S8. Complete Western blots for Fig. 5E.

Table S1. RNA-seq coverage statistics (provided in Excel).

Table S2. Keratinocyte genes that are up-regulated or down-regulated by IL-36 treatment (provided in Excel).

Table S3. Overlap between the *IL36_182* set and keratinocyte genes up-regulated by IL-17 (provided in Excel).

Table S4. Results of pathway enrichment analysis (provided in Excel).

Table S5. Rare homozygous *IL1RL2* variants observed in the Born in Bradford cohort.

Table S6. Full blood counts of individuals with homozygous *IL1RL2* mutations and controls.

Table S7. Immune serology results.

Table S8. Skin donor demographics.

Table S9. Oligonucleotide primers used in the study.

Table S10. Raw data for in vivo and ex vivo experiments (provided in Excel).

REFERENCES AND NOTES

1. C. Gabay, J. E. Towne, Regulation and function of interleukin-36 cytokines in homeostasis and pathological conditions. *J. Leukoc. Biol.* **97**, 645–652 (2015).
2. A. Onoufriadis, M. A. Simpson, A. E. Pink, P. Di Meglio, C. H. Smith, V. Pullabhatla, J. Knight, S. L. Spain, F. O. Nestle, A. D. Burden, F. Capon, R. C. Trembath, J. N. Barker, Mutations in *IL36RN/IL1F5* are associated with the severe episodic inflammatory skin disease known as generalized pustular psoriasis. *Am. J. Hum. Genet.* **89**, 432–437 (2011).
3. A. D. Burden, B. Kirby, *Psoriasis and Related Disorders*, in *Rook's Textbook of Dermatology*, C. E. M. Griffiths, J. N. Barker, T. Bleiker, R. J. Chalmers, D. Creamer, Eds. (Wiley-Blackwell, 2016), chap. 35.
4. M. A. Lowes, M. Suárez-Fariñas, J. G. Krueger, Immunology of psoriasis. *Annu. Rev. Immunol.* **32**, 227–255 (2014).
5. A. Johnston, X. Xing, L. Wolterink, D. H. Barnes, Z. Yin, L. Reingold, J. M. Kahlenberg, P. W. Harms, J. E. Gudjonsson, IL-1 and IL-36 are dominant cytokines in generalized pustular psoriasis. *J. Allergy Clin. Immunol.* **140**, 109–120 (2017).
6. S. Hussain, D. M. Berki, S.-E. Choon, A. D. Burden, M. H. Allen, J. I. Arostegui, A. Chaves, M. Duckworth, A. D. Irvine, M. Mockenhaupt, A. A. Navarini, M. M. B. Seyger, P. Soler-Palacin, C. Prins, L. Valeyrie-Allanore, M. A. Vicente, R. C. Trembath, C. H. Smith, J. N. Barker, F. Capon, IL36RN mutations define a severe autoinflammatory phenotype of generalized pustular psoriasis. *J. Allergy Clin. Immunol.* **135**, 1067–1070.e9 (2015).
7. X. Zuo, L. Sun, X. Yin, J. Gao, Y. Sheng, J. Xu, J. Zhang, C. He, Y. Qiu, G. Wen, H. Tian, X. Zheng, S. Liu, W. Wang, W. Li, Y. Cheng, L. Liu, Y. Chang, Z. Wang, Z. Li, L. Li, J. Wu, L. Fang, C. Shen, F. Zhou, B. Liang, G. Chen, H. Li, Y. Cui, A. Xu, X. Yang, F. Hao, L. Xu, X. Fan, Y. Li, R. Wu, X. Wang, X. Liu, M. Zheng, S. Song, B. Ji, H. Fang, J. Yu, Y. Sun, Y. Hui, F. Zhang, R. Yang, S. Yang, X. Zhang, Whole-exome SNP array identifies 15 new susceptibility loci for psoriasis. *Nat. Commun.* **6**, 6793 (2015).
8. L. Tortola, E. Rosenwald, B. Abel, H. Blumberg, M. Schäfer, A. J. Coyle, J.-C. Renauld, S. Werner, J. Kisielow, M. Kopf, Psoriasiform dermatitis is driven by IL-36–mediated DC-keratinocyte crosstalk. *J. Clin. Invest.* **122**, 3965–3976 (2012).
9. Y. Carrier, H.-L. Ma, H. E. Ramon, L. Napierata, C. Small, M. O'Toole, D. A. Young, L. A. Fouser, C. Nickerson-Nutter, M. Collins, K. Dunussi-Joannopoulos, Q. G. Medley, Inter-regulation of Th17 cytokines and the IL-36 cytokines in vitro and in vivo: Implications in psoriasis pathogenesis. *J. Invest. Dermatol.* **131**, 2428–2437 (2011).
10. A. Johnston, X. Xing, A. M. Guzman, M. Riblett, C. M. Loyd, N. L. Ward, C. Wohn, E. P. Prens, F. Wang, L. E. Maier, S. Kang, J. J. Voorhees, J. T. Elder, J. E. Gudjonsson, IL-1F5, -F6, -F8, and -F9: A novel IL-1 family signaling system that is active in psoriasis and promotes keratinocyte antimicrobial peptide expression. *J. Immunol.* **186**, 2613–2622 (2011).
11. J. E. Towne, B. R. Renshaw, J. Douangpanya, B. P. Lipsky, M. Shen, C. A. Gabel, J. E. Sims, Interleukin-36 (IL-36) ligands require processing for full agonist (IL-36α, IL-36β, and IL-36γ) or antagonist (IL-36Ra) activity. *J. Biol. Chem.* **286**, 42594–42602 (2011).
12. K. L. Cheung, R. Jarrett, S. Subramaniam, M. Salimi, D. Gutowska-Owsiak, Y.-L. Chen, C. Hardman, L. Xue, V. Cerundolo, G. Ogg, Psoriatic T cells recognize neolipid antigens generated by mast cell phospholipase delivered by exosomes and presented by CD1a. *J. Exp. Med.* **213**, 2399–2412 (2016).
13. W. R. Swindell, H. A. Remmer, M. K. Sarkar, X. Xing, D. H. Barnes, L. Wolterink, J. J. Voorhees, R. P. Nair, A. Johnston, J. T. Elder, J. E. Gudjonsson, Proteogenomic analysis of psoriasis reveals discordant and concordant changes in mRNA and protein abundance. *Genome Med.* **7**, 86 (2015).
14. K. E. Nograles, L. C. Zaba, E. Guttman-Yassky, J. Fuentes-Duculan, M. Suárez-Fariñas, I. Cardinale, A. Khatcherian, J. Gonzalez, K. C. Pierson, T. R. White, C. Pensabene, I. Coats, I. Novitskaya, M. A. Lowes, J. G. Krueger, Th17 cytokines interleukin (IL)-17 and IL-22 modulate distinct inflammatory and keratinocyte-response pathways. *Br. J. Dermatol.* **159**, 1092–1102 (2008).
15. J. E. Hawkes, J. E. Gudjonsson, N. L. Ward, The snowballing literature on imiquimod-induced skin inflammation in mice: A critical appraisal. *J. Invest. Dermatol.* **137**, 546–549 (2017).
16. L. van der Fits, S. Mourits, J. S. A. Voerman, M. Kant, L. Boon, J. D. Laman, F. Cornelissen, A.-M. Mus, E. Florencia, E. P. Prens, E. Lubberts, Imiquimod-induced psoriasis-like skin inflammation in mice is mediated via the IL-23/IL-17 axis. *J. Immunol.* **182**, 5836–5845 (2009).
17. Y. Cai, X. Shen, C. Ding, C. Qi, K. Li, X. Li, V. R. Jala, H.-g. Zhang, T. Wang, J. Zheng, J. Yan, Pivotal role of dermal IL-17-producing γδ T cells in skin inflammation. *Immunity* **35**, 596–610 (2011).
18. P. Di Meglio, J. H. Duarte, H. Ahlfors, N. D. L. Owens, Y. Li, F. Villanova, I. Tosi, K. Hirota, F. O. Nestle, U. Mrowietz, M. J. Gilchrist, B. Stockinger, Activation of the aryl hydrocarbon receptor dampens the severity of inflammatory skin conditions. *Immunity* **40**, 989–1001 (2014).

19. V. M. Narasimhan, K. A. Hunt, D. Mason, C. L. Baker, K. J. Karczewski, M. R. Barnes, A. H. Barnett, C. Bates, S. Bellary, N. A. Bockett, K. Giorda, C. J. Griffiths, H. Hemingway, Z. Jia, M. A. Kelly, H. A. Khawaja, M. Lek, S. McCarthy, R. McEachan, A. O'Donnell-Luria, K. Paigen, C. A. Parisinos, E. Sheridan, L. Southgate, L. Tee, M. Thomas, Y. Xue, M. Schnall-Levin, P. M. Petkov, C. Tyler-Smith, E. R. Maher, R. C. Trembath, D. G. MacArthur, J. Wright, R. Durbin, D. A. van Heel, Health and population effects of rare gene knockouts in adult humans with related parents. *Science* **352**, 474–477 (2016).
20. G. Yi, J. A. Ybe, S. S. Saha, G. Caviness, E. Raymond, R. Ganesan, M. L. Mbow, C. C. Kao, Structural and functional attributes of the interleukin-36 receptor. *J. Biol. Chem.* **291**, 16597–16609 (2016).
21. F. Ahsan, P. Moura-Alves, U. Guhlich-Bornhof, M. Klemm, S. H. E. Kaufmann, J. Maertzdorf, Role of interleukin 36γ in host defense against tuberculosis. *J. Infect. Dis.* **214**, 464–474 (2016).
22. World Health Organization (WHO), Global Tuberculosis Report 2015 (WHO, 2015); http://apps.who.int/iris/bitstream/10665/191102/1/9789241565059_eng.pdf.
23. M. S. Gresnigt, B. Rösler, C. W. M. Jacobs, K. L. Becker, L. A. B. Joosten, J. W. M. van der Meer, M. G. Netea, C. A. Dinarello, F. L. van de Veerdonk, The IL-36 receptor pathway regulates *Aspergillus fumigatus*-induced Th1 and Th17 responses. *Eur. J. Immunol.* **43**, 416–426 (2013).
24. L.-H. Lian, K. A. Milora, K. K. Manupipatpong, L. E. Jensen, The double-stranded RNA analogue polyinosinic-polycytidylic acid induces keratinocyte pyroptosis and release of IL-36γ. *J. Invest. Dermatol.* **132**, 1346–1353 (2012).
25. Y. Zheng, F. Niyonsaba, H. Ushio, S. Ikeda, I. Nagaoka, K. Okumura, H. Ogawa, Microbicidal protein psoriasin is a multifunctional modulator of neutrophil activation. *Immunology* **124**, 357–367 (2008).
26. S. Shao, T. Cao, L. Jin, B. Li, H. Fang, J. Zhang, Y. Zhang, J. Hu, G. Wang, Increased lipocalin-2 contributes to the pathogenesis of psoriasis by modulating neutrophil chemotaxis and cytokine secretion. *J. Invest. Dermatol.* **136**, 1418–1428 (2016).
27. M. Quaranta, B. Knapp, N. Garzorz, M. Mattii, V. Pullabhatla, D. Pennino, C. Andres, C. Traidl-Hoffmann, A. Cavani, F. J. Theis, J. Ring, C. B. Schmidt-Weber, S. Eyerich, K. Eyerich, Intraindividual genome expression analysis reveals a specific molecular signature of psoriasis and eczema. *Sci. Transl. Med.* **6**, 244ra90 (2014).
28. R. Lande, E. Botti, C. Jandus, D. Dojcinovic, G. Fanelli, C. Conrad, G. Chamilos, L. Feldmeyer, B. Marinari, S. Chon, L. Vence, V. Riccieri, P. Guillaume, A. A. Navarini, P. Romero, A. Costanzo, E. Piccolella, M. Gilliet, L. Frasca, The antimicrobial peptide LL37 is a T-cell autoantigen in psoriasis. *Nat. Commun.* **5**, 5621 (2014).
29. A. M. D'Erme, D. Wilsmann-Theis, J. Wagenpfeil, M. Hölzel, S. Ferring-Schmitt, S. Sternberg, M. Wittmann, B. Peters, A. Bosio, T. Bieber, J. Wenzel, IL-36γ (IL-1F9) is a biomarker for psoriasis skin lesions. *J. Invest. Dermatol.* **135**, 1025–1032 (2015).
30. A. M. Foster, J. Baliwag, C. S. Chen, A. M. Guzman, S. W. Stoll, J. E. Gudjonsson, N. L. Ward, A. Johnston, IL-36 promotes myeloid cell infiltration, activation, and inflammatory activity in skin. *J. Immunol.* **192**, 6053–6061 (2014).
31. C. Sheridan, New class PCSK9 blockers stride into cholesterol market. *Nat. Biotechnol.* **33**, 785–786 (2015).
32. S. Noda, J. G. Krueger, E. Guttman-Yassky, The translational revolution and use of biologics in patients with inflammatory skin diseases. *J. Allergy Clin. Immunol.* **135**, 324–336 (2015).
33. B. E. Strober, R. Bissonnette, D. Fiorentino, A. B. Kimball, L. Naldi, N. H. Shear, K. Goyal, S. Fakharzadeh, S. Calabro, W. Langholff, Y. You, C. Galindo, S. Lee, M. G. Lebwohl, Comparative effectiveness of biologic agents for the treatment of psoriasis in a real-world setting: Results from a large, prospective, observational study (Psoriasis Longitudinal Assessment and Registry [PSOLAR]). *J. Am. Acad. Dermatol.* **74**, 851–861.e4 (2016).
34. Y. Liu, J. Zhou, K. P. White, RNA-seq differential expression studies: More sequence or more replication? *Bioinformatics* **30**, 301–304 (2014).
35. S. K. Mahil, S. Twelves, K. Farkas, N. Setta-Kaffetzi, A. D. Burden, J. E. Gach, A. D. Irvine, L. Képíró, M. Mockenhaupt, H. H. Oon, J. Pinner, A. Ranki, M. M. B. Seyger, P. Soler-Palacin, E. R. Storan, E. S. Tan, L. Valeyrie-Allanore, H. S. Young, R. C. Trembath, S.-E. Choon, M. Szell, Z. Bata-Csorgo, C. H. Smith, P. Di Meglio, J. N. Barker, F. Capon, AP1S3 mutations cause skin autoinflammation by disrupting keratinocyte autophagy and up-regulating IL-36 production. *J. Invest. Dermatol.* **136**, 2251–2259 (2016).
36. B. Langmead, S. L. Salzberg, Fast gapped-read alignment with Bowtie 2. *Nat. Methods* **9**, 357–359 (2012).
37. S. Anders, P. T. Pyl, W. Huber, HTSeq—A Python framework to work with high-throughput sequencing data. *Bioinformatics* **31**, 166–169 (2015).
38. M. I. Love, W. Huber, S. Anders, Moderated estimation of fold change and dispersion for RNA-seq data with DESeq2. *Genome Biol.* **15**, 550 (2014).

Acknowledgments: We are grateful to the patients and volunteers who took part in this study. We thank B. Stockinger for her support; the Francis Crick Institute Biological Research Facility for expert breeding and maintenance of the mice; and the Flow Cytometry Facility, the Histopathology Facility, and Y. Li for their assistance with histology and quantification. We also thank Amgen for providing the M616 anti–IL-36R neutralizing antibody. **Funding:** We acknowledge the support from the Department of Health via the National Institute for Health Research (NIHR) BioResource Clinical Research Facility and comprehensive Biomedical Research Centre award at Guy's and St. Thomas' NHS Foundation Trust in partnership with King's College London and King's College Hospital NHS Foundation Trust (guysbrc-2012-1). This paper presents independent research funded by the NIHR under its Collaboration for Leadership in Applied Health Research and Care for Yorkshire and Humber. Core support for Born in Bradford was also provided by the Wellcome Trust (WT101597). This work was funded by a Medical Research Council (MRC) Stratified Medicine award (MR/L011808/1) and was supported in part by a Wellcome Trust strategic award (WT 102627) to R.C.T. S.K.M. is supported by an MRC Clinical Training Fellowship (MR/L001543/1). M.C.'s Ph.D. studentship is funded by the Psoriasis Association. The animal work was conducted at the Francis Crick Institute, which receives its core funding from Cancer Research UK, the MRC, and the Wellcome Trust. **Author contributions:** F.C. designed the study and supervised the experimental work. S.K.M. carried out the experiments, with input from M.P. P.D.M. performed the animal work. M.C., N.D., I.M.C., H.A., and F.D.C. implemented the RNA-seq and the downstream data analysis. J.N.B., C.H.S., R.C.T., and J.W. coordinated the recruitment of patients and healthy volunteers. F.C. wrote the manuscript, with input from S.K.M., P.D.M., N.D., C.H.S., F.D.C, and J.N.B. **Competing interests:** F.C. and J.N.B. have received funding from Boehringer-Ingelheim. All other authors declare no other competing interests. **Data and materials availability:** The RNA-seq data reported in this paper are archived at the Gene Expression Omnibus Repository (www.ncbi.nlm.nih.gov/geo) under accession no. GSE96601.

Submitted 17 March 2017
Resubmitted 16 June 2017
Accepted 21 August 2017
Published 11 October 2017
10.1126/scitranslmed.aan2514

Citation: S. K. Mahil, M. Catapano, P. Di Meglio, N. Dand, H. Ahlfors, I. M. Carr, C. H. Smith, R. C. Trembath, M. Peakman, J. Wright, F. D. Ciccarelli, J. N. Barker, F. Capon, An analysis of IL-36 signature genes and individuals with *IL1RL2* knockout mutations validates IL-36 as a psoriasis therapeutic target. *Sci. Transl. Med.* **9**, eaan2514 (2017).

Science Translational Medicine

An analysis of IL-36 signature genes and individuals with *IL1RL2* knockout mutations validates IL-36 as a psoriasis therapeutic target

Satveer K. Mahil, Marika Catapano, Paola Di Meglio, Nick Dand, Helena Ahlfors, Ian M. Carr, Catherine H. Smith, Richard C. Trembath, Mark Peakman, John Wright, Francesca D. Ciccarelli, Jonathan N. Barker and Francesca Capon

Sci Transl Med **9**, eaan2514.
DOI: 10.1126/scitranslmed.aan2514

Nixing IL-36 in psoriasis

Plaque psoriasis is a common T cell–driven autoimmune disease affecting the skin. Targeted biologics impeding the IL-17 inflammatory cytokine family exist but do not provide universal clinical benefit. Mahil *et al.* convincingly identify IL-36 as an important driver of psoriasis and suggest that blocking IL-36 signaling could bring relief to psoriasis patients. Their results stem from genetic analyses, as well as ex vivo experimentation with patient samples and in vivo treatment of a mouse model. Individuals naturally deficient in IL-36 signaling did not have any overt immunodeficiency, suggesting that interrupting IL-36 would be a safe approach for treating disease.

Science Translational Medicine
AAAS

www.sciencetranslationalmedicine.org/cgi/content/full/9/411/eaan2514/DC1

Supplementary Materials for

An analysis of IL-36 signature genes and individuals with *IL1RL2* knockout mutations validates IL-36 as a psoriasis therapeutic target

Satveer K. Mahil, Marika Catapano, Paola Di Meglio, Nick Dand, Helena Ahlfors, Ian M. Carr, Catherine H. Smith, Richard C. Trembath, Mark Peakman, John Wright, Francesca D. Ciccarelli, Jonathan N. Barker, Francesca Capon*

*Corresponding author. Email: francesca.capon@kcl.ac.uk

Published 11 October 2017, *Sci. Transl. Med.* **9**, eaan2514 (2017)
DOI: 10.1126/scitranslmed.aan2514

The PDF file includes:

Other Supplementary Material for this manuscript includes the following:
(available at
www.sciencetranslationalmedicine.org/cgi/content/full/9/411/eaan2514/DC1)

Table S1. RNA-seq coverage statistics (provided in Excel).
Table S2. Keratinocyte genes that are up-regulated or down-regulated by IL-36 treatment (provided in Excel).
Table S3. Overlap between the *IL36_182* set and keratinocyte genes up-regulated by IL-17 (provided in Excel).
Table S4. Results of pathway enrichment analysis (provided in Excel).
Table S10. Raw data for in vivo and ex vivo experiments (provided in Excel).

Materials and Methods

Human subjects

Inclusion criteria for patient recruitment were a diagnosis of moderate-to-severe plaque psoriasis (Psoriasis Area Severity Index >10) and washout from immune-modulators (at least 2 days for topical agents and 6 weeks for systemic treatment).

Individuals with homozygous *IL1RL2* variants (n=12) were identified by mining the exome sequence data relating to the Born in Bradford cohort (*19*). Ethnically-matched controls (n=4) were recruited from Bradford Teaching Hospitals NHS Foundation Trust.

Full blood counts and serology tests were provided by Viapath, Guy's and St Thomas' Hospitals NHS Foundation Trust.

Cell and tissue culture

Primary keratinocyte cultures were maintained in Epilife medium (Gibco) containing Supplement 7 (Gibco) and 1% penicillin-streptomycin (Gibco). Based on the results of preliminary kinetic studies (fig. S7), cultures were stimulated for 24 hours with 20ng/ml IL-36α, -β, –γ (Bio-Techne) or vehicle control. Cells and culture supernatants were then harvested for RNA isolation and ELISA, respectively. RNA samples were processed with the RNeasy Plus Mini kit (Qiagen). RNA-seq libraries were then prepared with the Illumina TruSeq Stranded Total RNA preparation kit and sequenced on an Illumina HiSeq 3000 system.

For the assessment of keratinocyte responses to mechanical trauma, primary keratinocytes from 2 healthy donors were grown to complete confluence and linear scratch wounds covering 40-50% of the well surface were created with a sterile pipette tip. After 4 hours, cells and culture supernatants were harvested for RNA isolation and ELISA, respectively.

Paired 6mm punch biopsies were obtained from lesional and adjacent non-lesional skin of psoriatic patients (n=10, table S8). Samples were immediately quartered and cultured for 24 hours in IMDM (Sigma) containing 2% penicillin-streptomycin-glutamine solution (Sigma), 10% knockout serum replacement factor (Gibco) and either 5ng/ml IL-36Ra (Bio-Techne) or PBS (Gibco).

PBMCs cultured in RPMI (Gibco) supplemented with 10% FBS and 1% penicillin-streptomycin were treated with 50ng/ml IL-36α for 7 hours or 50ng/ml PMA (Sigma)/250ng/ml Ionomycin (VWR International) for 5 hours or 5µg/ml poly(I:C) (Invivogen) for 24 hours.

For the assessment of IL-17 secreting T cells, T-cell Xtend (Oxford Immunotec) was added to whole blood one day after collection, and PBMC isolation was performed. PBMCs were maintained in RPMI/GlutaMAX (Gibco) supplemented with 10% AB Serum (Sigma), 1% penicillin-streptomycin and 1% amphotericin B (Invitrogen). Cells were pre-incubated with 1µl/ml Infanrix 5-in-1 vaccine (GlaxoSmithKline), 20µg/ml *Candida albicans* extracts (Greer) or PBS for 48 hours.

Real-time PCR, ELISA and ELISPOT

Dr. Woolf, Prof. Taams and Dr. Fear (King's College London) kindly donated RNA samples they had isolated from skin-resident T lymphocytes, monocytes/macrophages/dendritic cells and B cells, respectively. The remaining RNAs were isolated using the mirVana kit (Life Technologies) (human skin biopsies), a Polytron PT 3000 tissue homogenizer (Kinematika) with TRIzol (Life Technologies) (mouse skin) or the GeneJET RNA purification kit (Thermo Fisher Scientific) (all cultured cells). Gene expression was assessed by real-time PCR using the primers listed in table S9 or TaqMan assays (Life Technologies). Transcript levels were normalized to *HuPO*, *B2M* or *B2m* expression (measured with Applied Biosystems TaqMan probes). IL-17, IL-36γ, IL-8 and TNFα production were measured with the Human IL-17 Quantikine ELISA Kit (Bio-techne), Human IL-36γ ELISA Kit (Sigma), Human IL-8 ELISA Kit (Sigma) and Human TNFα ELISA Kit (Sigma), respectively. IL-17 producing T cells were measured with IL-17A T cell ELISPOT assay (U-Cytech Biosciences). The mean number of spots in stimulated samples was normalized to the mean number of spots in untreated samples to derive a stimulation index.

Immunofluorescence microscopy

Tissue sections (8µm) cut from frozen skin biopsies were stained with 1:50 rabbit anti-human CD3 (Dako) or 1:50 mouse anti-human CD11c (Bio-Rad). Slides were imaged using an A1R confocal microscope (Nikon) and at least 5 z-stacks images per sample were

taken. The number of positive cells per field were counted using NIS-Elements Advanced Research software (Nikon).

Western blotting

Proteins were isolated from skin biopsies using a Bullet Blender Tissue Homogeniser (Next Advance) with non-denaturing cell lysis buffer (50 mMTrisHCl pH 7.4, 150 mMNaCl, 2% Triton X-100, 1% SDS, 10 mM EDTA, 1:100 protease inhibitor cocktail, 200mM calyculin). Protein lysates were loaded onto 10% polyacrylamide gels and electrophoresed at 100V in 1X running buffer (25mM Tris-Base, 1.92M Glycine, 0.1% SDS). Proteins were transferred onto a polyvinylidene fluoride (Roche Diagnostics) membrane that had been equilibrated in cold absolute methanol for 2 minutes and in 1X transfer buffer (25mM Tris-Base, 192mM glycine, 20% methanol) for 5 minutes. Proteins were transferred using a Mini Trans-Blot Electrophoresis transfer cell apparatus at 200mA for 1 hour at 4°C. Membranes were probed with 1:500 mouse monoclonal anti-p-p38 (Santa Cruz Biotechnology), 1:500 mouse monoclonal anti-p38α/β (Santa Cruz Biotechnology) or 1:2000 mouse monoclonal anti-hsc70 (Santa Cruz Biotechnology). Densitometric analysis was undertaken with Image J, which is available at https://imagej.nih.gov/ij/.

In-vivo IL-36 signaling blockade

Full thickness skin biopsies from mice were collected on day 7 of treatment for histological staining, RNA extraction and skin digestion. Following embedding in paraffin, tissue sections were stained with haematoxylin and eosin. Images were acquired at 10x magnification with an Olympus VS120 slide scanner. Five measurements of epidermal and scale thickness were taken in three sections per mouse.

For flow cytometry analysis of infiltrating immune cells, skin was digested for 2 hours at 37°C, using 400 mg/ml Liberase TL (Roche) and 1 mg/ml collagenase D (Roche) in IMDM medium, as described elsewhere (*18*). For intracellular cytokine staining, cells were stimulated for 4 hours with 500 ng/ml phorbol 12, 13-dibutyrate and 500ng/ml ionomycin in the presence of 1 mg/ml brefeldin A and Fc block (BD Bioscience), while simultaneously stained for surface markers. Cells were then fixed with 3.8% paraformaldehyde, permeabilized with 0.1% NP-40, and stained with anti-IL-17A and anti-IL-22 antibodies (Biolegend). Cells were acquired on a FACS Fortessa (BD Biosciences).

Pathogenicity predictions

The mutation status of all *IL1RL2* wild-type and mutant individuals was validated by Sanger sequencing, using the primers reported in table S9. The pathogenic potential of non-synonymous variants was assessed with the following programs: CADD (cadd.gs.washington.edu), Condel (bg.upf.edu/fannsdb/), SIFT (sift.jcvi.org), PROVEAN (provean.jcvi.org/) and PolyPhen-2 (genetics.bwh.harvard.edu/pph2/).

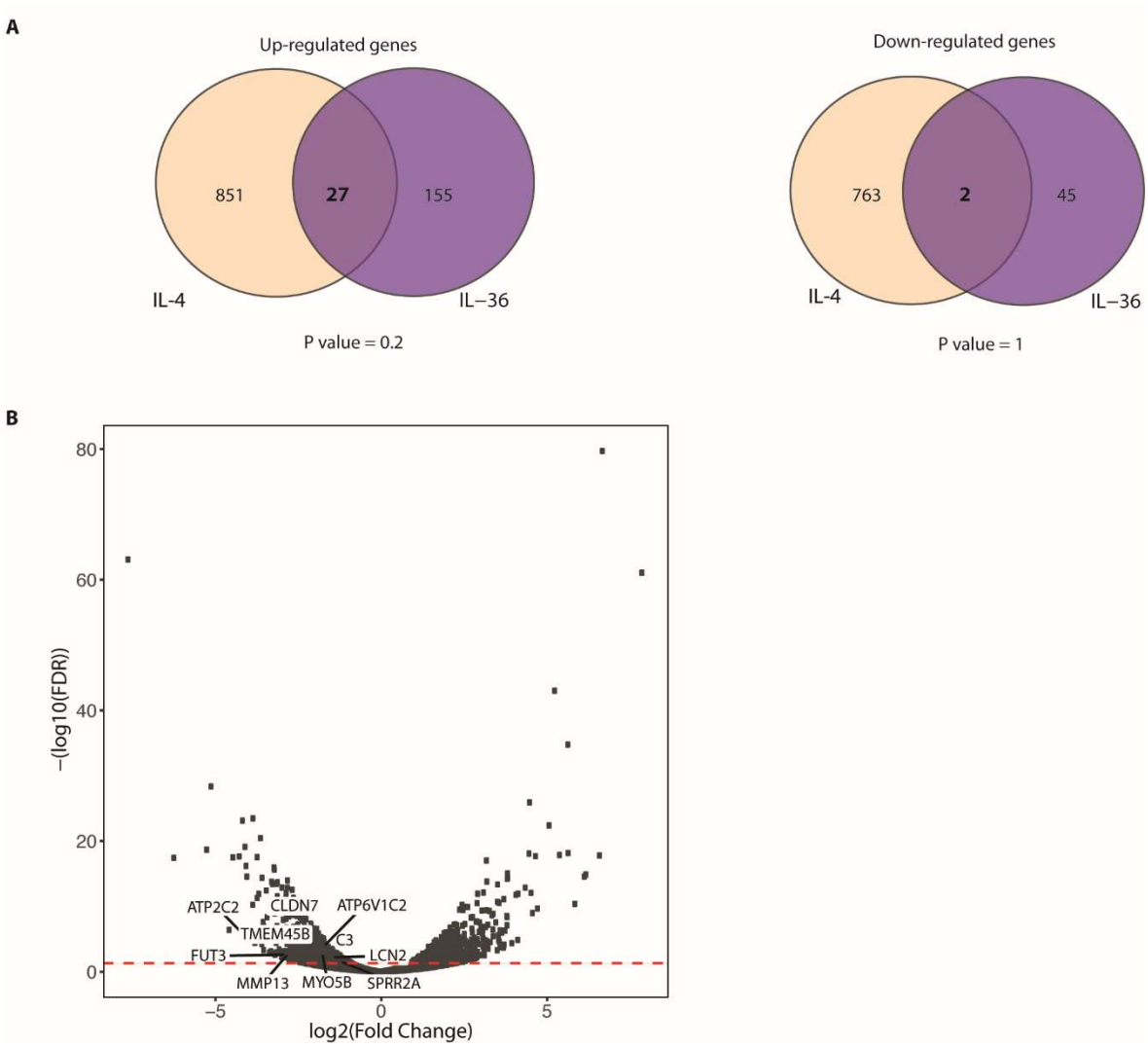

Fig. S1. IL-4 target genes are an appropriate negative control for IL-36 enrichment analyses, because there is no overlap between IL-4 and IL-36 signature genes. (**A**) The Venn diagrams show the overlap between the genes that are differentially expressed following stimulation of keratinocyte cultures with IL-4 or IL-36. Up-regulated genes (FDR<0.05, FC≥2) are shown on the left and down-regulated genes (FDR<0.05; FC≤-2) on the right. The *P* values reported under the diagram were obtained using the hyper-geometric distribution. (**B**) A number of keratinocyte genes (labelled in the volcano plot) that are up-regulated by IL-36 are down-regulated by IL-4.

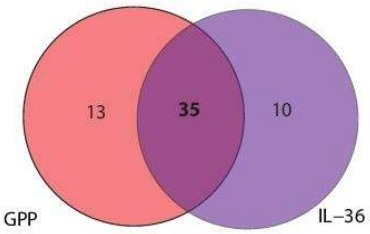

Most significantly enriched pathways shared between IL-36 and GPP

Canonical Pathway	-log(FDR)			
	IL–36α	IL–36β	IL–36γ	GPP
Atherosclerosis Signaling	9.8	9.6	10.2	13.2
Role of IL–17A in Psoriasis	13.1	11.0	12.6	7.3
Granulocyte Adhesion and Diapedesis	7.8	7.3	9.2	5.9
Agranulocyte Adhesion and Diapedesis	6.8	6.2	6.9	4.8
Acute Phase Response Signaling	5.5	4.8	6.7	6.1
p38 MAPK Signaling	5.2	5.0	5.9	4.8
LXR/RXR Activation	5.2	4.0	5.8	5.6
Communication between Immune Cells	7.0	5.1	6.7	3.9
Differential Regulation of Cytokines Production in Intestinal Cells by IL-17A and IL-17F	4.5	3.4	4.3	4.5
Role of IL-17F in Allergic Inflammatory Airway Diseases	4.2	3.1	5.1	3.4

Fig. S2. The pathways that underlie the pathogenesis of GPP are enriched within the IL-36 transcriptome. The Venn diagram shows the intersection of the pathways that are over-represented in GPP and in the three IL-36 datasets. The 10 most significantly enriched pathways are reported on the right.

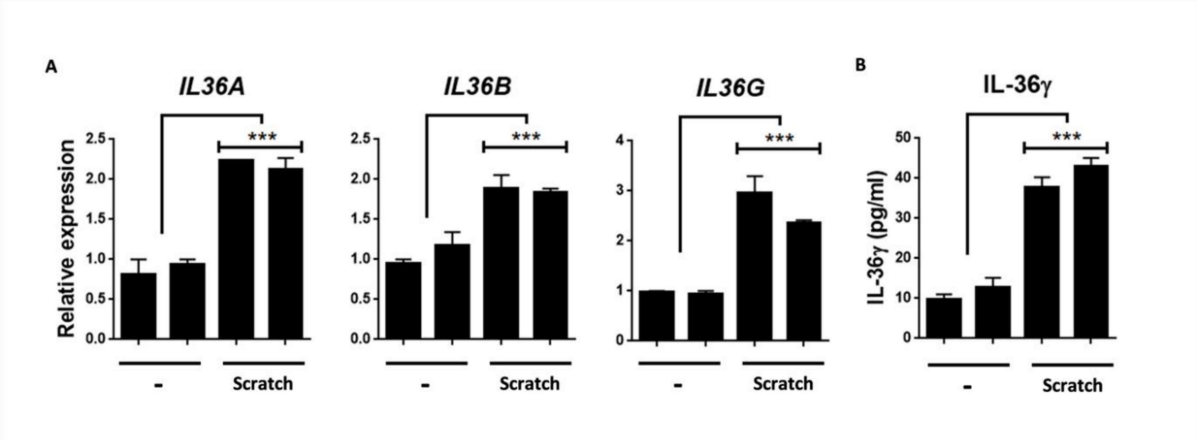

Fig. S3. Mechanical trauma up-regulates IL-36 production by cultured keratinocytes. Scratch wounds were created in primary keratinocyte monolayers derived from the skin of 2 healthy donors. After 4h, gene expression was compared in intact vs. scratched cultures, using real-time PCR (**A**) and cytokine release was assessed by ELISA (**B**). Data are presented as mean +/- SEM. *P* values were calculated by Student's t-test. ***$P \leq 0.001$.

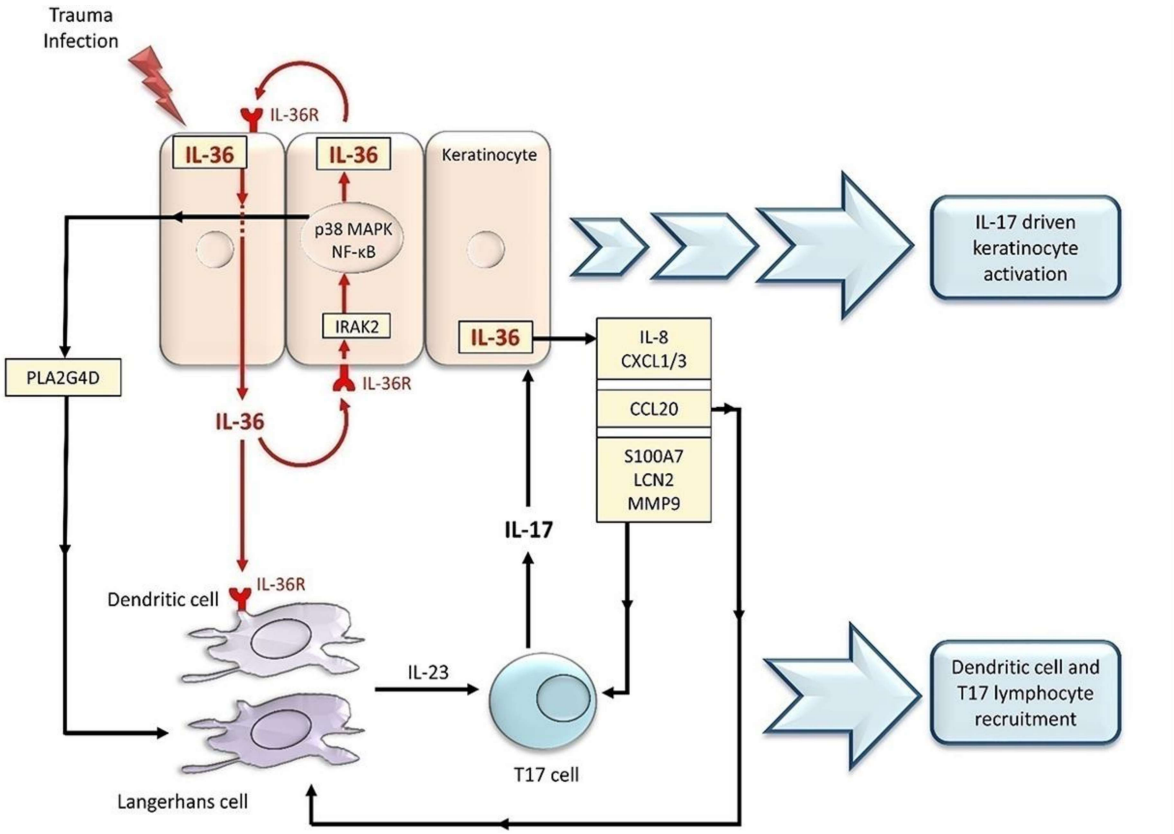

Fig. S4. Proposed pathogenic model illustrating the role of IL-36 as an amplifier of T_H17 signaling in psoriasis. IL-36 cytokines produced by keratinocytes activate dendritic cells (directly) and Langerhans cells (via PLA2G4D), leading to the polarization of TH17 lymphocytes. The ensuing IL-17 release promotes further IL-36 production by keratinocytes, resulting in autocrine and paracrine chemokine induction. IL-36 target genes identified by keratinocyte RNA-seq are shown in yellow boxes.

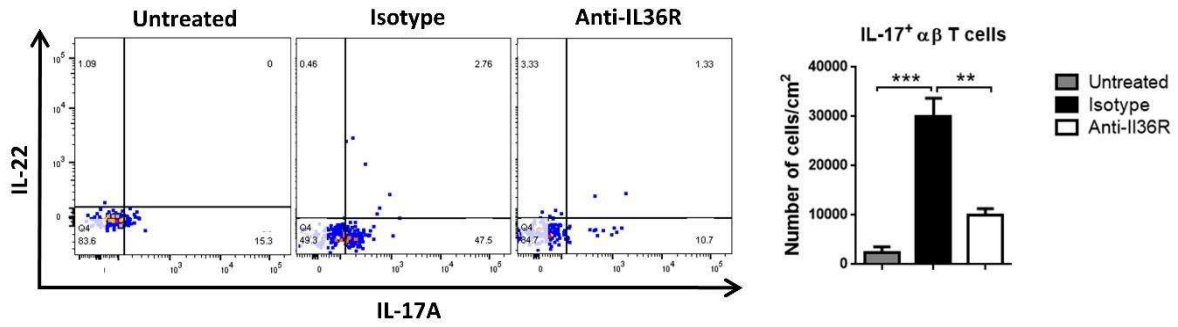

Fig. S5. In vivo IL-36 signaling blockade reduces the infiltration of IL-17–producing αβ T cells in imiquimod-induced psoriasiform dermatitis. Flow cytometry was performed on skin cell suspensions obtained from imiquimod-treated mice that had received daily injections of anti-IL36R or an isotype-matched control antibody (n=5 per group). Normal skin obtained from mice (n=3) that had not been treated with imiquimod was analyzed as a reference sample. Representative FACS plot (left) and quantification (right) of IL-17 and IL-22 producing TCRβ+ T-cells gated within live CD45+ cells. Data for each treatment group are presented as the mean +/- SEM. *P* values were calculated with one-way ANOVA followed by Dunnett's post-test. ***P*<0.01, ****P*≤ 0.001.

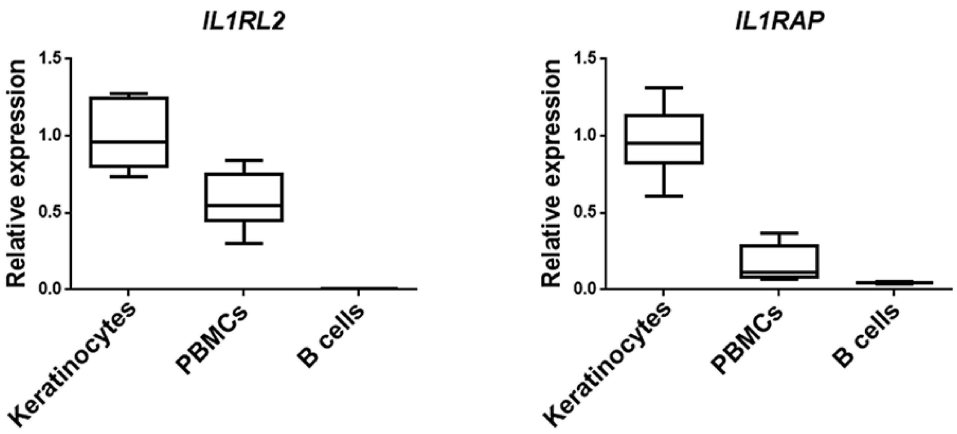

Fig. S6. The genes encoding the IL-36R subunits are expressed in PBMCs. *IL1RL2* and *IL1RAP* transcript levels were measured by real-time PCR and compared to those observed in cell types where the IL-36 receptor is highly expressed (keratinocytes) or virtually undetectable (B cells). Each bar shows the median and range of expression values, observed in 2-5 healthy donors.

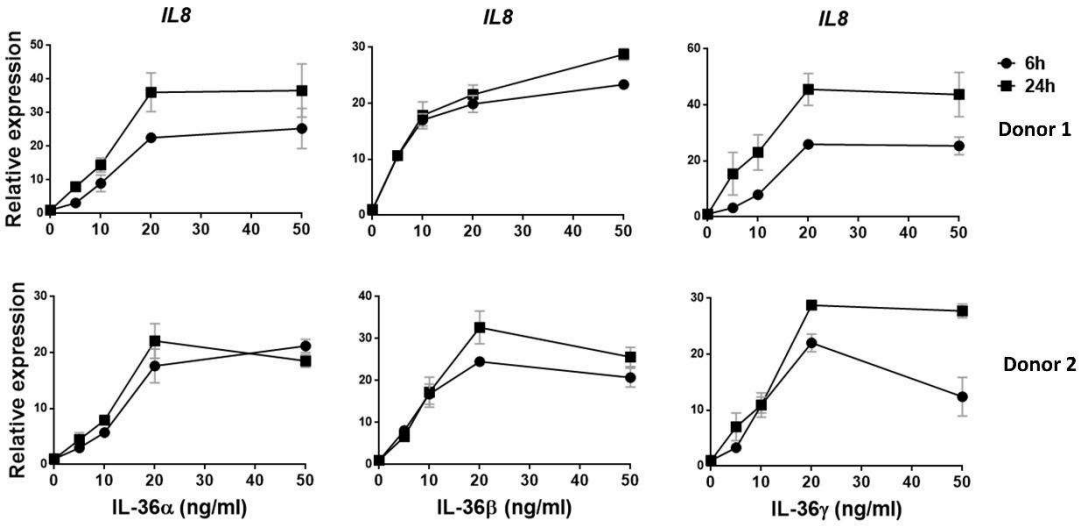

Fig. S7. Dose- and time-dependent effects of IL-36 cytokines in primary keratinocytes. Primary keratinocytes obtained from 2 independent healthy donors were treated with increasing concentrations (5-50ng/ml) of IL-36α, -β or –γ, for 6 or 24 hours. The effects of cytokine treatment were then measured by real-time PCR, using the up-regulation of *IL8* expression as a readout. Data from two independent donors are presented as the mean +/- SEM.

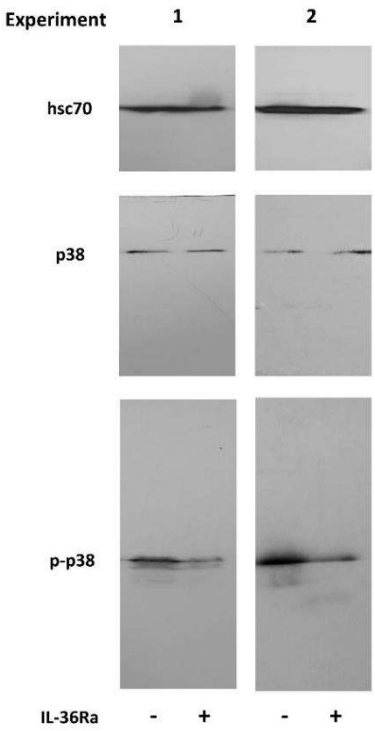

Fig. S8. Complete Western blots for Fig. 5E. The membrane was first probed with anti-p-p38 and anti-hsc70 antibodies (images were taken after different exposure times). It was then stripped and re-probed with anti-p38.

Table S5. Rare homozygous *IL1RL2* variants observed in the Born in Bradford cohort.

		Pathogenicity predictions (Score)					
Variant (rs ID)	**CADD[1]**	**Condel**	**SIFT**	**PROVEAN**	**PolyPhen-2**	**Consensus[2]**	**N. of homozygotes**
p.Ala197Asp c.590C>A (rs772278646)	22.7	Deleterious (0.827)	Damaging (0.007)	Deleterious (-3.23)	Possibly damaging (0.451)	**Deleterious**	1
p.Ile229Met c.687C>G (rs150242167)	24.6	Deleterious (0.966)	Damaging (0.003)	Neutral (-2.24)	Possibly damaging (0.844)	**Deleterious**	1
p.Ile355Thr c.1064T>C (rs138105991)	4.0	Neutral (0.262)	Tolerated (0.120)	Deleterious (-2.84)	Benign (0.037)	Benign	1
p.Ala471Thr c.1411G>A (rs75091099)	22.0	Deleterious (0.55)	Tolerated (0.064)	Deleterious (-2.78)	Possibly damaging (0.600)	**Deleterious**	9
p.Pro543Leu c.1628C>T (rs529060003)	23.4	Deleterious (0.855)	Damaging (0.031)	Deleterious (-3.92)	Benign (0.231)	**Deleterious**	1
p.Pro546Leu c.1637C>T (rs72998581)	13.1	Neutral (0.241)	Tolerated (0.070)	Neutral (-2.28)	Benign (0.006)	Benign	1

[1]Although the CADD algorithm does not return qualitative predictions, scores greater than 15 are typically considered as evidence ofpathogenicity.[2]Variants were designated as deleterious when at least 4 out of 5 programs returned a prediction of pathogenicity. Individuals who were homozygous for the underlined variants were recalled for further phenotyping.

Table S6. Full blood counts of individuals with homozygous *IL1RL2* mutations and controls.

Participant ID	*Hb (g/L)*	*WBC (10^9/L)*	*Neut (10^9/L)*	*Lymph (10^9/L)*	*Mono (10^9/L)*	*Eo (10^9/L)*	*Baso (10^9/L)*	*Plt (10^9/L)*
P1	12.5	7.12	4.5	1.95	0.47	0.16	0.04	282
P2	13.4	5.67	3.44	1.66	0.49	0.05	0.02	282
P3	15.5	6.53	3.34	2.36	0.43	0.37	0.02	267
P4	12.5	6.73	4.74	1.47	0.28	0.21	0.02	275
P5	14.1	8.01	5.18	2.18	0.36	0.27	0.02	307
P6	12.5	5.65	3.29	1.89	0.33	0.09	0.06	347
P7	13.2	6.89	4.14	2.19	0.33	0.09	0.1	406
P8	13.3	7.7	5.96	1.32	0.33	0.15	0.01	241
P9	12.3	9.54	6.29	2.16	0.48	0.11	0.06	253
P10	11.8	8.04	5.33	1.87	0.34	0.32	0.02	329
P11	12	6.81	3.6	2.49	0.37	0.08	0.03	231
P12	12.2	7.48	4.17	2.53	0.32	0.31	0.02	282
C1	13.3	8.3	5.9	1.91	0.35	0.11	0.03	288
C2	12.2	9.29	5.72	2.6	0.56	0.37	0.04	229
C3	14.3	9.92	6.77	2.59	0.4	0.13	0.03	290
C4	14.4	4.39	2.05	1.94	0.32	0.05	0.02	210

Individuals highlighted in bold were recalled for further phenotyping. Hb, haemoglobin (reference range 11.5-15.5); WBC, white blood cell count (4-11); Neut, neutrophil count (2.2-6.3); Lymph, lymphocyte count (1.3-4); Mono, monocyte count (0.2-1); Eo, eosinophil count, (0-0.4); Baso, basophil count (0-0.1); Plt, platelet count (150-450).

Table S7. Immune serology results.

Participant ID	*IgG (g/L)*	*IgA (g/L)*	*IgM (g/L)*	*Aspergillus IgG (mgA/L)*	*VZV IgG*	*HiB IgG (mg/L)*	*Tetanus IgG (IU/ml)*	*Measles IgG*
P1	11.4	1.13	0.75	13.1	positive	n/a	0.18	positive
P2	12.2	2.78	1	22.3	positive	n/a	1.07	positive
P3	15.9	3.13	1.23	17.5	positive	n/a	3.46	positive
P4	11.7	2.06	2.3	84.7	positive	n/a	0.17	indeterminate*
P5	13.9	2.3	1.46	18.5	positive	n/a	1.7	positive
P6	11.9	2.35	0.94	33.3	positive	5.34	6.5	positive
C1	10.9	0.95	1.09	36.5	n/a	5.75	2.12	positive
C2	17.8	3.22	1.15	11.6	positive	1.48	1.57	indeterminate*
C3	16.9	2.6	1.08	54.8	positive	0.42	4.4	positive
C4	16.7	3.41	2.05	34.4	positive	2.27	1.46	positive

IgG reference range 6.34-18.11; IgA (0.87-4.12); IgM (0.53-2.23); Aspergillus IgG (0-39.9); HiB IgG, Haemophilus influenza IgG (>0.14); Tetanus toxoid IgG (>0.14); VZV varicella zoster virus; n/a, test was not performed since there was no evidence of vaccination or past infection from the clinical history and/or medical records. *'Indeterminate' indicates an inconclusive test result.

Table S8. Skin donor demographics.

Participant ID	*Sex*	*Age*	*Ethnicity*	*Disease status*	*Experiment*
KC 1	F	34	European	Unaffected	IL-36 stimulation of primary keratinocytes
KC 2	F	55	European	Unaffected	IL-36 stimulation of primary keratinocytes, scratch assay
KC 3	F	46	European	Unaffected	IL-36 stimulation of primary keratinocytes, scratch assay
KC 4	F	40	African	Unaffected	IL-36 stimulation of primary keratinocytes
Ps 1	M	51	European	Affected by severe Ps	*Ex-vivo* IL-36Ra treatment (Real-time PCR)
Ps 2	M	37	African	Affected by severe Ps	*Ex-vivo* IL-36Ra treatment (Real-time PCR)
Ps 3	M	43	European	Affected by severe Ps	*Ex-vivo* IL-36Ra treatment (Real-time PCR)
Ps 4	F	47	European	Affected by severe Ps	*Ex-vivo* IL-36Ra treatment (Real-time PCR)
Ps 5	F	55	European	Affected by severe Ps	*Ex-vivo* IL-36Ra treatment (Real-time PCR)
Ps 6	M	37	European	Affected by severe Ps	*Ex-vivo* IL-36Ra treatment (IF microscopy)
Ps 7	F	58	African	Affected by severe Ps	*Ex-vivo* IL-36Ra treatment (IF microscopy)
Ps 8	M	22	East Asian	Affected by severe Ps	*Ex-vivo* IL-36Ra treatment (IF microscopy)
Ps 9	F	58	European	Affected by severe Ps	*Ex-vivo* IL-36Ra treatment (Western blotting)
Ps 10	F	53	East Asian	Affected by severe Ps	*Ex-vivo* IL-36Ra treatment (Western blotting)

IF, immunofluorescence

Table S9. Oligonucleotide primers used in the study.

Target	*Primer ID*	*Sequence (5' to 3')*	*Annealing temperature (°C)*	*Application*
CAMP	LL37_Fwd	GCTGGGTGATTTCTTCCGGA	60	Real-time
	LL37_Rev	CCTGGGTACAAGATTCCGCA		PCR
CCL20	CCL20_Fwd	GCGAATCAGAAGCAAGCAACT	60	Real-time
	CCL20_Rev	TTGCGCACACAGACAACTTT		PCR
HuPO	HuPO_Fwd	GCTTCCTGGAGGGTGTCC	60	Real-time
	HuPO_Rev	GGACTCGTTTGTACCCGTTG		PCR
IFIT1	IFIT1_Fwd	TAGGCAGAGATCGCATACCC	60	Real-time
	IFIT1_Rev	GCTTTCAAATCCCTTCCGCT		PCR
IL17A	IL17A_Fwd	CTACAACCGATCCACCTCACCTTG	60	Real-time
	IL17A_Rev	GGTAGTCCACGTTCCCATCAGC		PCR
IL6	IL6_Fwd	AAAGAGGCACTGGCAGAAAA	60	Real-time
	IL6_Rev	GCTCTGGCTTGTTCCTCACT		PCR
IL8	IL8_Fwd	TTGGCAGCCTTCCTGATTTC	60	Real-time
	IL8_Rev	AACTTCTCCACAACCCTCT		PCR
IL36A	IL36A_Fwd	GGCCTGAATGGACTCAATCT	60	Real-time
	IL36A_Rev	ACTTCACAGGCTCGGGTTG		PCR
IL36B	IL36B_Fwd	CAGCATTAAGCCTGTCACTC	60	Real-time
	IL36B_Rev	GCACAGAAGAGACAGAGATC		PCR
IL36G	IL36G_Fwd	GGGCCGTCTATCAATCAATG	60	Real-time
	IL36G_Rev	TGATAACAGCAACAGTGACTG		PCR
IL1RL2	IL1RL2_1_Fwd	CAGTCTTTGGGGAAACGTGG	58	Sanger
Exon 1	IL1RL2_1_Rev	TCTCTGTTTCCTCTTCCGCG		sequencing
IL1RL2	IL1RL2_2_Fwd	TCCAGACTCAAGAAACTCCCA	58	Sanger
Exon 2	IL1RL2_2_Rev	TCTGGTCTGAGGTGCCATTT		sequencing
IL1RL2	IL1RL2_3_Fwd	GCAGAGGGTTTGCACAGTG	62	Sanger
Exon 3	IL1RL2_3_Rev	TAACTGGAGGAAGGTGGTGG		sequencing
IL1RL2	IL1RL2_4_Fwd	TCTGCTGCCTATCTATCCATCT	58	Sanger
Exon 4	IL1RL2_4_Rev	GACCTAGAATCACTCCTGCTCA		sequencing
IL1RL2	IL1RL2_5_Fwd	GCTTATTGATGGTCTGCTCTGT	58	Sanger
Exon 5	IL1RL2_5_Rev	GGAAACTGGGTGTGTATAGGAT		sequencing
IL1RL2	IL1RL2_6_Fwd	TTGCCCCTTGTGGTCTCTC	58	Sanger
Exon 6	IL1RL2_6_Rev	TGTTTGCTTTGTATGCCCGG		sequencing
IL1RL2	IL1RL2_7_Fwd	GGATAACATGATGGCCCAAAGT	58	Sanger
Exon 7	IL1RL2_7_Rev	CACAGCCTCACTCCAACAAC		sequencing
IL1RL2	IL1RL2_8_Fwd	TTCTGCTCCCATACCACTTTT	58	Sanger
Exon 8	IL1RL2_8_Rev	TGATGCTGGTGATTAGGGACA		sequencing
IL1RL2	IL1RL2_9_Fwd	GGAGATGATGTCCCTTGGCA	60	Sanger
Exon 9	IL1RL2_9_Rev	CAAGCAGGAATCTCAGGCAC		sequencing

IL1RL2	IL1RL2_10_Fwd	TGAGCTGAGATTGCATCCCT	60	Sanger
Exon 10	IL1RL2_10_Rev	CAGATCCTCTCACTAGTACGCA		sequencing
IL1RL2	IL1RL2_11_Fwd	AACTGACGGCAAGGTGGAG	60	Sanger
Exon 11	IL1RL2_11_Rev	CCTCTTCTCTACGCCTGAGC		sequencing
IRAK2	IRAK2_Fwd	CCTCCTCTGAGGCCTGTGT	60	Real-time
	IRAK2_Rev	TGATCTCAATTTGCCACGAA		PCR
KRT10	KRT10_Fwd	AGCATGGCAACTCACATCAG	60	Real-time
	KRT10_Rev	TGTCGATCTGAAGCAGGATG		PCR
KRT16	KRT16_Fwd	GAGATCAAAGACTACAGTCC	60	Real-time
	KRT16_Rev	CATGCTCATACTTGGTCCTG		PCR
LCN2	LCN2_Fwd	TCACCTCCGTCCTGTTTAGG	60	Real-time
	LCN2_Rev	AGGTAACTCGTTAATCCAGGGTAA		PCR
MMP9	MMP9_Fwd	GATCATTCCTCAGTGCCGGA	60	Real-time
	MMP9_Rev	TTCAGGGCGAGGACCATAGA		PCR
PLA2G4D	PLA2G4D_Fwd	TTGAGTGAGGCCGACCCTTA	60	Real-time
	PLA2G4D_Rev	GCTCCAGAACATTCTTGACCTG		PCR
RSAD2	PLA2G4D_Fwd	TCCGTCATGTCCTCTTCCAC	60	Real-time
	PLA2G4D_Rev	CTGTGACAGCTTTGACGAGG		PCR
S100A7	S100A7_Fwd	AACTTCCTTAGTGCCTGTGACAA	60	Real-time
	S100A7_Rev	TCCTTTTTCTCAAAGACATCGGC		PCR

4. Discussion

The recent characterisation of IL-36 cytokines as innate mediators of epithelial inflammation has led to a growing interest into the pathogenic role of these molecules [134]. In this context, the current study investigated IL-36 signalling as a shared disease mediator for common and rare forms of psoriasis, while also exploring the therapeutic potential of IL-36 blockade.

4.1 The pathogenic role of IL-36 cytokines in psoriasis

While the pathogenesis of common plaque psoriasis has been extensively investigated in recent years, the molecular mechanisms underlying cutaneous autoinflammation in pustular psoriasis remain poorly defined. Hence, very little information is available on potential drug targets [121].

While excessive IL-36 signalling had previously been demonstrated in patients bearing *IL36RN* mutations [96], [97], the transcriptome data generated in this thesis suggest that this pathway is also de-regulated in *IL36RN*-negative individuals, as the latter accounted for the majority of the GPP microarray dataset that was examined here. Further, IL-36 production can be increased by *AP1S3* disease alleles (as shown here) and *CARD14* over-expression [27], which again suggests that mutations in different disease genes converge on the de-regulation of IL-36 signalling.

Importantly, established pustular psoriasis genes (*IL36RN*, *AP1S3* and *CARD14*) only account for a minority of reported cases [29], [99], [108]. Thus, additional genetic determinants for the disease

will need to be uncovered and functionally characterised, to demonstrate that IL-36 signalling perturbation is a pervasive feature of the disease.

Due to the rarity of GPP, gene discovery will require multi-centre recruitment of patient cohorts that have been phenotyped using standardised criteria. The 100,000 Genomes Project, which seeks to facilitate the diagnosis of rare genetic diseases by means of whole genome sequencing, will help to achieve this [239]. An additional international initiative is the European Rare and Severe Psoriasis Expert Network (ERASPEN), which aims to formalise the diagnostic criteria for pustular psoriasis subtypes and promote the collection of patient samples [240].

Although whole exome sequencing remains the preferred approach for the discovery of causal variants in rare diseases, success rates remain variable (25-50%) especially in genetically heterogeneous conditions, so that alternative strategies are being explored [241]. In a recent study, Cummings et al compared patient RNA-seq data from disease-relevant tissue to the corresponding Genotype Tissue Expression (GTEx) reference panel [241]. Novel intronic and exonic splice site-altering mutations were thus identified, providing a genetic diagnosis in patients with rare muscle disorders for whom prior analysis of DNA sequencing data had failed to uncover a disease allele. Since GTEx also comprises skin transcriptome data [242], this approach may enable the identification of further pustular psoriasis genes and the assessment of how mutations may impact on IL-36 signalling.

Although the transcriptomic work in this study has improved understanding of the downstream targets of IL-36α, -β and -γ, these molecules do not exist in isolation within inflamed tissues. It would

thus be interesting to explore whether IL-36 can synergise with other key psoriasis cytokines such as IL-17 and TNFα, as this would generate further insights into the pro-inflammatory cross-talk that contributes to disease states.

4.2 The therapeutic potential of IL-36 blockade

IL-36 has been shown here to contribute to the development of both pustular and plaque psoriasis; two conditions characterised by differing clinical presentations and genetic architectures. In support of the common pathogenic mechanisms proposed in this thesis, plaque psoriasis is consistently observed at a higher frequency in patients with pustular psoriasis than in the general population [99]. The management of these patients with disease co-occurrence is challenging: although TNFα and IL-12/IL-23 antagonists can successfully treat plaques, their efficacy in pustular phenotypes is significantly inferior, and no agents currently exist that can effectively target both forms of psoriasis concurrently.

Blockade of IL-36 signalling may thus represent a unifying treatment for both diseases. In pustular psoriasis, it could reverse the widespread IL-36 upregulation that results from germline mutations in *IL36RN*, *AP1S3*, *CARD14* and other, as yet unidentified disease genes. In the case of plaque psoriasis, IL-36 blockers could counter the consequences of T17 driven, IL-36 over-expression in skin. In fact, the data generated here show that treatment with IL-36 antagonists results in decreased chemokine production and hence, reduced infiltration of inflammatory cells into the dermis and the epidermis.

Since the transcriptome analyses in this thesis demonstrated substantial redundancy between the downstream activities of IL-36α, -β and γ, the above experiments targeted the IL-36 receptor (using

a recombinant form of the human IL-36 receptor antagonist or a murine anti-IL36R antibody) rather than individual cytokines. Going forward, this is likely to be the optimal therapeutic strategy. Indeed, monoclonal antibodies that block the IL-36 receptor are being developed by Boehringer Ingelheim and AnaptysBio [243]–[245].

An alternative approach to IL-36 signalling blockade involves the inhibition of IL-36 proteolytic processing [246]. This is supported by emerging research demonstrating that the activation of IL-36 cytokines is regulated by keratinocyte and neutrophil-derived proteases [140]–[143]. If these enzymes prove amenable to pharmacological inhibition with orally available small molecules, a very cost-effective treatment strategy could be developed [247]. However, recent studies suggest that IL-36α, -β and -γ are activated by distinct proteases [140]–[143], so that a single agent may not be capable of mediating pan-IL-36 signalling blockade. In the future, the characterization of further molecules that regulate IL-36 production or bio-activity is likely to identify additional targets for therapeutic intervention.

4.3 The translational potential of human knockout studies

This study examined human gene knockouts recruited from the Born in Bradford cohort [212] to determine the long-term effects of IL-36 signalling inhibition on host immunity. This was based on the assumption that the phenotype of individuals harbouring homozygous LoF mutations in *IL1RL2* would mimic the effects of pharmacological receptor blockade.

Clinical, serological and molecular profiling of these individuals did not reveal any abnormalities in the immune responses to bacterial, viral and fungal pathogens. Moreover, no evidence of skin, gut

or lung pathology could be uncovered by searches of medical records or clinical examinations. The analyses in this project were, however, limited by the nature of the biological material that was available at the time (whole blood and saliva samples). Given the prominent role of IL-36 in barrier defences, further interrogation of epithelial-specific immune responses would therefore be valuable. In particular, skin samples could be analysed *ex-vivo* to complement the assessment of the circulating immune cells performed here.

Of note IL-36 has been implicated in the response to *Candida albicans* [152], a fungal pathogen which causes opportunistic infections of the skin/mucosae when host immunity is impaired. Thus, skin explants obtained from *IL1RL2* knockouts and controls could be stimulated with *C. albicans* and cytokine release could be compared in the two groups. Further, given that IL-36 has been shown to mediate the resolution of epithelial damage [172], it would be interesting to assess the response to skin trauma in the knockouts. This could be achieved by culturing knockout and control-derived keratinocyte monolayers and mimicking the effects of wounding using techniques such as the 'scratch assay' [248].

The application of a recall-by-genotype approach similar to ours has recently enabled the pre-clinical assessment of apolipoprotein C3 as a novel drug target [200]. Saleheen et al found that human *APOC3* knockouts recruited in Pakistan were healthy and had reduced fasting plasma triglyceride levels with blunted post-prandial triglyceride rises. This suggested that apolipoprotein C3 may in the future be successfully targeted for the treatment of hyperlipidaemia.

The scope for continuing such innovative work is dependent on the ongoing discovery of human gene knockouts, which will require larger-scale sequencing of populations enriched for parental relatedness. To this end, the East London Genes and Health (ELG&H) study aims to exome sequence and consent for recall 100,000 British individuals from Pakistani and Bangladeshi communities [249]. The analysis of such an extended resource will also increase the statistical power for genotype-phenotype correlations since numerous individuals with identical homozygous LoF alleles may be found.

More broadly, the scientific community is now aspiring to a global 'Human Knockout Project' [213], which will pool in a single database the results obtained from large population studies such as ELG&H, Born in Bradford and PROMIS, with a view to cataloguing all known human knockouts. This will be an invaluable resource for both academic researchers and pharmaceutical companies, and if appropriate consent for recall has been obtained from study participants, will enable additional deep phenotyping for therapeutic target validation.

In conclusion, this project has provided novel insights into a shared pathogenic role for IL-36 in pustular and plaque psoriasis. The observation of beneficial effects of IL-36 signalling inhibition in several experimental models now paves the way for early phase clinical trials. Importantly, this thesis also demonstrates the utility of human knockout research in the pre-clinical assessment of drug targets, and signals a paradigm shift in genetics research towards genotype-driven phenotyping. Harnessing the power of population-level sequence data in this manner may reap major health benefits in the future.

5. References

[1] F. O. Nestle, D. H. Kaplan, and J. Barker, "Psoriasis," *N. Engl. J. Med.*, vol. 361, no. 5, pp. 496–509, Jul. 2009.

[2] E. Christophers, "Psoriasis--epidemiology and clinical spectrum," *Clin. Exp. Dermatol.*, vol. 26, no. 4, pp. 314–320, Jun. 2001.

[3] R. Parisi, D. P. M. Symmons, C. E. M. Griffiths, D. M. Ashcroft, and Identification and Management of Psoriasis and Associated ComorbidiTy (IMPACT) project team, "Global epidemiology of psoriasis: a systematic review of incidence and prevalence," *J. Invest. Dermatol.*, vol. 133, no. 2, pp. 377–385, Feb. 2013.

[4] J. Schmitt and G. Wozel, "The psoriasis area and severity index is the adequate criterion to define severity in chronic plaque-type psoriasis," *Dermatol. Basel Switz.*, vol. 210, no. 3, pp. 194–199, 2005.

[5] V. Bronsard *et al.*, "What are the best outcome measures for assessing quality of life in plaque type psoriasis? A systematic review of the literature," *J. Eur. Acad. Dermatol. Venereol. JEADV*, vol. 24 Suppl 2, pp. 17–22, Apr. 2010.

[6] R. C. Lamb *et al.*, "Screening for anxiety and depression in people with psoriasis: a cross-sectional study in a tertiary referral setting," *Br. J. Dermatol.*, Jul. 2016.

[7] G. K. Perera, P. Di Meglio, and F. O. Nestle, "Psoriasis," *Annu. Rev. Pathol.*, vol. 7, pp. 385–422, 2012.

[8] J. C. Henes *et al.*, "High prevalence of psoriatic arthritis in dermatological patients with psoriasis: a cross-sectional study," *Rheumatol. Int.*, vol. 34, no. 2, pp. 227–234, Feb. 2014.

[9] J. M. Gelfand, A. L. Neimann, D. B. Shin, X. Wang, D. J. Margolis, and A. B. Troxel, "Risk of myocardial infarction in patients with psoriasis," *JAMA*, vol. 296, no. 14, pp. 1735–1741, Oct. 2006.

[10] E. J. Samarasekera, J. M. Neilson, R. B. Warren, J. Parnham, and C. H. Smith, "Incidence of cardiovascular disease in individuals with psoriasis: a systematic review and meta-analysis," *J. Invest. Dermatol.*, vol. 133, no. 10, pp. 2340–2346, Oct. 2013.

[11] O. Ahlehoff *et al.*, "Psoriasis is associated with clinically significant cardiovascular risk: a Danish nationwide cohort study," *J. Intern. Med.*, vol. 270, no. 2, pp. 147–157, Aug. 2011.

[12] M. Murphy, P. Kerr, and J. M. Grant-Kels, "The histopathologic spectrum of psoriasis," *Clin. Dermatol.*, vol. 25, no. 6, pp. 524–528, Dec. 2007.

[13] M. A. Lowes, M. Suárez-Fariñas, and J. G. Krueger, "Immunology of psoriasis," *Annu. Rev. Immunol.*, vol. 32, pp. 227–255, 2014.

[14] S. K. Mahil, F. Capon, and J. N. Barker, "Genetics of psoriasis," *Dermatol. Clin.*, vol. 33, no. 1, pp. 1–11, Jan. 2015.

[15] A. S. Lønnberg, L. Skov, A. Skytthe, K. O. Kyvik, O. B. Pedersen, and S. F. Thomsen, "Heritability of psoriasis in a large twin sample," *Br. J. Dermatol.*, vol. 169, no. 2, pp. 412–416, Aug. 2013.

[16] J. T. Elder, R. P. Nair, S. W. Guo, T. Henseler, E. Christophers, and J. J. Voorhees, "The genetics of psoriasis," *Arch. Dermatol.*, vol. 130, no. 2, pp. 216–224, Feb. 1994.

[17] F. Capon, R. C. Trembath, and J. N. Barker, "An update on the genetics of psoriasis," *Dermatol. Clin.*, vol. 22, no. 4, pp. 339–347, vii, Oct. 2004.

[18] R. C. Trembath *et al.*, "Identification of a major susceptibility locus on chromosome 6p and evidence for further disease loci revealed by a two stage genome-wide search in psoriasis," *Hum. Mol. Genet.*, vol. 6, no. 5, pp. 813–820, May 1997.

[19] R. P. Nair *et al.*, "Evidence for two psoriasis susceptibility loci (HLA and 17q) and two novel candidate regions (16q and 20p) by genome-wide scan," *Hum. Mol. Genet.*, vol. 6, no. 8, pp. 1349–1356, Aug. 1997.

[20] C. D. Veal *et al.*, "Family-based analysis using a dense single-nucleotide polymorphism-based map defines genetic variation at PSORS1, the major psoriasis-susceptibility locus," *Am. J. Hum. Genet.*, vol. 71, no. 3, pp. 554–564, Sep. 2002.
[21] C. A. Alper, C. E. Larsen, D. P. Dubey, Z. L. Awdeh, D. A. Fici, and E. J. Yunis, "The haplotype structure of the human major histocompatibility complex," *Hum. Immunol.*, vol. 67, no. 1–2, pp. 73–84, Feb. 2006.
[22] R. P. Nair *et al.*, "Genome-wide scan reveals association of psoriasis with IL-23 and NF-kappaB pathways," *Nat. Genet.*, vol. 41, no. 2, pp. 199–204, Feb. 2009.
[23] Genetic Analysis of Psoriasis Consortium & the Wellcome Trust Case Control Consortium 2 *et al.*, "A genome-wide association study identifies new psoriasis susceptibility loci and an interaction between HLA-C and ERAP1," *Nat. Genet.*, vol. 42, no. 11, pp. 985–990, Nov. 2010.
[24] B.-J. Feng *et al.*, "Multiple Loci within the major histocompatibility complex confer risk of psoriasis," *PLoS Genet.*, vol. 5, no. 8, p. e1000606, Aug. 2009.
[25] X. Yin *et al.*, "Genome-wide meta-analysis identifies multiple novel associations and ethnic heterogeneity of psoriasis susceptibility," *Nat. Commun.*, vol. 6, p. 6916, Apr. 2015.
[26] Y. Okada *et al.*, "Fine mapping major histocompatibility complex associations in psoriasis and its clinical subtypes," *Am. J. Hum. Genet.*, vol. 95, no. 2, pp. 162–172, Aug. 2014.
[27] C. T. Jordan *et al.*, "Rare and common variants in CARD14, encoding an epidermal regulator of NF-kappaB, in psoriasis," *Am. J. Hum. Genet.*, vol. 90, no. 5, pp. 796–808, May 2012.
[28] C. T. Jordan *et al.*, "PSORS2 is due to mutations in CARD14," *Am. J. Hum. Genet.*, vol. 90, no. 5, pp. 784–795, May 2012.
[29] D. M. Berki *et al.*, "Activating CARD14 Mutations Are Associated With Generalized Pustular Psoriasis but Rarely Account for Familial Recurrence in Psoriasis Vulgaris," *J. Invest. Dermatol.*, Jul. 2015.
[30] P. E. Stuart *et al.*, "Association of β-defensin copy number and psoriasis in three cohorts of European origin," *J. Invest. Dermatol.*, vol. 132, no. 10, pp. 2407–2413, Oct. 2012.
[31] R. de Cid *et al.*, "Deletion of the late cornified envelope LCE3B and LCE3C genes as a susceptibility factor for psoriasis," *Nat. Genet.*, vol. 41, no. 2, pp. 211–215, Feb. 2009.
[32] F. Capon *et al.*, "Identification of ZNF313/RNF114 as a novel psoriasis susceptibility gene," *Hum. Mol. Genet.*, vol. 17, no. 13, pp. 1938–1945, Jul. 2008.
[33] M. Cargill *et al.*, "A large-scale genetic association study confirms IL12B and leads to the identification of IL23R as psoriasis-risk genes," *Am. J. Hum. Genet.*, vol. 80, no. 2, pp. 273–290, Feb. 2007.
[34] E. Ellinghaus *et al.*, "Genome-wide association study identifies a psoriasis susceptibility locus at TRAF3IP2," *Nat. Genet.*, vol. 42, no. 11, pp. 991–995, Nov. 2010.
[35] L. C. Tsoi *et al.*, "Identification of 15 new psoriasis susceptibility loci highlights the role of innate immunity," *Nat. Genet.*, vol. 44, no. 12, pp. 1341–1348, Dec. 2012.
[36] L. C. Tsoi *et al.*, "Enhanced meta-analysis and replication studies identify five new psoriasis susceptibility loci," *Nat. Commun.*, vol. 6, p. 7001, May 2015.
[37] X. Zuo *et al.*, "Whole-exome SNP array identifies 15 new susceptibility loci for psoriasis," *Nat. Commun.*, vol. 6, p. 6793, Apr. 2015.
[38] K. K.-H. Farh *et al.*, "Genetic and epigenetic fine mapping of causal autoimmune disease variants," *Nature*, vol. 518, no. 7539, pp. 337–343, Feb. 2015.
[39] J. A. Tennessen *et al.*, "Evolution and functional impact of rare coding variation from deep sequencing of human exomes," *Science*, vol. 337, no. 6090, pp. 64–69, Jul. 2012.
[40] A. Coventry *et al.*, "Deep resequencing reveals excess rare recent variants consistent with explosive population growth," *Nat. Commun.*, vol. 1, p. 131, 2010.
[41] T. A. Manolio *et al.*, "Finding the missing heritability of complex diseases," *Nature*, vol. 461, no. 7265, pp. 747–753, Oct. 2009.

[42] J. Bowes *et al.*, "Dense genotyping of immune-related susceptibility loci reveals new insights into the genetics of psoriatic arthritis," *Nat. Commun.*, vol. 6, p. 6046, Feb. 2015.
[43] Y. Sheng *et al.*, "Sequencing-based approach identified three new susceptibility loci for psoriasis," *Nat. Commun.*, vol. 5, p. 4331, Jul. 2014.
[44] X. Yin *et al.*, "Genome-wide meta-analysis identifies multiple novel associations and ethnic heterogeneity of psoriasis susceptibility," *Nat. Commun.*, vol. 6, p. 6916, Apr. 2015.
[45] H. Cheng *et al.*, "Identification of a missense variant in LNPEP that confers psoriasis risk," *J. Invest. Dermatol.*, vol. 134, no. 2, pp. 359–365, Feb. 2014.
[46] L.-D. Sun *et al.*, "Association analyses identify six new psoriasis susceptibility loci in the Chinese population," *Nat. Genet.*, vol. 42, no. 11, pp. 1005–1009, Nov. 2010.
[47] H. Tang *et al.*, "A large-scale screen for coding variants predisposing to psoriasis," *Nat. Genet.*, vol. 46, no. 1, pp. 45–50, Jan. 2014.
[48] P. E. Stuart *et al.*, "Genome-wide association analysis identifies three psoriasis susceptibility loci," *Nat. Genet.*, vol. 42, no. 11, pp. 1000–1004, Nov. 2010.
[49] D. Ellinghaus *et al.*, "Combined analysis of genome-wide association studies for Crohn disease and psoriasis identifies seven shared susceptibility loci," *Am. J. Hum. Genet.*, vol. 90, no. 4, pp. 636–647, Apr. 2012.
[50] R. Lande *et al.*, "Plasmacytoid dendritic cells sense self-DNA coupled with antimicrobial peptide," *Nature*, vol. 449, no. 7162, pp. 564–569, Oct. 2007.
[51] F. O. Nestle *et al.*, "Plasmacytoid predendritic cells initiate psoriasis through interferon-alpha production," *J. Exp. Med.*, vol. 202, no. 1, pp. 135–143, Jul. 2005.
[52] L. C. Zaba *et al.*, "Psoriasis is characterized by accumulation of immunostimulatory and Th1/Th17 cell-polarizing myeloid dendritic cells," *J. Invest. Dermatol.*, vol. 129, no. 1, pp. 79–88, Jan. 2009.
[53] Y. Qian *et al.*, "The adaptor Act1 is required for interleukin 17-dependent signaling associated with autoimmune and inflammatory disease," *Nat. Immunol.*, vol. 8, no. 3, pp. 247–256, Mar. 2007.
[54] P. M. Elias *et al.*, "Epidermal vascular endothelial growth factor production is required for permeability barrier homeostasis, dermal angiogenesis, and the development of epidermal hyperplasia: implications for the pathogenesis of psoriasis," *Am. J. Pathol.*, vol. 173, no. 3, pp. 689–699, Sep. 2008.
[55] T. Mabuchi and N. Hirayama, "Binding Affinity and Interaction of LL-37 with HLA-C*06:02 in Psoriasis," *J. Invest. Dermatol.*, vol. 136, no. 9, pp. 1901–1903, Sep. 2016.
[56] R. Lande *et al.*, "The antimicrobial peptide LL37 is a T-cell autoantigen in psoriasis," *Nat. Commun.*, vol. 5, p. 5621, 2014.
[57] A. Arakawa *et al.*, "Melanocyte antigen triggers autoimmunity in human psoriasis," *J. Exp. Med.*, vol. 212, no. 13, pp. 2203–2212, Dec. 2015.
[58] K. L. Cheung *et al.*, "Psoriatic T cells recognize neolipid antigens generated by mast cell phospholipase delivered by exosomes and presented by CD1a," *J. Exp. Med.*, vol. 213, no. 11, pp. 2399–2412, Oct. 2016.
[59] H. Chiba *et al.*, "Cloning of a gene for a novel epithelium-specific cytosolic phospholipase A2, cPLA2delta, induced in psoriatic skin," *J. Biol. Chem.*, vol. 279, no. 13, pp. 12890–12897, Mar. 2004.
[60] M. Quaranta *et al.*, "Intraindividual genome expression analysis reveals a specific molecular signature of psoriasis and eczema," *Sci. Transl. Med.*, vol. 6, no. 244, p. 244ra90, Jul. 2014.
[61] American Academy of Dermatology Work Group *et al.*, "Guidelines of care for the management of psoriasis and psoriatic arthritis: section 6. Guidelines of care for the treatment of psoriasis and psoriatic arthritis: case-based presentations and evidence-based conclusions," *J. Am. Acad. Dermatol.*, vol. 65, no. 1, pp. 137–174, Jul. 2011.

[62] A. Nast *et al.*, "European S3-Guidelines on the systemic treatment of psoriasis vulgaris--Update 2015--Short version--EDF in cooperation with EADV and IPC," *J. Eur. Acad. Dermatol. Venereol. JEADV*, vol. 29, no. 12, pp. 2277–2294, Dec. 2015.
[63] D. Tartar, T. Bhutani, M. Huynh, T. Berger, and J. Koo, "Update on the immunological mechanism of action behind phototherapy," *J. Drugs Dermatol. JDD*, vol. 13, no. 5, pp. 564–568, May 2014.
[64] R. S. Stern and PUVA Follow-Up Study, "The risk of squamous cell and basal cell cancer associated with psoralen and ultraviolet A therapy: a 30-year prospective study," *J. Am. Acad. Dermatol.*, vol. 66, no. 4, pp. 553–562, Apr. 2012.
[65] R. S. Stern and PUVA Follow up Study, "The risk of melanoma in association with long-term exposure to PUVA," *J. Am. Acad. Dermatol.*, vol. 44, no. 5, pp. 755–761, May 2001.
[66] S. K. Mahil, F. Capon, and J. N. Barker, "Update on psoriasis immunopathogenesis and targeted immunotherapy," *Semin. Immunopathol.*, vol. 38, no. 1, pp. 11–27, Jan. 2016.
[67] J. Kim and J. G. Krueger, "Highly Effective New Treatments for Psoriasis Target the IL-23/Type 17 T Cell Autoimmune Axis," *Annu. Rev. Med.*, vol. 68, pp. 255–269, Jan. 2017.
[68] L. C. Zaba *et al.*, "Amelioration of epidermal hyperplasia by TNF inhibition is associated with reduced Th17 responses," *J. Exp. Med.*, vol. 204, no. 13, pp. 3183–3194, Dec. 2007.
[69] L. C. Zaba *et al.*, "Effective treatment of psoriasis with etanercept is linked to suppression of IL-17 signaling, not immediate response TNF genes," *J. Allergy Clin. Immunol.*, vol. 124, no. 5, pp. 1022–1010.e1–395, Nov. 2009.
[70] T. Bongartz, A. J. Sutton, M. J. Sweeting, I. Buchan, E. L. Matteson, and V. Montori, "Anti-TNF antibody therapy in rheumatoid arthritis and the risk of serious infections and malignancies: systematic review and meta-analysis of rare harmful effects in randomized controlled trials," *JAMA*, vol. 295, no. 19, pp. 2275–2285, May 2006.
[71] S. K. Mahil, T. C. Andrews, C. Brierley, J. N. Barker, and C. H. Smith, "Demyelination during tumour necrosis factor antagonist therapy for psoriasis: a case report and review of the literature," *J. Dermatol. Treat.*, vol. 24, no. 1, pp. 38–49, Feb. 2013.
[72] C. E. M. Griffiths *et al.*, "Comparison of ustekinumab and etanercept for moderate-to-severe psoriasis," *N. Engl. J. Med.*, vol. 362, no. 2, pp. 118–128, Jan. 2010.
[73] K. A. Papp *et al.*, "Efficacy and safety of ustekinumab, a human interleukin-12/23 monoclonal antibody, in patients with psoriasis: 52-week results from a randomised, double-blind, placebo-controlled trial (PHOENIX 2)," *Lancet Lond. Engl.*, vol. 371, no. 9625, pp. 1675–1684, May 2008.
[74] C. L. Leonardi *et al.*, "Efficacy and safety of ustekinumab, a human interleukin-12/23 monoclonal antibody, in patients with psoriasis: 76-week results from a randomised, double-blind, placebo-controlled trial (PHOENIX 1)," *Lancet Lond. Engl.*, vol. 371, no. 9625, pp. 1665–1674, May 2008.
[75] A. D. Burden *et al.*, "The British Association of Dermatologists' Biologic Interventions Register (BADBIR): design, methodology and objectives," *Br. J. Dermatol.*, vol. 166, no. 3, pp. 545–554, Mar. 2012.
[76] A. Blauvelt *et al.*, "Secukinumab is superior to ustekinumab in clearing skin of subjects with moderate-to-severe plaque psoriasis up to 1 year: Results from the CLEAR study," *J. Am. Acad. Dermatol.*, vol. 76, no. 1, pp. 60–69.e9, Jan. 2017.
[77] R. G. Langley *et al.*, "Secukinumab in plaque psoriasis--results of two phase 3 trials," *N. Engl. J. Med.*, vol. 371, no. 4, pp. 326–338, Jul. 2014.
[78] C. E. M. Griffiths *et al.*, "Comparison of ixekizumab with etanercept or placebo in moderate-to-severe psoriasis (UNCOVER-2 and UNCOVER-3): results from two phase 3 randomised trials," *Lancet Lond. Engl.*, vol. 386, no. 9993, pp. 541–551, Aug. 2015.
[79] K. Papp *et al.*, "Tildrakizumab (MK-3222), an anti-interleukin-23p19 monoclonal antibody, improves psoriasis in a phase IIb randomized placebo-controlled trial," *Br. J. Dermatol.*, vol. 173, no. 4, pp. 930–939, Oct. 2015.
[80] K. B. Gordon *et al.*, "A Phase 2 Trial of Guselkumab versus Adalimumab for Plaque Psoriasis," *N. Engl. J. Med.*, vol. 373, no. 2, pp. 136–144, Jul. 2015.

[81] P. Schafer, “Apremilast mechanism of action and application to psoriasis and psoriatic arthritis,” *Biochem. Pharmacol.*, vol. 83, no. 12, pp. 1583–1590, Jun. 2012.
[82] K. Papp *et al.*, “Apremilast, an oral phosphodiesterase 4 (PDE4) inhibitor, in patients with moderate to severe plaque psoriasis: Results of a phase III, randomized, controlled trial (Efficacy and Safety Trial Evaluating the Effects of Apremilast in Psoriasis [ESTEEM] 1),” *J. Am. Acad. Dermatol.*, vol. 73, no. 1, pp. 37–49, Jul. 2015.
[83] K. A. Papp *et al.*, “Tofacitinib, an oral Janus kinase inhibitor, for the treatment of chronic plaque psoriasis: Long-term efficacy and safety results from 2 randomized phase-III studies and 1 open-label long-term extension study,” *J. Am. Acad. Dermatol.*, vol. 74, no. 5, pp. 841–850, May 2016.
[84] H. Bachelez *et al.*, “Tofacitinib versus etanercept or placebo in moderate-to-severe chronic plaque psoriasis: a phase 3 randomised non-inferiority trial,” *Lancet Lond. Engl.*, vol. 386, no. 9993, pp. 552–561, Aug. 2015.
[85] N. Punwani *et al.*, “Downmodulation of key inflammatory cell markers with a topical Janus kinase 1/2 inhibitor,” *Br. J. Dermatol.*, vol. 173, no. 4, pp. 989–997, Oct. 2015.
[86] B. E. Strober *et al.*, “Comparative effectiveness of biologic agents for the treatment of psoriasis in a real-world setting: Results from a large, prospective, observational study (Psoriasis Longitudinal Assessment and Registry [PSOLAR]),” *J. Am. Acad. Dermatol.*, vol. 74, no. 5, pp. 851–861.e4, May 2016.
[87] A. Saggini, S. Chimenti, and A. Chiricozzi, “IL-6 as a druggable target in psoriasis: focus on pustular variants,” *J. Immunol. Res.*, vol. 2014, p. 964069, 2014.
[88] A. Robinson *et al.*, “Treatment of pustular psoriasis: from the Medical Board of the National Psoriasis Foundation,” *J. Am. Acad. Dermatol.*, vol. 67, no. 2, pp. 279–288, Aug. 2012.
[89] H. B. Naik and E. W. Cowen, “Autoinflammatory pustular neutrophilic diseases,” *Dermatol. Clin.*, vol. 31, no. 3, pp. 405–425, Jul. 2013.
[90] X. Li *et al.*, “Mutation analysis of the IL36RN gene in Chinese patients with generalized pustular psoriasis with/without psoriasis vulgaris,” *J. Dermatol. Sci.*, vol. 76, no. 2, pp. 132–138, Nov. 2014.
[91] S. Polesie and A. G. Lidholm, “Secukinumab in the Treatment of Generalized Pustular Psoriasis: A Case report,” *Acta Derm. Venereol.*, vol. 97, no. 1, pp. 124–125, 04 2017.
[92] J. Saunier, S. Debarbieux, D. Jullien, L. Garnier, S. Dalle, and L. Thomas, “Acrodermatitis Continua of Hallopeau Treated Successfully with Ustekinumab and Acitretin after Failure of Tumour Necrosis Factor Blockade and Anakinra,” *Dermatol. Basel Switz.*, Nov. 2014.
[93] M. Cassandra, E. Conte, and B. Cortez, “Childhood pustular psoriasis elicited by the streptococcal antigen: a case report and review of the literature,” *Pediatr. Dermatol.*, vol. 20, no. 6, pp. 506–510, Dec. 2003.
[94] N. Weigle and S. McBane, “Psoriasis,” *Am. Fam. Physician*, vol. 87, no. 9, pp. 626–633, May 2013.
[95] K. Asumalahti *et al.*, “Genetic analysis of PSORS1 distinguishes guttate psoriasis and palmoplantar pustulosis,” *J. Invest. Dermatol.*, vol. 120, no. 4, pp. 627–632, Apr. 2003.
[96] S. Marrakchi *et al.*, “Interleukin-36-receptor antagonist deficiency and generalized pustular psoriasis,” *N. Engl. J. Med.*, vol. 365, no. 7, pp. 620–628, Aug. 2011.
[97] A. Onoufriadis *et al.*, “Mutations in IL36RN/IL1F5 are associated with the severe episodic inflammatory skin disease known as generalized pustular psoriasis,” *Am. J. Hum. Genet.*, vol. 89, no. 3, pp. 432–437, Sep. 2011.
[98] M. Tauber *et al.*, “IL36RN Mutations Affect Protein Expression and Function: A Basis for Genotype-Phenotype Correlation in Pustular Diseases,” *J. Invest. Dermatol.*, vol. 136, no. 9, pp. 1811–1819, Sep. 2016.
[99] S. Hussain *et al.*, “IL36RN mutations define a severe autoinflammatory phenotype of generalized pustular psoriasis,” *J. Allergy Clin. Immunol.*, Nov. 2014.

[100] N. Setta-Kaffetzi *et al.*, "Rare pathogenic variants in IL36RN underlie a spectrum of psoriasis-associated pustular phenotypes," *J. Invest. Dermatol.*, vol. 133, no. 5, pp. 1366–1369, May 2013.
[101] K. Sugiura *et al.*, "A novel IL36RN/IL1F5 homozygous nonsense mutation, p.Arg10X, in a Japanese patient with adult-onset generalized pustular psoriasis," *Br. J. Dermatol.*, vol. 167, no. 3, pp. 699–701, Sep. 2012.
[102] J. M. Ellingford, G. C. M. Black, T. H. Clayton, M. Judge, C. E. M. Griffiths, and R. B. Warren, "A novel mutation in IL36RN underpins childhood pustular dermatosis," *J. Eur. Acad. Dermatol. Venereol. JEADV*, vol. 30, no. 2, pp. 302–305, Feb. 2016.
[103] A. Körber *et al.*, "Mutations in IL36RN in patients with generalized pustular psoriasis," *J. Invest. Dermatol.*, vol. 133, no. 11, pp. 2634–2637, Nov. 2013.
[104] M. Farooq *et al.*, "Mutation analysis of the IL36RN gene in 14 Japanese patients with generalized pustular psoriasis," *Hum. Mutat.*, vol. 34, no. 1, pp. 176–183, Jan. 2013.
[105] T. Takeichi *et al.*, "A newly revealed IL36RN mutation in sibling cases complements our IL36RN mutation statistics for generalized pustular psoriasis," *J. Dermatol. Sci.*, vol. 85, no. 1, pp. 58–60, Jan. 2017.
[106] M. Hayashi *et al.*, "Novel IL36RN gene mutation revealed by analysis of 8 Japanese patients with generalized pustular psoriasis," *J. Dermatol. Sci.*, vol. 76, no. 3, pp. 267–269, Dec. 2014.
[107] N. Kanazawa, T. Nakamura, N. Mikita, and F. Furukawa, "Novel IL36RN mutation in a Japanese case of early onset generalized pustular psoriasis," *J. Dermatol.*, vol. 40, no. 9, pp. 749–751, Sep. 2013.
[108] N. Setta-Kaffetzi *et al.*, "AP1S3 mutations are associated with pustular psoriasis and impaired Toll-like receptor 3 trafficking," *Am. J. Hum. Genet.*, vol. 94, no. 5, pp. 790–797, May 2014.
[109] J. Hirst *et al.*, "Distinct and overlapping roles for AP-1 and GGAs revealed by the 'knocksideways' system," *Curr. Biol. CB*, vol. 22, no. 18, pp. 1711–1716, Sep. 2012.
[110] Y. Guo, C. Chang, R. Huang, B. Liu, L. Bao, and W. Liu, "AP1 is essential for generation of autophagosomes from the trans-Golgi network," *J. Cell Sci.*, vol. 125, no. Pt 7, pp. 1706–1715, Apr. 2012.
[111] S. Hussey, L. H. Travassos, and N. L. Jones, "Autophagy as an emerging dimension to adaptive and innate immunity," *Semin. Immunol.*, vol. 21, no. 4, pp. 233–241, Aug. 2009.
[112] H.-M. Lee *et al.*, "Autophagy negatively regulates keratinocyte inflammatory responses via scaffolding protein p62/SQSTM1," *J. Immunol. Baltim. Md 1950*, vol. 186, no. 2, pp. 1248–1258, Jan. 2011.
[113] R. Mössner *et al.*, "Palmoplantar Pustular Psoriasis Is Associated with Missense Variants in CARD14, but Not with Loss-of-Function Mutations in IL36RN in European Patients," *J. Invest. Dermatol.*, vol. 135, no. 10, pp. 2538–2541, Oct. 2015.
[114] A. Johnston *et al.*, "IL-1 and IL-36 are dominant cytokines in generalized pustular psoriasis," *J. Allergy Clin. Immunol.*, Dec. 2016.
[115] C. M. Henry, G. P. Sullivan, D. M. Clancy, I. S. Afonina, D. Kulms, and S. J. Martin, "Neutrophil-Derived Proteases Escalate Inflammation through Activation of IL-36 Family Cytokines," *Cell Rep.*, Jan. 2016.
[116] I. Aksentijevich *et al.*, "An autoinflammatory disease with deficiency of the interleukin-1-receptor antagonist," *N. Engl. J. Med.*, vol. 360, no. 23, pp. 2426–2437, Jun. 2009.
[117] A. A. de Jesus, S. W. Canna, Y. Liu, and R. Goldbach-Mansky, "Molecular mechanisms in genetically defined autoinflammatory diseases: disorders of amplified danger signaling," *Annu. Rev. Immunol.*, vol. 33, pp. 823–874, 2015.
[118] Y. Dombrowski *et al.*, "Cytosolic DNA triggers inflammasome activation in keratinocytes in psoriatic lesions," *Sci. Transl. Med.*, vol. 3, no. 82, p. 82ra38, May 2011.
[119] V. Kopfnagel, M. Wittmann, and T. Werfel, "Human keratinocytes express AIM2 and respond to dsDNA with IL-1β secretion," *Exp. Dermatol.*, vol. 20, no. 12, pp. 1027–1029, Dec. 2011.

[120] F. L. Zhong *et al.*, "Germline NLRP1 Mutations Cause Skin Inflammatory and Cancer Susceptibility Syndromes via Inflammasome Activation," *Cell*, vol. 167, no. 1, pp. 187–202.e17, Sep. 2016.
[121] A. Robinson *et al.*, "Treatment of pustular psoriasis: from the Medical Board of the National Psoriasis Foundation," *J. Am. Acad. Dermatol.*, vol. 67, no. 2, pp. 279–288, Aug. 2012.
[122] S. Imafuku *et al.*, "Efficacy and safety of secukinumab in patients with generalized pustular psoriasis: A 52-week analysis from phase III open-label multicenter Japanese study," *J. Dermatol.*, vol. 43, no. 9, pp. 1011–1017, Sep. 2016.
[123] K. Yamasaki, H. Nakagawa, Y. Kubo, K. Ootaki, and Japanese Brodalumab Study Group, "Efficacy and safety of brodalumab in patients with generalized pustular psoriasis and psoriatic erythroderma: results from a 52-week, open-label study," *Br. J. Dermatol.*, vol. 176, no. 3, pp. 741–751, Mar. 2017.
[124] M. Viguier, P. Guigue, C. Pagès, A. Smahi, and H. Bachelez, "Successful treatment of generalized pustular psoriasis with the interleukin-1-receptor antagonist Anakinra: lack of correlation with IL1RN mutations," *Ann. Intern. Med.*, vol. 153, no. 1, pp. 66–67, Jul. 2010.
[125] U. Hüffmeier, M. Wätzold, J. Mohr, M. P. Schön, and R. Mössner, "Successful therapy with anakinra in a patient with generalized pustular psoriasis carrying IL36RN mutations," *Br. J. Dermatol.*, vol. 170, no. 1, pp. 202–204, Jan. 2014.
[126] M. Tauber, M. Viguier, C. Le Gall, A. Smahi, and H. Bachelez, "Is it relevant to use an interleukin-1-inhibiting strategy for the treatment of patients with deficiency of interleukin-36 receptor antagonist?," *Br. J. Dermatol.*, vol. 170, no. 5, pp. 1198–1199, May 2014.
[127] L. Puig, D. Barco, E. Vilarrasa, and A. Alomar, "Treatment of acrodermatitis continua of Hallopeau with TNF-blocking agents: case report and review," *Dermatol. Basel Switz.*, vol. 220, no. 2, pp. 154–158, 2010.
[128] L. Di Costanzo, M. Napolitano, C. Patruno, M. Cantelli, and N. Balato, "Acrodermatitis continua of Hallopeau (ACH): two cases successfully treated with adalimumab," *J. Dermatol. Treat.*, vol. 25, no. 6, pp. 489–494, Dec. 2014.
[129] R. Bissonnette *et al.*, "Increased expression of IL-17A and limited involvement of IL-23 in patients with palmo-plantar (PP) pustular psoriasis or PP pustulosis; results from a randomised controlled trial," *J. Eur. Acad. Dermatol. Venereol. JEADV*, vol. 28, no. 10, pp. 1298–1305, Oct. 2014.
[130] "APRICOT Trial," *APRICOT*. [Online]. Available: http://apricot-trial.com/. [Accessed: 21-Mar-2017].
[131] D. M. Berki *et al.*, "Loss of IL36RN function does not confer susceptibility to psoriasis vulgaris," *J. Invest. Dermatol.*, vol. 134, no. 1, pp. 271–273, Jan. 2014.
[132] J. E. Sims *et al.*, "A new nomenclature for IL-1-family genes," *Trends Immunol.*, vol. 22, no. 10, pp. 536–537, Oct. 2001.
[133] M. S. Gresnigt and F. L. van de Veerdonk, "Biology of IL-36 cytokines and their role in disease," *Semin. Immunol.*, vol. 25, no. 6, pp. 458–465, Dec. 2013.
[134] C. Gabay and J. E. Towne, "Regulation and function of interleukin-36 cytokines in homeostasis and pathological conditions," *J. Leukoc. Biol.*, vol. 97, no. 4, pp. 645–652, Apr. 2015.
[135] Y. Carrier *et al.*, "Inter-regulation of Th17 cytokines and the IL-36 cytokines in vitro and in vivo: implications in psoriasis pathogenesis," *J. Invest. Dermatol.*, vol. 131, no. 12, pp. 2428–2437, Dec. 2011.
[136] K. A. Milora, H. Fu, O. Dubaz, and L. E. Jensen, "Unprocessed Interleukin-36α Regulates Psoriasis-Like Skin Inflammation in Cooperation With Interleukin-1," *J. Invest. Dermatol.*, vol. 135, no. 12, pp. 2992–3000, Dec. 2015.
[137] N. Li *et al.*, "Alarmin function of cathelicidin antimicrobial peptide LL37 through IL-36γ induction in human epidermal keratinocytes," *J. Immunol. Baltim. Md 1950*, vol. 193, no. 10, pp. 5140–5148, Nov. 2014.

[138] L.-H. Lian, K. A. Milora, K. K. Manupipatpong, and L. E. Jensen, "The double-stranded RNA analogue polyinosinic-polycytidylic acid induces keratinocyte pyroptosis and release of IL-36γ," *J. Invest. Dermatol.*, vol. 132, no. 5, pp. 1346–1353, May 2012.
[139] J. E. Towne *et al.*, "Interleukin-36 (IL-36) ligands require processing for full agonist (IL-36α, IL-36β, and IL-36γ) or antagonist (IL-36Ra) activity," *J. Biol. Chem.*, vol. 286, no. 49, pp. 42594–42602, Dec. 2011.
[140] J. S. Ainscough *et al.*, "Cathepsin S is the major activator of the psoriasis-associated proinflammatory cytokine IL-36γ," *Proc. Natl. Acad. Sci. U. S. A.*, Mar. 2017.
[141] T. Macleod *et al.*, "Neutrophil Elastase-mediated proteolysis activates the anti-inflammatory cytokine IL-36 Receptor antagonist," *Sci. Rep.*, vol. 6, p. 24880, Apr. 2016.
[142] C. M. Henry, G. P. Sullivan, D. M. Clancy, I. S. Afonina, D. Kulms, and S. J. Martin, "Neutrophil-Derived Proteases Escalate Inflammation through Activation of IL-36 Family Cytokines," *Cell Rep.*, vol. 14, no. 4, pp. 708–722, Feb. 2016.
[143] D. M. Clancy, C. M. Henry, G. P. Sullivan, and S. J. Martin, "Neutrophil extracellular traps can serve as platforms for processing and activation of IL-1 family cytokines," *FEBS J.*, Apr. 2017.
[144] S. S. Saha *et al.*, "Signal Transduction and Intracellular Trafficking by the Interleukin 36 Receptor," *J. Biol. Chem.*, vol. 290, no. 39, pp. 23997–24006, Sep. 2015.
[145] J. E. Towne, K. E. Garka, B. R. Renshaw, G. D. Virca, and J. E. Sims, "Interleukin (IL)-1F6, IL-1F8, and IL-1F9 signal through IL-1Rrp2 and IL-1RAcP to activate the pathway leading to NF-kappaB and MAPKs," *J. Biol. Chem.*, vol. 279, no. 14, pp. 13677–13688, Apr. 2004.
[146] A. M. Foster *et al.*, "IL-36 promotes myeloid cell infiltration, activation, and inflammatory activity in skin," *J. Immunol. Baltim. Md 1950*, vol. 192, no. 12, pp. 6053–6061, Jun. 2014.
[147] A. Johnston *et al.*, "IL-1F5, -F6, -F8, and -F9: a novel IL-1 family signaling system that is active in psoriasis and promotes keratinocyte antimicrobial peptide expression," *J. Immunol. Baltim. Md 1950*, vol. 186, no. 4, pp. 2613–2622, Feb. 2011.
[148] D. E. Smith, B. R. Renshaw, R. R. Ketchem, M. Kubin, K. E. Garka, and J. E. Sims, "Four new members expand the interleukin-1 superfamily," *J. Biol. Chem.*, vol. 275, no. 2, pp. 1169–1175, Jan. 2000.
[149] P. T. Walsh and P. G. Fallon, "The emergence of the IL-36 cytokine family as novel targets for inflammatory diseases," *Ann. N. Y. Acad. Sci.*, Oct. 2016.
[150] G. Yi *et al.*, "Structural and Functional Attributes of the Interleukin-36 Receptor," *J. Biol. Chem.*, vol. 291, no. 32, pp. 16597–16609, Aug. 2016.
[151] M. S. Gresnigt *et al.*, "The IL-36 receptor pathway regulates Aspergillus fumigatus-induced Th1 and Th17 responses," *Eur. J. Immunol.*, vol. 43, no. 2, pp. 416–426, Feb. 2013.
[152] F. L. van de Veerdonk *et al.*, "IL-38 binds to the IL-36 receptor and has biological effects on immune cells similar to IL-36 receptor antagonist," *Proc. Natl. Acad. Sci. U. S. A.*, vol. 109, no. 8, pp. 3001–3005, Feb. 2012.
[153] A. Puel *et al.*, "Chronic mucocutaneous candidiasis in humans with inborn errors of interleukin-17 immunity," *Science*, vol. 332, no. 6025, pp. 65–68, Apr. 2011.
[154] S. Vigne *et al.*, "IL-36 signaling amplifies Th1 responses by enhancing proliferation and Th1 polarization of naive CD4+ T cells," *Blood*, vol. 120, no. 17, pp. 3478–3487, Oct. 2012.
[155] N. Segueni *et al.*, "Limited Contribution of IL-36 versus IL-1 and TNF Pathways in Host Response to Mycobacterial Infection," *PloS One*, vol. 10, no. 5, p. e0126058, 2015.
[156] F. Ahsan, P. Moura-Alves, U. Guhlich-Bornhof, M. Klemm, S. H. E. Kaufmann, and J. Maertzdorf, "Role of Interleukin 36γ in Host Defense Against Tuberculosis," *J. Infect. Dis.*, vol. 214, no. 3, pp. 464–474, Aug. 2016.
[157] M.-A. Boutet *et al.*, "Distinct Expression of IL-36α, β, γ, their antagonist IL-36Ra and IL-38 in psoriasis, rheumatoid arthritis and Crohn's disease," *Clin. Exp. Immunol.*, Dec. 2015.
[158] M. Keermann *et al.*, "Expression of IL-36 family cytokines and IL-37 but not IL-38 is altered in psoriatic skin," *J. Dermatol. Sci.*, vol. 80, no. 2, pp. 150–152, Nov. 2015.

[159] A. M. D'Erme *et al.*, "IL-36γ (IL-1F9) is a biomarker for psoriasis skin lesions," *J. Invest. Dermatol.*, vol. 135, no. 4, pp. 1025–1032, Apr. 2015.
[160] J. Kim *et al.*, "The Spectrum of Mild to Severe Psoriasis Vulgaris Is Defined by a Common Activation of IL-17 Pathway Genes, but with Key Differences in Immune Regulatory Genes," *J. Invest. Dermatol.*, vol. 136, no. 11, pp. 2173–2182, Nov. 2016.
[161] H. Blumberg *et al.*, "Opposing activities of two novel members of the IL-1 ligand family regulate skin inflammation," *J. Exp. Med.*, vol. 204, no. 11, pp. 2603–2614, Oct. 2007.
[162] L. Tortola *et al.*, "Psoriasiform dermatitis is driven by IL-36-mediated DC-keratinocyte crosstalk," *J. Clin. Invest.*, vol. 122, no. 11, pp. 3965–3976, Nov. 2012.
[163] S. Vigne *et al.*, "IL-36R ligands are potent regulators of dendritic and T cells," *Blood*, vol. 118, no. 22, pp. 5813–5823, Nov. 2011.
[164] S. Mutamba, A. Allison, Y. Mahida, P. Barrow, and N. Foster, "Expression of IL-1Rrp2 by human myelomonocytic cells is unique to DCs and facilitates DC maturation by IL-1F8 and IL-1F9," *Eur. J. Immunol.*, vol. 42, no. 3, pp. 607–617, Mar. 2012.
[165] D. Dietrich *et al.*, "Interleukin-36 potently stimulates human M2 macrophages, Langerhans cells and keratinocytes to produce pro-inflammatory cytokines," *Cytokine*, vol. 84, pp. 88–98, Aug. 2016.
[166] C. Bridgewood, M. Stacey, A. Alase, D. Lagos, A. Graham, and M. Wittmann, "IL-36γ has proinflammatory effects on human endothelial cells," *Exp. Dermatol.*, Sep. 2016.
[167] C. Gabay and J. E. Towne, "Regulation and function of interleukin-36 cytokines in homeostasis and pathological conditions," *J. Leukoc. Biol.*, vol. 97, no. 4, pp. 645–652, Apr. 2015.
[168] A. Nishida *et al.*, "Increased Expression of Interleukin-36, a Member of the Interleukin-1 Cytokine Family, in Inflammatory Bowel Disease," *Inflamm. Bowel Dis.*, vol. 22, no. 2, pp. 303–314, Feb. 2016.
[169] S. E. Russell *et al.*, "IL-36α expression is elevated in ulcerative colitis and promotes colonic inflammation," *Mucosal Immunol.*, vol. 9, no. 5, pp. 1193–1204, Sep. 2016.
[170] K. Scheibe *et al.*, "IL-36R signalling activates intestinal epithelial cells and fibroblasts and promotes mucosal healing in vivo," *Gut*, Jan. 2016.
[171] A. D. Cohen, J. Dreiher, and S. Birkenfeld, "Psoriasis associated with ulcerative colitis and Crohn's disease," *J. Eur. Acad. Dermatol. Venereol. JEADV*, vol. 23, no. 5, pp. 561–565, May 2009.
[172] O. Medina-Contreras *et al.*, "Cutting Edge: IL-36 Receptor Promotes Resolution of Intestinal Damage," *J. Immunol. Baltim. Md 1950*, vol. 196, no. 1, pp. 34–38, Jan. 2016.
[173] Y. A. Bochkov, K. M. Hanson, S. Keles, R. A. Brockman-Schneider, N. N. Jarjour, and J. E. Gern, "Rhinovirus-induced modulation of gene expression in bronchial epithelial cells from subjects with asthma," *Mucosal Immunol.*, vol. 3, no. 1, pp. 69–80, Jan. 2010.
[174] R. T. Chustz *et al.*, "Regulation and function of the IL-1 family cytokine IL-1F9 in human bronchial epithelial cells," *Am. J. Respir. Cell Mol. Biol.*, vol. 45, no. 1, pp. 145–153, Jul. 2011.
[175] R. A. Ramadas, S. L. Ewart, Y. Iwakura, B. D. Medoff, and A. M. LeVine, "IL-36α exerts pro-inflammatory effects in the lungs of mice," *PloS One*, vol. 7, no. 9, p. e45784, 2012.
[176] R. A. Ramadas, X. Li, D. M. Shubitowski, S. Samineni, M. Wills-Karp, and S. L. Ewart, "IL-1 Receptor antagonist as a positional candidate gene in a murine model of allergic asthma," *Immunogenetics*, vol. 58, no. 10, pp. 851–855, Oct. 2006.
[177] S. Frey *et al.*, "The novel cytokine interleukin-36α is expressed in psoriatic and rheumatoid arthritis synovium," *Ann. Rheum. Dis.*, vol. 72, no. 9, pp. 1569–1574, Sep. 2013.
[178] C. Lamacchia *et al.*, "The severity of experimental arthritis is independent of IL-36 receptor signaling," *Arthritis Res. Ther.*, vol. 15, no. 2, p. R38, Mar. 2013.
[179] A. Derer *et al.*, "Blockade of IL-36 receptor signaling does not prevent from TNF-induced arthritis," *PloS One*, vol. 9, no. 8, p. e101954, 2014.

[180] A. Chiricozzi *et al.*, "Crosstalk between skin inflammation and adipose tissue-derived products: pathogenic evidence linking psoriasis to increased adiposity," *Expert Rev. Clin. Immunol.*, vol. 12, no. 12, pp. 1299–1308, Dec. 2016.
[181] E. J. P. van Asseldonk *et al.*, "The effect of the interleukin-1 cytokine family members IL-1F6 and IL-1F8 on adipocyte differentiation," *Obes. Silver Spring Md*, vol. 18, no. 11, pp. 2234–2236, Nov. 2010.
[182] H.-G. Eichler *et al.*, "Bridging the efficacy-effectiveness gap: a regulator's perspective on addressing variability of drug response," *Nat. Rev. Drug Discov.*, vol. 10, no. 7, pp. 495–506, 01 2011.
[183] J. W. Scannell, A. Blanckley, H. Boldon, and B. Warrington, "Diagnosing the decline in pharmaceutical R&D efficiency," *Nat. Rev. Drug Discov.*, vol. 11, no. 3, pp. 191–200, Mar. 2012.
[184] B. Munos, "Lessons from 60 years of pharmaceutical innovation," *Nat. Rev. Drug Discov.*, vol. 8, no. 12, pp. 959–968, 2009.
[185] J. A. Dimasi, "Risks in new drug development: approval success rates for investigational drugs," *Clin. Pharmacol. Ther.*, vol. 69, no. 5, pp. 297–307, May 2001.
[186] T. Tuntland *et al.*, "Implementation of pharmacokinetic and pharmacodynamic strategies in early research phases of drug discovery and development at Novartis Institute of Biomedical Research," *Front. Pharmacol.*, vol. 5, p. 174, 2014.
[187] R. M. Plenge, E. M. Scolnick, and D. Altshuler, "Validating therapeutic targets through human genetics," *Nat. Rev. Drug Discov.*, vol. 12, no. 8, pp. 581–594, Aug. 2013.
[188] "Exploring biological space." [Online]. Available: http://www.nature.com/horizon/chemicalspace/background/figs/odyssey_f1.html. [Accessed: 24-Apr-2017].
[189] D. G. MacArthur and C. Tyler-Smith, "Loss-of-function variants in the genomes of healthy humans," *Hum. Mol. Genet.*, vol. 19, no. R2, pp. R125–130, Oct. 2010.
[190] D. G. MacArthur *et al.*, "A systematic survey of loss-of-function variants in human protein-coding genes," *Science*, vol. 335, no. 6070, pp. 823–828, Feb. 2012.
[191] J. C. Cohen, E. Boerwinkle, T. H. Mosley, and H. H. Hobbs, "Sequence variations in PCSK9, low LDL, and protection against coronary heart disease," *N. Engl. J. Med.*, vol. 354, no. 12, pp. 1264–1272, Mar. 2006.
[192] J. D. Horton, J. C. Cohen, and H. H. Hobbs, "PCSK9: a convertase that coordinates LDL catabolism," *J. Lipid Res.*, vol. 50 Suppl, pp. S172–177, Apr. 2009.
[193] M. Abifadel *et al.*, "Mutations in PCSK9 cause autosomal dominant hypercholesterolemia," *Nat. Genet.*, vol. 34, no. 2, pp. 154–156, Jun. 2003.
[194] C. Sheridan, "New class PCSK9 blockers stride into cholesterol market," *Nat. Biotechnol.*, vol. 33, no. 8, pp. 785–786, Aug. 2015.
[195] "Make no mistake: PCSK9 and the FOURIER clinical outcome study represent a triumph for genetic-driven drug discovery," *Plenge Gen @rplenge*, 24-Mar-2017. [Online]. Available: http://www.plengegen.com/blog/pcsk9-fourier/. [Accessed: 24-Apr-2017].
[196] R. Liu *et al.*, "Homozygous defect in HIV-1 coreceptor accounts for resistance of some multiply-exposed individuals to HIV-1 infection," *Cell*, vol. 86, no. 3, pp. 367–377, Aug. 1996.
[197] G. Hütter *et al.*, "Long-term control of HIV by CCR5 Delta32/Delta32 stem-cell transplantation," *N. Engl. J. Med.*, vol. 360, no. 7, pp. 692–698, Feb. 2009.
[198] C. Flexner, "HIV drug development: the next 25 years," *Nat. Rev. Drug Discov.*, vol. 6, no. 12, pp. 959–966, Dec. 2007.
[199] Emerging Risk Factors Collaboration *et al.*, "Lipid-related markers and cardiovascular disease prediction," *JAMA*, vol. 307, no. 23, pp. 2499–2506, Jun. 2012.
[200] D. Saleheen *et al.*, "Human knockouts and phenotypic analysis in a cohort with a high rate of consanguinity," *Nature*, vol. 544, no. 7649, pp. 235–239, Apr. 2017.

[201] STABILITY Investigators *et al.*, "Darapladib for preventing ischemic events in stable coronary heart disease," *N. Engl. J. Med.*, vol. 370, no. 18, pp. 1702–1711, May 2014.
[202] M. L. O'Donoghue *et al.*, "Effect of darapladib on major coronary events after an acute coronary syndrome: the SOLID-TIMI 52 randomized clinical trial," *JAMA*, vol. 312, no. 10, pp. 1006–1015, Sep. 2014.
[203] K. Schmidt, A. Noureen, F. Kronenberg, and G. Utermann, "Structure, function, and genetics of lipoprotein (a)," *J. Lipid Res.*, vol. 57, no. 8, pp. 1339–1359, Aug. 2016.
[204] E. T. Lim *et al.*, "Distribution and medical impact of loss-of-function variants in the Finnish founder population," *PLoS Genet.*, vol. 10, no. 7, p. e1004494, Jul. 2014.
[205] M. Saleh *et al.*, "Differential modulation of endotoxin responsiveness by human caspase-12 polymorphisms," *Nature*, vol. 429, no. 6987, pp. 75–79, May 2004.
[206] J. T. Seto *et al.*, "ACTN3 genotype influences muscle performance through the regulation of calcineurin signaling," *J. Clin. Invest.*, vol. 123, no. 10, pp. 4255–4263, Oct. 2013.
[207] A.-K. Niemi and K. Majamaa, "Mitochondrial DNA and ACTN3 genotypes in Finnish elite endurance and sprint athletes," *Eur. J. Hum. Genet. EJHG*, vol. 13, no. 8, pp. 965–969, Aug. 2005.
[208] A. B. Jørgensen, R. Frikke-Schmidt, B. G. Nordestgaard, and A. Tybjærg-Hansen, "Loss-of-function mutations in APOC3 and risk of ischemic vascular disease," *N. Engl. J. Med.*, vol. 371, no. 1, pp. 32–41, Jul. 2014.
[209] TG and HDL Working Group of the Exome Sequencing Project, National Heart, Lung, and Blood Institute *et al.*, "Loss-of-function mutations in APOC3, triglycerides, and coronary disease," *N. Engl. J. Med.*, vol. 371, no. 1, pp. 22–31, Jul. 2014.
[210] M. Lek *et al.*, "Analysis of protein-coding genetic variation in 60,706 humans," *Nature*, vol. 536, no. 7616, pp. 285–291, 18 2016.
[211] P. Sulem *et al.*, "Identification of a large set of rare complete human knockouts," *Nat. Genet.*, vol. 47, no. 5, pp. 448–452, May 2015.
[212] V. M. Narasimhan *et al.*, "Health and population effects of rare gene knockouts in adult humans with related parents," *Science*, vol. 352, no. 6284, pp. 474–477, Apr. 2016.
[213] J. Kaiser, "The hunt for missing genes," *Science*, vol. 344, no. 6185, pp. 687–689, May 2014.
[214] J. T. Minion, F. Butcher, N. J. Timpson, and M. J. Murtagh, "The ethics conundrum in Recall by Genotype (RbG) research: Perspectives from birth cohort participants," *bioRxiv*, p. 124636, Apr. 2017.
[215] L. J. Corbin *et al.*, "Causal Analyses, Statistical Efficiency And Phenotypic Precision Through Recall-By-Genotype Study Design," *bioRxiv*, p. 124586, Apr. 2017.
[216] V. M. Narasimhan, Y. Xue, and C. Tyler-Smith, "Human Knockout Carriers: Dead, Diseased, Healthy, or Improved?," *Trends Mol. Med.*, vol. 22, no. 4, pp. 341–351, Apr. 2016.
[217] F. A. Ran, P. D. Hsu, J. Wright, V. Agarwala, D. A. Scott, and F. Zhang, "Genome engineering using the CRISPR-Cas9 system," *Nat. Protoc.*, vol. 8, no. 11, pp. 2281–2308, Nov. 2013.
[218] "CRISPR Design." [Online]. Available: http://crispr.mit.edu/. [Accessed: 04-May-2017].
[219] T. Aasen and J. C. Izpisúa Belmonte, "Isolation and cultivation of human keratinocytes from skin or plucked hair for the generation of induced pluripotent stem cells," *Nat. Protoc.*, vol. 5, no. 2, pp. 371–382, Feb. 2010.
[220] P. Di Meglio *et al.*, "Activation of the aryl hydrocarbon receptor dampens the severity of inflammatory skin conditions," *Immunity*, vol. 40, no. 6, pp. 989–1001, Jun. 2014.
[221] K. J. Livak and T. D. Schmittgen, "Analysis of relative gene expression data using real-time quantitative PCR and the 2(-Delta Delta C(T)) Method," *Methods San Diego Calif*, vol. 25, no. 4, pp. 402–408, Dec. 2001.
[222] C. A. Schneider, W. S. Rasband, and K. W. Eliceiri, "NIH Image to ImageJ: 25 years of image analysis," *Nat. Methods*, vol. 9, no. 7, pp. 671–675, Jul. 2012.

[223] M. Kircher, D. M. Witten, P. Jain, B. J. O'Roak, G. M. Cooper, and J. Shendure, "A general framework for estimating the relative pathogenicity of human genetic variants," *Nat. Genet.*, vol. 46, no. 3, pp. 310–315, Mar. 2014.
[224] A. González-Pérez and N. López-Bigas, "Improving the assessment of the outcome of nonsynonymous SNVs with a consensus deleteriousness score, Condel," *Am. J. Hum. Genet.*, vol. 88, no. 4, pp. 440–449, Apr. 2011.
[225] P. Kumar, S. Henikoff, and P. C. Ng, "Predicting the effects of coding non-synonymous variants on protein function using the SIFT algorithm," *Nat. Protoc.*, vol. 4, no. 7, pp. 1073–1081, 2009.
[226] Y. Choi, G. E. Sims, S. Murphy, J. R. Miller, and A. P. Chan, "Predicting the functional effect of amino acid substitutions and indels," *PloS One*, vol. 7, no. 10, p. e46688, 2012.
[227] I. Adzhubei, D. M. Jordan, and S. R. Sunyaev, "Predicting functional effect of human missense mutations using PolyPhen-2," *Curr. Protoc. Hum. Genet.*, vol. Chapter 7, p. Unit7.20, Jan. 2013.
[228] "Babraham Bioinformatics - FastQC A Quality Control tool for High Throughput Sequence Data." [Online]. Available: http://www.bioinformatics.babraham.ac.uk/projects/fastqc/. [Accessed: 13-May-2017].
[229] "Babraham Bioinformatics - Trim Galore!" [Online]. Available: https://www.bioinformatics.babraham.ac.uk/projects/trim_galore/. [Accessed: 13-May-2017].
[230] B. Langmead and S. L. Salzberg, "Fast gapped-read alignment with Bowtie 2," *Nat. Methods*, vol. 9, no. 4, pp. 357–359, Mar. 2012.
[231] S. Anders, P. T. Pyl, and W. Huber, "HTSeq--a Python framework to work with high-throughput sequencing data," *Bioinforma. Oxf. Engl.*, vol. 31, no. 2, pp. 166–169, Jan. 2015.
[232] O. An, G. M. Dall'Olio, T. P. Mourikis, and F. D. Ciccarelli, "NCG 5.0: updates of a manually curated repository of cancer genes and associated properties from cancer mutational screenings," *Nucleic Acids Res.*, vol. 44, no. D1, pp. D992–999, Jan. 2016.
[233] M. I. Love, W. Huber, and S. Anders, "Moderated estimation of fold change and dispersion for RNA-seq data with DESeq2," *Genome Biol.*, vol. 15, no. 12, p. 550, 2014.
[234] "GWAS Catalog." [Online]. Available: https://www.ebi.ac.uk/gwas/. [Accessed: 04-May-2017].
[235] D. Smedley *et al.*, "BioMart--biological queries made easy," *BMC Genomics*, vol. 10, p. 22, Jan. 2009.
[236] F. O. Nestle, P. Di Meglio, J.-Z. Qin, and B. J. Nickoloff, "Skin immune sentinels in health and disease," *Nat. Rev. Immunol.*, vol. 9, no. 10, pp. 679–691, Oct. 2009.
[237] L. van der Fits *et al.*, "Imiquimod-induced psoriasis-like skin inflammation in mice is mediated via the IL-23/IL-17 axis," *J. Immunol. Baltim. Md 1950*, vol. 182, no. 9, pp. 5836–5845, May 2009.
[238] P. Di Meglio *et al.*, "Activation of the aryl hydrocarbon receptor dampens the severity of inflammatory skin conditions," *Immunity*, vol. 40, no. 6, pp. 989–1001, Jun. 2014.
[239] "The 100,000 Genomes Project," *Genomics England*, 21-Jul-2014. .
[240] "Eraspen - Home." [Online]. Available: http://eraspen.eu/. [Accessed: 23-Apr-2017].
[241] B. B. Cummings *et al.*, "Improving genetic diagnosis in Mendelian disease with transcriptome sequencing," *Sci. Transl. Med.*, vol. 9, no. 386, Apr. 2017.
[242] "GTEx Portal." [Online]. Available: https://www.gtexportal.org/home/. [Accessed: 03-May-2017].
[243] "ANB019," *AnaptysBio*. .
[244] J. Wolf and L. K. Ferris, "Anti-IL-36R antibodies, potentially useful for the treatment of psoriasis: a patent evaluation of WO2013074569," *Expert Opin. Ther. Pat.*, vol. 24, no. 4, pp. 477–479, Apr. 2014.
[245] "ANTI IL-36R ANTIBODIES." [Online]. Available: http://www.freepatentsonline.com/20150203584.pdf. [Accessed: 03-May-2017].

[246] S. J. Martin, C. HENRY, and G. SULLIVAN, “Use of inhibitors of il-36 proteolytic processing for the treatment and/or reduction of inflammation,” WO2016042131 A1, 24-Mar-2016.
[247] A. Aslam and C. E. M. Griffiths, “Drug therapies in dermatology,” *Clin. Med. Lond. Engl.*, vol. 14, no. 1, pp. 47–53, Feb. 2014.
[248] G. Fitsialos *et al.*, “Transcriptional signature of epidermal keratinocytes subjected to in vitro scratch wounding reveals selective roles for ERK1/2, p38, and phosphatidylinositol 3-kinase signaling pathways,” *J. Biol. Chem.*, vol. 282, no. 20, pp. 15090–15102, May 2007.
[249] “Home | East London Genes & Health.” [Online]. Available: http://www.genesandhealth.org/. [Accessed: 23-Apr-2017].

6. Appendix I: Oliogonucleotide primers

Table 6.1 Oligonucleotide primers used in the study

Target	Primer ID	Sequence (5' to 3')	Annealing temperature (°C)	Application
AP1M1	AP1M1_HindIII_ Fwd	GTAAAGCTTATGTCCGCCAGCGCCG TCTAC	60	Cloning *AP1M1* into plasmid
	AP1M1_BamHI_ Rev	GATGGATCCCTGGGTCCGGAGCTG GTAATC		
AP1S3	AP1S3_1_Fwd	CTCCAGCGCTCCTTGCTC	56	CRISPR
Exon 1	AP1S3_1_Rev	GGATCGAATGAATGAATGGA		validation
AP1S3	AP1S3_2_Fwd	TTTCAGTGTCTTTGCAGAACG	59	CRISPR
Exon 2	AP1S3_2_Rev	CCCCAGCCTTCAAAGATTTC		validation
AP1S3	AP1S3_3_Fwd	GACTGCATATTCGTGGGAAAA	59	CRISPR
Exon 3	AP1S3_3_Rev	GCTGAGATGGGGACTGTAGC		Validation
AP1S3	AP1S3_4_Fwd	GGCAGATGTTTCCCCTGATA	59	CRISPR
Exon 4	AP1S3_4_Rev	TCATCATCATCATCATCATCTTTC		Validation
AP1S3	AP1S3_5_Fwd	ATTTCACAGTCTGCGGAAGG	59	CRISPR
Exon 5	AP1S3_5_Rev	TGGGAGGCGTTGCTTATTTA		Validation
AP1S1	AP1S1_2_Fwd	GGGCTGGATGTTGGAAGAAA	59	CRISPR
Exon 2	AP1S1_2_Rev	GTCCTCCAGATGTCCTCAGC		Validation
AP1S2	AP1S2_2_Fwd	CATGTAAATGCCCCATCCCC	59	CRISPR
Exon 2	AP1S2_2_Rev	TCACTGAAGTCTGCAATTTCCT		Validation
AP1S3	AP1S3_Fwd	GCTCTTCAGTCGACAAGGGA	60	Real-time PCR
	AP1S3_Rev	GCGTCAAGAGCTCATTGTCC		
AP1S2	AP1S2_Fwd	ACTGCAGGAGGAAGCTGAAAC	60	Real-time PCR
	AP1S2_Rev	GAAGCGGCTTAGCAAAACAGT		

AP1S1	AP1S1_Fwd	ATACTTTGGCAGTGTGTGCG	60	Real-time PCR
	AP1S1_Rev	CCTCTTGCAGTAGGTCAGCC		
AP1S3	sgRNA-top	CACCGTTCAGATTATTCTCTCCCG	-	CRISPR guide
Exon 2	sgRNA-bottom	AAACCGGGAGAGAATAATCTGAAC		RNAs
AP1S3 **coding region**	ON-TARGET plus SMARTpool human *AP1S3* siRNA	CUACACAUGUUCUGGAUAA AAGAAGAUCACCCGGGAAA GGAAAUUACGGCUACAGAA CAUUCAUAUUAGAGUGGUU	-	siRNA mediated gene silencing
Non-targeting	ON-TARGET plus Non-targeting pool siRNA	UGGUUUACAUGUCGACUAA UGGUUUACAUGUUGUGUGA UGGUUUACAUGUUUUCUGA UGGUUUACAUGUUUUCCUA	-	Control primers for siRNA mediated gene silencing
CAMP	LL37_Fwd	GCTGGGTGATTTCTTCCGGA	60	Real-time PCR
	LL37_Rev	CCTGGGTACAAGATTCCGCA		
CCL20	CCL20_Fwd	GCGAATCAGAAGCAAGCAACT	60	Real-time PCR
	CCL20_Rev	TTGCGCACACAGACAACTTT		
FBXL5	FBXL5_Fwd	AGGACATTGTTGGACTAAGGACT	56	Seq CRISPR
	FBXL5_Rev	TGAAGTAGGGCAGATCTTGGT		off target
HuPO	HuPO_Fwd	GCTTCCTGGAGGGTGTCC	60	Real-time PCR
	HuPO_Rev	GGACTCGTTTGTACCCGTTG		
IFIT1	IFIT1_Fwd	TAGGCAGAGATCGCATACCC	60	Real-time PCR
	IFIT1_Rev	GCTTTCAAATCCCTTCCGCT		
IL1B	IL1B_Fwd	GCCCTAAACAGATGAAGTGCTC	60	Real-time PCR
	IL1B_Rev	GAACCAGCATCTTCCTCAG		
IL17A	IL17A_Fwd	CTACAACCGATCCACCTCACCTTG	60	Real-time PCR
	IL17A_Rev	GGTAGTCCACGTTCCCATCAGC		
IL6	IL6_Fwd	AAAGAGGCACTGGCAGAAAA	60	Real-time PCR

	IL6_Rev	GCTCTGGCTTGTTCCTCACT		
IL8	IL8_Fwd	TTGGCAGCCTTCCTGATTTC	60	Real-time PCR
	IL8_Rev	AACTTCTCCACAACCCTCT		
IL36A	IL36A_Fwd	GGCCTGAATGGACTCAATCT	60	Real-time PCR
	IL36A_Rev	ACTTCACAGGCTCGGGTTG		
IL36B	IL36B_Fwd	ACTTCACAGGCTCGGGTTG	60	Real-time PCR
	IL36B_Rev	CAGCATTAAGCCTGTCACTC		
IL36G	IL36G_Fwd	GGGCCGTCTATCAATCAATG	60	Real-time PCR
	IL36G_Rev	TGATAACAGCAACAGTGACTG		
IL1RL2	IL1RL2_1_Fwd	CAGTCTTTGGGGAAACGTGG	58	Sanger seq
Exon 1	IL1RL2_1_Rev	TCTCTGTTTCCTCTTCCGCG		
IL1RL2	IL1RL2_2_Fwd	TCCAGACTCAAGAAACTCCCA	58	Sanger seq
Exon 2	IL1RL2_2_Rev	TCTGGTCTGAGGTGCCATTT		
IL1RL2	IL1RL2_3_Fwd	GCAGAGGGTTTGCACAGTG	62	Sanger seq
Exon 3	IL1RL2_3_Rev	TAACTGGAGGAAGGTGGTGG		
IL1RL2	IL1RL2_4_Fwd	TCTGCTGCCTATCTATCCATCT	58	Sanger seq
Exon 4	IL1RL2_4_Rev	GACCTAGAATCACTCCTGCTCA		
IL1RL2	IL1RL2_5_Fwd	GCTTATTGATGGTCTGCTCTGT	58	Sanger seq
Exon 5	IL1RL2_5_Rev	GGAAACTGGGTGTGTATAGGAT		
IL1RL2	IL1RL2_6_Fwd	TTGCCCCTTGTGGTCTCTC	58	Sanger seq
Exon 6	IL1RL2_6_Rev	TGTTTGCTTTGTATGCCCGG		
IL1RL2	IL1RL2_7_Fwd	GGATAACATGATGGCCCAAAGT	58	Sanger seq
Exon 7	IL1RL2_7_Rev	CACAGCCTCACTCCAACAAC		
IL1RL2	IL1RL2_8_Fwd	TTCTGCTCCCATACCACTTTT	58	Sanger seq
Exon 8	IL1RL2_8_Rev	TGATGCTGGTGATTAGGGACA		
IL1RL2	IL1RL2_9_Fwd	GGAGATGATGTCCCTTGGCA	60	Sanger seq

Exon 9	IL1RL2_9_Rev	CAAGCAGGAATCTCAGGCAC		
IL1RL2	IL1RL2_10_Fwd	TGAGCTGAGATTGCATCCCT	60	Sanger seq
Exon 10	IL1RL2_10_Rev	CAGATCCTCTCACTAGTACGCA		
IL1RL2	IL1RL2_11_Fwd	AACTGACGGCAAGGTGGAG	60	Sanger seq
Exon 11	IL1RL2_11_Rev	CCTCTTCTCTACGCCTGAGC		
IRAK2	IRAK2_Fwd	CCTCCTCTGAGGCCTGTGT	60	Real-time PCR
	IRAK2_Rev	TGATCTCAATTTGCCACGAA		
KRT10	KRT10_Fwd	AGCATGGCAACTCACATCAG	60	Real-time PCR
	KRT10_Rev	TGTCGATCTGAAGCAGGATG		
KRT16	KRT16_Fwd	GAGATCAAAGACTACAGTCC	60	Real-time PCR
	KRT16_Rev	CATGCTCATACTTGGTCCTG		
LCN2	LCN2_Fwd	TCACCTCCGTCCTGTTTAGG	60	Real-time PCR
	LCN2_Rev	AGGTAACTCGTTAATCCAGGGTAA		
MMP9	MMP9_Fwd	GATCATTCCTCAGTGCCGGA	60	Real-time PCR
	MMP9_Rev	TTCAGGGCGAGGACCATAGA		
PALD1	PALD1_Fwd	TTTTGGTGAGGGTGCAAGC	59	Seq CRISPR
	PALD1_Rev	CAGAAGGTGGAAAAGTGACCA		off target
PLA2G4D	PLA2G4D_Fwd	TTGAGTGAGGCCGACCCTTA	60	Real-time PCR
	PLA2G4D_Rev	GCTCCAGAACATTCTTGACCTG		
RSAD2	RSAD2_Fwd	TCCGTCATGTCCTCTTCCAC	60	Real-time PCR
	RSAD2_Rev	CTGTGACAGCTTTGACGAGG		
S100A7	S100A7_Fwd	AACTTCCTTAGTGCCTGTGACAA	60	Real-time PCR
	S100A7_Rev	TCCTTTTTCTCAAAGACATCGGC		
TG	TG_Fwd	GCCTTCAACTCTGCCTTTATTCA	56	Seq CRISPR
	TG_Rev	AAACCACAGAGCCAGCAGAA		off target
TNF	TNF_Fwd	CCCAGGGACCTCTCTCTAATCA	60	Real-time PCR

	TNF_Rev	GCTACAGGCTTGTCACTCGG		
TREM1	TREM1_Fwd	CTGAAAAGCACAGGGTCAGG	56	Seq CRISPR
	TREM1_Rev	ATGGATGTGGCTGGAAGTCA		off target

Seq, sequencing.

7. Appendix II: Web resources

CADD	http://cadd.gs.washington.edu/
dbSNP	http://www.ncbi.nlm.nih.gov/SNP/
DESeq2	https://bioconductor.org/packages/release/bioc/html/DESeq2.html
Ensembl genome browser	http://www.ensembl.org/index.html
ERASPEN	http://www.eraspen.eu
FastQC	https://www.bioinformatics.babraham.ac.uk/projects/fastqc/
GTEx Portal	https://www.gtexportal.org/home/
GWAS catalogue	https://www.ebi.ac.uk/gwas/
ImageJ	http://imagej.nih.gov/ij/
PolyPhen-2	http://genetics.bwh.harvard.edu/pph2/
Primer3	http://www.bioinformatics.nl/cgi-bin/primer3plus/primer3plus.cgi/
Primer BLAST	http://www.ncbi.nlm.nih.gov/tools/primer-blast/
PROVEAN	http://provean.jcvi.org/index.php
SIFT	http://sift.jcvi.org/
UCSC genome browser	http://genome.ucsc.edu/